Exploration and Geological Services Division, Yukon Region

BULLETIN 10

Geology and mineral occurrences of the Slats Creek, Fairchild Lake and "Dolores Creek" areas, Wernecke Mountains (106D/16, 106C/13, 106C/14), Yukon Territory

Derek J. Thorkelson[1,2]

with contributions from
C.A. Wallace[2], J.K. Mortensen[3], R.A. Creaser[4], V.J. McNicoll[5], M.E. Villeneuve[5], and P.W. Layer[6]

[1]Department of Earth Sciences, Simon Fraser University, Burnaby, British Columbia, Canada V5A 1S6
[2]Formerly with the Canada/Yukon Geoscience Office, Whitehorse, Yukon
[3]Earth and Ocean Sciences, University of British Columbia, Vancouver, British Columbia
[4]Earth and Atmospheric Sciences, University of Alberta, Edmonton, Alberta
[5]Geological Survey of Canada, Ottawa, Ontario
[6]Geophysical Institute, University of Alaska, Fairbanks, Alaska

2000

105-00737/

Published under the authority of the Minister of Indian Affairs and Northern Development, Ottawa, 2000.
http://www.inac.gc.ca
Printed in Whitehorse, Yukon, 2000.

© Minister of Public Works and Government Services Canada

QS-Y145-000-EE-A1 Catalogue No. R71-62/2000E ISBN 0-662-29168-9

This, and other Yukon Geology Program publications, may be obtained from:
Geoscience and Information Sales
c/o Whitehorse Mining Recorder
102-302 Main Street
Whitehorse, Yukon Y1A 2B5 Canada
phone (867) 667-3266, fax (867) 667-3267
Visit the Yukon Geology Program web site at www.yukonweb.com/government/geoscience/

In referring to this publication, please use the following citation:
Thorkelson, Derek J., 2000. Geology and mineral occurrences of the Slats Creek, Fairchild Lake and "Dolores Creek" areas, Wernecke Mountains (106D/16, 106C/13, 106C/14), Yukon Territory. Exploration and Geological Services Division, Yukon, Indian and Northern Affairs Canada, Bulletin 10, 73p.

Production by K-L Services, Whitehorse, Yukon.

Cover: Angular unconformity between Lower Paleozoic dolostone and Lower Proterozoic dolostone, near confluence of Bond Creek and Wind River, 10 km west of study area, Wernecke Mountains (view to the southwest). Age difference across unconformity is at least 1.2 billion years. Pre-Paleozoic folding probably occurred mainly during Racklan Orogeny, and geometry may have been affected by subsequent Corn Creek Orogeny. About 7 km of intervening strata are present between the two dolostone successions in the eastern part of the study area.

Preface

This study of three 1:50 000 scale map sheets provides a seminal revision of the Proterozoic geological history of northern Yukon, including definition and regional correlation of stratigraphic sequences, magmatism and deformation. The geologic record of northern Yukon is now known to extend into the Early Proterozoic, and to include four rather than three Proterozoic stratigraphic sequences. These are the Wernecke Supergroup, Pinguicula Group, Hematite Creek Group, and Windermere Supergroup. Mafic dykes record igneous activity at 1.72 Ga, and 1.27 Ga. A major pulse of hydrothermal-phreatic activity produced the intrusive Wernecke Breccias at 1.6 Ga, and was followed by minor hydrothermal activity at 1.38 and 1.27 Ga. Two events of contractional deformation are recognized, in the Racklan Orogeny (pre-1.72 Ga), marked by the unconformity of the Pinguicula Group on the Wernecke Supergroup, and the Corn Creek Orogeny (1.0-0.76 Ga), marked by the unconformity of the Windermere on the Hematite Creek Group.

This study also provides the geological framework needed to assess the mineral potential and explore these map areas and other extensive parts of northern Yukon with similar geology. The Wernecke Breccias contain occurrences of copper-cobalt-gold-silver-uranium, with mineralogical and textural similarities to the huge Olympic Dam copper-uranium-gold-silver deposit being mined in South Australia. This study demonstrates that the two are the same age at 1.6 Ga. Other mineralization in the area includes Early Proterozoic sedimentary-exhalative lead-zinc occurrences and Cretaceous and/or Tertiary base metal and rare gold-rich veins.

Fieldwork from 1992 to 1996 was funded by the Canada/Yukon Co-operation Agreement on Mineral Resource Development. Lithoprobe additionally supported the fieldwork in 1996. Logistical support was provided by the Canada/Yukon Geoscience Office, a jointly managed program with the Department of Indian Affairs and Northern Development as scientific authority, and the Yukon Department of Economic Development as administering agency.

Grant Abbott
Chief Geologist and Regional Manager
Exploration and Geological Services Division
Indian and Northern Affairs Canada

Shirley Abercrombie
Manager, Mineral Resources Program
Department of Economic Development
Yukon Government

Preface

Cette étude qui porte sur trois cartes à l'échelle de 1/50 000 présente une révision fondamentale de la géologie protérozoïque du nord du Yukon. Elle inclut une définition et une corrélation régionale des séquences stratigraphiques, des roches magmatiques et des déformations. Le profil géologique de cette région comprend maintenant le Protérozoïque précoce et quatre (au lieu de trois) séquences stratigraphiques protérozoïques qui sont le Supergroupe de Wernecke, le Groupe de Pinguicula, le Groupe de Hematite Creek et le Supergroupe de Windermere. La mise en place des dykes mafiques a été datée à 1,72 Ga et à 1,27 Ga. Un épisode majeur d'activité hydrothermale-phréatique est à l'origine des brèches intrusives de Wernecke à 1,6 Ga; une activité hydrothermale mineure a suivi à 1,38 et 1,27 Ga. Deux épisodes de déformation par contraction s'observent dans l'orogène de Racklan (avant 1,72 Ga), par la discordance du Groupe de Pinguicula sur le Supergroupe de Wernecke, et dans l'orogène de Corn Creek (1,0-0,76 Ga), par la discordance du Supergroupe de Windermere sur le Groupe d'Hematite Creek.

Cette étude offre la cadre géologique nécessaire à l'évaluation du potentiel minéral des régions cartographiques en question et d'autres grandes étendues géologiquement apparentées du nord du Yukon ainsi qu'à leur prospection. Les brèches de Wernecke recèlent des indices de cuivre-cobalt-or-argent-uranium, semblables par la minéralogie et la texture à l'énorme gisement de cuivre-uranium-or-argent d'Olympic Dam exploité en Australie-Méridionale. Selon l'étude, les deux gisements datent de 1.6 Ga. Parmi les autres minéralisations décelées dans la région, mentionnons des occurrences de plomb-zinc logées dans des roches sédimentaires exhalatives du Protérozoïque précoce et des filons de métaux communs et de rares filons aurifères du Crétacé et(ou) du Tertiaire.

Les travaux de terrain exécutés de 1992 à 1996 ont été financés dans le cadre de l'Entente Canada-Yukon sur l'exploitation minière. Lithoprobe a fourni un appui additionnel en 1996. Le Bureau de géoscience Canada-Yukon, programme géré conjointement avec le ministère des Affaires indiennes et le Développement du Nord, sur le plan scientifique, et le ministère de l'Expansion économique du Yukon, sur le plan administratif, a fourni un appui logistique.

Grant Abbott
Géologue en chef et gestionnaire régional
Division des services géologiques et d'exploration
Affaires indiennes et du Nord Canada

Shirley Abercrombie
Gestionnaire, Programme des ressources minérales
Ministère de l'Expansion économique
Gouvernement du Yukon

Contents

Preface/Préface

Abstract 1

Résumé 3

Introduction
- Location, physiography and access 5
- Acknowledgements 6

Stratigraphy
- Introduction 7
- Basement age and affinity 7
- Wernecke Supergroup 7
  - Introduction 7
  - Fairchild Lake Group (PFL) 12
  - Quartet Group (PQ) 13
  - Gillespie Lake Group (PGL) 13
  - Synthesis of Wernecke Supergroup deposition 14
- Slab Volcanics (PSv) 16
- Pinguicula Group (PP) 18
  - Introduction 18
  - Unit descriptions 20
- Hematite Creek Group (PHC) 21
  - Introduction 21
  - Stratigraphic description 22
  - Depositional history and significance 22
- Windermere Supergroup 25
  - Introduction 25
  - Units in the study area 25
  - Synthesis of depositional history 28
- Upper Proterozoic to Lower Paleozoic sedimentary rocks (PCs) 29
- Lower Paleozoic sedimentary rocks (CDs) 29
  - Description 29

Intrusive Rocks
- Wernecke Breccia (PWb) 31
  - Introduction 31
  - Physical and mineralogical characteristics 31
  - Style of breccia emplacement 33
  - Timing of brecciation and hydrothermal activity 36
  - Unconformable relationship with the Pinguicula Group 38
  - Model for brecciation and mineralization 39
- Igneous Rocks 39
  - Introduction 39
  - Bonnet Plume River intrusions (EPd) 39
  - Lamprophyre (EPl) 40
  - Bear River dykes (MPd) 41

Structural History
- Introduction 43
- Phase 1: SE-directed contraction (first event of Racklan Orogeny) 43
- Phase 2: Kink band formation (second event of Racklan Orogeny) 44
- Phase 3: Explosive brecciation (Wernecke Breccia development) 44
- Phase 4: Shearing, faulting 44
- Phase 5: West-directed contraction (Corn Creek Orogeny) 45
- Phase 6: Hayhook extension 45

Phase 7: Laramide contraction 46
Phase 8: Transpression along the Snake River Fault system 46
Phase 9: Extensional block faulting 47

Mineral Occurrences
Introduction 48
Sedimentary exhalative occurrences 48
Wernecke Breccia-related occurrences 48
Mineral enrichments 50
Characteristics of selected occurrences 51
Vein occurrences 52

Regional Synthesis
Introduction 53
Geological history 53
>1.73 Ga 53
1.73-1.59 Ga 53
1.59-1.27 Ga 54
1.27-0.8 Ga 54
800-550 Ma 55

References 56

Appendices 63
Appendix 1: Age determinations 64
Appendix 2: Neodymium model ages 65
Appendix 3: Geochemical analyses 66
Appendix 4: Assays 68

Figures
Figure 1. Location of the study area in northeastern Yukon 5
Figure 2. Simplified geology of the study area 8
Figure 3. Schematic thickness-stratigraphic columns of the study area 9
Figure 4. Time-stratigraphic column of the study area 10
Figure 5. Proterozoic geology of central Yukon and the western Northwest Territories 11
Figure 6. Wavy-laminated and cross-laminated siltstone of the Fairchild Lake Group 12
Figure 7. East-southeast-verging overturned syncline in upper Fairchild Lake Group 12
Figure 8. Easterly verging folds in upper Fairchild Lake Group and lower Quartet Group 12
Figure 9. Minor folds in thinly bedded dolostone of Gillespie Lake Group 13
Figure 10. Mud-crack casts in silty dolostone of the Gillespie Lake Group 13
Figure 11. Resistant dolostone (PGL) overlying 250-m-thick recessive shale succession (PGLs) within Gillespie Lake Group 13
Figure 12. Suggested correlation of Proterozoic successions in the Wernecke, Ogilvie, and Mackenzie Mountains, and the western Arctic 16
Figure 13. Slab volcanics (PSV) of the Slab mineral occurrence 17
Figure 14. Angular unconformity between basal Pinguicula Group (PPa) and underlying Gillespie Lake Group (PGL) 18
Figure 15. Pinguicula Group, units A, B, and C (PPa; PPb; PPc), underlain by the Quartet Group (PQ) 20
Figure 16. Clasts of zebra dolostone (Z) and micritic carbonate in intraclast conglomerate of Pinguicula Group unit C 21
Figure 17. Interbedded dolostone, shale, and micaceous sandstone in the stratigraphically middle part of the Hematite Creek Group 22
Figure 18. Thinly bedded dolostone and shale of the Hematite Creek Group 22
Figure 19. Geological map of the southeastern study area and a small region of map area 106C/11, to the south 23
Figure 20. Small stromatolites in dolostone beds near top of Hematite Creek Group 24
Figure 21. Angular unconformity between folded dolostone and shale of the Hematite Creek Group (PHC) and overlying Sayunei conglomerate (PSA) of the Windermere Supergroup 25
Figure 22. Subrounded clasts of siltstone and dolostone in Sayunei Formation 26

Figure 23. Lower Windermere Supergroup: 200-m-thick basal conglomerate of the Sayunei Formation (PSA) disconformably overlain by Profeit dolostone (PTP), 7 km south of Mt. Profeit 26
Figure 24. Geological map of the northeastern study area 27
Figure 25. Geological map of the southwestern study area 29
Figure 26. Angular unconformity between Lower Paleozoic carbonate (CDs) and underlying deformed Gillespie Lake Group (PGL) 30
Figure 27. Typical Wernecke Breccia (ca. 1.6 Ga) from the Pika occurrence 31
Figure 28. Clasts of quartz-albite syenite of the Bonnet Plume River intrusions in Wernecke Breccia 31
Figure 29. Angular fragments of fine-grained anorthosite (white) of the Bonnet Plume River intrusions in Wernecke Breccia (dark grey matrix) 31
Figure 30. Well-rounded cobble-sized clast of altered siltstone of the Wernecke Supergroup in Wernecke Breccia 32
Figure 31. Geological map of the central study area 34
Figure 32. Geological map of the north-central part of map 106C/14 35
Figure 33. Non-conformity between black shale of the basal Fifteenmile Group (PF) and Ogilvie Mountains breccia (PWb) 36
Figure 34. Geological relations at the Pika mineral occurrence, in the west-central part of map 106C/14 37
Figure 35. One of the Bear River mafic dykes (mPd; ca. 1.27 Ga) crosscutting steeply dipping dolostone beds of Gillespie Lake Group (PGL), south of Bear River. 41
Figure 36. Two parallel, vertically dipping, dioritic Bear River dykes (ca. 1.27 Ga) crosscutting tilted dolostone of Gillespie Lake Group (PGL), north of Tow mineral occurrence 41
Figure 37. Thrust relationship between Gillespie Lake Group (PGL; hanging wall) and Lower Paleozoic carbonate (CDs) 46
Figure 38. Mineral occurrences (Yukon Minfile, 1997) in the study area relative to major geological structures 49
Figure 39. Background metal concentrations in metasomatized but visibly non-mineralized samples of Wernecke Breccia 50

In Pocket

Geoscience Map 1998-9 106D/16
Geoscience Map 1998-10 106C/13
Geoscience Map 1998-11 106C/14

Abstract

The study area provides a clear record of the Proterozoic geological evolution of northern and central Yukon Territory. The area lies in the Wernecke Mountains of east-central Yukon, approximately 150 km north-northeast of the town of Mayo, and 20 km west of the Yukon-Northwest Territories border. The rocks record events of sedimentation, magmatism and deformation ranging in age from Early Proterozoic to Tertiary. Rocks of Early Proterozoic age predominate, but strata of Middle Proterozoic, Late Proterozoic, and Early Paleozoic ages are also abundant.

The oldest strata belong to the Wernecke Supergroup, which is divided into the Fairchild Lake Group (lowest), the Quartet Group (middle), and the Gillespie Lake Group (highest). These strata form two clastic-to-carbonate grand cycles, apparently recording two periods of subsidence and basinal infilling. Stratigraphic thickness is estimated at about 13 km, inferring deposition on a passive continental margin or intracratonic rift basin.

The Wernecke Supergroup was crosscut by dioritic to syenitic dykes and stocks (ca. 1.72 Ga), and undated biotite lamprophyre, folded and kinked during Racklan Orogeny, and then intruded by the hydrothermal-phreatic Wernecke Breccias (ca. 1.6 Ga). The relative timing between Racklan orogenesis and the igneous events remains uncertain. The ca. 1.72 Ga intrusions, herein named the Bonnet Plume River intrusions, may be correlative with a newly recognized stratigraphic unit, the Slab volcanics. The volcanic rocks sit as a 250-m-thick megaclast in one of the Wernecke Breccia zones, at the Slab mineral occurrence. The Wernecke Breccias and adjacent country rocks have been variably metasomatized and locally mineralized. The breccias are coeval with similar fragmental and metasomatic rocks at the Olympic Dam mine, in South Australia, and may have been generated in the same general magmatic and hydrothermal regime.

The Pinguicula Group unconformably overlies the Wernecke Supergroup. The Pinguicula Group contains three formations and consists of mainly siltstone and shale overlain by dolostone, some of which displays prominent zebra texture. The unconformity truncates not only folds, foliations, and kink bands in the Wernecke Supergroup, but also the Bonnet Plume River intrusions and zones of Wernecke Breccia. These relations confirm that Racklan Orogeny was an Early Proterozoic event, and constrain the age of the Pinguicula Group to <1.6 Ga. Pinguicula strata range up to 3.5 km thick, and were apparently deposited in rift basins produced in a cycle of modest crustal extension associated with emplacement of the nearby Hart River sills (ca. 1.38 Ga). One of the sills crosscuts the lowest formation of the Pinguicula Group.

The dioritic Bear River dykes (ca. 1.27 Ga) intrude the Gillespie Lake Group and have the same age as the Mackenzie dyke swarm in cratonic rocks of the Northwest Territories. Dyke emplacement was followed by sedimentary deposition of the Hematite Creek Group, formerly the upper part of the Pinguicula Group. The Hematite Creek Group, which is up to 1 km thick, contains abundant detrital zircon (beyond the study area) and muscovite grains (within the study area) of Grenvillian age. The grains range as young as ca. 1033 Ma, constraining Hematite Creek Group deposition to no earlier than the late Middle Proterozoic. The Hematite Creek Group, and several other broadly correlative successions extending from Alaska to the Northwest Territories, apparently received sediment from the Grenville orogen via trans-continental river systems.

The Windermere Supergroup unconformably overlies the Hematite Creek Group in the study area. The deformational event recorded by this unconformity is herein named the Corn Creek Orogeny, and represents the second of two important periods of Proterozoic contraction in Yukon. The Windermere Supergroup, which is about 2.5 km thick in the study area, displays prominent facies changes involving glacial, conglomeratic, silty and dolomitic deposits. Deposition began sometime after ca. 755 Ma and ended sometime after ca. 600 Ma, spanning the Sturtian and Varangian glaciations. The facies changes in the Windermere are abrupt and imply a protracted history of synsedimentary crustal extension, possibly generated during separation of the North American and Australian continents.

Upper Proterozoic to Lower Paleozoic strata overlie the Windermere succession in the eastern part of the study area. In the west, however, Lower Paleozoic rocks lie directly on the Wernecke Supergroup, revealing a prominent lacuna of about 1 billion years. The Paleozoic strata represent mainly a carbonate bank environment – part of Mackenzie Platform, which extends from the Northwest Territories to western Yukon.

All geological units in the study area were folded during the Cretaceous to Early Tertiary Laramide orogeny. In the northeastern corner of the study area, dextral transpression along the Snake River Fault, probably in the Early Tertiary, produced southwest-verging folds and thrust faults in Upper Proterozoic and Lower Paleozoic rocks. The degree to which strike-slip deformation in the Tertiary and possibly earlier times has affected the structural geometry of the study area is

uncertain, but may be responsible for the prominent set of north- to northwest-trending faults in the northern Wernecke and Richardson mountains.

Mineral occurrences are numerous and belong to three general types. Sedimentary exhalative Pb-Zn occurrences are the oldest, and are restricted to the Gillespie Lake Group in the south-central part of the map area. Hydrothermal disseminated and vein Cu-Co-Au-Ag-U mineralization related to Wernecke Breccias are widespread, and are metallogenetically and texturally similar to those at the Olympic Dam deposit in South Australia. Base metal and rare gold-rich veins are the youngest occurrences. They crosscut geological units as young as the Windermere Supergroup, and may be as young as Tertiary. The veins are concentrated in the eastern part of the map area and appear to form the northern end of a long belt of similar occurrences.

Résumé

La région étudiée offre une bonne vue d'ensemble de l'évolution géologique du Protérozoïque dans le nord et le centre du Yukon. Elle est située dans les monts Wernecke, dans le centre-est du Yukon, à quelque 150 km au nord-nord-est du village de Mayo et à 20 km à l'ouest de la frontière entre le Yukon et les Territoires du Nord-Ouest. On y observe des manifestations de sédimentation, de magmatisme et de déformation dont l'âge s'échelonne du Protérozoïque inférieur au Tertiaire. Les roches du Protérozoïque inférieur sont prédominantes, mais les couches du Protérozoïque moyen et supérieur ainsi que du Paléozoïque sont également abondantes.

Les couches les plus anciennes font partie du Supergroupe de Wernecke, lequel est reparti en trois groupes, soit les groupes inférieur de Fairchild Lake, intermédiaire de Quartet et supérieur de Gillespie Lake. Ces couches comportent deux cycles sédimentaires complets allant des roches détritiques aux roches carbonatées, et semblent montrer deux périodes de subsidence et de remplissage de bassin. Leur épaisseur totale de quelque 13 km laisse supposer que la sédimentation s'est produite sur une marge continentale passive ou dans un bassin d'effondrement.

Le Supergroupe de Wernecke a été traversé par des dykes et des stocks de composition dioritiques à syénitiques (env. 1,71 Ga) et de lamprophyre à biotite (non-daté), puis déformé par des plis et des kinks au cours de l'Orogenèse de Racklan, et enfin pénétré par les brèches hydrothermales phréatiques de Wernecke (env. 1,6 Ga). La datation relative entre l'Orogénèse de Racklan et les épisodes intrusifs demeure indéterminée. Les intrusions datant d'environ 1,71 Ga, nommés ici intrusions de Bonnet Plume River, seraient en corrélation avec une unité stratigraphique nouvellement reconnue, soit les roches volcaniques de Slab. Ces roches volcaniques se présentent sous la forme d'un mégaclaste de 250 m d'épaisseur au sein d'une des zones bréchiques de Wernecke, à l'indice Slab. Les Brèches de Wernecke et les roches encaissantes adjacentes ont subi divers degrés de métasomatisme et sont, par endroit, minéralisées. Elles sont contemporaines des roches fragmentées et métasomatiques identiques, rencontrées dans la mine Olympic Dam, en Australie-Méridionale; elles ont vraisemblablement été formées par le même régime magmatique et hydrothermal général.

Le Groupe de Pinguicula repose en discordance sur le Supergroupe de Wernecke. Il renferme trois formations et est composé principalement de siltstones et de shales recouverts de dolomies, dont certaines montrent une texture rubanée. La discordance a tronqué non seulement les plis, les schistosités et les kinks du Supergroupe de Wernecke mais aussi les intrusions de Bonnet Plume River et les zones bréchiques de Wernecke. Ces relations confirment l'âge protérozoïque inférieur de l'Orogenèse de Racklan et situent l'âge du Groupe de Pinguicula à <1,6 Ga. Les couches de Pinguicula, qui atteignent jusqu'à 3,5 km d'épaisseur, auraient été déposées dans des bassins d'effondrement formés lors d'une phase d'extension crustale de faible amplitude associée à la mise en place des filons-couches avoisinants de Hart River (env. 1,38 Ga). Un de ces filons-couches recoupe la formation inférieure du Groupe de Pinguicula.

Les dykes dioritiques de Bear River (env. 1,27 Ga) ont pénétré le Groupe de Gillespie Lake et sont du même âge que le réseau de dykes de Mackenzie se rencontrant dans les roches cratoniques des Territoires du Nord-Ouest. Cet événement a été suivi par la sédimentation du Groupe d'Hematite Creek, qui correspondait anciennement à la partie supérieure du Groupe de Pinguicula. Le Groupe d'Hematite Creek, dont l'épaisseur peut atteindre 1 km, renferme d'abondants zircons détritiques (au-delà de la région étudiée) et des grains de muscovite détritique (au sein de la région étudiée) d'âge grenvillien. L'âge minimum de ces grains est d'environ 1 033 Ma; le dépôt du Groupe d'Hematite Creek ne s'est donc pas produit avant le Protérozoïque moyen tardif. Ce groupe et plusieurs autres successions généralement corrélatives, qui s'étendent de l'Alaska jusqu'aux Territoires du Nord-Ouest, semblent avoir été alimentés en sédiments de l'orogenèse grenvillienne par le biais de systèmes fluviaux transcontinentaux.

Dans la région d'étude, le Supergroupe de Windermere repose en discordance sur le Groupe d'Hematite Creek. La déformation qui s'inscrit dans cette discordance porte le nom d'Orogenèse de Corn Creek; elle représente la seconde des deux plus importantes périodes de contraction protérozoïque au Yukon. Dans la zone d'étude, le Supergroupe de Windermere, d'environ 2,5 km d'épaisseur, montre des changements marqués de faciès mettant en cause des dépôts glaciaires, conglomératiques, silteux et dolomitiques. Le début de la sédimentation est postérieur à environ 755 Ma et la fin est postérieure à environ 600 Ma; elle englobe les glaciations sturtiennes et varangiennes. Dans le Supergroupe de Windemere, les changements de faciès sont brusques, traduisant une longue phase d'extension synsédimentaire de la croûte, qui a vraisemblablement débuté lors de la séparation des continents nord-américain et australien.

Dans la partie orientale de la région d'étude, les couches du Protérozoïque supérieur au Paléozoïque inférieur recouvrent la succession de Windermere. Toutefois, dans la partie occidentale, les roches du Paléozoïque inférieur reposent directement sur le Supergroupe de Wernecke, révélant un hiatus important d'environ 1 Ga. Les couches du Paléozoïque représentent principalement un environnement de plate-forme carbonatée, soit une partie de la plate-forme de Mackenzie, qui s'étend des Territoires du Nord-Ouest jusqu'à l'ouest du Yukon.

Toutes les unités géologiques de la région étudiée ont été plissées au cours de l'orogenèse laramienne, du Crétacé au Tertiaire inférieur. Dans l'angle nord-est de la région d'étude, une transpression dextre le long de la Faille de Snake River, qui s'est sans doute produite au cours du Tertiaire inférieur, a formé des plis et des failles de chevauchement de vergence

sud-ouest dans les roches du Protérozoïque supérieur et du Paléozoïque inférieur. On ne sait pas vraiment jusqu'à quel point la géométrie structurale de la région d'étude a été affectée par la déformation à rejet horizontal d'âge tertiaire et sans doute d'âge plus ancien. On croit toutefois que cette déformation pourrait être la cause d'importantes failles d'orientation nord et nord-ouest dans la partie septentrionale des monts Wernecke et dans les monts Richardson.

Les nombreuses occurrences de minéraux appartiennent à trois grands types. Les occurrences de sulfures exhalatifs sédimentaires à Pb-Zn sont les plus anciennes; elles sont confinées au Groupe de Gillespie Lake situé dans le centre-sud de la région cartographiée. Les dissémination et les veines hydrothermales (Cu-Co-Au-Ag-U) apparentées aux Brèches de Wernecke apparaissent sur de grandes étendues. Du point de vue métallogénique et textural, ces occurrences sont semblables à celles du gisement Olympic Dam, en Autralie-Méridionale. Les veines de métaux communs et de rares veines aurifères, sont les occurrences les plus récentes. Elles recoupent des unités géologiques aussi jeunes que celles du Supergroupe de Windermere, et pourraient être aussi récentes que le Tertiaire. Ces veines, concentrées dans la partie orientale de la région cartographiée, semblent former l'extrémité septentrionale d'une longue zone d'occurrences similaires.

Introduction

This report describes the geology of three adjoining map areas in the Wernecke Mountains of northeastern Yukon (106D/16, 106C/13 and 106C/14), collectively referred to as the study area (Fig. 1). The main goals of this report are to clarify the geological history of the study area, to place mineral occurrences therein in an improved geological context, and to relate these findings to the geology of the surrounding region. This information is intended to enhance the effectiveness of mineral exploration programs, to provide a basis for decisions on land use, and to improve our understanding of the early geological evolution of Yukon Territory.

Coloured geological maps of the study area, published at 1:50,000 scale (Thorkelson and Wallace, 1998a, 1998b, 1998c), are essential companions of this report. Several black-and-white maps are included on the pages of the report itself (inset maps on Fig. 1), but many geological details are displayed only on the large-format coloured maps.

The author carried out geological investigations in the study area as Project Geologist for the Canada/Yukon Geoscience Office (1992-1995), and as Assistant Professor of Earth Sciences at Simon Fraser University (1995-1999). During the first three years of the project, Carol A. Wallace ably assisted the author. The investigations were built on a platform of previous publications from government agencies, academic researchers, and mineral exploration companies. The most valuable publication for this program of study was the preliminary map of R.T. Bell (1986a). Work was augmented by collaboration with colleagues in government and academe, and with geologists from several companies involved in mineral exploration programs in the Wernecke Mountains. Geological studies in the region by the author and collaborators remain in progress.

Fieldwork was carried out from helicopter-supported two-person camps for two months in each summer of 1992, 1993 and 1994. A preliminary geological map and report were released in the winter following each of these field seasons (Thorkelson and Wallace, 1993a,b; 1994a,b; 1995a,b). In each of the summers of 1995 and 1996, fieldwork was limited to about ten days, and no new government reports were released. In 1997, 1998, and 1999, summary articles were published in annual Lithoprobe volumes for the SNORCLE transect. Geochemical and geochronological data were collected during the program but few data were included in any of the reports and articles. In this report, a large amount of geochemical and geochronological data is included as appendices (Tables A1-1, A2-1, A3-1 and A4-1). Topographic maps at 1:50,000 scale, produced by the Surveys and Mapping Branch, Natural Resources Canada, formed the base for the geological maps.

Location, physiography and access

The study area consists of map areas 106D/16, 106C/13 and 106C/14. It is located in northeastern Yukon Territory approximately 110 km north of the Keno Hill mining district, 150 km northeast of the town of Mayo, and 250 km east-northeast of Dawson City (Fig. 1; Thorkelson and Wallace,

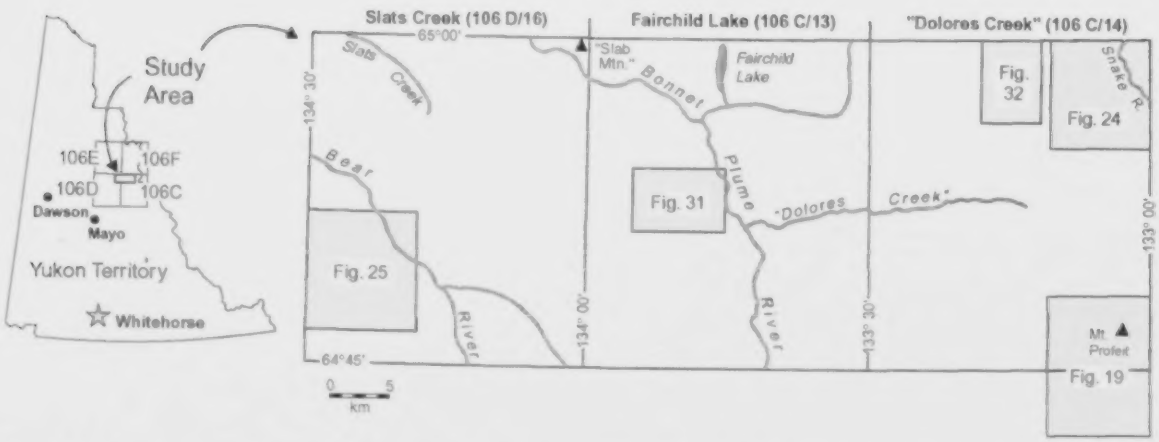

Figure 1. Location of the study area in northeastern Yukon, covering three 1:50,000 scale map areas. Inset maps are included in this report as figures.

1999). The eastern edge of the study area lies only 17 km west of the Northwest Territories. The map areas, each of which is approximately 24 km wide (east-west) and 28 km long (north-south), combine for a total area of nearly 2000 km^2. The area is remote and mountainous, with peaks rising to over 2200 m (7000 ft.) from valleys as low as 600 m (2000 ft.). Forming part of the Arctic watershed, the area is drained by the Wind, Bear, Bonnet Plume, and Snake rivers which drain into the Peel River, which runs into the Mackenzie River, which flows into the Arctic Ocean.

The area may be accessed by helicopter, or by small fixed-wing aircraft. Three airstrips are present, one alongside the Bear River (central 106D/16), one beside the Bonnet Plume River (northeastern corner of 106D/16), and the third near the headwaters of "Dolores Creek"[1] (central 106C/14). Presently, the strips by the Bear and Bonnet Plume rivers are in good condition, whereas the one at Dolores Creek is in poor condition. Float planes can land on Fairchild Lake (106C/13), on "Glacier Lake" in the east-central part of map 106C/13, and on a small unnamed lake in the southern part of map area 106C/14. Under optimal conditions, floatplanes may also be able to land on sections of the various rivers. Access to nearby regions is possible by float plane to Gillespie Lake and Pinguicula Lake, to the south of the study area and the Quartet Lakes, northwest of the study area. In the winter, additional access is possible by track-drive equipment along a crude winter road known as the Wind River trail, which begins at the Keno Hill mining district, north of Mayo.

Acknowledgements

The project was principally funded by the Canada/Yukon Geoscience Office (1992-1996), through an Economic Development Agreement between the Canadian and Yukon governments. Additional funds were provided in 1996 by a Lithoprobe grant to the author at Simon Fraser University.

The author thanks Carol Wallace for reliable and enthusiastic geological research and assistance; Grant Abbott for framing the research program, and for participating in joint field excursions; Charlie Roots for guidance and access to unpublished data; Jim Mortensen for geochronology and reminiscence; Rob Creaser for geochronology and tracer isotope analysis; Vicki McNicoll, Paul Layer and Michael Villeneuve for isotopic age determinations; Tony Fallick and Richard Taylor for stable isotope analysis; Andrew Conly for mineral compositions and paragenesis; and Stephen Johnston, Craig Hart, Don Murphy, Ted Fuller, John Kowalchuk, Julie Hunt, Danièle Héon, Mike Stammers, David Caulfield, Mark Baknes, Murray Jones, Randy Vance, Tom Bell, Don Norris, Dick Bell, Bob Thompson, Hu Gabrielse, John Wheeler, Gerry Ross, Peter Mustard, Don Cook, Fred Cook, Geri Eisbacher, Rob Rainbird, Tony LeCheminant, Johnny Winter, Bob Lane, Tom Pollock, Doug Eaton, Rob Carne, Roger Hulstein, Sunil Gandhi, Glen Shevchenko, and several others for sharing geological ideas and information on the geology of northwestern Canada. Will VanRanden is thanked for computer drafting and patience. Pat Johnstone, Katrin Breitsprecher and Sheryl Beaudoin provided technical support and assistance with manuscript preparation at Simon Fraser University. Logistical support and courtesies extended to us in the field by the Newmont-Westmin-Pamicon-Equity joint venture, and by BHP Minerals, significantly reduced the costs and increased the effectiveness of the field program. Don Cook, Don Norris and Diane Emond reviewed the manuscript and provided numerous suggestions, which led to substantial improvements. The author remains singularly responsible for any errors, omissions, or shortcomings of this report.

[1] This is an informal name, however for brevity, use of quotes is omitted in the rest of the text.

Stratigraphy

Introduction

Sedimentary successions dominate the bedrock geology of the study area (Figs. 2, 3). They range in age from >1.72 Ga (Early Proterozoic) to ca. 0.4 Ga (Early Paleozoic), spanning over a quarter of Earth history (Fig. 4). From oldest to youngest, the successions include the Wernecke Supergroup, the Pinguicula Group, the Windermere Supergroup, and Paleozoic rocks of Mackenzie platform. The cumulative thickness of these strata is about 22 km. Deposition occurred in environments ranging from stable platform to rift basin. Sedimentation was punctuated by periods of uplift and erosion, and in some cases by deformation, magmatism and mineralization. Although the region was affected by at least three events of contractional deformation, including Mesozoic to Early Cenozoic Cordilleran orogenesis, it remained inboard from convergent plate-edge processes such as arc magmatism and terrane obduction.

A framework for understanding Proterozoic successions in western North America was established by Young et al. (1979) who recognized three major divisions: Sequence A (~1.7 to ~1.2 Ga), Sequence B (~1.2 to ~0.8 Ga), and Sequence C (~0.8 to 0.57 Ga; shown on the inset map in Fig. 5). The sequences were shown to be separated by major unconformities. Sedimentary successions from one region were considered broadly correlative with those of the same sequence in another region. The utility of this framework has been most enduring for Sequence C, as correlations within this division have been increasingly supported by subsequent geological studies. Some correlations within Sequences A and B have been strengthened by recent work, while others have been re-assigned or discarded. This outcome is not surprising, as Sequences A and B together span about 1 billion years.

In the study area, Sequence A is represented by the Wernecke Supergroup, the Slab volcanics, and the Pinguicula Group; Sequence B is represented by the Hematite Creek Group; and Sequence C is represented by the Windermere Supergroup (Fig. 5). The sequences are well exposed, and separated from one another by prominent angular unconformities (Eisbacher, 1978). The Slab volcanic succession is a newly defined unit, which is shown to lie between the Wernecke Supergroup and the Pinguicula Group. Strata formerly called the Pinguicula Group and considered to belong to Sequence B have been divided into two parts. The lower part retains the name Pinguicula Group but has been re-assigned to Sequence A. The upper part is herein called the Hematite Creek Group, and remains in Sequence B.

Basement age and affinity

Crystalline basement to the sedimentary successions is nowhere exposed. Therefore, the age of the crust beneath the study area is unknown, and may range from Early Proterozoic to Archean. The combination of thick sedimentary successions and an overall continental setting infers that the region is underlain by attenuated continental crust, most probably a thinned, westward continuation of the North American craton. Prior to the attenuation, the last major tectonic event to affect this part of the North American craton probably occurred during convergence and suturing of Precambrian terranes along the Fort Simpson, Wopmay and Trans-Hudson orogenic belts between 1.84 and 2.0 Ga (Hoffman, 1989; Villeneuve et al., 1991). Consequently, at about 1.84 Ga, the North American craton is likely to have extended westward beyond its current Cordilleran limit, and may have been sutured to the craton of another continent. Seismic reflection profiles to the east, extending from the Fort Simpson magmatic arc to the Slave craton suggest that the Proterozoic sequences were deposited on a westward continuation of the ca. 1.84 Ga Fort Simpson magmatic terrane (Cook et al., 1998). Following deposition, lithospheric extension and crustal attenuation in Yukon and adjacent areas probably signify separation of cratonic North America from continental crust to the west. The rifting produced deep intracratonic basins, and ultimately a passive margin. The continental mass which separated from North America was probably Early Proterozoic to Archean crust of southern to eastern Australia (Eisbacher, 1985; Bell and Jefferson,1987; Ross et al., 1992).

Wernecke Supergroup

Introduction

The Wernecke Supergroup is the oldest exposed succession in the study area, and is also the oldest non-crystalline rock in the Canadian Cordillera. The succession was first mapped by Wheeler (1954) and formally described and named by Delaney (1981). Eisbacher (1981) referred to the succession as the Wernecke Assemblage, but Delaney's report is considered the definitive work on the subject and his terminology is followed here. The Wernecke Supergroup crops out as numerous inliers spanning nearly the entire width of Yukon, mainly between latitudes 64° and 66°N (Fig. 5). Combined field and geochronological data indicate that the Wernecke Supergroup was deposited prior to ca. 1.725 Ga (see section on the Bonnet Plume River intrusions). These strata are among the first indicators of the geological environment in western Canada following widespread Early Proterozoic cratonization of ancestral North America, a crustal region considered by Rogers (1996) to constitute part of the Precambrian continent Arctica.

The Wernecke Supergroup is the most abundant succession in the study area. It consists of three main components: the Fairchild Lake Group, the Quartet Group, and the Gillespie Lake Group (Figs. 2, 3, 4). Delaney (1981) estimated the thickness of the Wernecke Supergroup to be at least 14 km, similar to the 12.9 km minimum estimate made in this report. Precise measurement of unit thickness is hampered by several phases of deformation that have produced strain varying from large folds and faults to cleavage, kink-banding and crenulation. Given these uncertainties, the estimates given

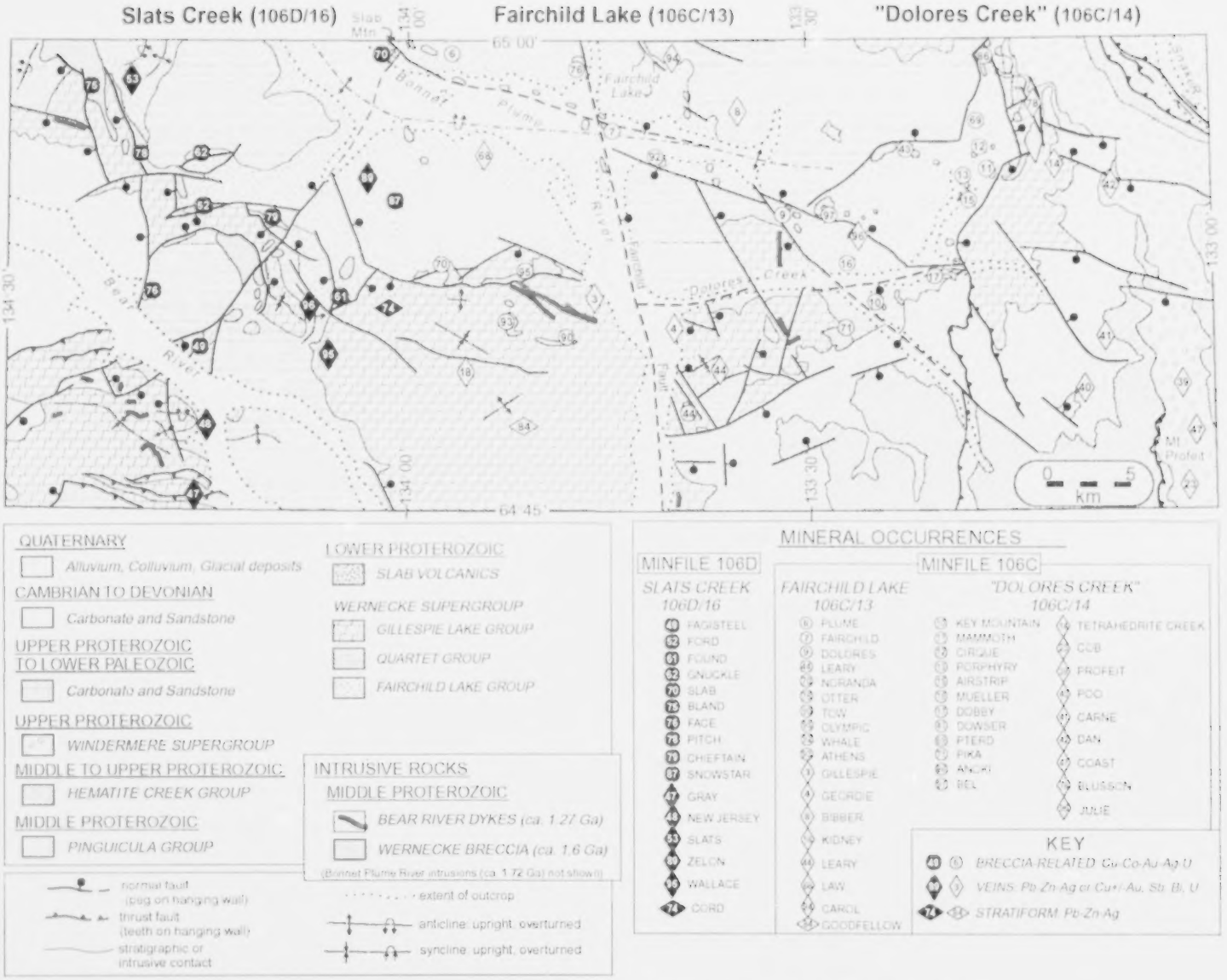

Figure 2. Simplified geology of the study area showing main geological units and mineral occurrences (Yukon Minfile, 1997).

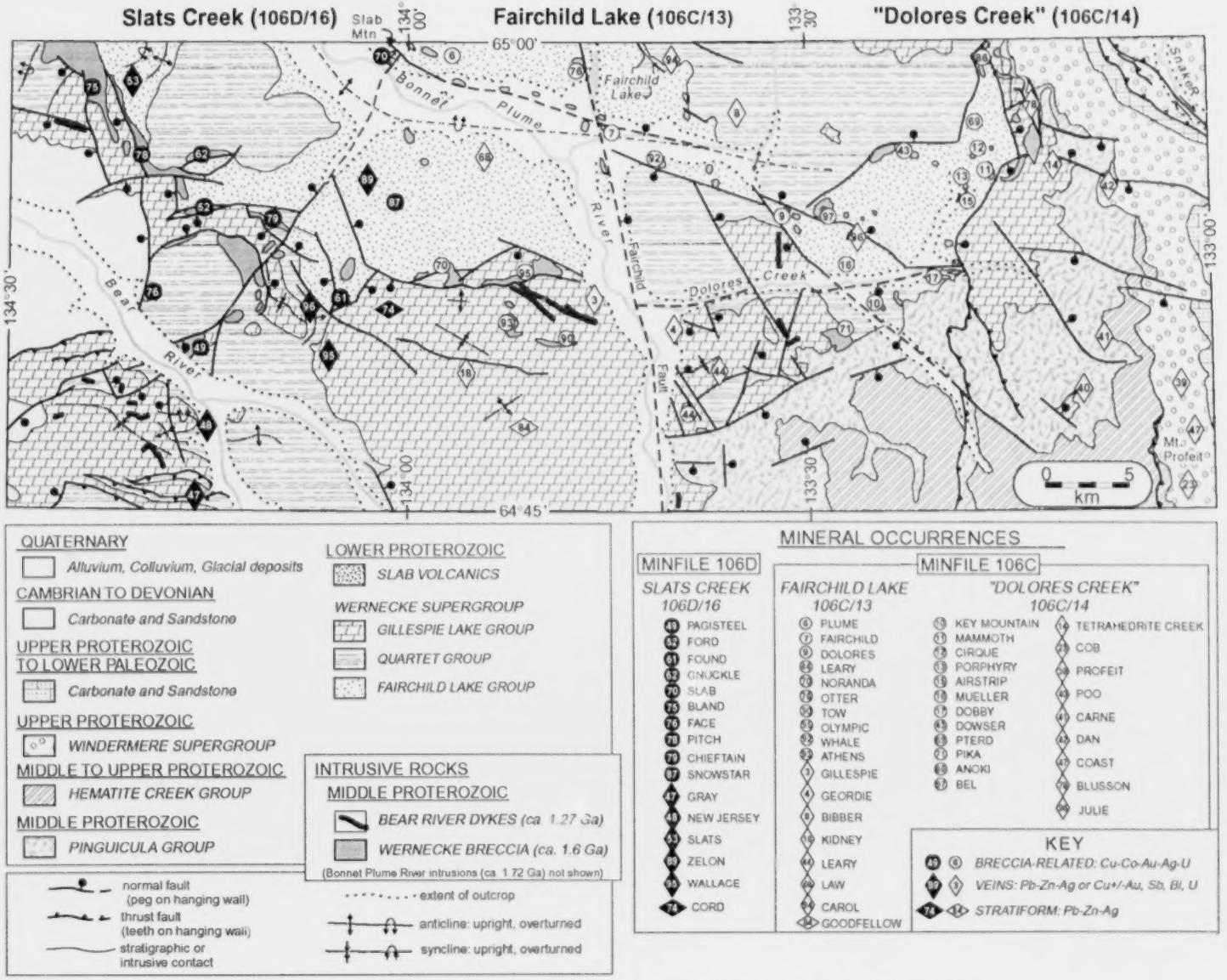

Figure 2. *Simplified geology of the study area showing main geological units and mineral occurrences (Yukon Minfile, 1997).*

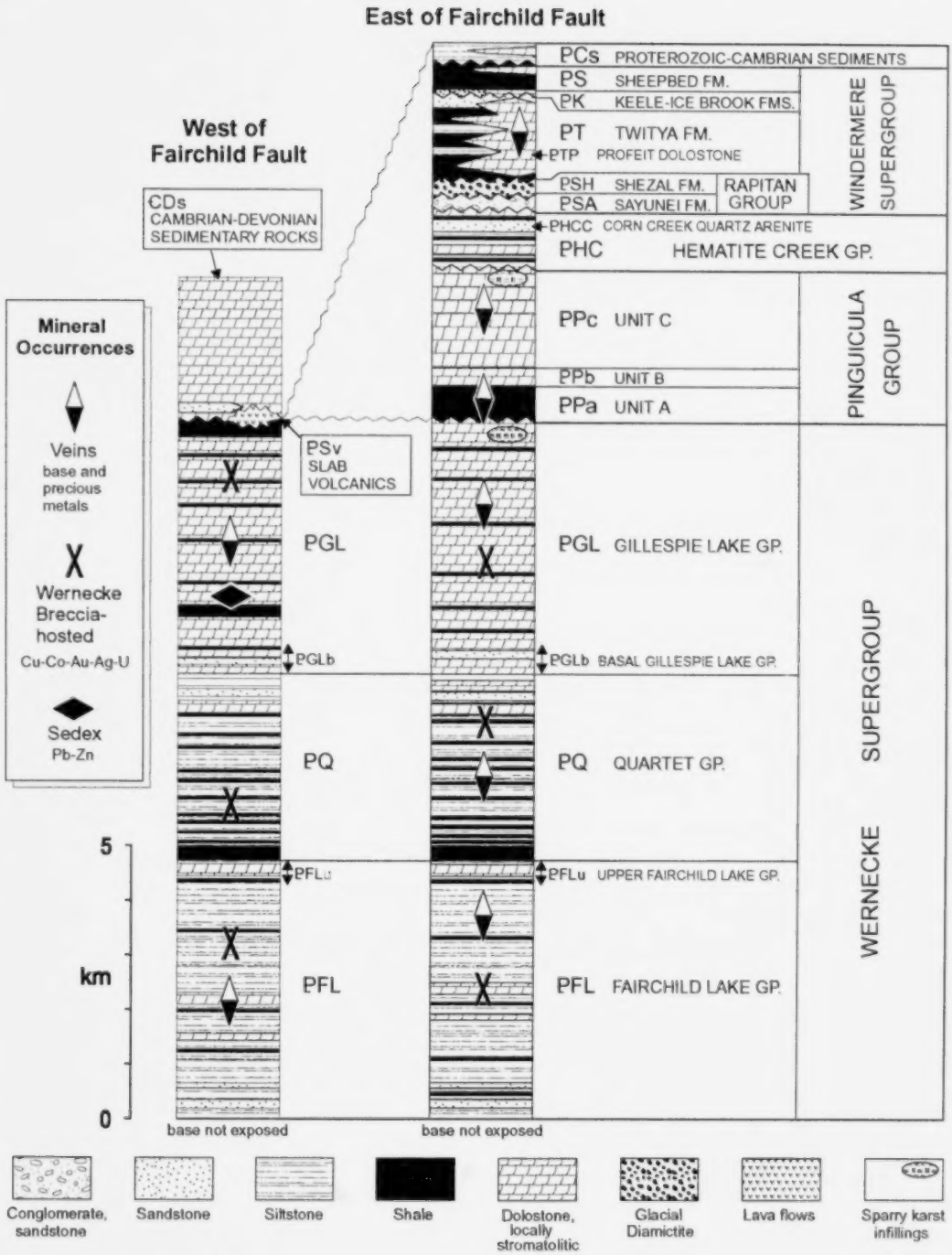

Figure 3. *Schematic thickness-stratigraphic columns of the study area, showing main lithologies and generalized positions of mineral occurrence types (for actual mineral occurrence locations, see Fig. 2). About 7 km of Precambrian strata that are exposed east of the Fairchild Fault (units PPa to PCs) are cut out beneath the sub-Paleozoic unconformity to the west of the Fairchild Fault.*

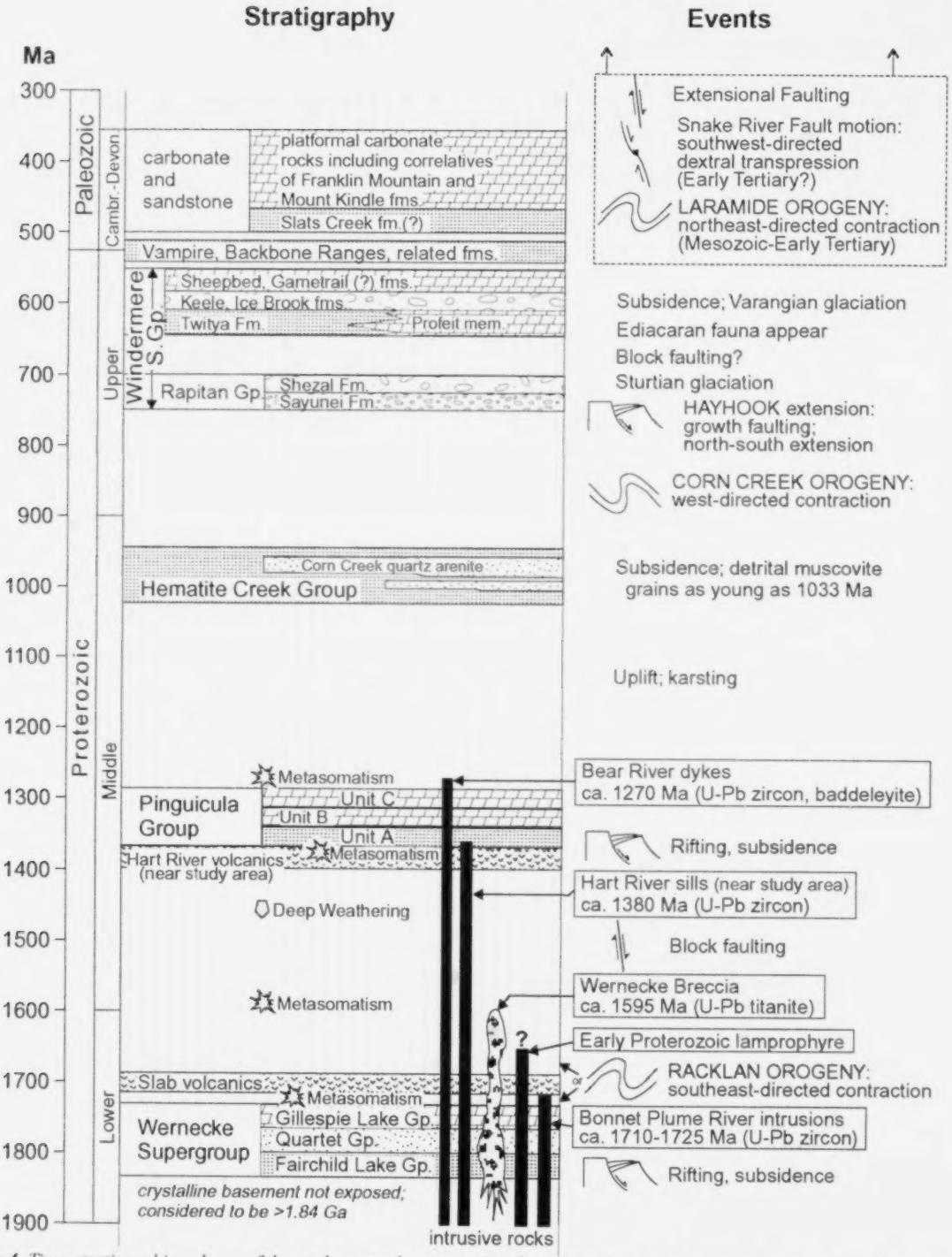

Figure 4. *Time-stratigraphic column of the study area, showing major depositional, intrusive, metasomatic, and deformational events.*

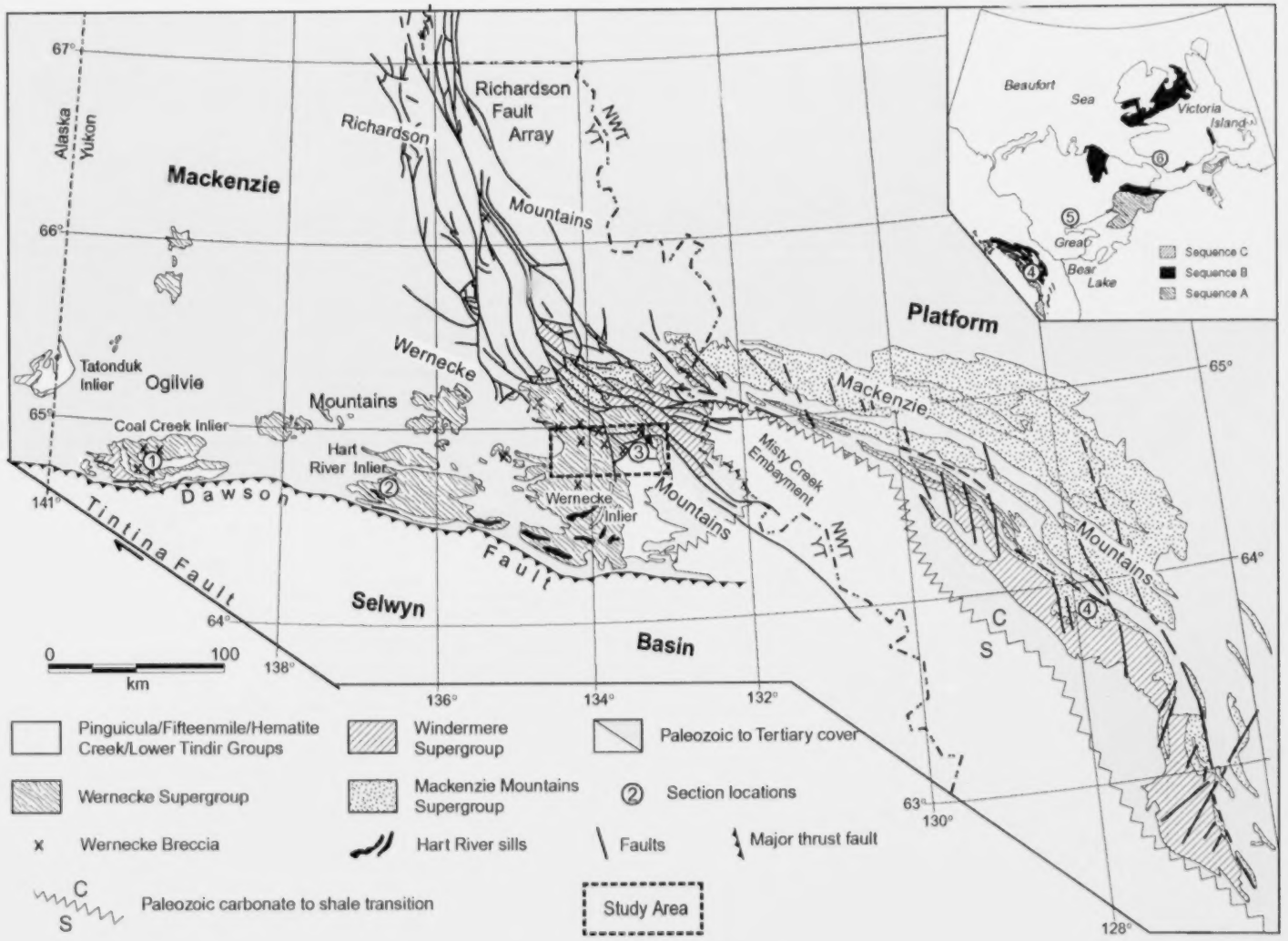

Figure 5. *Proterozoic geology of central Yukon and the western Northwest Territories, showing location of the study area in the Wernecke Mountains. Modified from Abbott (1997). Inset shows relevant geological features of the western Arctic.*

herein are considered to be within 20% of the original stratigraphic thickness.

Fairchild Lake Group (PFL)

The Fairchild Lake Group is the oldest non-crystalline rock in the Canadian Cordillera. The base of the group is not exposed, but it may rest directly on crystalline basement from which it has been structurally decoupled during contractional deformation. In this report, it has been mapped as a single unit (PFL) except where an upper unit (PFLu) has been distinguished. Below the upper unit, Fairchild Lake Group strata consist of mainly greenish grey-weathering, parallel- to cross-laminated siltstone (Fig. 6), dark shale, and light grey-weathering, very fine-grained sandstone, with minor brown-weathering dolostone.

The thickest section of sub-PFLu strata, estimated at 4.6 km thick, is on the overturned limb of a south-verging anticline southwest of Fairchild Lake (Fig. 2). The overturned nature of this section is indicated by truncations in cross laminations, and bedding which dips more steeply than cleavage. The upper Fairchild Lake Group (PFLu), about 200 m thick, is characterized by alternating successions of platy, brown- to buff-weathering dolostone and black-weathering siltstone (Fig. 7). A 10-m-thick, locally conspicuous white-weathering, medium-grained, recrystallized limestone unit near the top of the succession serves as a regional marker unit (Fig. 8). In Delaney's (1981) nomenclature, the lower Fairchild Lake Group succession is subdivided into units F-1 to F-4, and the upper Fairchild Lake Group is called unit F-TR. Structural complications, probable facies changes, and the wide spacing of traverses in this regional mapping program precluded consistent application of Delaney's nomenclature.

In locations of high strain, generally in tight folds, sedimentary rocks have been transformed into slate, phyllite, or fine-grained chloritoid- or garnet-porphyroblastic muscovite-chlorite-quartz schist. Commonly, the penetrative foliation has been deformed into kink bands. These fabrics are best developed between the Slab mineral occurrence (Fig. 2; Yukon Minfile, 1997) and Fairchild Lake, where Wernecke Breccia (ca. 1595 Ma) crosscuts them. Muscovite-bearing fine-grained schist from near the Slab and Plume occurrences (Yukon Minfile, 1997) was dated by the $^{40}Ar/^{39}Ar$ method at the University of Alaska (Table A1-1; P.W. Layer, pers. comm., 1996). Plateau ages for the samples are 980 ± 15 Ma and 833 ± 17 Ma. These dates are significantly younger than the age of the breccias, which crosscut them, and must be considered as ages of cooling rather than the times of schist formation. Their integrated ages are somewhat older than the plateau ages because the Ar that was released at high temperatures was isotopically "older." In the final step of Ar heating, the sample with a plateau age of ca. 980 Ma released Ar with an isotopic age of 1775 ± 132 Ma.

Minor occurrences of tuffaceous rock in the Fairchild Lake Group northwest of the study area were reported by

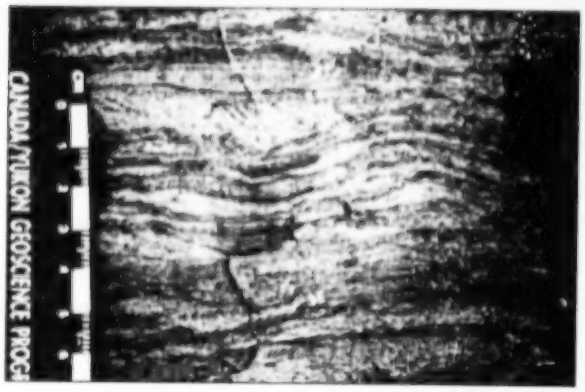

Figure 6. *Wavy-laminated and cross-laminated siltstone of the Fairchild Lake Group.*

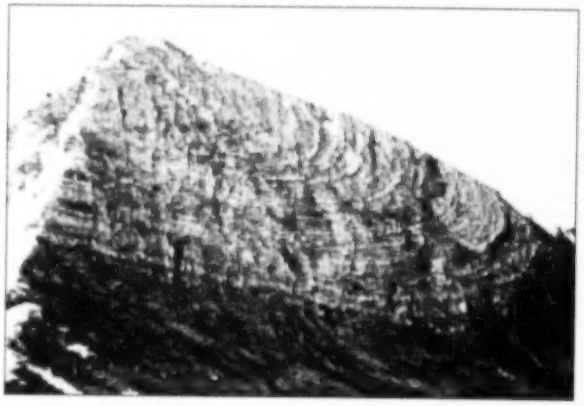

Figure 7. *East-southeast-verging overturned syncline in upper Fairchild Lake Group in northwestern part of study area. Fold is considered to have developed during Racklan Orogeny. View to the west-southwest.*

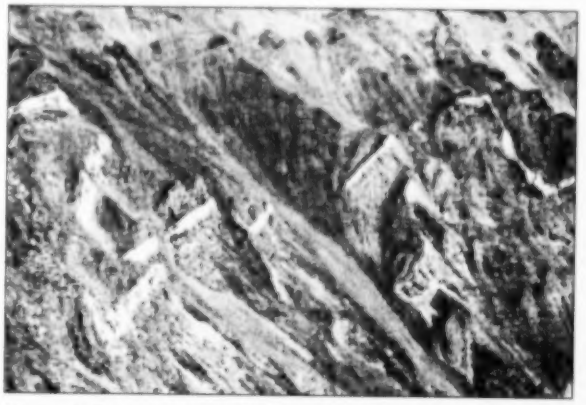

Figure 8. *Easterly verging folds in upper Fairchild Lake Group and lower Quartet Group delineated by a 10-m-thick white-weathering dolostone marker unit of the upper Fairchild Lake Group in northeastern part of study area. View to the north.*

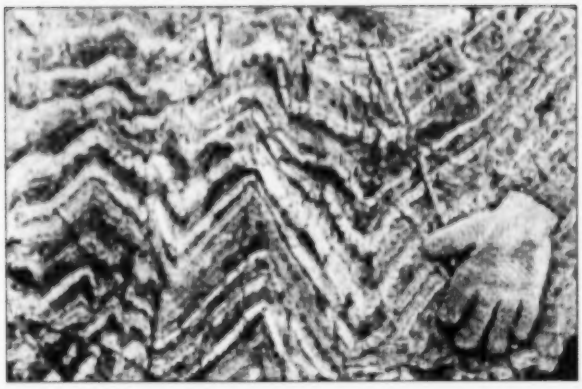

Figure 9. *Minor folds in thinly bedded dolostone of Gillespie Lake Group, west of the Bonnet Plume River, south of the Tow mineral occurrence (shown in Fig. 2.).*

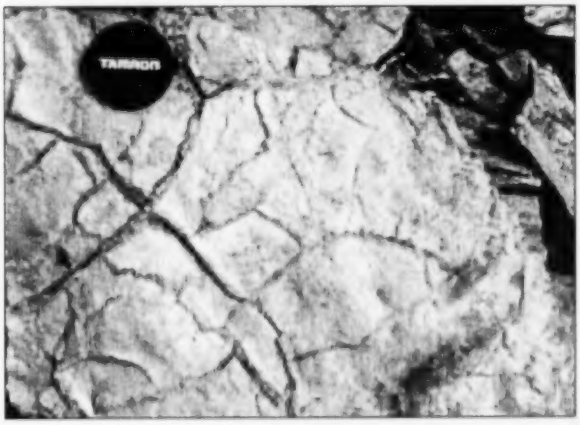

Figure 10. *Mud-crack casts in silty dolostone of the Gillespie Lake Group.*

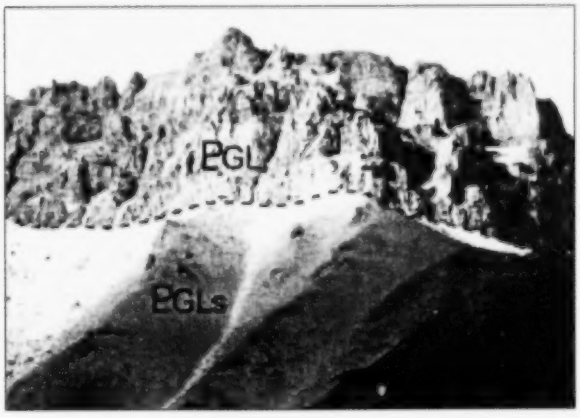

Figure 11. *Resistant dolostone (PGL) overlying 250-m-thick recessive shale succession (PGLs) within Gillespie Lake Group, northeast of the Goodfellow mineral occurrence (Fig. 2). View to the north.*

Hulstein (1994; personal communication, 1995). Those near the Gremlin occurrence (Yukon Minfile, 1997) in map area 106E/2 were visited by the author in 1996 and identified as metamorphosed laminated siltstone, some of which contains mm-long porphyroblasts of chloritoid (which may have been mistaken for chloritized phenocrysts). Those near the Flatulent occurrence (Yukon Minfile, 1997) in map area 106E/4, considered by R. Hulstein (pers. comm., 1995) to be distal airfall deposits, were not re-examined by the author. The possibility remains that a small proportion of the Fairchild Lake Group may contain a minor proportion of distal airfall material, but medial and proximal volcanic rocks are absent.

Quartet Group (PQ)

The Quartet Group (PQ) is the middle unit of the Wernecke Supergroup (Fig. 3). The lowest unit of the Quartet Group, called Q1 by Delaney (1981), is black, carbonaceous, somewhat pyritic shale, which gradationally overlies the upper Fairchild Lake Group. This unit commonly displays slaty cleavage, which has been locally deformed into a finely spaced crenulation cleavage. Above the basal shale, the Quartet Group comprises a succession of dark grey- to rusty-weathering pyritic shale, siltstone and thinly bedded (5-20 cm), very fine-grained sandstone (Q2 of Delaney, 1981). Bedding surfaces are generally planar, although the coarser beds are wavy- to cross-laminated. Toward the top of the succession the layers typically coarsen and thicken to 50-100-cm-thick beds of fine-grained quartz arenite. At the top of the Quartet Group, these sandstone beds are interbedded with brown- to orange-weathering silty dolostone, marking the onset of Gillespie Lake sedimentation. These sedimentological trends infer deep, anoxic conditions at the beginning of Quartet sedimentation followed by general shallowing. The thickest section of the Quartet Group, estimated at 3.4 km, extends from about 6 to 13 km east of Fairchild Lake (Fig. 2). Although the top of the section is well defined by basal Gillespie Lake strata, the base of the section is a fault. The absence of a stratigraphic base to this section infers that the Quartet Group may be somewhat thicker, perhaps by 0.5-1 km, than the section estimate of 3.4 km.

Gillespie Lake Group (PGL)

The basal Gillespie Lake Group (unit G-TR in Delaney, 1981) gradationally overlies the Quartet Group, and is distinguished from the upper Quartet by its abundance of orange-weathering dolostone beds. The alternating layers of grey-weathering siltstone and orange-weathering dolostone give this basal unit a distinctive banded appearance. The remainder of the Gillespie Lake Group (units G-2 to G-7 in Delaney, 1981) is dominated by orange-weathering, fine-grained dolostone and silty dolostone (Fig. 9). Most of the beds are plane- to wavy-laminated and devoid of other macroscopic features, but the scattered presence of cross-laminations, algal mats, stromatolites, pisolites, intraclasts, and mud-crack casts (Fig. 10) provide compelling evidence

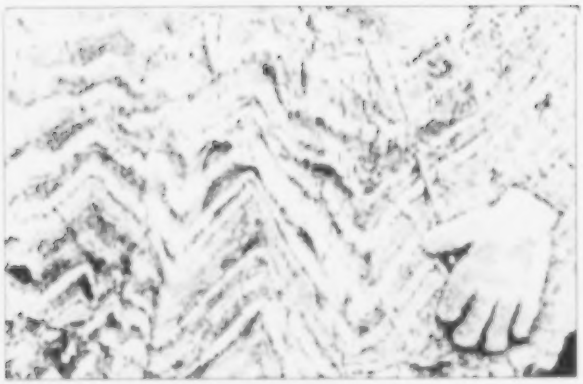

Figure 9. Minor folds in thinly bedded dolostone of Gillespie Lake Group, west of the Bonnet Plume River, south of the Tow mineral occurrence (shown in Fig. 2).

Figure 10. Mud-crack casts in silty dolostone of the Gillespie Lake Group.

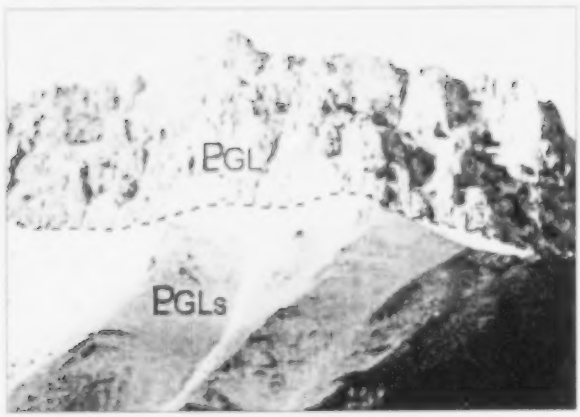

Figure 11. Resistant dolostone (PGL) overlying 250-m-thick recessive shale succession (PGLs) within Gillespie Lake Group, northeast of the Goodfellow mineral occurrence (Fig. 2). View to the north.

Hulstein (1994; personal communication, 1995). Those near the Gremlin occurrence (Yukon Minfile, 1997) in map area 106E/2 were visited by the author in 1996 and identified as metamorphosed laminated siltstone, some of which contains mm-long porphyroblasts of chloritoid (which may have been mistaken for chloritized phenocrysts). Those near the Flatulent occurrence (Yukon Minfile, 1997) in map area 106E/4, considered by R. Hulstein (pers. comm., 1995) to be distal airfall deposits, were not re-examined by the author. The possibility remains that a small proportion of the Fairchild Lake Group may contain a minor proportion of distal airfall material, but medial and proximal volcanic rocks are absent.

Quartet Group (PQ)

The Quartet Group (PQ) is the middle unit of the Wernecke Supergroup (Fig. 3). The lowest unit of the Quartet Group, called Q1 by Delaney (1981), is black, carbonaceous, somewhat pyritic shale, which gradationally overlies the upper Fairchild Lake Group. This unit commonly displays slaty cleavage, which has been locally deformed into a finely spaced crenulation cleavage. Above the basal shale, the Quartet Group comprises a succession of dark grey- to rusty-weathering pyritic shale, siltstone and thinly bedded (5-20 cm), very fine-grained sandstone (Q2 of Delaney, 1981). Bedding surfaces are generally planar, although the coarser beds are wavy- to cross-laminated. Toward the top of the succession the layers typically coarsen and thicken to 50-100-cm-thick beds of fine-grained quartz arenite. At the top of the Quartet Group, these sandstone beds are interbedded with brown- to orange-weathering silty dolostone, marking the onset of Gillespie Lake sedimentation. These sedimentological trends infer deep, anoxic conditions at the beginning of Quartet sedimentation followed by general shallowing. The thickest section of the Quartet Group, estimated at 3.4 km, extends from about 6 to 13 km east of Fairchild Lake (Fig. 2). Although the top of the section is well defined by basal Gillespie Lake strata, the base of the section is a fault. The absence of a stratigraphic base to this section infers that the Quartet Group may be somewhat thicker, perhaps by 0.5-1 km, than the section estimate of 3.4 km.

Gillespie Lake Group (PGL)

The basal Gillespie Lake Group (unit G-TR in Delaney, 1981) gradationally overlies the Quartet Group, and is distinguished from the upper Quartet by its abundance of orange-weathering dolostone beds. The alternating layers of grey-weathering siltstone and orange-weathering dolostone give this basal unit a distinctive banded appearance. The remainder of the Gillespie Lake Group (units G-2 to G-7 in Delaney, 1981) is dominated by orange-weathering, fine-grained dolostone and silty dolostone (Fig. 9). Most of the beds are plane- to wavy-laminated and devoid of other macroscopic features, but the scattered presence of cross-laminations, algal mats, stromatolites, pisolites, intraclasts, and mud-crack casts (Fig. 10) provide compelling evidence

of shallow-water to intertidal depositional conditions. The thickest succession of the group, estimated to be 4.7 km, forms the south limb of a broad syncline west of the Bonnet Plume River, south of the Tow occurrence (Yukon Minfile, 1997). Near the top of that section, the dolostone succession is punctuated by alternating layers of siltstone and shale ranging from a few metres to 250 m thick (Fig. 11). Scattered throughout the Gillespie Lake Group are black and grey diagenetic chert nodules and pseudo-beds.

Pockets, veins and stockwork of red-weathering sparry carbonate are locally abundant, particularly near the base of the Group, south of Bear River. The spar is generally interpreted as chemical infilling of karst cavities developed during periods of diastemic emergence (Thorkelson and Wallace, 1993a). A region of sparry carbonate containing angular nodules of pyrite and chalcopyrite up to 5 cm across is well exposed 2.5 km southwest of the Gnuckle mineral occurrence (Yukon Minfile, 1997). At this locality, which is near major normal faults and large zones of metasomatized breccia, the spar may be a product of hydrothermal activity instead of karsting.

Facies changes within the Gillespie Lake Group are locally pronounced. South of Bear River, in the southwestern part of the study area (Fig. 2), a thick layer (approximately 200 m) of fine-grained epiclastic rock is present within the dolostone succession. This layer comprises a lower member of green-weathering laminated mudstone, and an upper member of brown- to black-weathering shale and dolomitic siltstone. Across Bear River, to the north, the epiclastic succession is absent, and well-exposed strata, which lie an equal distance above the Quartet Group are dolomitic. More subtle facies changes within the Gillespie Lake Group are highlighted by the seemingly sporadic appearance of stromatolites, thin lenses of black siltstone, and silty dolostone beds containing cross laminations. As noted by Delaney (1981), detailed stratigraphic work is necessary to understand the nature and significance of the many facies changes recorded in the Wernecke and Ogilvie mountains.

Delaney (1981) estimated the Gillespie Lake Group to be >4 km thick, and divided it into eight units. Except for the basal unit, the author, in the process of regional mapping, did not consistently recognize these units. Mustard et al. (1990), working at Mount Good about 50 km to the south, suggested that a 1.2 km succession in that area could represent the entire Gillespie Lake Group, and could be correlated with Delaney's (1981) eight units. They accounted for the great difference in thickness by suggesting that Delaney overestimated the thickness of the Gillespie Lake succession. The results presented in this report, however, corroborate the >4 km thickness estimated by Delaney (1981), and indicate that either the Gillespie Lake Group thins dramatically toward Mt. Good, or the sections near Mt. Good represent a fraction of the total succession. The author prefers the latter because the Gillespie Lake Group appears to be fairly uniform in thickness throughout a broad area of the Wernecke Mountains, as determined from numerous low-level flights in aircraft.

Two reports have suggested that volcanic rocks were deposited within the Gillespie Lake Group. In one report, Mustard et al. (1990, p. 46) identified a "volcanic bed... [containing] clay-filled amygdules and green phenocrysts" near Mount Good. They interpreted this unit as a volcanic flow or tuff. A sample of that unit evaluated for geochronology by the Geological Survey of Canada yielded a few "zircon-like crystals," none of which were "magmatic," and many of which were "xenocrystic from country rock" (R.R. Parrish, written communication to C.F. Roots, 1991). In the other report, Abbott (1993) considered the Hart River volcanics (ca. 1.38 Ga) located in the Ogilvie Mountains 110 km west-southwest of the study area, to lie within the Gillespie Lake Group. Subsequently, Abbott (1997) argued that these volcanic rocks lie stratigraphically above, and are significantly younger than, the Gillespie Lake succession. Thus, the evidence cited by Mustard et al. (1990), which is based on a brief field inspection, remains as the only possible indication of synsedimentary volcanism in the Gillespie Lake Group.

Thin stratiform laminae of galena and sphalerite occur in black siltstone of the Gillespie Lake Group in the study area at the Cord and Goodfellow mineral occurrences (Fig. 2; Yukon Minfile, 1997), 16-19 km south and southwest of Fairchild Lake (Fig. 2). These enrichments are interpreted as products of metalliferous exhalations of the "sedex" variety during Gillespie Lake sedimentation (Campbell and McClintock, 1980; Hardy and Campbell, 1981; Eaton, 1983). There are no known correlatives of these exhalative occurrences.

Synthesis of Wernecke Supergroup deposition

The depositional history of the Wernecke Supergroup as described by Delaney (1981), and generally corroborated in this study, may be understood in terms of two main clastic-to-carbonate grand cycles. In the first cycle, siltstone and minor carbonate of the lower Fairchild Lake Group grades up into a conspicuous succession of interbedded carbonate and shale. This progression reflects general shallowing and sediment starvation of the basin, although the carbonates themselves appear to be "distal representatives of... carbonates which may have fringed the margin of the Wernecke Basin..." (Delaney, 1981, p. 8). The black, pyritic shales of the lower Quartet Group mark inception of the second cycle, which indicate continuing sediment starvation in a deeper water environment. Higher in the Quartet, increased sediment influx is indicated by interbedded shale and siltstone, which generally coarsens upward and grades into the thick, platformal carbonates of the Gillespie Lake Group, completing the second grand cycle. Shallow water to locally emergent conditions were maintained during deposition of the Gillespie Lake Group.

The pair of clastic-to-carbonate cycles in the Wernecke succession may be interpreted as two stages of basin subsidence and sediment infilling. The first cycle may represent initial basin development. Deepening of the basin

at the start of the second cycle may reflect a subsequent pulse of subsidence and marine transgression. If genesis of the Wernecke basin is cast in terms of continental rifting, then the two grand cycles may equate to two stages of lithospheric stretching, subsidence, and thermal deepening of the basin. The accumulation of >4 km of shallow-water carbonates at the end of the second cycle indicates protracted subsidence of the Wernecke basin. The abrupt facies changes noted in the Gillespie Lake Group infer that normal faulting played an important role in basin architecture.

The absence of firm correlations between the Wernecke Supergroup and other successions is problematic. The Belt-Purcell succession in the southern Canadian Cordillera and the adjacent United States was considered as a possible correlative (Aitken and McMechan, 1992). However, it is now known to range in age mainly from 1370-1470 Ma (Anderson and Davis, 1995; Aleinikoff et al., 1996; Doughty and Chamberlain, 1996), and is therefore ca. 0.3 billion years younger than the Wernecke Supergroup. The Muskwa assemblage in northeastern Canada may be equivalent to the Wernecke Supergroup, although R.T. Bell, who worked extensively in both successions (e.g., Bell, 1968; 1978) did not draw such a correlation. A small inlier of Proterozoic strata at Cap Mountain in the Northwest Territories was loosely correlated with the Wernecke Supergroup by Aitken and McMechan (1992), but is now known, on the basis of detrital zircon ages, to be younger than about 1.03 Ga (Villeneuve et al., 1998). The Cap Mountain strata are more reasonably correlated with the Mackenzie Mountains Supergroup or the Hematite Creek Group (cf. Villeneuve et al., 1998).

The Wernecke Supergroup most plausibly correlates with the lower part of the Hornby Bay Group in the Coppermine Homocline east of Great Bear Lake in the Northwest Territories (Fig. 12; Young et al., 1979; Cook and MacLean, 1995; Abbott et al., 1997). The "lower" Hornby Bay Group, for the purpose of this correlation, is considered to be the carbonate East River formation, and the underlying clastic Lady Nye, Fault River, and Big Bear formations. These formations have a cumulative thickness estimated by Bowring and Ross (1985) at 3.4 km, and by Ross and Donaldson (1989) at 1.3 km. The overlying Kaertok Formation of the "upper" Hornby Bay Group is necessarily excluded from correlation, because one of its constituents, the Narakay volcanics, is dated at 1663 ± 8 Ma (Bowring and Ross, 1985) and is ca. 60 million years younger than the minimum age of the Wernecke Supergroup. Correlation is further denied on the basis of the contractional-syntectonic character of the Kaertok Formation (Cook and MacLean, 1995), which contrasts with the relatively quiescent sedimentation of the Wernecke Supergroup. However, it is possible that strata correlative with the Kaertok Formation were deposited in the Wernecke Mountains region, perhaps as the upper part of the Wernecke Supergroup, and subsequently eroded prior to deposition of the overlying Pinguicula Group. Discontinuous seismic reflection and drill hole data between the Wernecke Mountains and the Coppermine region indicate plausible stratigraphic continuity between the lower Hornby Bay Group and the Wernecke succession (Cook et al., 1992; Cook and MacLean, 1995). If this correlation is correct, then the strata thicken by up to ten times between the Hornby Bay exposures and those in the Wernecke Mountains. This trend is generally supported by the geophysical model of the Wernecke basin as a deep miogeocline (e.g., Cook et al.,1992).

Is the Wernecke Supergroup a product of late Early Proterozoic continental break-up? Paleocurrent data and interpretations of Delaney (1981) support this idea. Sediment dispersal patterns are generally toward the south, with only minor transport in northerly directions. In his synthesis, Delaney (1981) considered the Wernecke Supergroup to have been deposited in a miogeoclinal, not an intracratonic, environment. Following Norris (1972), he argued that the basin margin followed an east-west trend to the north of the Wernecke and Ogilvie mountains, curving southward in the Northwest Territories to follow the general trend of the Cordilleran orogen (Fig. 5). Seismic and aeromagnetic data were subsequently used to corroborate such an arcuate basin configuration (Cook et al., 1991, 1992; Dredge Mitchelmore and Cook, 1994), although the basin margin may lie far to the east of the Cordilleran orogen — possibly east of the Coppermine Homocline.

Although Delaney postulated basin development in response to collisional orogenesis in the Wopmay region of the Northwest Territories, the great sediment thickness and abundance of platformal carbonate rocks in the succession are more favourably accommodated by a rifted margin setting. If a rifted margin origin is adopted, then the absence of volcanic rocks in the succession may indicate that the Wernecke Supergroup was deposited on the lower plate of a simple-shear extensional fault system (cf. Wernicke, 1985). Rift-related magmatism, if it did occur, may have been restricted to more westerly, axial parts of the rift. Alternatively, rift magmatism may have occurred early in the history of extension, and was thereby restricted to a deeper, presently unexposed level of the Fairchild Lake Group or its substratum.

A rift environment for the Wernecke depocentre is attractive from a Yukon perspective, but is troublesome when viewed in the context of the entire Canadian and northern U.S. Cordillera. The problem lies in the absence of Wernecke-aged successions south of central Yukon. If the entire western margin of ancestral North America underwent rifting prior to ca. 1.72 Ga, then other successions of Wernecke Supergroup age should be expected elsewhere along the margin. Instead, the oldest dated strata exposed in southwestern Canada and the northwestern U.S. is the ca. 1.4 Ga Belt-Purcell Supergroup. This succession, however, is regarded as an intracratonic basin between North America and another continent, probably eastern Australia, on the basis of paleocurrents and detrital zircon ages (Ross et al, 1992; Doughty et al., 1998). Therefore, generation of the "Wernecke miogeocline" may have been restricted to the northern Canadian Cordillera,

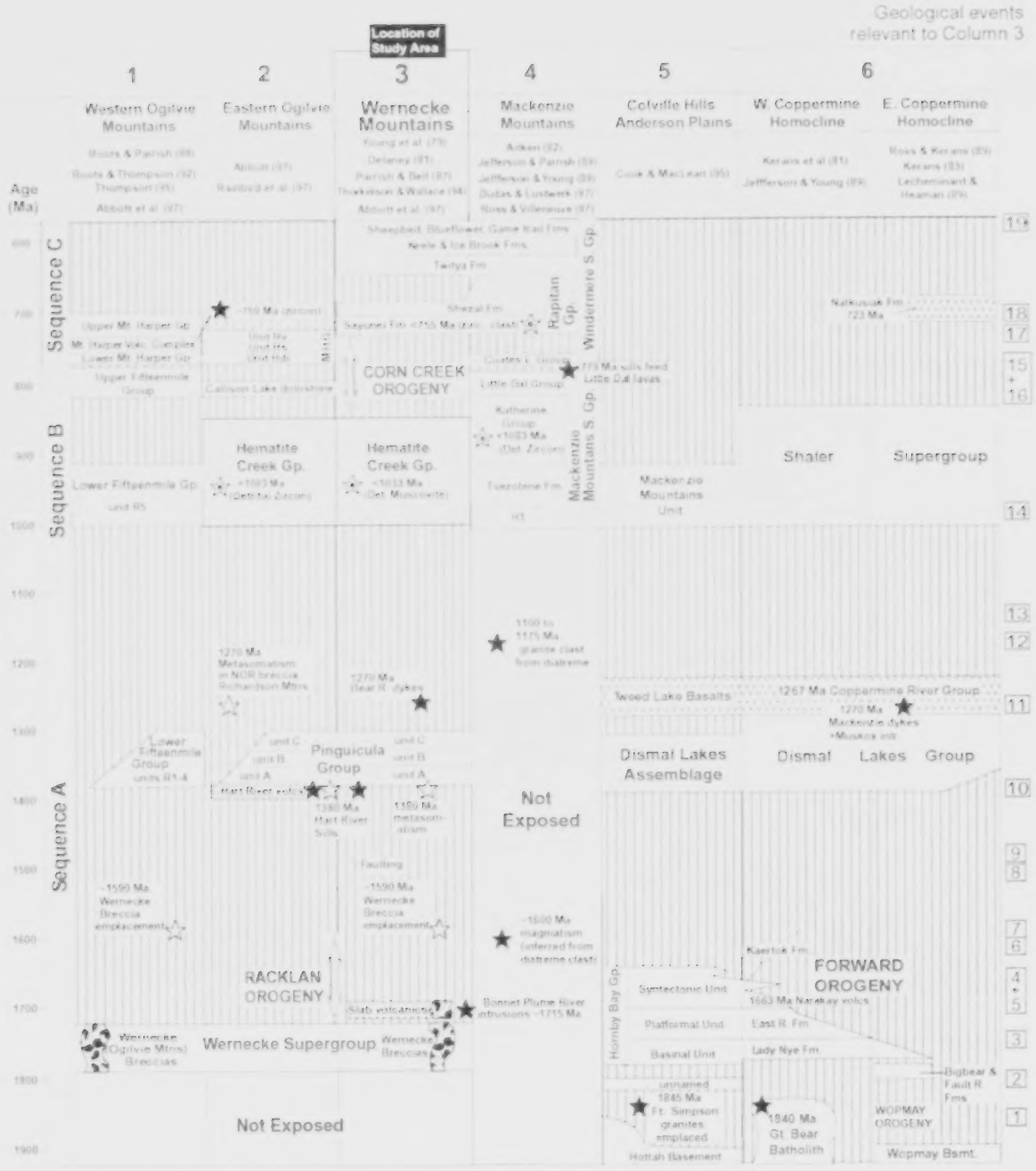

Figure 12. Suggested correlation of Proterozoic successions in the Wernecke, Ogilvie, and Mackenzie Mountains, and the western Arctic (modified from Cook and Macleam, 1995; Abbott, 1997; and Thorkelson et al., 1998). Geological events relevant to the Wernecke Mountains, numbered along the right margin, are discussed in the section entitled Geological History. Ages of certain events are indicated with stars: black stars = intrusive events; white stars = metasomatic events; white stars with black dots = detrital mineral ages.

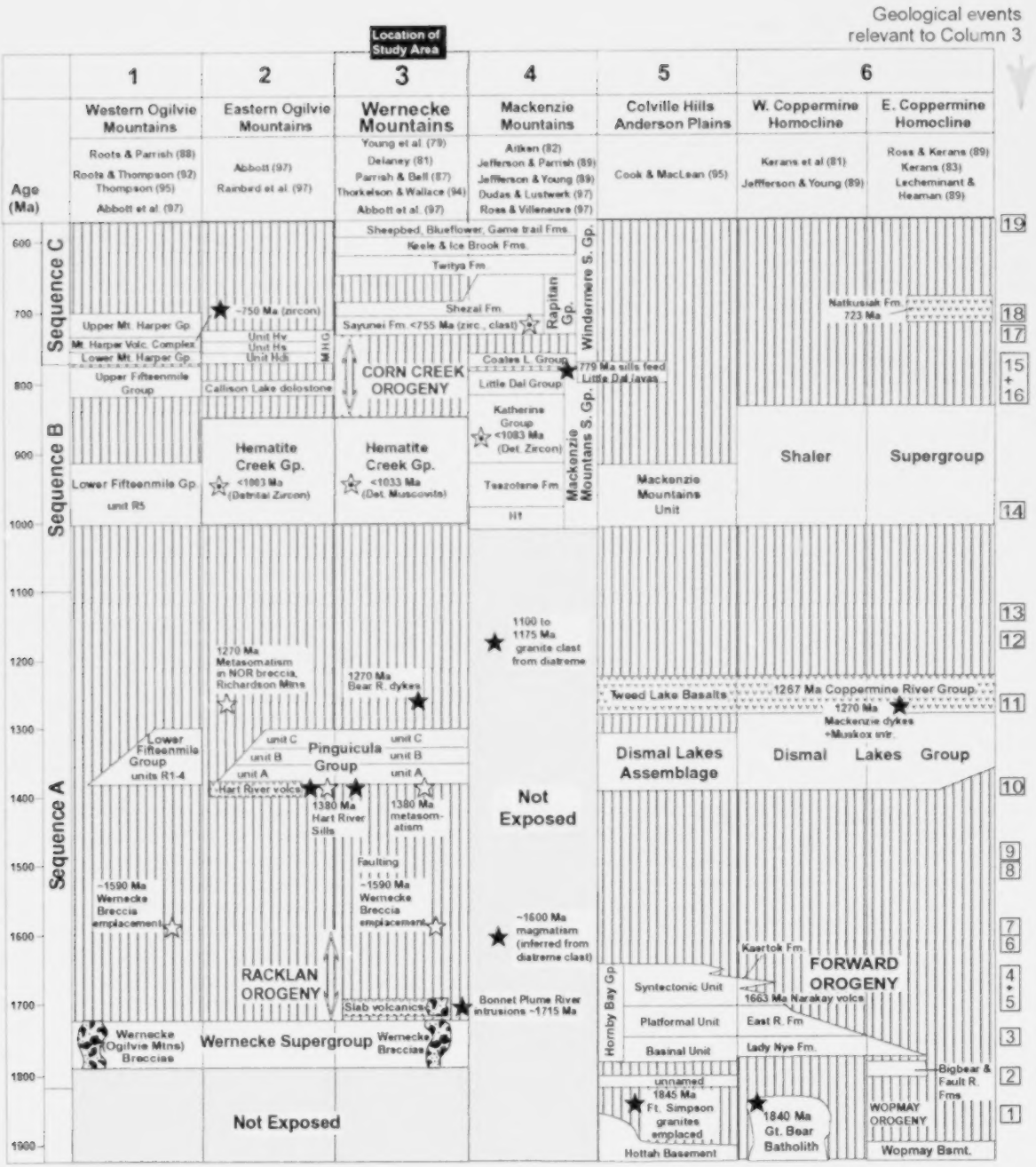

Figure 12. *Suggested correlation of Proterozoic successions in the Wernecke, Ogilvie, and Mackenzie Mountains, and the western Arctic (modified from Cook and Maclean, 1995; Abbott, 1997; and Thorkelson et al., 1998). Geological events relevant to the Wernecke Mountains, numbered along the right margin, are discussed in the section entitled Geological History. Ages of certain events are indicated with stars: black stars = intrusive events; white stars = metasomatic events; white stars with black dots = detrital mineral ages.*

whilst more southerly regions remained relatively undisturbed. The configuration of the Wernecke rift system may have been oriented quite differently from the present Cordilleran outline which is generally thought to reflect the shape of the rifted margin generated by Late Proterozoic "Windermere" rifting and subsequent Lower Paleozoic extension (e.g. Cook et al., 1991; Ross, 1991).

Slab Volcanics (PSv)

The Slab volcanic succession was first recognized by members of the Newmont-Westmin-Pamicon-Equity mineral exploration venture in 1992, and described by Thorkelson and Wallace (1993a, 1994a). Named after "Slab Mountain" at the Slab mineral occurrence (Yukon Minfile, 1997; Thorkelson and Wallace, 1994a), the Slab volcanics are preserved as an isolated, apparently down-dropped block (0.25 x 0.6 km) at the northern edge of the study area, northeast of the Bonnet Plume River (Figs. 2, 3, 4, 13). These volcanic strata were tentatively assigned to the Pinguicula Group by Thorkelson and Wallace (1993a, b), but are now regarded on the basis of field and isotopic evidence as relics of a previously unrecognized stratigraphic interval, younger than the Wernecke Supergroup and older than the Pinguicula Group. Geochemical similarities (Table A3-1) between the Slab volcanics (mafic-intermediate composition) and quartz-albite syenite (ca. 1.725 Ga) of the Bonnet Plume River intrusions suggest a co-magmatic relationship (although Nd model ages are somewhat different; Table A2-1). Further work is necessary to test this hypothesis. Evidence that the Slab volcanics are younger than 1.71 Ga is limited to their appearance of being less deformed and less altered than dykes and stocks of the Bonnet Plume River intrusions.

The Slab volcanics consist of about forty steeply dipping lava flows, totaling about 250 m thick. Each flow is 4-7 m thick, alternating with minor beds of clastic rock including rounded-pebble conglomerate, sandstone, and volcanic breccia. Many of the lavas have dense flow bottoms and scoriaceous flow tops which indicate stratigraphic tops-to-the-northwest, consistent with the facing direction of basal scours in the conglomerate and sandstone beds. The lava flows have a slight maroon tint to their grey colour, and commonly contain amygdules of quartz, white and orange calcite, biotite, chlorite, and apatite. The flows are aphyric, except for a few which contain scattered phenocrysts

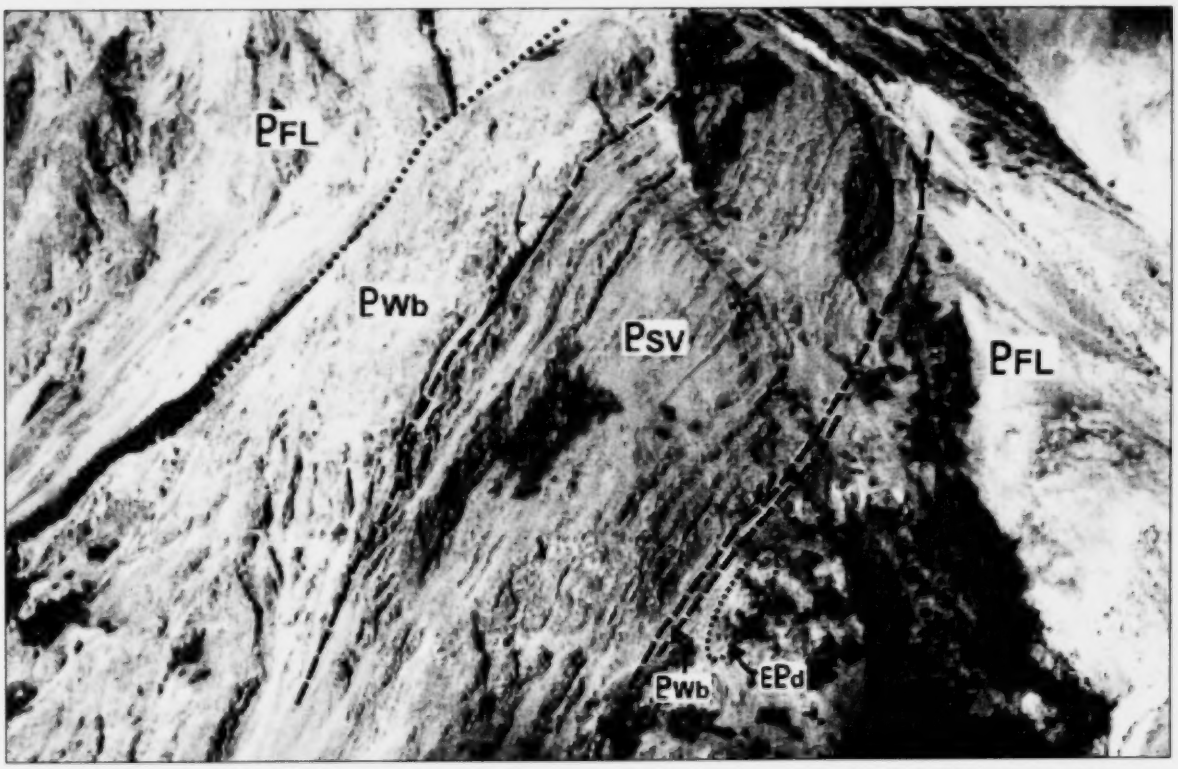

Figure 13. *Slab volcanics (PSV) of the Slab mineral occurrence situated between Wernecke Breccia (PWb) and altered siltstone to kink-banded schist of the Fairchild Lake Group (PFL; Fig. 2). A small body of the Bonnet Plume River intrusions (EPd) is located approximately. Thickness of Slab volcanics is about 250 m. Stratigraphic top of the volcanic rocks is to the left. View to the north.*

(1-3 mm) of plagioclase and anhedral, apparently corroded pyroxene. Groundmass consists of weakly flow-aligned laths of plagioclase intergrown with biotite and interstitial quartz. In contrast to cleaved and kinked siltstone of the Fairchild Lake Group to the east of the faulted volcanic succession, the lavas are not folded and are devoid of secondary petrofabrics. J.K. Mortensen dated rutile from the Slab volcanics at ca. 1.38 Ga (Table A1-1). A provisional depleted-mantle Nd isotopic model age from one of the flows was calculated at 3.00 Ga (Table A2-1; R.A. Creaser, pers. comm., 1995).

The Slab volcanics are not included in the Wernecke Supergroup because their apparent subaerial origin is inconsistent with marine conditions represented by the Wernecke Supergroup. At the time of their formation, the volcanic rocks probably covered tens or perhaps hundreds of square kilometres. The down-dropped block at "Slab Mountain" is apparently the only part of the succession which has not been completely removed by erosion. The absence of volcanic strata within or beneath the exposed base of Pinguicula Group implies that this erosion occurred before deposition of the Pinguicula Group, during the same interval as deep weathering of the Wernecke Supergroup and Wernecke Breccia (Fig. 4). The volcanic rocks are not included in the Pinguicula Group because volcanic strata are apparently absent in the Pinguicula Group, despite the original descriptions of Eisbacher (1978).

The block of Slab volcanics (Fig. 13) appears to be entirely surrounded by intrusive breccia dated at ca. 1.59 Ga (R.A. Creaser, pers. comm., 1994). Megaclasts up to 20 m across (perhaps more) of schist and diorite of the country rock are contained in the breccia (Bell and Delaney, 1977). The breccia belongs to a set of large fragmental zones known as Wernecke Breccia, which were generated by explosive expansion of fluids. Along the western flank of the Slab volcanics block, a narrow (0.1-1 m) fault zone of cataclasite and slickensides separates the volcanic rocks from a tabular zone of Wernecke Breccia. The eastern margin of the volcanic block lies close to schist of the Fairchild Lake Group and diorite of the Bonnet Plume River intrusions. Where the contact is well exposed, a narrow strip (2-5 m) of Wernecke Breccia is visible, separating the volcanic rocks from the schist and diorite. A boulder-sized clast (0.5 m diameter) of biotitic amygdaloidal volcanic rock, apparently derived from the volcanic succession, was observed in the breccia immediately to the northwest of the volcanic rocks.

By what mechanisms were the Slab volcanics emplaced into their current position? The presence of megaclasts of country rock and boulder-sized volcanic clasts in the zone of Wernecke Breccia suggests that the block of Slab volcanics was engulfed during the collapse phase of Wernecke Breccia formation. Most plausibly, the block foundered into a cavernous vent area, in the manner of diatreme fallback breccias, following rapid expulsion of volatiles and entrained particles. Subsequent faulting adjusted the position of the volcanic block, but was not the primary mechanism of block emplacement.

The foregoing observations from "Slab Mountain" indicate: (1) the Slab volcanics were deposited as a succession of mainly subaerial lavas at least 250 m thick on a substrate of Wernecke Supergroup, either before or after Racklan Orogeny, but definitely before Wernecke Breccia emplacement; (2) parts of the Slab volcanics, including a large intact piece of the succession, collapsed into a zone of Wernecke Breccia at ca. 1.59 Ga; and (3) faulting of unknown age, and hydrothermal activity at ca. 1.38 Ga (causing growth of rutile), modified the assemblage.

Pinguicula Group (PP)

Introduction

The Pinguicula Group is a carbonate and siliciclastic succession deposited with angular unconformity on the Lower Proterozoic Wernecke Supergroup (Fig. 14). Eisbacher (1978, 1981) divided the succession into six formations, units A-F. Recent work, however, indicates that a major unconformity exists within the succession (Thorkelson et al., 1998). For this reason, strata originally defined as the Pinguicula Group are herein separated into two groups (Figs. 3, 4). The lower part of the original Pinguicula Group (Eisbacher's units A-C) retains the name Pinguicula Group. The upper part (Eisbacher's units D-F) is herein named the Hematite Creek Group, and is described separately.

The break between the Hematite Creek Group and the Pinguicula Group was placed at the unit C-D boundary because unit C is locally karsted, and because correlative strata in the eastern Ogilvie Mountains are separated by an angular unconformity which locally cuts out the entirety of Pinguicula units A-C (Abbott, 1997). In the study area, and in areas to the

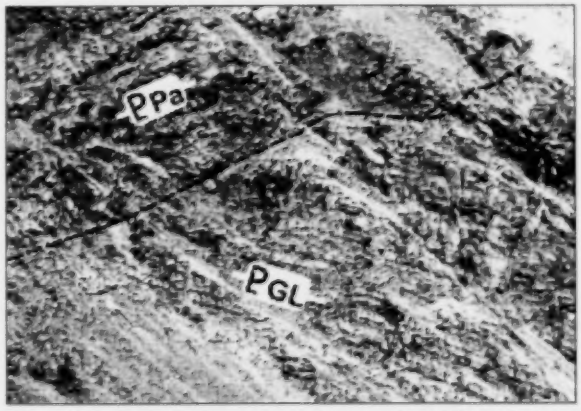

***Figure 14**. Angular unconformity between basal Pinguicula Group (PPa) and underlying Gillespie Lake Group (PGL), at eastern edge of study area near Pika Minfile occurrence (Fig. 2). Field of view is approximately 200 m wide. View to the southwest.*

south (Eisbacher, 1981) and north (D.K. Norris, pers. comm., 1998), all units in the Pinguicula-Hematite Creek successions are broadly conformable.

The Pinguicula Group has been considered part of Sequence B, as defined by Young et al. (1979). However, as indicated in the following discussion, the base of the Pinguicula Group is now considered to be about the same age as the Hart River sills, ca. 1.38 Ga. Consequently, the Pinguicula Group now falls within the age-range of Sequence A of Young et al. (1979), but is about 350 million years younger than the Wernecke Supergroup, also of Sequence A. Clearly, the use of sequences A and B in establishing correlation among Lower to Middle Proterozoic strata is less useful than originally envisaged. In northwestern Canada, the Pinguicula Group may correlate with the lower parts of the Fifteenmile Group in the Ogilvie Mountains (units R1-R4 of Thompson, 1995), and the Dismal Lakes Group in the Northwest Territories (Fig. 12).

The Pinguicula Group represents a period of basin development and basinal to platformal sedimentation in Yukon. Contact relations and stratigraphic characteristics are well displayed in and near the study area where the Pinguicula Group was originally defined (Eisbacher, 1978). In the study area, the Pinguicula Group (as defined here) reaches a maximum thickness of about 2720 m. However, south of the study area, unit A thickens by about 800 m, bringing the maximum cumulative thickness of the Pinguicula Group to about 3520 m.

In the study area (Fig. 2), the redefined Pinguicula Group unconformably overlies the Wernecke Supergroup (> ca. 1725 Ma) and intrusive breccia zones called Wernecke Breccia (ca. 1595 Ma; Table A1-1). About 20 km to the south, unit A of the Pinguicula Group is crosscut by a small stock which has recently been dated at ca. 1380 Ma (Table A1-1; J. Mortensen, pers. comm., 1997). This age is similar to those of the Hart River sills, which are well exposed in the southern Wernecke and eastern Ogilvie mountains (Abbott, 1997). In the eastern Ogilvie Mountains, strata that have been recently assigned to the Pinguicula Group unconformably overlie the Hart River sills, and the Hart River volcanics, which have been correlated with the Hart River sills (Abbott, 1997).

These relations appear incongruous, since the Hart River sills are indicated to be both younger and older than the Pinguicula Group. There are two possible explanations. One is that the "Pinguicula" strata in the eastern Ogilvie Mountains may not belong to the Pinguicula Group and may actually belong entirely to the younger Hematite Creek Group. The other, and currently preferred explanation, is that Hart River magmatism overlapped in age with the onset of Pinguicula deposition, in an environment of crustal extension. Regardless which explanation is correct, unit A of the Pinguicula Group in the Wernecke Mountains was definitely intruded by dioritic magma at ca. 1.38 Ga, indicating that the base of the Pinguicula Group is ca. 1.38 Ga or older. The base of the Pinguicula Group is therefore constrained between ca. 1.38 Ga and the age of the underlying Wernecke Breccia, ca. 1.59 Ga. Deposition of the Pinguicula Group is likely to have ended by ca. 1270 Ma when the Bear River dykes were emplaced (Table A1-1). These dykes may have fed a basaltic volcanic succession, which is nowhere preserved. If Pinguicula deposition had continued past ca. 1270 Ma, then the succession might be expected to contain basaltic lavas related to the Bear River dykes.

Detrital zircons from greywacke at the base of unit A in the study area were dated by the U-Pb method (Table A1-1). The zircons range in age from 1841 ± 4 Ma to 3078 ± 10 Ma. All but the oldest date cluster into two groups: 1841-1983 Ma, and 2496-2719 Ma. Detrital zircon ages from these basal beds indicate sediment provenance from Early Proterozoic to Archean terranes. Zircons in the range 1841-1983 may have come from the western Canadian Shield, notably felsic igneous rocks of the Fort Simpson, Wopmay, and Thelon-Talston zones (Hoffman, 1989). The remainder of the zircons are Archean in age and could have come from the Slave, Rae, or Hearne cratons in the western part of the Shield. Although the western Canadian Shield is a reasonable source region, local crystalline basement is a plausible alternative. The nature of the cratonic substrate of Yukon and the westernmost Northwest Territories is unknown and may contain components of both Proterozoic and Archean crust. Conceivably, all of the sediment of Proterozoic to Archean provenance in the basal Pinguicula Group could have been derived from local continental crust that was exposed in the early history of Pinguicula deposition. Such exposures may have been produced by block faulting during formation of the Pinguicula basin, and subsequently covered during deposition of the Pinguicula Group and younger strata.

The environment of deposition of the Pinguicula Group progressed from a mid- to deep-water shale basin (unit A) to a mid-water carbonate shelf (unit B), to a subtidal or intertidal carbonate bank (unit C). Near-surface sedimentary structures such as mudcracks, intraclasts, interference ripples, and stromatolites are rare in units A-C. However, zebra texture in unit C is considered a product of shallow-water processes, as argued below.

All units of the Pinguicula Group are thinnest to the north of the study area, in map-area 106F/3 (Eisbacher, 1981; Norris, 1982). Unit A thickens through the study area, and continues to thicken south of the study area, reaching maximum thickness in the southern part of map-area 106C/11. This trend is consistent with a southward-deepening initial basin configuration (Eisbacher, 1981). Units B and C, however, thin from the study area toward the south, apparently indicating a trough-like basin geometry toward the end of Pinguicula deposition. Some southward thinning of unit C could be a consequence of sub-Hematite Group erosion. Basin development may have been related to Hart River sill emplacement and crustal extension.

Unit descriptions

Unit A of the Pinguicula Group (Fig. 15) is characterized by maroon-, green- and black-weathering shale and siltstone (100-600 m thick), underlain by a thin (0-10 m) basal succession of conglomerate and greenish grey- to rusty-weathering, locally pyritic sandstone. Unit A is much less competent than overlying units B and C, and its variation in thickness is partly due to internal deformation. The shale and siltstone of unit A are generally planar bedded and laminated. The conglomerate is dominated by clasts of siltstone probably derived from the Wernecke Supergroup. The clasts are subrounded to rounded, from 1 to 30 cm long, and are supported by a sandy matrix. South of the Pika occurrence (Yukon Minfile, 1997), the conglomerate contains pebbles and detrital hematite derived from Wernecke Breccia.

Variations in the thickness of unit A are evident both gradually and abruptly. Gradual thickening occurs from northeast to southwest in the study area. This trend continues to the south where the shale changes colour from hues of maroon and green to black and rusty-brown, and thickens to about 1400 m in the southwestern part of map area 106C/11, where it is crosscut by Hart River diorite. An abrupt change of thickness is evident in the west-central part of the study area, from thin in the vicinity of the Pika mineral occurrence, to thick in the vicinity of the Key Mountain occurrence (Yukon Minfile, 1997; Fig. 2). The long northwest-trending fault, which separates the two areas, may have served as a northeast-side-down growth fault, permitting thicker strata of unit A to accumulate on the downfaulted block. If this interpretation is correct, then the fault must have been reactivated with the opposite sense of motion sometime after deposition of the Hematite Creek Group, as indicated by the current sense of displacement (Fig. 2).

Eisbacher (1981) reported volcanic rocks in unit A, which he named the "Kohse Creek volcanics." Despite numerous inspections, no volcanic rocks were found in unit A or in any of the Pinguicula strata in either the study area or farther south near Kohse Creek (106C/11). The author suspects that the Kohse Creek volcanics do not exist. On the mountains directly north and south of Kohse Creek, dioritic dykes and sills crosscut Pinguicula Group and Wernecke Supergroup strata (Blusson, 1974). These intrusive rocks may have been misidentified by Eisbacher as volcanic rocks, a possibility accepted by Eisbacher (pers. comm., 1994). However, if the Kohse Creek volcanics do exist, they are likely correlative with the Hart River volcanics which, by means of correlation with the Hart River sills, may have erupted at the onset of Pinguicula deposition.

Unit B consists of medium-bedded, orange-weathering, laminated dolostone and limestone up to 320 m thick (Fig. 15). Variations in thickness may be partly of depositional origin, and partly due to internal deformation. Unit B overlies unit A conformably and gradationally. A few beds of maroon siltstone are scattered throughout the unit, and are in greater abundance near the base, suggesting depositional continuity with unit A. Beds up to 60 cm thick hosting rounded intraclasts of grey-weathering limestone are common near the base of the unit. Crossbeds are present locally. Thin beds of grey carbonate are common near the top of unit B. Overall, unit B is characterized by consistency of bed thickness and rock types.

Unit C is up to 1800 m thick and consists of thin- to very thick-bedded or massive, grey- to yellowish grey-weathering micritic limestone and dolostone. Eisbacher reported a thickness of 200 m from south of the study area; apparently the unit thins significantly in that direction. Unit C abruptly to gradationally overlies unit B (Fig. 15). Original micritic texture is commonly overprinted by narrow (1- to 15-mm-wide) en-echelon bands of white sparry dolostone, known as zebra texture (Wallace et al., 1994). Local intraformational conglomerates or "storm beds" within unit C contain

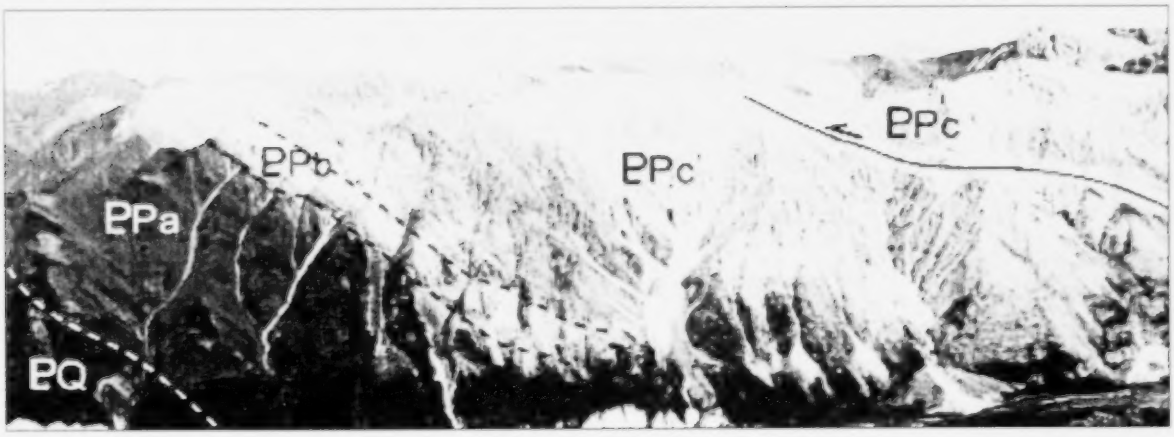

Figure 15. *Pinguicula Group, units A, B, and C (PPa; PPb; PPc), underlain by the Quartet Group (PQ), south of Dolores Creek and southeast of Key Mountain mineral occurrence (Fig. 2). A west-verging thrust fault doubles the thickness of unit C. View to the east-northeast.*

Unit descriptions

Unit A of the Pinguicula Group (Fig. 15) is characterized by maroon-, green- and black-weathering shale and siltstone (100-600 m thick), underlain by a thin (0-10 m) basal succession of conglomerate and greenish grey- to rusty-weathering, locally pyritic sandstone. Unit A is much less competent than overlying units B and C, and its variation in thickness is partly due to internal deformation. The shale and siltstone of unit A are generally planar bedded and laminated. The conglomerate is dominated by clasts of siltstone probably derived from the Wernecke Supergroup. The clasts are subrounded to rounded, from 1 to 30 cm long, and are supported by a sandy matrix. South of the Pika occurrence (Yukon Minfile, 1997), the conglomerate contains pebbles and detrital hematite derived from Wernecke Breccia.

Variations in the thickness of unit A are evident both gradually and abruptly. Gradual thickening occurs from northeast to southwest in the study area. This trend continues to the south where the shale changes colour from hues of maroon and green to black and rusty-brown, and thickens to about 1400 m in the southwestern part of map area 106C/11, where it is crosscut by Hart River diorite. An abrupt change of thickness is evident in the west-central part of the study area, from thin in the vicinity of the Pika mineral occurrence, to thick in the vicinity of the Key Mountain occurrence (Yukon Minfile, 1997; Fig. 2). The long northwest-trending fault, which separates the two areas, may have served as a northeast-side-down growth fault, permitting thicker strata of unit A to accumulate on the downfaulted block. If this interpretation is correct, then the fault must have been reactivated with the opposite sense of motion sometime after deposition of the Hematite Creek Group, as indicated by the current sense of displacement (Fig. 2).

Eisbacher (1981) reported volcanic rocks in unit A, which he named the "Kohse Creek volcanics." Despite numerous inspections, no volcanic rocks were found in unit A or in any of the Pinguicula strata in either the study area or farther south near Kohse Creek (106C/11). The author suspects that the Kohse Creek volcanics do not exist. On the mountains directly north and south of Kohse Creek, dioritic dykes and sills crosscut Pinguicula Group and Wernecke Supergroup strata (Blusson, 1974). These intrusive rocks may have been misidentified by Eisbacher as volcanic rocks, a possibility accepted by Eisbacher (pers. comm., 1994). However, if the Kohse Creek volcanics do exist, they are likely correlative with the Hart River volcanics which, by means of correlation with the Hart River sills, may have erupted at the onset of Pinguicula deposition.

Unit B consists of medium-bedded, orange-weathering, laminated dolostone and limestone up to 320 m thick (Fig. 15). Variations in thickness may be partly of depositional origin, and partly due to internal deformation. Unit B overlies unit A conformably and gradationally. A few beds of maroon siltstone are scattered throughout the unit, and are in greater abundance near the base, suggesting depositional continuity with unit A. Beds up to 60 cm thick hosting rounded intraclasts of grey-weathering limestone are common near the base of the unit. Crossbeds are present locally. Thin beds of grey carbonate are common near the top of unit B. Overall, unit B is characterized by consistency of bed thickness and rock types.

Unit C is up to 1800 m thick and consists of thin- to very thick-bedded or massive, grey- to yellowish grey-weathering micritic limestone and dolostone. Eisbacher reported a thickness of 200 m from south of the study area; apparently the unit thins significantly in that direction. Unit C abruptly to gradationally overlies unit B (Fig. 15). Original micritic texture is commonly overprinted by narrow (1- to 15-mm-wide) en-echelon bands of white sparry dolostone, known as zebra texture (Wallace et al., 1994). Local intraformational conglomerates or "storm beds" within unit C contain

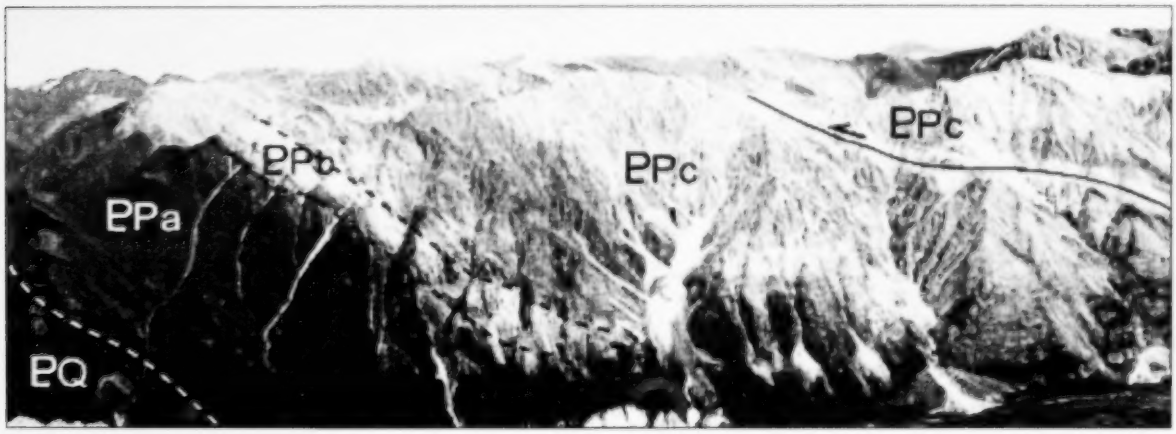

Figure 15. *Pinguicula Group, units A, B, and C (PPa; PPb; PPc), underlain by the Quartet Group (PQ), south of Dolores Creek and southeast of Key Mountain mineral occurrence (Fig. 2). A west-verging thrust fault doubles the thickness of unit C. View to the east-northeast.*

intraclasts of both grey micrite and zebra dolostone (Fig. 16). The presence of zebra dolostone as rip-up clasts infers that the zebra texture in unit C developed at or near the sediment surface, shortly after micrite deposition and prior to lithification. Pods and lenses up to 50 m wide of pinkish grey-weathering, very coarse dolomite spar are common within a few km of the Poo mineral occurrence (Yukon Minfile, 1997). These sparry zones crosscut both bedding and zebra texture, and appear to have developed from dissolution and open space filling in a karst environment. This karsting is attributed to emergent conditions prior to deposition of the overlying Hematite Creek Group.

Hematite Creek Group (PHC)

Introduction

The Hematite Creek Group consists of shallow-water clastic and carbonate units formerly considered the upper parts (units D-F) of the Pinguicula Group (Eisbacher, 1981). These units are here removed from the Pinguicula Group because new age determinations indicate that they are younger than the lower Pinguicula units by about 300 million years (Fig. 4; Table A1-1), and because of evidence for unconformity described in the section on the Pinguicula Group. The Corn Creek quartz arenite is the only unit which has been distinguished from the rest of the Hematite Creek Group. It is herein considered a facies of the Hematite Creek Group, and is broadly equivalent to unit E of the original Pinguicula Group (Eisbacher, 1981). Units D, E and F are not recognized in this report and their usage is provisionally abandoned. The Hematite Creek Group is overlain with angular unconformity by the Windermere Supergroup, whose deposition began at about 780 Ma (Ross, 1991). The Hematite Creek Group is clearly pre-Windermere in age, but post- ca. 1 Ga (details given below), and thus it is most favourably retained in Sequence B of Young et al. (1979).

The Hematite Creek Group is well exposed in the southeastern study area, as well as a few km to the south in the vicinity of Hematite Creek and Pinguicula Lake (106C/11). The original descriptions of units D-F by Eisbacher (1981), and those provided in this report, are sufficient to define the lithologic character of the Hematite Creek Group. Although detailed type sections have not been identified, the southern quarter of map area 106C/14 combined with the adjoining northern quarter of map area 106C/11 is recommended as the type locality for the Hematite Creek Group. Detailed stratigraphic work is required to produce proper type sections, and is likely to result in the identification of formations and members within the group.

The Hematite Creek Group crops out in the Hart River inlier (Pinguicula Group unit D of Abbott, 1997). It is considered correlative with parts of the Fifteenmile Group in the Coal Creek inlier, the Mackenzie Mountains Supergroup in western Northwest Territories, and the Shaler Supergroup on Victoria Island and in the Coppermine area (Rainbird et al., 1997). The Hematite Creek Group may also correlate with some or all of the upper Middle to Late Proterozoic strata at Cap Mountain in the southwestern Northwest Territories (Villeneuve et al., 1998), and a seismically imaged layer beneath the Imperial anticline in the west-central Northwest Territories (Cook and MacLean, 1999). Joint field excursions by J.G. Abbott and the author in 1995 and 1996 improved regional correlations in Yukon by recognizing stratigraphic similarities, including the local abundance of detrital muscovite in siltstone and fine-grained sandstone (Thorkelson et al., 1998).

Correlations within Sequence B have been strengthened by detrital zircon and muscovite populations yielding "Grenville-age" U-Pb dates of ca. 1.0-1.1 Ga (Rainbird et al., 1996, 1997; Abbott, 1997; Villeneuve et al., 1998). Isotopic ages of detrital muscovite grains from the Hematite Creek Group in the study area are strikingly similar to the zircon dates from other units of Sequence B (Thorkelson et al., 1998). Six muscovite grains from unit D were analyzed by the $^{40}Ar/^{39}Ar$ method by the Geological Survey of Canada (Table A1-1; M.E. Villeneuve, pers. comm., 1997). Five of the grains yielded ages between 1033 ± 9 Ma and 1114 ± 12 Ma, remarkably similar to the age of the Grenville-age zircons reported from the other successions of Sequence B (Rainbird et al., 1997). The sixth grain yielded an age of 2441 ± 19 Ma and may have been derived from elsewhere in the Canadian Shield. Detrital zircon ages from the Hematite Creek Group range from 1271 ± 10 Ma to 1650 ± 3 Ma. Five of the dates fall into the range 1437-1475 Ma. These zircon ages differ markedly from those of the basal Pinguicula Group, which range from 1841-3078 Ma.

Figure 16. *Clasts of zebra dolostone (Z) and micritic carbonate in intraclast conglomerate of Pinguicula Group unit C. Long dimension of photograph is about 25 cm.*

Stratigraphic description

The Hematite Creek Group is a diverse succession of carbonate and clastic rocks up to 1050 m thick, which overlies unit C of the Pinguicula Group. At the base, it commonly consists of up to 100 m of black-weathering shale intercalated with orange-weathering stromatolitic dolostone. Overlying the basal strata is thin to very thick-bedded, buff-, grey- and orange-weathering dolostone, intercalated with various lithotypes including: black-weathering shale; thin- to medium-bedded, black-, maroon- and buff-weathering, locally muscovite-bearing siltstone and sandstone; finely laminated grey- to maroon-weathering nodular limestone; and thick-bedded, locally cross-bedded, grey-weathering quartz arenite (Figs. 3; 17, 18). The dolostone beds, which constitute about 50% of the succession, commonly contain small (0.5-5 cm) dolostone rip-up clasts, nodules, and thin replacement-beds of black-weathering chert, and orange- to white-weathering nodules of sparry calcite, quartz, and jasper. Clusters of small (5- to15-cm-wide), closely spaced, orange-weathering stromatolites are uncommon, but scattered throughout the succession. Siltstone commonly displays desiccation cracks and ripple marks, locally with interference wave patterns. The siliciclastic component generally coarsens and is more mature up-section. Quartz arenite occurs as subordinate, thin tongues in the lower parts of the succession, and as thick layers (up to 200 m) toward the top, where it commonly predominates (Fig. 3).

Eisbacher (1981) named the quartz-arenite-dominated part of the Hematite Creek Group "unit E, Corn Creek quartzite" (of the original Pinguicula Group). However, in the process of regional mapping, the author was unable to reliably separate the Corn Creek strata from the rest of the Hematite Creek Group because quartz-arenite beds are interlayered throughout the succession, and because both micritic and stromatolitic dolostone occur above even the thickest quartz-arenite successions. The quartz-arenite component is therefore regarded as the Corn Creek lithofacies (PHCC) of the Hematite Creek Group, rather than as a separate unit.

Eisbacher (1981) identified a "unit F" of the Pinguicula Group, which he described as "thinly bedded particulate limestone." The strata of unit F were re-examined by the author in 1994 and are preferably described as finely laminated, locally nodular limestone underlain by a succession of maroon siltstone. These strata are exposed in an area of approximately 3 km^2, about 7 km south-southwest of Mount Profeit (Fig.19). They overlie a quartz-arenite-dominated part of the succession in a folded and thrust-faulted part of the Hematite Creek Group. Unit F and other parts of the Hematite Creek Group are overlain with angular unconformity by the basal conglomerate of the Windermere Supergroup. Despite their local prominence, the strata of unit F are likely to correlate with similar units in the region, particularly maroon siltstone and stromatolitic to massive dolostone which lie between thick tongues of quartz arenite located 1 km south of the study area at longitude 133°20' W (Fig. 20). For this reason, the strata which Eisbacher called unit F are not regarded as a distinct formation of the Hematite Creek Group, and may not be the highest strata preserved in the succession. Additional stratigraphic work is necessary to address the position and importance of Eisbacher's unit F.

Depositional history and significance

The Hematite Creek Group was deposited in shallow water as indicated by abundant near-surface sedimentary structures such as mudcracks, intraclasts, and stromatolites. Interference ripples in siltstone units suggest a shore-face origin. The tongues of quartz arenite in the Corn Creek facies may have been deposited in a beach or bar setting, whereas the dolostone successions may have been deposited in lagoonal or carbonate bank environments. More work is needed to properly characterize the sedimentary facies of this group,

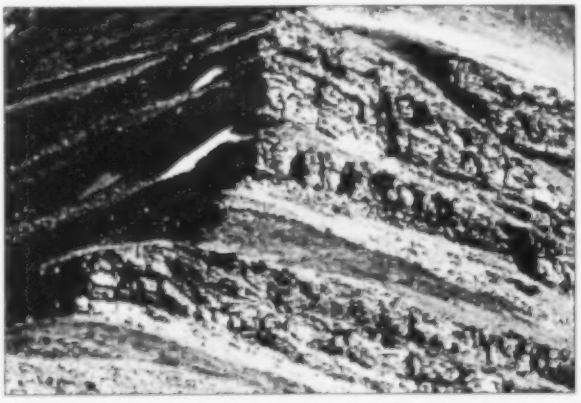

Figure 17. *Interbedded dolostone, shale, and micaceous sandstone in the stratigraphically middle part of the Hematite Creek Group, in the east-central part of 106C/14, east of the Carne mineral occurrence (Fig. 2). Distance along ridge is approximately 100 m. View to the southeast.*

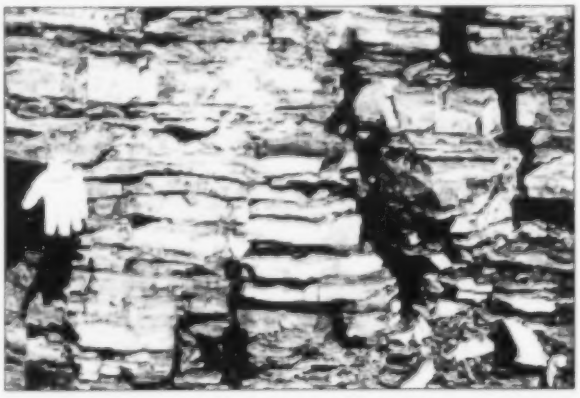

Figure 18. *Thinly bedded dolostone and shale of the Hematite Creek Group.*

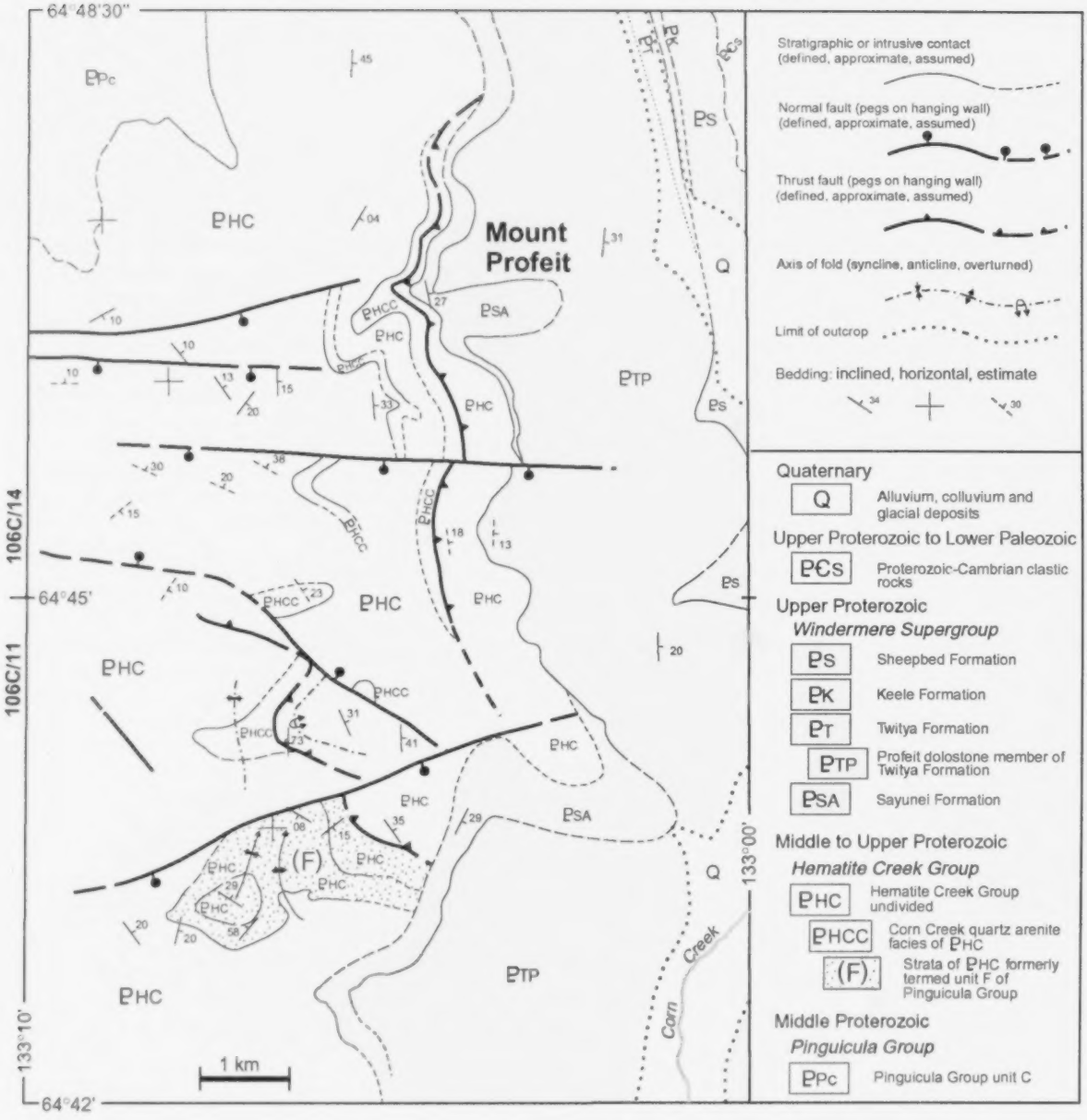

Figure 19. *Geological map of the southeastern study area (see Figs. 1 and 2 for location), and a small region of map area 106C/11, to the south. Folds and thrust faults in the Hematite Creek and Pinguicula groups are truncated by the Windermere Supergroup (shading). East-trending normal faults appear to be growth faults controlling pronounced variations in thickness of the basal conglomerate (PSA) of the Windermere Supergroup. Entire strata formerly called Pinguicula Group unit F by Eisbacher (1981) shown with stippling, provided for historical comparison.*

Figure 20. *Small stromatolites in dolostone beds near top of Hematite Creek Group.*

but the general environment of deposition can be broadly categorized as a carbonate-clastic platform without significant deep-water facies.

The Hematite Creek Group was deposited on the Pinguicula Group after an extensive hiatus. The age of the Pinguicula Group may extend from >1380 Ma to ca. 1270 Ma, although deposition most likely began at ca. 1380 Ma and ended a few million years or tens of million years later. The Hematite Creek Group is constrained to be younger than its youngest detrital mineral age, 1033 ± 9 Ma (Table A1-1). Thus, a lacuna of perhaps 300 million years is apparent between the groups. In the study area, evidence for this time-break is restricted to local karst features. In the eastern Ogilvie Mountains, however, an angular unconformity is present (Abbott, 1997), confirming a significant break between deposition of the groups.

The basin into which the Hematite Creek Group was deposited was tectonically active, and may have formed in response to Grenvillian orogenesis. The Grenville orogeny in Canada and correlative events on several continents were major events of magmatism, deformation and mountain building that extended from about 1250-1000 Ma (Hoffman, 1989; Ross et al., 1992). Paleocurrents and detrital zircon dates support the idea that the Grenville orogen in eastern Canada was a major source of clastic sediment in several Sequence B successions (Rainbird et al., 1992; 1997).

Direct evidence for Grenville-age activity in northwestern Canada is limited to granitic clasts, dated at ca. 1135 Ma (Jefferson and Parrish, 1989) and ca. 1129 Ma (Mortensen and Colpron, 1998), from the Coates Lake diatreme (of uncertain age), N.W.T. The diatreme crosscuts the Mackenzie Mountains Supergroup (Fig. 12), southeast of the study area. Whether the granitic clasts represent the development of a plutonized orogenic basement of Grenville age onto which Sequence B strata were deposited (Jefferson and Parrish, 1989), or an isolated stock emplaced at depth after the beginning of Sequence B sedimentation, is an important question. The most likely answer is that Grenville-age magmatism was extremely limited, as inferred by the apparent absence of exposed Grenville-age igneous rocks. In particular, the Wernecke Supergroup, Muskwa Assemblage, and Belt-Purcell Supergroup are devoid of known Grenville-age intrusions. The clast in the Coates Lake Diatreme is most favourably regarded as a sample of a rare, deep-seated intrusion, and not representative of substantial basement reworking. From this perspective, the statement by Jefferson and Parrish (1989) that the age of the clast defines "a maximum age for the Mackenzie Mountains Supergroup" is considered unjustified. The lower parts of the Mackenzie Mountains Supergroup may have been already deposited when a small volume of granitic magma intruded and solidified within the underlying crust.

It is unclear whether the crust of western Canada was generally stable, or undergoing modest contractional, extensional, or transcurrent tectonics at the time of the Grenville orogeny. Despite the absence of definitive evidence for Grenville-age deformation, and the weak case for granitic magmatism, the possibility remains that development of some basins of Sequence B were linked in some manner to the latter stages of the Grenville orogeny. One way in which these events may have been linked is through the Albany-Frazer tectonic belt in Australia, of Grenville age (Moores, 1991; Ross et al., 1992). This possibility is reasonable if ancestral Australia lay next to western Canada in the Proterozoic, as suggested by Bell and Jefferson (1987).

Ages of detrital minerals from the Hematite Creek Group infer sediment derivation from mainly the Grenville orogen in eastern North America and the mid-continent of the United States. All of the zircon dates, and five of the six muscovite dates, are younger than the zircon ages from the Pinguicula Group (Table A1-1). The oldest zircon from the Hematite Creek Group is ca. 1650 Ma, for which few local or regional sources are known. The nearest known source is the Narakay Volcanic Complex of the Hornby Bay Group in the Northwest Territories (Bowring and Ross, 1985). Five zircons gave ages in the mid-1400s. The most likely source for these grains is a suite of anorogenic granites in the central U.S. (Anderson and Morrison, 1992; Rainbird et al., 1997). Two zircons gave ages of ca. 1270 Ma, which are identical within error to the age of the Bear River dykes in the study area, and the Mackenzie dyke swarm and Coppermine volcanics (LeCheminant and Heaman, 1989) in the Northwest Territories. The oldest muscovite grain (ca. 2440 Ma) could have come from the western Canadian Shield. The remainder of the muscovite ages are between 1100 and 1000 Ma, and are most favourably explained by derivation from the Grenville orogen.

Rainbird et al. (1992, 1997) proposed that a trans-continental river system, in the style of the Amazon River, carried detritus from the eroding Grenville orogen to western and northwestern North America. Sediment from this river was deposited in basins of Sequence B. At the time when these sediments reached the Yukon region, the Pinguicula Group

had already been deposited, uplifted and locally tilted. The influx of clastic detritus into a carbonate platform produced a succession of alternating clastic and carbonate deposits, which characterizes the Hematite Creek Group. Thick tongues of mature sand, probably deposited on beaches and bars, became dominant in the upper parts of the Hematite Creek succession, forming the Corn Creek lithofacies, while carbonate and mudrock sedimentation continued in subordinate form, probably in lagoons and tidal flats.

Windermere Supergroup

Introduction

In the study area, the Windermere Supergroup rests with angular unconformity on the Hematite Creek Group (Figs. 4, 19, 21; Eisbacher, 1978). In contrast to the largely platformal Hematite Creek Group, the oldest Windermere sediments were deposited in more dynamic environments involving rifting and glaciation (Ross, 1991; Aitken, 1991; Narbonne and Aitken, 1995). Upper Windermere strata indicate a return to more stable conditions. Following correlations with strata in southern British Columbia by Gabrielse (1972), Eisbacher (1981) recognized five formations of the Windermere Supergroup in the Wernecke and Mackenzie mountains. All five are present in the study area, where total thickness is at least 2500 m.

The Windermere Supergroup is the main component of Sequence C (Young et al., 1979). The Windermere succession, and correlative strata which crop out from Alaska to Mexico, is considered to have formed in response to rifting and possible passive margin development (Eisbacher, 1981; Ross, 1991; Young, 1995; Mustard and Roots, 1997). Isotopic age determinations from rare volcanic rocks near the base of the succession, and correlations with strata on other continents

***Figure 21**. Angular unconformity between folded dolostone and shale of the Hematite Creek Group (PHC) and overlying Sayunei conglomerate (PSA) of the Windermere Supergroup, on northwest flank of Mt. Profeit. Folds are product of Corn Creek Orogeny. View to the southeast.*

(Eisbacher, 1985; Bell and Jefferson, 1987; Young, 1992) indicate that deposition began at ca. 780 Ma. Correlations and stratigraphic details are provided in numerous reports including Eisbacher (1981; 1985), Gabrielse and Campbell (1991), and Narbonne and Aitken (1995).

In the northern Cordillera, the Windermere Supergroup can be divided into two main sedimentary packages (Figs. 3, 4). The lower is the Rapitan Group, which consists largely of sediment gravity flows and tillites of proglacial and glacial origin (Eisbacher, 1981, 1985). The upper package consists of three clastic-carbonate grand cycles comprising (1) the Twitya-Keele formations, (2) the Sheepbed-Gametrail formations; and (3) the Blueflower-Risky formations (Narbonne and Aitken, 1995). Rocks of the third grand cycle are not present in the study area. The terms Hay Creek Group and Ekwi Supergroup have been used for parts of the Windermere succession in northern Canada (e.g., Yeo et al., 1978; Eisbacher, 1985; Norris and Dyke, 1997), but usage of these names has been discontinued in some recent publications (e.g., Narbonne and Aitken, 1995) and will not be applied in this report.

Current evidence infers that the Windermere Supergroup should also include the Coates Lake Group and an undated basalt member at the top of the uppermost Little Dal Formation (Sequence B) in the Mackenzie Mountains (Aitken, 1981). These strata were deposited in extensional basins prior to deposition of the Rapitan Group (Jefferson and Parrish, 1989). The basalt has been chemically linked to the nearby Tsezotene sills (Dudas and Lustwerk, 1997) and a quartz diorite plug (Jefferson and Parrish, 1989). The plug was dated by U-Pb (zircon) at 777 +2.5/-1.8 Ma, and the sills were dated by U-Pb (baddeleyite) at ca. 779 Ma (Fig. 12; LeCheminant et al., 1992). The basalt has also been correlated with the Mt. Harper Group volcanics, dated at 751 +26/-18 Ma (Mustard and Roots, 1997). Correlation among these "early Windermere" igneous rocks and the Little Dal basalt infers that the basalt and the overlying Coates Lake Group are favourably regarded as some of the first deposits of Sequence C in the northern Cordillera. Unconformities bounding the Coates Lake Group (Jefferson and Parrish, 1989) are best regarded as intra-supergroup, syntectonic features similar to those within the Rapitan Group (e.g., Eisbacher, 1981; this report).

Units in the study area

RAPITAN GROUP

The Rapitan Group is the lowest part of the Windermere Supergroup in the Wernecke Mountains, and consists of two units, the Sayunei and Shezal formations. Both are well exposed in the northeastern part of the study area (Fig. 2).

Sayunei Formation (PSA)

The Sayunei Formation is a poorly stratified succession of orange-, brown- and grey-weathering, matrix- to clast-

had already been deposited, uplifted and locally tilted. The influx of clastic detritus into a carbonate platform produced a succession of alternating clastic and carbonate deposits, which characterizes the Hematite Creek Group. Thick tongues of mature sand, probably deposited on beaches and bars, became dominant in the upper parts of the Hematite Creek succession, forming the Corn Creek lithofacies, while carbonate and mudrock sedimentation continued in subordinate form, probably in lagoons and tidal flats.

Windermere Supergroup

Introduction

In the study area, the Windermere Supergroup rests with angular unconformity on the Hematite Creek Group (Figs. 4, 19, 21; Eisbacher, 1978). In contrast to the largely platformal Hematite Creek Group, the oldest Windermere sediments were deposited in more dynamic environments involving rifting and glaciation (Ross, 1991; Aitken, 1991; Narbonne and Aitken, 1995). Upper Windermere strata indicate a return to more stable conditions. Following correlations with strata in southern British Columbia by Gabrielse (1972), Eisbacher (1981) recognized five formations of the Windermere Supergroup in the Wernecke and Mackenzie mountains. All five are present in the study area, where total thickness is at least 2500 m.

The Windermere Supergroup is the main component of Sequence C (Young et al., 1979). The Windermere succession, and correlative strata which crop out from Alaska to Mexico, is considered to have formed in response to rifting and possible passive margin development (Eisbacher, 1981; Ross, 1991; Young, 1995; Mustard and Roots, 1997). Isotopic age determinations from rare volcanic rocks near the base of the succession, and correlations with strata on other continents (Eisbacher, 1985; Bell and Jefferson, 1987; Young, 1992) indicate that deposition began at ca. 780 Ma. Correlations and stratigraphic details are provided in numerous reports including Eisbacher (1981; 1985), Gabrielse and Campbell (1991), and Narbonne and Aitken (1995).

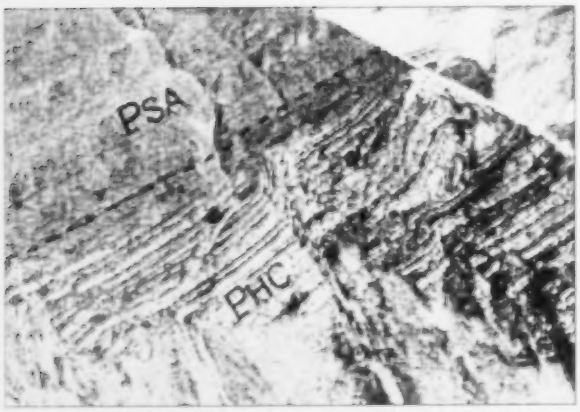

Figure 21. *Angular unconformity between folded dolostone and shale of the Hematite Creek Group (PHC) and overlying Sayunei conglomerate (PSA) of the Windermere Supergroup, on northwest flank of Mt. Profeit. Folds are product of Corn Creek Orogeny. View to the southeast.*

In the northern Cordillera, the Windermere Supergroup can be divided into two main sedimentary packages (Figs. 3, 4). The lower is the Rapitan Group, which consists largely of sediment gravity flows and tillites of proglacial and glacial origin (Eisbacher, 1981, 1985). The upper package consists of three clastic-carbonate grand cycles comprising (1) the Twitya-Keele formations, (2) the Sheepbed-Gametrail formations; and (3) the Blueflower-Risky formations (Narbonne and Aitken, 1995). Rocks of the third grand cycle are not present in the study area. The terms Hay Creek Group and Ekwi Supergroup have been used for parts of the Windermere succession in northern Canada (e.g., Yeo et al., 1978; Eisbacher, 1985; Norris and Dyke, 1997), but usage of these names has been discontinued in some recent publications (e.g., Narbonne and Aitken, 1995) and will not be applied in this report.

Current evidence infers that the Windermere Supergroup should also include the Coates Lake Group and an undated basalt member at the top of the uppermost Little Dal Formation (Sequence B) in the Mackenzie Mountains (Aitken, 1981). These strata were deposited in extensional basins prior to deposition of the Rapitan Group (Jefferson and Parrish, 1989). The basalt has been chemically linked to the nearby Tsezotene sills (Dudas and Lustwerk, 1997) and a quartz diorite plug (Jefferson and Parrish, 1989). The plug was dated by U-Pb (zircon) at 777 +2.5/-1.8 Ma, and the sills were dated by U-Pb (baddeleyite) at ca. 779 Ma (Fig. 12; LeCheminant et al., 1992). The basalt has also been correlated with the Mt. Harper Group volcanics, dated at 751 +26/-18 Ma (Mustard and Roots, 1997). Correlation among these "early Windermere" igneous rocks and the Little Dal basalt infers that the basalt and the overlying Coates Lake Group are favourably regarded as some of the first deposits of Sequence C in the northern Cordillera. Unconformities bounding the Coates Lake Group (Jefferson and Parrish, 1989) are best regarded as intra-supergroup, syntectonic features similar to those within the Rapitan Group (e.g., Eisbacher, 1981; this report).

Units in the study area

RAPITAN GROUP

The Rapitan Group is the lowest part of the Windermere Supergroup in the Wernecke Mountains, and consists of two units, the Sayunei and Shezal formations. Both are well exposed in the northeastern part of the study area (Fig. 2).

Sayunei Formation (PSA)

The Sayunei Formation is a poorly stratified succession of orange-, brown- and grey-weathering, matrix- to clast-

supported conglomerate and friable sandstone (Figs. 22, 23). The conglomerate contains clasts of subangular to rounded pebbles, cobbles and boulders of mainly quartz arenite, carbonate, siltstone, and micaceous siltstone, all of which may have been derived from the Pinguicula Group. The unit is discontinuous, and varies in thickness from 0 to 210 m. Abrupt variations in thickness appear to be related to east-trending normal faults in the underlying Hematite Creek Group, in the southeastern corner of the study area and in the adjoining map area a few kilometres to the south (Fig. 19). Where the Sayunei is absent, the stratigraphically higher Twitya Formation sits directly on the Hematite Creek Group (Fig. 19). A maximum age of deposition for the Sayunei formation in the Mackenzie Mountains was provided by a clast of leucogranite dated at 755 ± 18 Ma (Fig. 12; Ross and Villeneuve, 1997).

Shezal Formation (PSH)

The Shezal Formation consists of massive, unstratified, green- to rusty brown-weathering, matrix-rich diamictite containing pebbles and cobbles of dolostone, quartz arenite, and (?)greenstone. The sedimentary matrix is commonly well cleaved. Eisbacher (1981) identified striated clasts in the diamictite, and considered it to be of glacial origin. Thickness is considered to be >300 m; a more accurate estimate is hindered by the lack of internal layering. Thicknesses of 500 to 800 m were reported from sections elsewhere in the Wernecke and Mackenzie mountains by Eisbacher (1981), and Narbonne and Aitken (1995). In those localities, the Shezal Formation is known to lie stratigraphically between the Sayunei and Twitya formations. In the study area, a thrust or oblique-slip fault (the Snake River Fault) places the Shezal Formation onto younger units of the Windermere Supergroup (Fig. 24). In several localities to the west and southwest of the thrust fault, the Sayunei and Twitya are in direct stratigraphic contact and not separated by the Shezal diamictite (Fig. 24). These relationships infer that the Shezal diamictite was distributed in discontinuous patches prior to deposition of the Twitya Formation, and that faulting has since juxtaposed Shezal-absent and Shezal-present successions.

POST-RAPITAN STRATA

Twitya Formation (PT)

The Twitya Formation consists of mainly siltstone and dolostone, with minor sandstone and "grit" (very coarse sandstone to pebble conglomerate). The dolostone is an informal member named Profeit dolostone by Eisbacher (1981). The Twitya Formation disconformably overlies Sayunei conglomerate, or where the Sayunei is absent, overlies the Hematite Creek Group with angular unconformity (Figs. 19, 24). Twitya siltstone is brown-, dun-, and locally maroon-weathering, thin-bedded and laminated, locally calcareous, and commonly cleaved. It hosts several discontinuous intervals of sandstone and grit up to 10 m thick. The sandstone and grit are commonly crossbedded and fill local scours in the host siltstone. The grit beds occur with increasing abundance toward the top of the formation, and contain rounded pebbles of siltstone, sandstone, and carbonate. Both the sandstone and the grit contain angular rip-up clasts of black or green siltstone, orange dolostone, and shale. Ediacaran fossils are present in the upper part of the Twitya Formation and younger Windermere units (Narbonne and Hofmann, 1987).

Profeit dolostone (PTP) forms layers of variable thickness within the Twitya Formation. It is massive to medium-bedded, light grey-weathering, and commonly fetid. Oolites, intraclasts, oncolites, stromatolites and algal mats are common, indicative of shallow water deposition. Zebra texture and vugs are present locally. At Mount Profeit, the dolostone is about 1200 m thick and represents the entire Twitya Formation

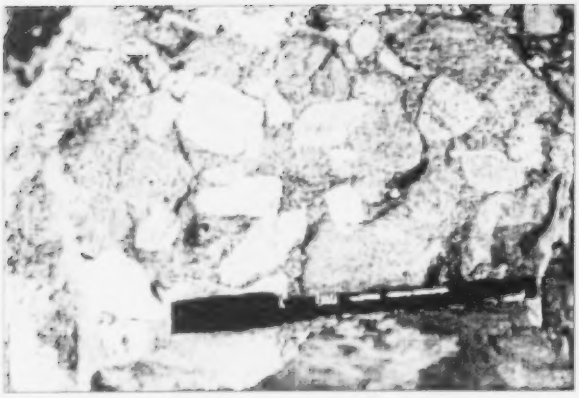

Figure 22. Subrounded clasts of siltstone and dolostone in Sayunei Formation (basal conglomerate of Windermere Supergroup).

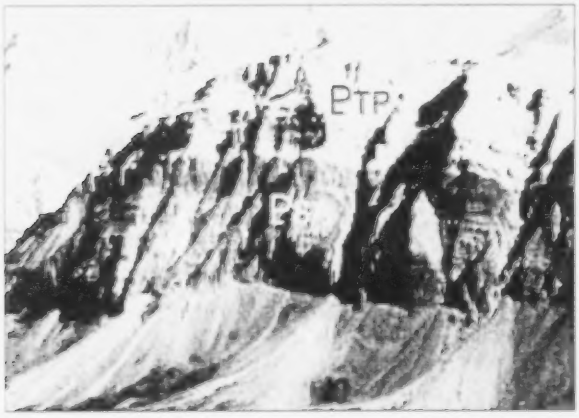

Figure 23. *Lower Windermere Supergroup: 200-m-thick basal conglomerate of the Sayunei Formation (PSA) disconformably overlain by Profeit dolostone (PTP), 7 km south of Mt. Profeit (Fig. 19). The Shezal Formation (PSH), which lies between these units in other localities, is absent. View to the southeast.*

supported conglomerate and friable sandstone (Figs. 22, 23). The conglomerate contains clasts of subangular to rounded pebbles, cobbles and boulders of mainly quartz arenite, carbonate, siltstone, and micaceous siltstone, all of which may have been derived from the Pinguicula Group. The unit is discontinuous, and varies in thickness from 0 to 210 m. Abrupt variations in thickness appear to be related to east-trending normal faults in the underlying Hematite Creek Group, in the southeastern corner of the study area and in the adjoining map area a few kilometres to the south (Fig. 19). Where the Sayunei is absent, the stratigraphically higher Twitya Formation sits directly on the Hematite Creek Group (Fig. 19). A maximum age of deposition for the Sayunei formation in the Mackenzie Mountains was provided by a clast of leucogranite dated at 755 ± 18 Ma (Fig. 12; Ross and Villeneuve, 1997).

Shezal Formation (PSH)

The Shezal Formation consists of massive, unstratified, green- to rusty brown-weathering, matrix-rich diamictite containing pebbles and cobbles of dolostone, quartz arenite, and (?)greenstone. The sedimentary matrix is commonly well cleaved. Eisbacher (1981) identified striated clasts in the diamictite, and considered it to be of glacial origin. Thickness is considered to be >300 m; a more accurate estimate is hindered by the lack of internal layering. Thicknesses of 500 to 800 m were reported from sections elsewhere in the Wernecke and Mackenzie mountains by Eisbacher (1981), and Narbonne and Aitken (1995). In those localities, the Shezal Formation is known to lie stratigraphically between the Sayunei and Twitya formations. In the study area, a thrust or oblique-slip fault (the Snake River Fault) places the Shezal Formation onto younger units of the Windermere Supergroup (Fig. 24). In several localities to the west and southwest of the thrust fault, the Sayunei and Twitya are in direct stratigraphic contact and not separated by the Shezal diamictite (Fig. 24). These relationships infer that the Shezal diamictite was distributed in discontinuous patches prior to deposition of the Twitya Formation, and that faulting has since juxtaposed Shezal-absent and Shezal-present successions.

POST-RAPITAN STRATA

Twitya Formation (PT)

The Twitya Formation consists of mainly siltstone and dolostone, with minor sandstone and "grit" (very coarse sandstone to pebble conglomerate). The dolostone is an informal member named Profeit dolostone by Eisbacher (1981). The Twitya Formation disconformably overlies Sayunei conglomerate, or where the Sayunei is absent, overlies the Hematite Creek Group with angular unconformity (Figs. 19, 24). Twitya siltstone is brown-, dun-, and locally maroon-weathering, thin-bedded and laminated, locally calcareous, and commonly cleaved. It hosts several discontinuous intervals of sandstone and grit up to 10 m thick. The sandstone and grit are commonly crossbedded and fill local scours in the host siltstone. The grit beds occur with increasing abundance toward the top of the formation, and contain rounded pebbles of siltstone, sandstone, and carbonate. Both the sandstone and the grit contain angular rip-up clasts of black or green siltstone, orange dolostone, and shale. Ediacaran fossils are present in the upper part of the Twitya Formation and younger Windermere units (Narbonne and Hofmann, 1987).

Profeit dolostone (PTP) forms layers of variable thickness within the Twitya Formation. It is massive to medium-bedded, light grey-weathering, and commonly fetid. Oolites, intraclasts, oncolites, stromatolites and algal mats are common, indicative of shallow water deposition. Zebra texture and vugs are present locally. At Mount Profeit, the dolostone is about 1200 m thick and represents the entire Twitya Formation

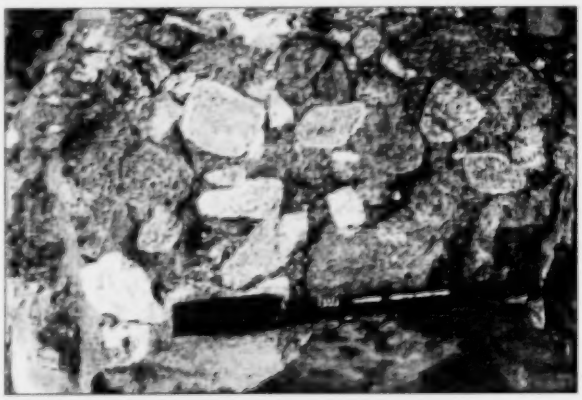

Figure 22. *Subrounded clasts of siltstone and dolostone in Sayunei Formation (basal conglomerate of Windermere Supergroup).*

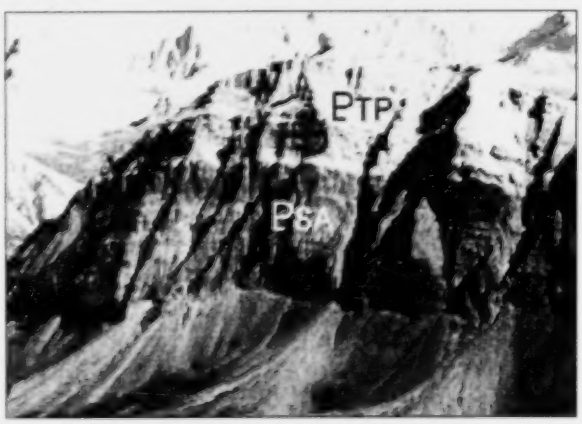

Figure 23. *Lower Windermere Supergroup: 200-m-thick basal conglomerate of the Sayunei Formation (PSA) disconformably overlain by Profeit dolostone (PTP), 7 km south of Mt. Profeit (Fig. 19). The Shezal Formation (PSH), which lies between these units in other localities, is absent. View to the southeast.*

(Fig. 23). It undergoes a spectacular facies change a few kilometres north of Mt. Profeit where it thins dramatically and separates into two main tongues, up to 45 m thick, within a thick succession of Twitya siltstone and grit (Eisbacher, 1981). In the northeastern part of the study area, the combined clastic and carbonate succession reaches 1.6 km thick.

Keele Formation (PK)

Conglomerate, diamictite and dolostone lie above the Twitya Formation (Fig. 24) and were considered by Eisbacher (1981) to belong to the Keele Formation, a usage followed in this report. The conglomerate overlies the Twitya Formation and consists of grey, rounded dolostone clasts, apparently derived from the Profeit dolostone. The overlying diamictite is

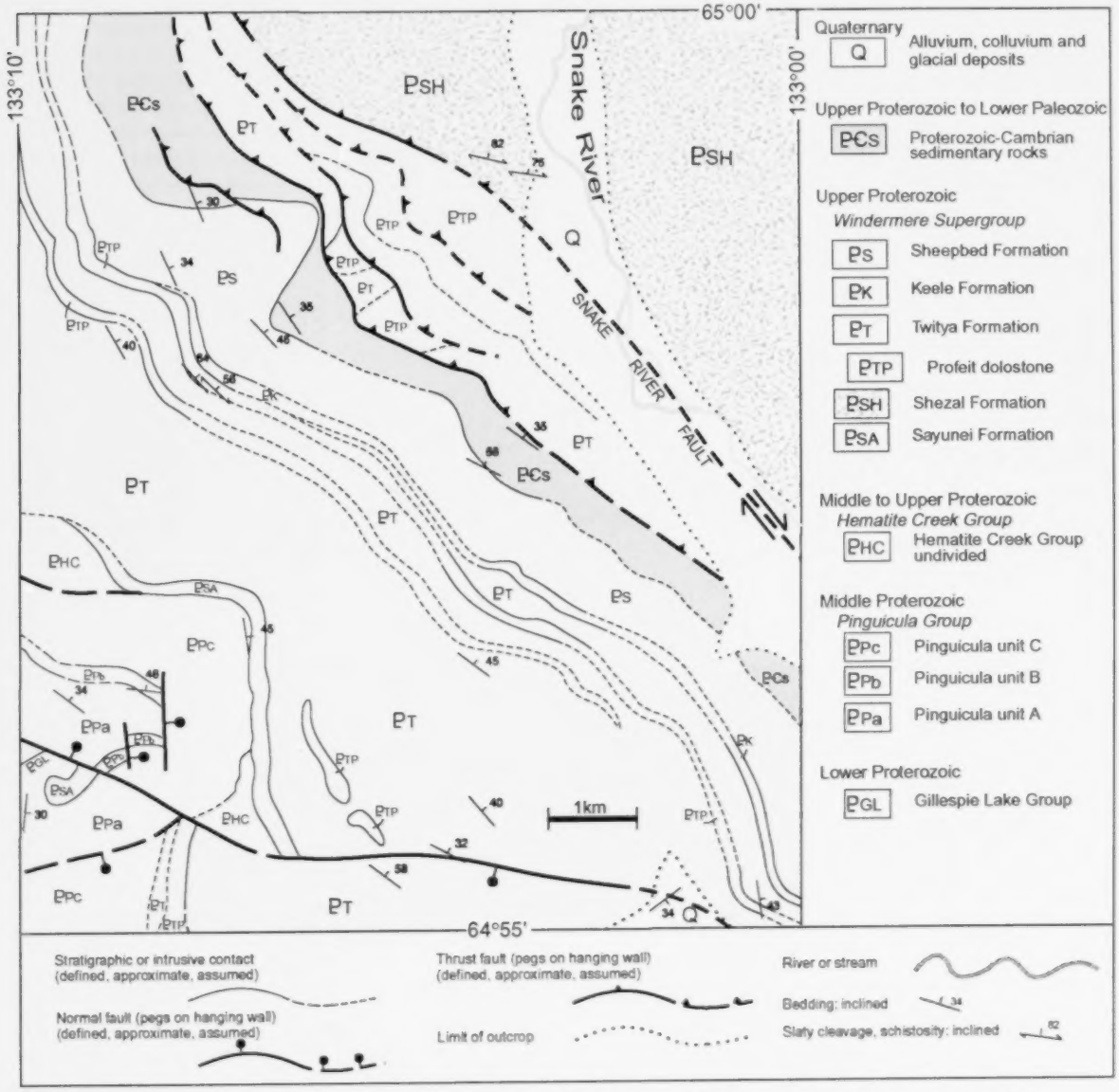

Figure 24. *Geological map of the northeastern study area (see Fig. 1 for location), showing thrust faults interpreted as transpressional features related to the dextral strike-slip Snake River Fault, and the angular unconformity between the Windermere Supergroup and the older Hematite Creek and Pinguicula groups. The Shezal Formation (PSH) of the Windermere Supergroup is present in the highest structural panel, but is missing from its correct position between the Sayunei and Twitya formations in the lowest panel.*

massive, light brown-weathering, and contains clasts of grey-weathering carbonate, light grey-weathering quartz sandstone, and black-weathering siltstone or (?)chert. The conglomerate and diamictite were observed at one location only, on a ridge crest at about latitude 64°58'N where they reach approximately 25 m thick. The diamictite may be correlative with the glaciogenic Ice Brook Formation in the Mackenzie Mountains (Aitken, 1991). Above the Twitya Formation is a thin succession (0- to 15-m-thick) of laminated, thin-bedded to massive, light orange- to cream-weathering micritic dolostone, known informally as the Teepee dolostone (Eisbacher, 1981; Aitken, 1991). The Keele Formation is discontinuous in the study area, and pinches out toward the northern and southern edges of the study area. In the Mackenzie Mountains, the Keele Formation ranges up to 500 m thick and is dominated by shoaling-upward cycles of dolostone and quartzite (Eisbacher, 1981).

Sheepbed Formation (PS)

The Sheepbed Formation overlies the Keele Formation. Where the Keele is absent, the Sheepbed sits directly on the Twitya Formation (Fig. 24). It is about 500 m thick and composed of recessive black-, dark brown-, and locally rusty-weathering shale, siltstone, and local calcareous siltstone. Toward the top of the succession are a few thin (<5 m) beds of buff- to grey-weathering silty limestone, which may correlate with the Gametrail Formation (Narbonne and Aitken, 1995). Flute casts and cross-beds are present locally in the siltstone.

Synthesis of depositional history

In the northern Cordillera, deposition of Sequence C first began in the Mackenzie and Ogilvie mountains. In the Mackenzie Mountains, the Little Dal basalt and the evaporite-bearing Coates Lake Group were deposited in extensional basins (Jefferson and Parrish, 1989). In the western Ogilvie Mountains, the broadly correlative Mt. Harper Group, including volcanic rocks with rift-signature geochemistry, were also deposited during crustal extension (Mustard and Roots, 1997). Deposition of these successions predated sedimentation in the Wernecke Mountains, where the Rapitan is the lowest formation. The extension, which controlled the deposition of Sequence C, is termed the Hayhook rift event (Fig. 4; Young et al., 1979; Jefferson and Parrish, 1989; Norris, 1997).

In the study area, Windermere sedimentation began with the Sayunei conglomerate, probably in a proglacial and synextensional environment dominated by sediment gravity flows (Eisbacher, 1985). The east-trending faults south of Mount Profeit coincide with sites of dramatic thickening of the Sayunei Formation, from 0 to 200 m. If these structures are growth faults, as they appear to be, then the direction of extension is inferred to be north-south. Northeast of the study area, deposition of jasper and hematite occurred at the top of the Sayunei Formation to form the huge Crest deposit of banded iron formation (Yeo, 1986).

Following Sayunei deposition, the Shezal Formation prograded over the conglomerates as a water-lain ice-marginal diamicton (Eisbacher, 1985). In the study area, the Shezal Formation is restricted to the highest identified structural panel in a minor thrust belt along the Snake River (Fig. 24). The contrast in the thickness of the Shezal deposits (>300 m) across these structures infers that the distribution of the Shezal diamicton prior to Twitya deposition was patchy. Young (1995) showed that the Rapitan glacial deposits and correlative Sturtian strata in Australia may have been produced by a once-continuous belt of glaciers which formed along highly elevated shoulders of an intracratonic rift valley (Young, 1995).

The Twitya Formation represents continued rift-related sedimentation, in the absence of glacial conditions, as carbonate mounds within a shale-turbidite basin. The overlying Keele Formation indicates carbonate-bank deposition, punctuated by Varangian-age (ca. 610 Ma) glaciation of the Ice Brook Formation. Subsequent marine transgression, possibly in response to another period of crustal extension, led to deposition of the shale-dominated Sheepbed Formation. Carbonate layers at the top of the Sheepbed (Gametrail Formation?) indicate a return to shallow-water conditions, after substantial infilling of the Sheepbed basin.

A lacuna of perhaps 50 million years probably exists between the Rapitan Group and the Twitya Formation. This unconformable relationship is evident from the uneven distribution of the Rapitan formations, and the estimated ages of the Rapitan, Twitya, and Keele successions. Beneath the Twitya Formation, formations of the Rapitan Group vary greatly in thickness, and are locally absent. Although the discontinuous nature of the Rapitan formations may be explained by localized, rift-controlled deposition, it may also be a product of a pre-Twitya depositional hiatus involving uplift and erosion.

Precambrian erosion as a cause of patchy preservation of the Rapitan Group is supported by the difference in interpreted ages of the Shezal and Twitya formations. The Rapitan strata are considered products of the Sturtian glaciation (700-800 Ma; Eisbacher, 1985), and are younger than 755 Ma, the age of a granite clast in the Sayunei Formation in the Northwest Territories (Ross and Villeneuve, 1997). In contrast, the upper part of the Twitya formation, with its <610 Ma Ediacaran fauna, is at least 90 million years younger (Hofmann et al., 1990; Young, 1995; G.M. Narbonne, pers. comm., 1996). The overlying Ice Brook Formation is regarded as a product of the Varangian glaciation (ca. 600 Ma; Eisbacher, 1985; Aitken, 1991; Young, 1995). The coarsely clastic Rapitan Group represents a period of rapid deposition, and is not an appealing unit to span the "missing" 700-610 Ma range of time. The Twitya Formation indicates more gradual sedimentation, but is considered unlikely to extend as far back in time as ca. 700 Ma (G.M. Narbonne, pers. comm., 1996), especially since the entire Twitya succession is represented locally by shallow-water carbonates of Profeit dolostone.

Upper Proterozoic to Lower Paleozoic sedimentary rocks (PCs)

A succession of quartz arenite, dolostone, siltstone and conglomerate overlies the Windermere Supergroup. It is restricted to the eastern edge of the study area, and was not studied in depth in this research program (Fig. 24). According to Narbonne et al. (1985), it correlates with the Backbone Ranges and Vampire formations, and unit 11 of Fritz et al. (1983). Quartz arenite and interbedded pinkish orange-weathering carbonate compose the succession in the northeastern part of the map area. The quartz arenite is typically trough cross-bedded to plane-bedded, grey- to rusty-weathering, with very well rounded grains cemented with either silica or brown-weathering carbonate. These units pinch out to the south-southeast, east of Mount Profeit, where they are replaced by a younger succession of dark grey- to buff-weathering carbonate and minor sandstone, and overlying conglomerate, dolostone and siltstone. Total thickness of unit PCs exposed in the map area is about 350 m (Narbonne et al., 1985).

Lower Paleozoic sedimentary rocks (CDs)

Description

Carbonate and clastic rocks of Lower Paleozoic age crop out in the western part of the study area, and to the east of the study area above unit PCs (Figs. 2, 3, 4). They belong to an assemblage of generally shallow-water strata, which extend in a broad arc from the Mackenzie Mountains to the Ogilvie Mountains (Fig. 5). This assemblage defines a shelf environment called Mackenzie Platform (Gordey and Anderson, 1993; for additional and alternative nomenclature

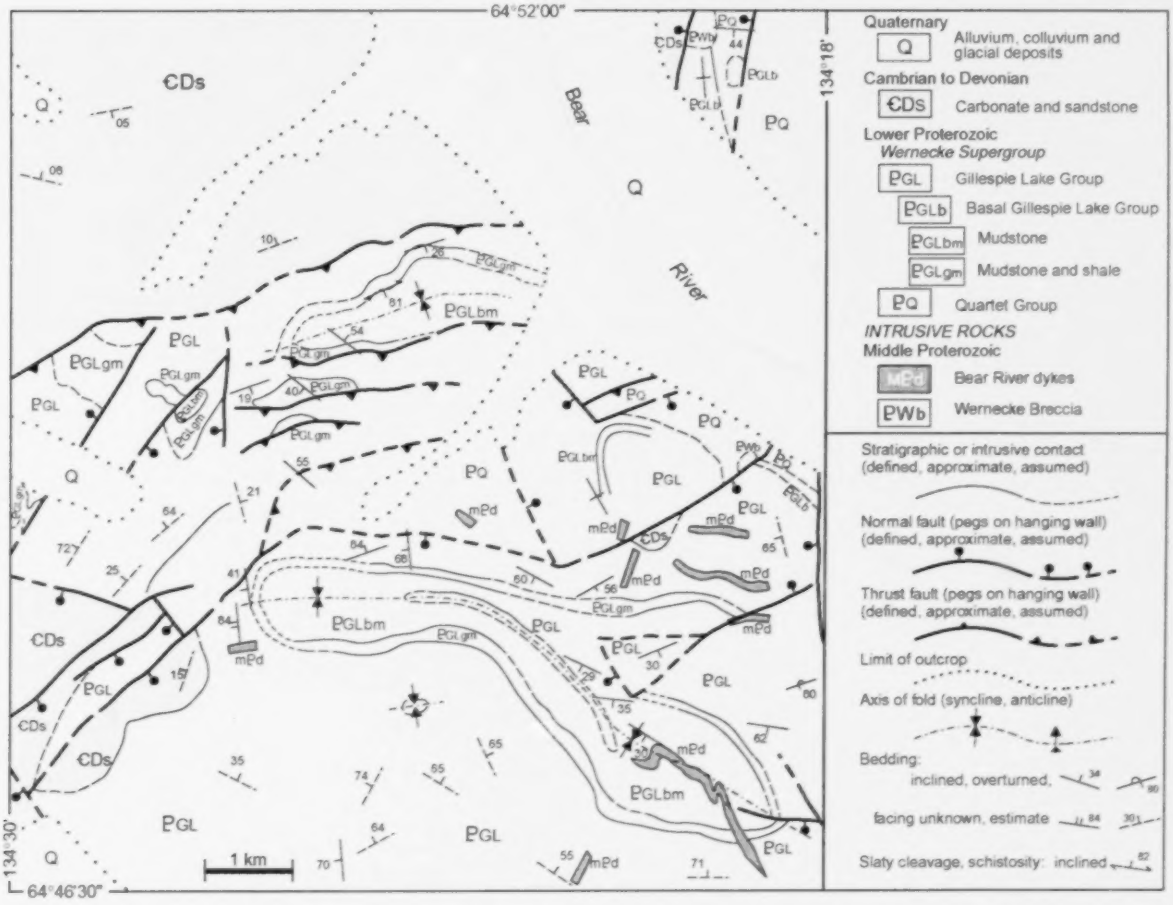

Figure 25. *Geological map of the southwestern study area (see Fig. 1 for location), showing north-verging folds and faults (Laramide orogeny), the ca. 1.27 Ga Bear River dykes (locally folded), and the unconformity between Paleozoic and Lower Proterozoic strata.*

see Abbott, 1997; Norris, 1997; and Fritz, 1997). Deeper water counterparts to this platform include the Richardson and Blackstone troughs of northern Yukon, and the Selwyn Basin of south-central Yukon (Norford, 1997; Cecile, 1982). Together, these basinal and platformal regions constitute a thick miogeoclinal wedge, which developed along the western edge (in present geographic coordinates) of ancestral North America. This miogeocline is considered to have developed in response to crustal extension and continental separation beginning in the Late Proterozoic with Windermere rifting and basin formation (Gabrielse and Campbell, 1991).

In the study area, the lowest strata comprise thinly bedded maroon- and green-weathering mudstone, siltstone, conglomerate, and dolostone. They are well exposed in the southwestern part of the study where they are perhaps 50 m thick, but are either very thin or absent to the north. They are tentatively correlated with the Middle Cambrian Slats Creek Formation (Fritz, 1997). Above these mainly siliciclastic rocks is a thick succession (ca. 2 km) of massive, commonly recrystallized grey dolostone. This carbonate succession was mapped by Green (1972) as units 8 and 10, and is probably correlative with unit CDb in northern Yukon (Norris, 1984), and the Franklin Mountain and Mount Kindle formations in the Mackenzie Mountains (Cecile, 1982). On the basis of these correlations, the dolostone is considered to range in age from Cambrian to Middle Devonian.

Unit CDs directly overlies the Lower Proterozoic Wernecke Supergroup in the western part of the map area (Figs. 25 (see previous page), 26). Missing are intervening strata of the Pinguicula Group, the Hematite Creek Group, the Windermere Supergroup and unit PCs. These intermediate-aged successions are abundant in the eastern part of the study area, where they have a cumulative thickness of about 7 km. Their complete absence in the west implies that either they were not deposited there, or they were eroded prior to deposition of unit CDs (or some combination of the two). In the opinion of the writer, substantial Proterozoic erosion is required to explain the missing strata, as non-deposition of all of these successions seems unlikely. As suggested in the section on Structural History, depositional and erosional patterns in both Proterozoic and Phanerozoic time may have been partly controlled by protracted activity of the Fairchild Fault (Fig. 2). This down-to-the-east normal fault merges to the north with the Richardson Fault Array (Fig. 5), which is known to have been active in both Proterozoic and Tertiary times (Norris, 1997, and related works).

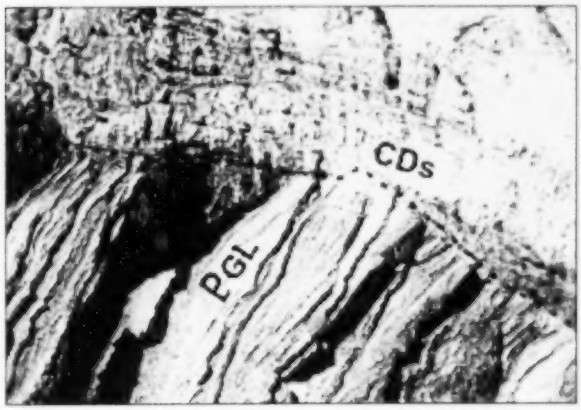

Figure 26. *Angular unconformity between Lower Paleozoic carbonate (CDs) and underlying deformed Gillespie Lake Group (PGL), near confluence of Bond Creek and Wind River, 10 km west of study area. Pre-Paleozoic folding probably occurred mainly during Racklan Orogeny, but geometry may have been affected by subsequent Corn Creek Orogeny. View is to the southwest.*

Intrusive Rocks

Wernecke Breccia (PWb)

Introduction

Numerous breccia zones known collectively as Wernecke Breccia are present within the Wernecke Supergroup in the study area and elsewhere in the Wernecke Mountains (Figs. 2, 4, 5). The breccia zones generally range in area from 0.1 to 10 km^2 and crop out in curvilinear arrays over an area of about 3500 km^2 (Archer and Schmidt, 1978; Bell, 1986a, b; Wheeler and McFeely, 1991; Thorkelson and Wallace, 1993b). Typical Wernecke Breccia consists of metasomatized, angular to subangular clasts in a hydrothermally precipitated matrix; disseminated or fracture-controlled specular hematite is ubiquitous. Lane (1990) called similar breccias in the Ogilvie Mountains (Fig. 5), 300 km west of the study area, the Ogilvie Mountains breccias. A single breccia zone hosting the Nor mineral occurrence is known from the Richardson Mountains, 150 km north-northwest of the study area (Fig. 5; Tempelman-Kluit, 1981). The brecciation and related hydrothermal activity occurred in early Middle Proterozoic time.

Considerable mineralization of Cu, Co, U, and Au in and around the breccia zones has been an intermittent focus of mineral exploration. Bell and Jefferson (1987), Bell (1989), Gandhi and Bell (1990) and Hitzman et al. (1992) noted similarities between Wernecke Breccia and other breccias of similar age and environment. These authors drew connections with breccias of the Olympic Dam mine in Australia on the basis of similar age, and physical and mineralogical characteristics, and probable proximity of ancestral North America with ancestral Australia in Proterozoic time. Chemical analyses of Wernecke Breccia are listed in Table A3-1.

Physical and mineralogical characteristics

Breccia clasts are mainly derived from dolostone, siltstone, slate, phyllite, and schist of the Wernecke Supergroup (Fig. 27). Clasts from igneous intrusions are locally abundant (Figs. 28, 29) where breccia zones crosscut or engulf dykes and stocks of the Bonnet Plume River intrusions (ca. 1.72 Ga). Volcanic clasts, derived from the Slab volcanics, have been observed in one location. At all localities, the clasts are set in a matrix composed of smaller rock fragments and a variety of hydrothermally deposited minerals which, although dominated by feldspars, micas, carbonates, quartz, and chlorite, locally include chalcopyrite, cobaltite, brannerite, and bornite. Clast colours vary from their source-rock colours of black, grey, brown and green, to alteration hues of pink, red and maroon, reflecting variable degrees of metasomatism. In most breccia zones, red and pink clasts are abundant, and secondary minerals such as dolomite and specular hematite are common as disseminated grains, fracture fillings, and veins. In many of the clasts, sedimentary laminations are visually

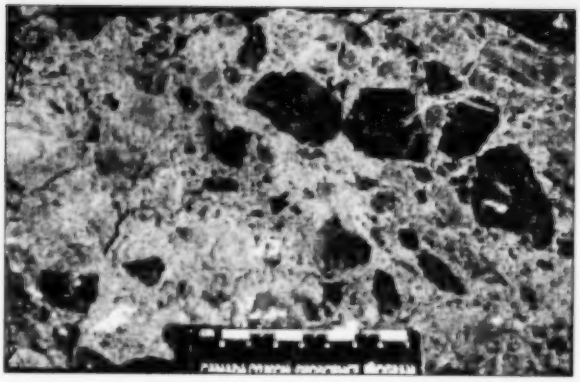

Figure 27. *Typical Wernecke Breccia (ca. 1.6 Ga) from the Pika occurrence (Fig. 2), containing variably metasomatized clasts of siltstone and dolostone.*

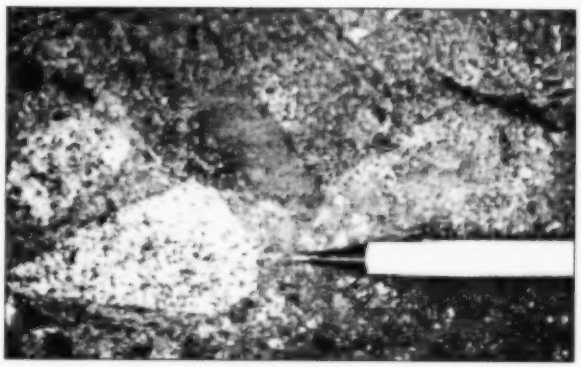

Figure 28. *Clasts of quartz-albite syenite (light grey, left of pencil; ca. 1.725 Ga) of the Bonnet Plume River intrusions in Wernecke Breccia (ca. 1.6 Ga) at the Porphyry mineral occurrence (106C/14; Fig. 2).*

Figure 29. *Angular fragments of fine-grained anorthosite (white) of the Bonnet Plume River intrusions in Wernecke Breccia (dark grey matrix) near margin of a fine-grained anorthosite megaclast, Olympic mineral occurrence, west of Bonnet Plume River (Fig. 2).*

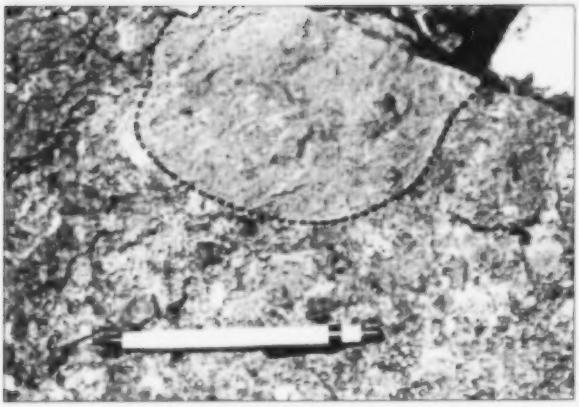

Figure 30. *Well-rounded cobble-sized clast of altered siltstone of the Wernecke Supergroup in Wernecke Breccia, Olympic mineral occurrence (Yukon Minfile, 1997).*

enhanced due to preferential reddening of alternating layers. Apparently metasomatism was more active along coarser, more permeable horizons. The red colouration is attributed to growth of disseminated earthy hematite and, in some cases, potassium feldspar. Wernecke Breccia is typically well cemented and indurated. At the Slab, Otter and Fairchild (Fig. 2) occurrences, breccia is moderately friable and the clasts are typically drab grey — apparently containing little earthy hematite. These differences may reflect variations in temperature, pressure and composition of the hydrothermal fluids.

Clasts of country rock are typically angular to subangular, but are locally subrounded to rounded (Fig. 30). Clast rounding is attributed to abrasion with wallrock and "milling" among clasts during breccia activity. At several localities, clasts have marked embayments, and are commonly rimmed with specularite. The irregular shapes of these clasts, which contrast with the angular to rounded shapes of most other fragments, is suggestive of soft-sediment deformation (Laznicka and Edwards, 1979). However, the Wernecke Supergroup, from which these clasts were derived, was fully lithified and locally metamorphosed prior to brecciation (details given below). The irregular, embayed clasts are more favourably considered as products of aqueous corrosion or "digestion" during breccia-related hydrothermal activity.

Clast sizes are generally in the granule, pebble and cobble-size ranges, although boulder-size clasts are scattered in many breccia zones. Megaclasts (>2 m in diameter) of sedimentary or metamorphic rock are present in some of the breccia zones, notably at the Face and Slab mineral occurrences (Fig. 2). At the Slab occurrence, megaclasts of schist and altered siltstone are common, some of which are 20 m or more across (Bell and Delaney, 1977). Megaclasts of intrusive rock are present in many of the breccia zones, including those at the Slab, Bel, Pika, Anoki, and Olympic mineral occurrences where blocks of diorite up to 0.5 km long are engulfed by breccia. At the Slab occurrence, breccia surrounds a rotated mega-block (0.25 x 0.6 km) of the Slab volcanics (Fig. 13).

Large metasomatic aureoles are typically present in the breccia zones and in the surrounding country rocks. Regionally, metasomatism began before and ended after brecciation, although specific metasomatic effects and timing vary among breccia zones. Generally, these effects include precipitation, in both clasts and matrix, of various phases including specular and earthy hematite, magnetite, dolomite, siderite, chlorite, biotite, muscovite, quartz, albite, microcline, rutile, titanite, brannerite, apatite, monazite, cobaltite, chalcopyrite, and (rare) bornite.

The igneous clasts in breccia zones are also typically metasomatized. Metasomatic effects on igneous protoliths include replacement of plagioclase by albite, potassium feldspar or scapolite, replacement of augite by chlorite or actinolite, and hornfelsic or fracture-controlled growth of carbonate, quartz, wollastonite, hematite and magnetite.

Laznicka and Edwards (1979) examined breccias in the Dolores Creek map area and concluded that metasomatism usually led to sodium enrichment and potassium depletion. Conly (1993) developed a generalized paragenetic sequence based on study of several specimens of breccia from the Slats Creek map area. Using optical and electron microscopy he determined that breccia matrix was dominated by early growth of feldspar, followed by quartz, mica, and carbonate, and late growth of mainly hematite. Chalcopyrite was inferred to have grown in the middle and late stages of paragenesis. Hitzman et al. (1992) developed a hydrothermal model based on sodic metasomatism (deepest), potassic metasomatism (mid-depth) and sericite-carbonate metasomatism (shallowest). This model was partly based on the premise that, at the time of Wernecke Breccia emplacement, the Wernecke Supergroup was essentially undeformed and that the stratigraphically lower parts of the Wernecke Supergroup were structurally deeper. However, recent work (summarized below and detailed in the Structural History section) has revealed that the Wernecke Supergroup was deformed into upright to overturned folds during the Racklan Orogeny, prior to the brecciation. This finding calls into question the field basis for the depth zones described by Hitzman et al. (1992), although the general idea that some breccia zones formed at greater depths and higher temperatures than others remains plausible.

Breccia matrix locally has streaks defined by variable grain size and mineral abundances, a characteristic probably produced by precipitation during rapid fluid streaming. Late-stage quartz and carbonate veins commonly cut across both clasts and matrix of previously cemented breccias. The breccias and surrounding metasomatic aureoles are locally enriched in Cu, Co, Au, Ag and U. Factors controlling metal distribution are poorly understood, although gold concentrations generally correlate with those of copper.

Mineralization is discussed further in the Mineral Occurrences section.

Contacts between breccia and country rock vary from abrupt to gradational. Some of the abrupt contacts are faults across which breccia is juxtaposed with unaltered, unbrecciated strata, commonly of the Gillespie Lake Group. Others, however, are intrusive contacts along which breccia was emplaced into unaltered country rock (Figs. 31, 32). This relationship was noted near the Pitch and Slats mineral occurrences (Fig. 2), where red-clast hematitic breccia intrudes siltstone and dolostone unaffected by metasomatism. There, metasomatism of breccia clearly preceded and did not continue after breccia emplacement. The reverse relationship is recognized in the Slab occurrence, where relatively unaltered breccia was emplaced into mineralized (Cu, Co, U), previously metasomatized rock. Crosscutting (intrusive) relations are evident at most locations, and are particularly well preserved at the Gremlin occurrence, 20 km northwest of the study area.

Gradational relationships between breccia and host rock are well developed in several places, especially around the Bland, Eaton, and Ford occurrences (Fig. 2). In such localities, unaltered host rock (typically dark siltstone) grades into altered host rock (typically purplish brown with red, bedding-controlled bands, and hematitic fractures) which grades into progressively more metasomatized and fractured rock toward the breccia. The transition from host rock to breccia occurs across a zone of crackle breccia in which highly fractured host rock has undergone incipient fragmentation. Metasomatic alteration increases toward the breccia zone, where clasts are typically reddened, and specular hematite is abundant, particularly in matrix. The width of the metasomatic aureole from unaltered siltstone to Wernecke Breccia ranges from metres to hundreds of metres. In contrast, at the Gnuckle mineral occurrence (Fig. 2), a zone of breccia is locally dominated by clasts of black shale that lack visible metasomatic effects. At this location, the shale clasts were apparently torn from country rock and rapidly cemented to form breccia without undergoing appreciable metasomatic alteration.

Petrofabrics indicate the timing of brecciation relative to other deformational events. Randomly oriented clasts of kinked schist and slate of the Fairchild Lake Group occur in Wernecke Breccia at the Slab and Julie occurrences (Fig. 2). The matrix of the breccia at these locations is devoid of secondary petrofabrics, indicating that synkinematic metamorphism and kinking (the first and second phases of deformation in the study area) preceded brecciation.

Style of breccia emplacement

Previous workers have suggested various modes of occurrence for Wernecke Breccia, including diatremes (Tempelman-Kluit, 1981; Bell and Delaney, 1977), phreatomagmatic explosions (Laznicka and Edwards, 1979), modified evaporite diapirs (Bell, 1989), or mud diapirs (Lane, 1990). The hypothesis of mud diapirism is untenable because the Wernecke Supergroup was lithified and locally metamorphosed at the time of brecciation. The hypothesis of evaporite diapirism is also rejected because brecciation occurred after development of cleavage and schistosity, kink bands, upright to overturned folds, and lower greenschist-grade metamorphism — features attributed to Racklan Orogeny. The possibility of salt preservation and diapiric uprise after Racklan Orogeny seems extremely remote. In addition, there is no stratigraphic evidence that a formation of evaporite ever existed beneath the Wernecke Supergroup.

Phreatomagmatic explosion as the cause of brecciation may, upon initial consideration, seem appealing because it recognizes the close spatial relationship between the Bonnet Plume River intrusions (mainly diorite) and Wernecke Breccia. The igneous intrusions typically occur as mega-clasts in breccia, or as small dykes and stocks near breccia zones. This spatial coincidence led Laznicka and Edwards (1979), and Laznicka and Gaboury (1988) to suggest that magmas emplaced into unconsolidated sediment of the Wernecke Supergroup triggered phreatomagmatic explosions and formation of Wernecke Breccia. Although this explanation accounts for the co-spatial relationship between the breccias and the igneous intrusions, it is rejected for three reasons. Firstly, the intrusions were emplaced about 100 million years prior to breccia formation (based on recent geochronology, Table A1-1). Secondly, the Wernecke Supergroup was entirely lithified, twice deformed, and variably metamorphosed up to lower greenschist grade before brecciation. Thirdly, juvenile igneous clasts have not been recorded by the author, or by any previous workers, despite considerable petrographic investigation.

The rejection of the unconsolidated-phreatomagmatic model leaves unresolved the issue of why the breccias and the igneous intrusions occur together. Perhaps the best explanation is that the hydrothermal solutions responsible for brecciation rose through the crust along the same pathways used previously by the magmas. Deep-seated fracture systems may have developed prior to or during igneous activity, and may have acted as long-lived "plumbing systems" for subsequent metasomatic events (cf. Roots and Thompson, 1988).

The diatreme model of breccia genesis is consistent with much, but not all, of the existing data. A diatreme origin can account for: (1) intrusion of breccia into a succession of rock which had previously undergone deformation and igneous intrusion; (2) intense fracturing of country rock; and (3) rounding of clasts by milling within moving breccia. However, two principal features of the breccias require qualification of this model. Firstly, breccia clasts were derived from the Wernecke Supergroup and the igneous intrusions it hosts. Importantly, clasts of lower crustal or mantle affinity, such as gneiss or peridotite, have not been reported from any of the breccias. Consequently, the clastic component of Wernecke Breccia appears to have originated almost entirely

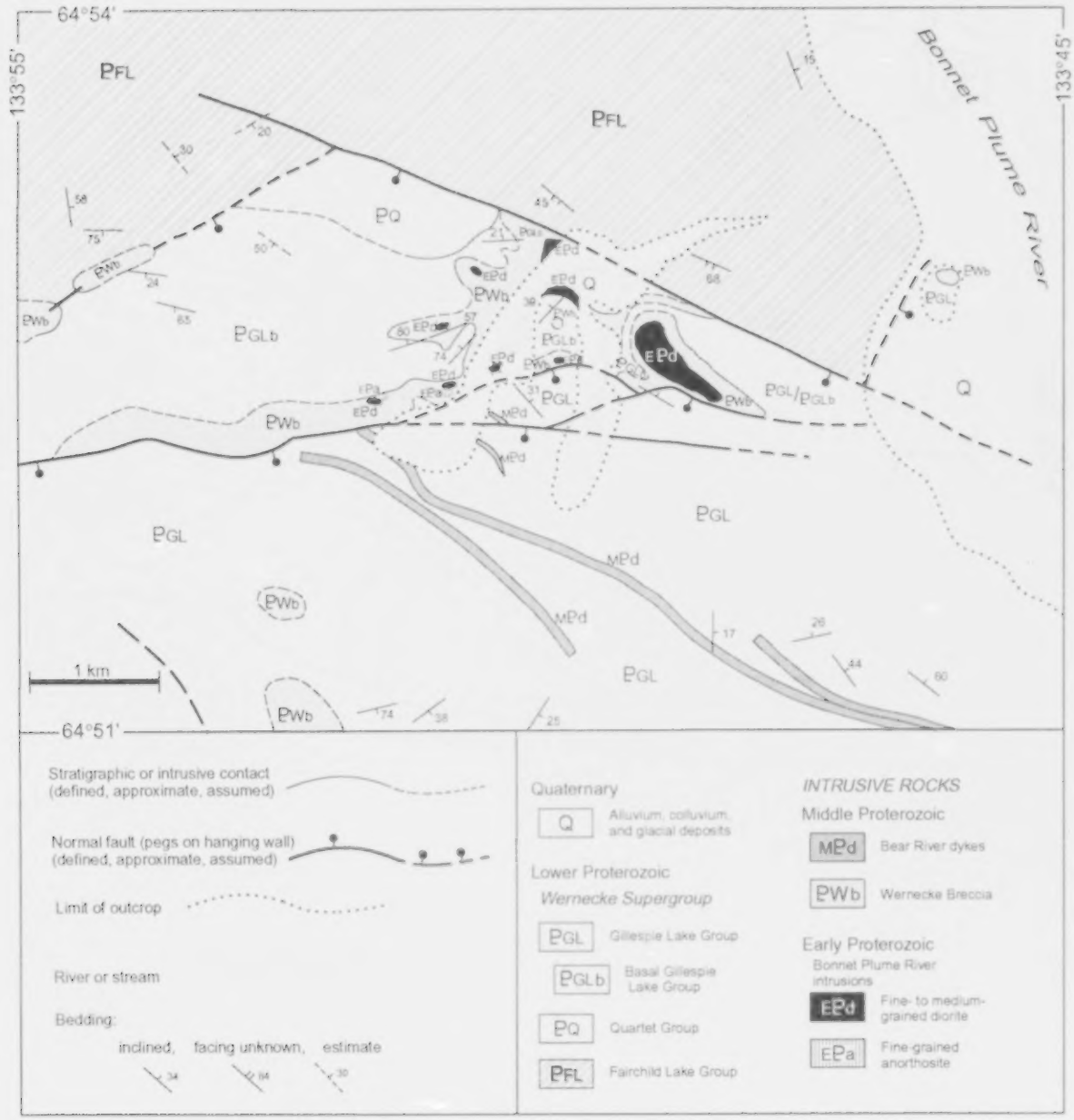

Figure 31. *Geological map of the central study area (see Fig. 1 for location), showing zones of Wernecke Breccia, distributed along normal faults, and containing numerous megaclasts of the Bonnet Plume River intrusions (ca. 1.71 Ga). The long dykes are correlated with the Bear River dykes (ca. 1.27 Ga). The faults to the north of the breccia zones locally cut out the entire Quartet Group, inferring a throw of about 4 km.*

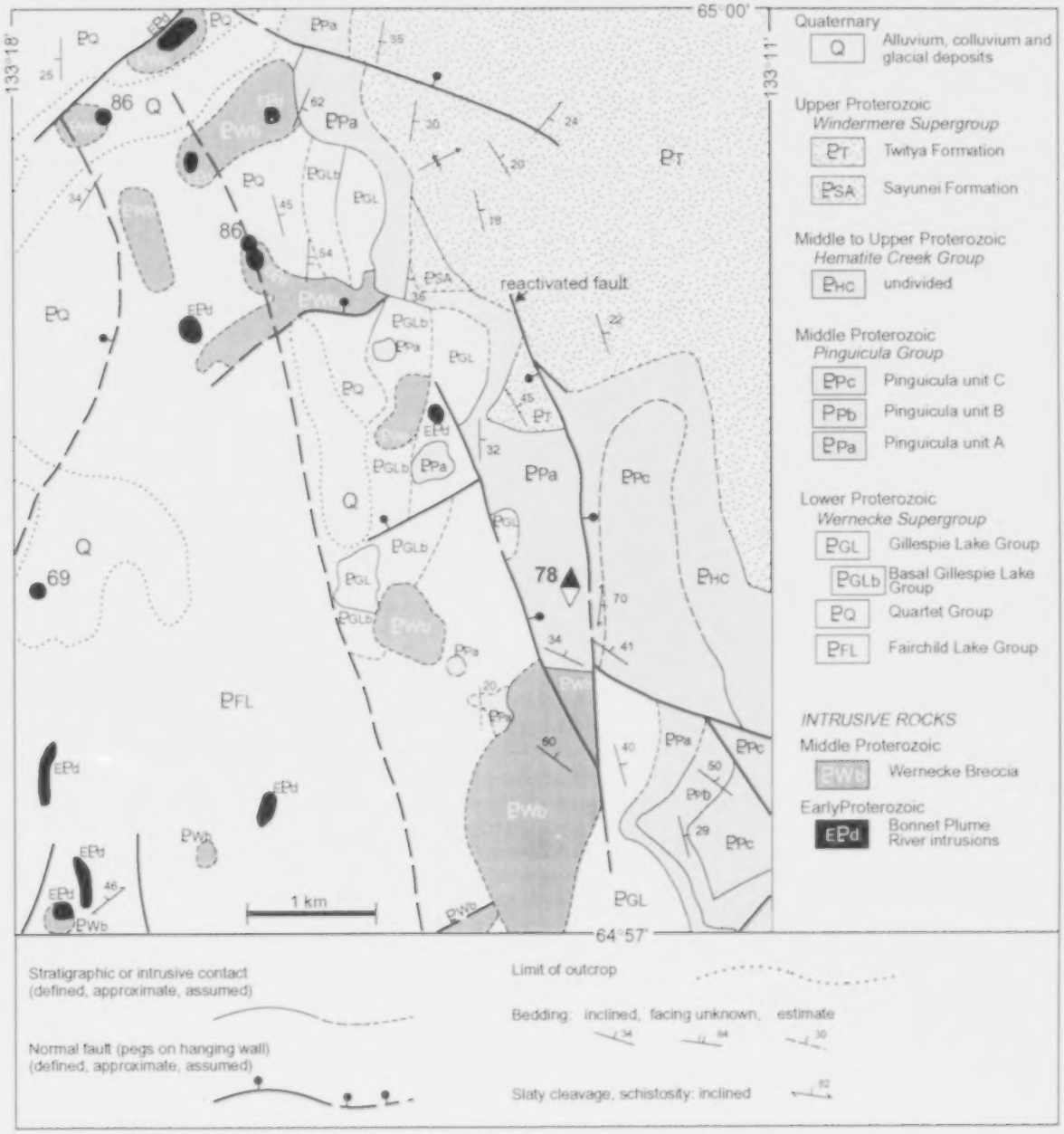

Figure 32. Geological map of the north-central part of map 106C/14, showing the unconformities separating the Pinguicula and Hematite Creek groups (light shading) from the Wernecke Supergroup and the Windermere Supergroup (stippling). Wernecke Breccia (dark shading), commonly enclosing bodies of the Bonnet Plume River intrusions (black) is nonconformably overlain by the Pinguicula Group. See Fig. 1 for location. Mineral occurrences (numbered) are listed in Figs. 2, 38.

Figure 31. Geological map of the central study area (see Fig. 1 for location), showing zones of Wernecke Breccia, distributed along normal faults, and containing numerous megaclasts of the Bonnet Plume River intrusions (ca. 1.71 Ga). The long dykes are correlated with the Bear River dykes (ca. 1.27 Ga). The faults to the north of the breccia zones locally cut out the entire Quartet Group, inferring a throw of about 4 km.

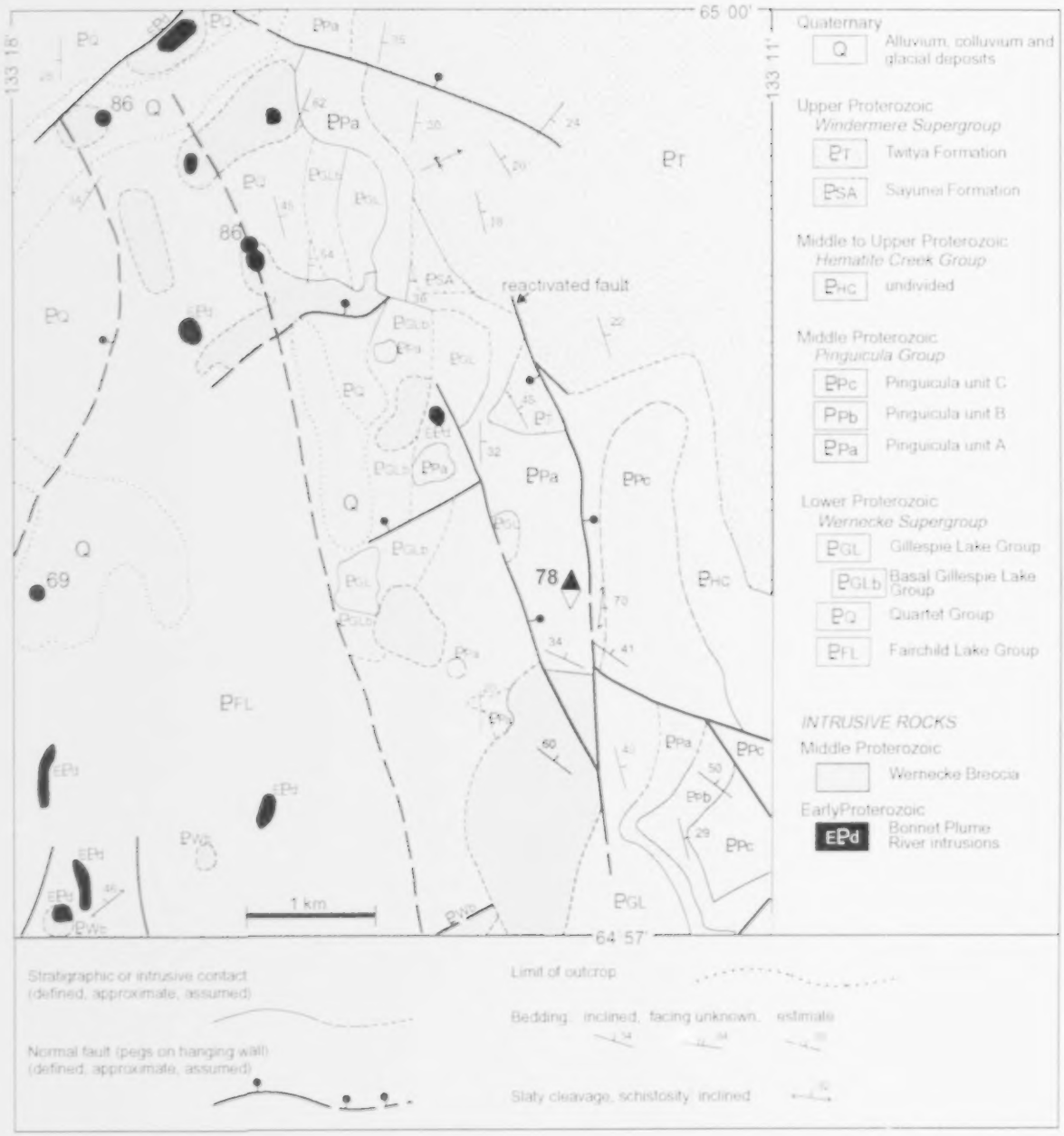

Figure 32. *Geological map of the north-central part of map 106C/14, showing the unconformities separating the Pinguicula and Hematite Creek groups (light shading) from the Wernecke Supergroup and the Windermere Supergroup (stippling). Wernecke Breccia (dark shading), commonly enclosing bodies of the Bonnet Plume River intrusions (black) is nonconformably overlain by the Pinguicula Group. See Fig. 1 for location. Mineral occurrences (numbered) are listed in Figs. 2, 38.*

within Wernecke Supergroup, although a deeper source for the mineralizing fluids is plausible. Secondly, the breccia zones are distributed in curvilinear arrays, and are typically related to steep faults. This style of distribution implies a strong supracrustal influence in the location of breccia development. Furthermore, the breccia zones do not tend to decrease in size and abundance with increasing depth. Zones of Wernecke Breccia thereby differ from typical diatremes which are generally depicted as downward-tapering conical pipes (e.g., Mitchell, 1991).

Wernecke Breccia is most favourably modeled as a set of hydrothermal and/or phreatic breccias whose location was partly determined by crustal features. Brecciation was probably largely caused by explosive expansion of volatile-rich fluids. Venting of the breccia may have occurred above the Slab volcanics or correlative strata. An igneous influence is implied by common enrichments of Fe, Cu and Co. The fluids may have been partly derived from volatile-rich residual liquids of hypothetical, fractionating tholeiitic magma chambers located beneath the Wernecke Supergroup (cf. Hitzman et al., 1992; Thorkelson and Wallace, 1993a). Breccia generation could represent a late magmatic stage, when the chambers were largely solidified, and fluids enriched in Fe and volatiles escaped toward the surface and boiled explosively.

Igneous intrusions of Wernecke Breccia-age (ca. 1.6 Ga) are unknown in Yukon (but are inferred beneath the Mackenzie Mountains in the Northwest Territories; Jefferson and Parrish, 1989). The Slab volcanics, with a probable age-range of 1.59-1.73 Ga, are the only known igneous rocks in the region, which could represent breccia-age magmatism. The Slab volcanics are presently correlated by the author with a stock of alkali-feldspar syenite of the Bonnet Plume River intrusions (ca. 1.72 Ga). The lack of an obvious igneous source (although appropriate intrusions may exist at depth) suggests that the breccia-forming fluids were released during general heating of the crust during a regional tectonic and thermal disturbance. Perhaps this fluid event is related to lithospheric extension and crustal heating related to a large upwelling of asthenospheric mantle.

Timing of brecciation and hydrothermal activity

Field observations and isotopic dates from this investigation have added important constraints to the timing of geological events related to breccia genesis. Previously, the only reliable isotopic date was a U-Pb monazite age of 1.27 ± 0.04 Ga from the Nor breccia in the Richardson Mountains (Fig. 12; Parrish and Bell, 1987). Although the date is considered analytically sound, its relevance to the breccia province as a whole was uncertain because the Nor breccia is about 130 km from the nearest neighbouring zones of Wernecke Breccia. Archer et al. (1986) reported other isotopic dates on U-bearing whole rocks and minerals such as brannerite and pitchblende. Their oldest date approached 1.2 Ga, but most were much younger. The highly discordant nature of these dates renders them difficult to interpret, and they are considered unreliable estimates of the ages of initial brecciation and subsequent hydrothermal activity (Parrish and Bell, 1987).

Three isotopic dates reveal that hydrothermal activity in Wernecke Breccia zones occurred in at least three pulses. Titanite (sphene) from the breccia zone on the eastern side of the Slab mineral occurrence was dated at ca. 1595 Ma (Table A1-1; Fig. 12; R.A. Creaser, pers. comm., 1994). This date is interpreted to represent the time of initial brecciation and hydrothermal activity. The second date was from the Slab volcanics, which lie within the Slab breccia zone. Rutile from mafic lava was dated at ca. 1380 Ma (Table A1-1; Fig. 12; J.K. Mortensen, pers. comm., 1997), and is considered to represent a second pulse of hydrothermal activity within the Slab breccia zone. The third date is from a Bear River dyke in the northwestern part of the study area, 2 km south of the Bland mineral occurrence. Baddeleyite from the dyke was dated at ca. 1270 Ma (Fig. 12; Mortensen, pers. comm., 1996; Thorkelson et al., 1998). The dyke, which lies about 1 km from a breccia zone, is crosscut by veinlets of earthy and specular hematite, a feature that characterizes much of the hydrothermal activity associated with Wernecke Breccia bodies. The baddeleyite date is considered to be the time of dyke emplacement, so the metasomatism is constrained to be ca. 1270 Ma or younger.

Almost all of the brecciation and metasomatism occurred during the first event (ca. 1.59 Ga). This relationship is evident from the nature of the contact between Wernecke Breccia and the Pinguicula / lower Fifteenmile groups. The contact is well exposed at several places in both the Wernecke and Ogilvie mountains. The ca. 1.38 Ga Pinguicula and Fifteenmile strata nonconformably overlie the breccia, and there is no evidence that hydrothermal activity extended above the contact (Fig. 33). Furthermore, a locally well developed

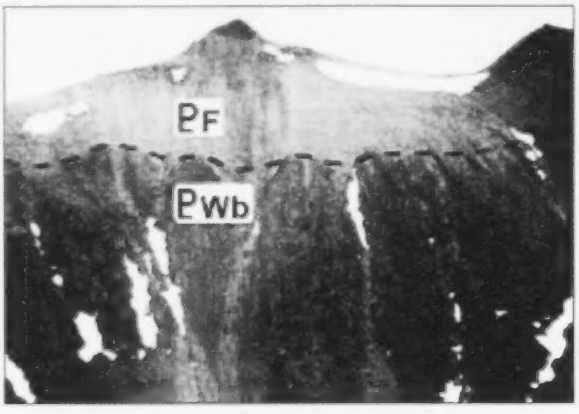

Figure 33. *Non-conformity between black shale of the basal Fifteenmile Group (PF) and Ogilvie Mountains breccia (PWb), in the Ogilvie Mountains. Ogilvie Mountains breccia is considered equivalent to Wernecke Breccia.*

regolith and weathered zone is present at the top of the breccia zones, confirming that brecciation and hydrothermal activity ended prior to Pinguicula / Fifteenmile sedimentation (Fig. 34). The subsequent hydrothermal events at ca. 1.38 Ga and <1.27 Ga are therefore considered to be minor and very localized.

The surges of hydrothermal fluids that brecciated and mineralized the Wernecke Supergroup were produced in a huge area of crust, spanning the Wernecke, Ogilvie and part of the Richardson mountains (Fig. 5). The fluid surges were probably generated by a sudden event of crustal heating. The simplest explanation for rapid heating is regional upwelling of mantle and emplacement of mafic igneous intrusions in the lower crust. A magmatic episode at the time of breccia formation, ca. 1.59 Ga, is not recognized in Yukon, although the undated Slab volcanic succession remains a possible candidate. Apparently, intrusive igneous rocks, which may have triggered hydrothermal activity and brecciation, are unexposed, and restricted to the middle and lower crust, as speculated by Laznicka and Gaboury (1988). Preliminary radiogenic isotope analysis suggests that the fluids involved in Wernecke brecciation may have been derived principally from upper crustal sources (R.A. Creaser, pers. comm., 1994).

Initial brecciation and metasomatism at 1595 Ma is not linked to concomitant igneous activity in Yukon, but it does coincide with emplacement of the Hiltaba intrusions and eruption of the Gawler Range volcanics in South Australia at about 1585-1595 Ma (Creaser, 1995). These igneous rocks are genetically linked to hematitic breccias at the Olympic Dam mine. Gandhi and Bell (1990) and Hitzman et al. (1992) have grouped the Wernecke Breccias in the same metallogenetic class as those at the Olympic Dam mine. Preliminary carbon and oxygen isotope data from carbonate minerals of Wernecke Breccia (R.P. Tayor and A. Fallick, pers. comm., 1994) are similar to those from the Olympic Dam mine (Oreskes and Einaudi, 1992). These similarities strengthen stratigraphic

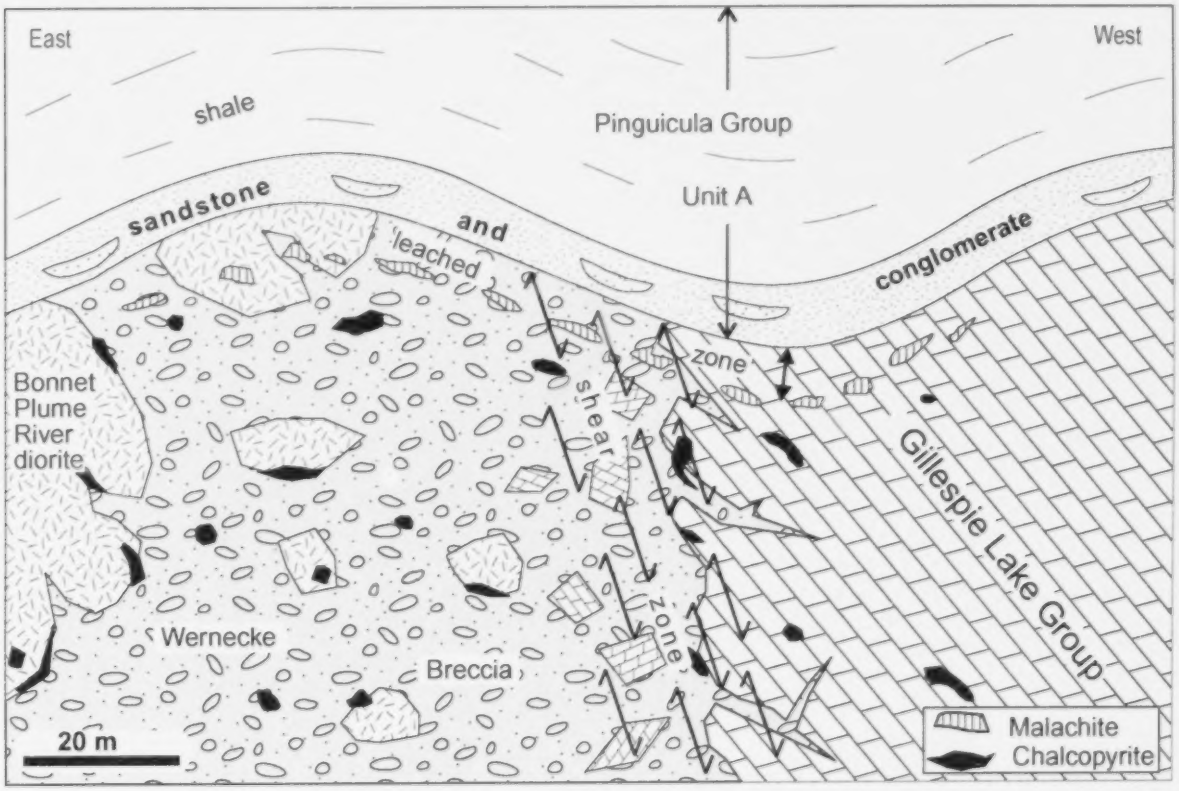

Figure 34. Geological relations at the Pika mineral occurrence, in the west-central part of map 106C/14 (see Fig. 2 for location). The geological history of this area includes: (1) deposition of the Gillespie Lake Group (Wernecke Supergroup); (2) intrusion of Bonnet Plume River diorite, and folding of the Wernecke Supergroup during Racklan Orogeny (relative timing of magmatism and deformation uncertain); (3) emplacement of Wernecke Breccia, metasomatism of breccia and host rock, and hydrothermal precipitation of chalcopyrite; (4) localized shearing; (5) deep weathering, and leaching of copper from chalcopyrite to form a weak supergene-oxide zone of malachite; (6) deposition of the Pinguicula Group; and (7) regional folding.

correlations between Australia and western Canada drawn previously by Bell and Jefferson (1987) who suggested that ancestral North America and Australia were linked in Proterozoic time. If these suggestions are correct, then the driving force for initial Wernecke brecciation could have been felsic igneous rocks similar to the Hiltaba intrusions and Gawler Range volcanics. The overall cause of Australian-Canadian brecciation at 1.59 Ga may be the impingement of a large mantle plume head, which caused regional heating of the continental lithosphere. In Yukon, heating may have been sufficient to drive metamorphic dehydration leading to voluminous hydrothermal activity in the upper crust. In South Australia, a higher thermal flux and mafic magmatism may have led to crustal melting and "anorogenic" felsic magmatism (Creaser, 1995).

Subsequent hydrothermal events may be tied to more local igneous events. Metasomatism at 1380 Ma was probably caused by emplacement of the Hart River mafic intrusions, which crop out 25-50 km to the south and southwest of the study area (Figs. 4, 5; Green, 1972; Abbott, 1997). Subsequent metasomatism at ca. 1270 Ma in the Richardson Mountains, and at ca. 1270 Ma or later in the study area, is most favourably linked to emplacement of the Bear River dykes, which intruded the western and central parts of the study area at ca. 1270 Ma (Table A1-1; Fig. 4). These dykes may be considered part of the large 1267-1270 Ma Mackenzie igneous event which includes the Muskox intrusion, the Coppermine lavas, and the giant radiating Mackenzie dyke swarm of the Northwest Territories and adjacent parts of the Canadian Shield (LeCheminant and Heaman, 1989; Francis, 1994). The 1.38 and 1.27 Ga events reflect episodic flow of hydrothermal solutions along igneous pathways and through the breccia zones.

Unconformable relationship with the Pinguicula Group

Brecciation and breccia-related metasomatism were complete before deposition of the Pinguicula Group (Wernecke Mountains) and the Fifteenmile Group (western Ogilvie Mountains). The basal strata of both groups abruptly truncate breccia textures and metasomatic alteration (Fig. 32). Beneath the unconformity in both locations, regolith formation and weak supergene oxide mineralization indicate widespread weathering during the Middle to Late Proterozoic. This interval is also considered as the time of erosion of the Slab volcanics (Fig. 4).

The sub-Pinguicula unconformity is well displayed at the Pika mineral occurrence, east of Bonnet Plume River and south of Dolores Creek (Fig. 34; Thorkelson and Wallace, 1994a). Beneath the unconformity at this location, weak supergene enrichment is evident in Gillespie Lake dolostone and a zone of Wernecke Breccia. The supergene zone sits between the unconformity and hypogene copper mineralization in the breccia, the dolostone, and bodies of the Bonnet Plume River intrusions. Directly beneath the overlying Pinguicula Group, and extending downward for about 12 m, the rocks are pale, friable, and devoid of Cu mineralization. The bottom metre of this pale zone contains abundant veinlets and disseminated grains of malachite. Beneath the malachite-rich zone, the breccia and dolostone have normal texture and colour. The pale, crumbly rock is interpreted as a leached zone produced by subaerial weathering prior to deposition of the Pinguicula Group. The thin zone hosting malachite is regarded as a weak supergene oxide zone. A corresponding supergene sulphide zone may be present but was not identified. Leaching and supergene oxide enrichment have also been observed near the Anoki mineral occurrence in the northeast part of the study area (Fig. 32).

In the western Ogilvie Mountains, the Ogilvie Mountains breccias have been described as intruding both the Wernecke Supergroup and the lower Fifteenmile Group (Lane, 1990; Thompson, 1995). Recent investigations of critical localities by the author and J.G. Abbott demonstrate that the Ogilvie Mountains breccias do not intrude any strata of the Fifteenmile Group. Instead, the Fifteenmile Group rests nonconformably on breccia that has been leached, locally silicified, and locally enriched by supergene oxide mineralization in a style strikingly similar to that of sub-Pinguicula rocks in the Wernecke Mountains (Fig. 33; Abbott et al., 1997).

Three localities in the Ogilvie Mountains, which had been mapped as breccia intruding the Fifteenmile Group, were closely examined. At one site, the basal Fifteenmile rests on crumbly, yellowish breccia. This "leached" breccia extends downward for about 1 m where it abruptly grades into breccia with normal characteristics such as green-red mottled colour, disseminated specular hematite, and a chlorite-carbonate matrix. At the base of the leached zone, malachite staining is locally present. The strong metasomatic alteration, which is pervasive in the breccia, is nowhere evident in the overlying Fifteenmile strata.

At the second site, the leached zone in the breccia underlying the Fifteenmile Group is 5 to 10 m thick. The top two metres of this zone are a silicic regolith consisting largely of red and white chalcedony. Above the unconformity, buff carbonate and maroon shale of the lower Fifteenmile Group show no evidence of brecciation or metasomatism. At the third site, a breccia body mapped by Thompson (1995) as Ogilvie Mountains breccia is herein considered to be younger than, and unrelated to the Ogilvie Mountains breccias. This breccia occurs in the lower Fifteenmile group as intensely fractured dolostone surrounded by veins of red-weathering white carbonate spar. Nowhere does the breccia show evidence of iron and silica metasomatism ubiquitous to the Ogilvie Mountains breccia and Wernecke Breccia. Rather, the breccia at this site belongs to a common type of carbonate-only breccias, probably related to dewatering or dolomitization, which occurs sporadically in most Early Proterozoic to Early Paleozoic dolostone formations in the Ogilvie and Mackenzie mountains.

Other localities, where zones of Ogilvie Mountains breccia were interpreted to lie within the Fifteenmile Group, were also investigated. In all cases, the Fifteenmile Group is either faulted against or unconformably overlies the breccia bodies. Evidence for Ogilvie Mountains breccia crosscutting any of the Fifteenmile strata is completely lacking. These observations confirm that the Fifteenmile Group, like the Pinguicula Group, was deposited on a substrate of Wernecke Supergroup and its hosted zones of Wernecke Breccia after a lacuna involving erosion, weathering, and regolith formation.

Model for brecciation and mineralization

A model relating igneous events, brecciation, and mineralization has been developed. In the first stage (pre-breccia stage), mineralization related to intrusive events preceded Wernecke brecciation. In this stage, dioritic intrusions were emplaced at ca. 1.71 Ga, and the Slab volcanics erupted between ca. 1.7 and 1.6 Ga. During this interval, probably during one or both of these igneous events, Cu-Co-Au mineralization occurred as fracture fillings and disseminated grains in the Wernecke Supergroup in a manner similar to copper-porphyry mineralization. Pre-breccia mineralization is well displayed at the Slab occurrence (Fig. 2), where the Wernecke Supergroup and Bonnet Plume River diorite are mineralized but crosscutting bodies of Wernecke Breccia are not. Pre-breccia metasomatic activity may have been local rather than widespread.

In the second stage (main brecciation), a large pulse of uprising Fe-rich fluids expanded explosively at ca. 1.595 Ga. These phreatic explosions produced numerous subterranean breccia zones whose initial porosity ranged from 10-70%. Widespread metasomatism and hydrothermal precipitation preceded, accompanied, and followed the brecciation. In some zones, brecciation occurred several times. Faulting may have been active concurrently. Venting above the breccia zones almost certainly occurred, perhaps forming maar-like explosion pits above the Slab volcanics or the Wernecke Supergroup. (Vent deposits are nowhere preserved because of extensive Middle and Late Proterozoic denudation.) Mineralization of Cu, Co, Au and U occurred during the hydrothermal activity. Most or all of the breccia zones are considered to have developed during this stage as younger rocks are generally unaffected by brecciation and metasomatism. In addition the large and potentially correlative breccia bodies at the Olympic Dam mine in Australia formed at this time.

In the third and fourth stages (late hydrothermal flow), some of the breccia zones served as conduits for hydrothermal fluids generated during the 1.38 Ga (Hart River) and 1.27 Ga (Bear River-Mackenzie) igneous events. These hydrothermal events are not evident in the preserved parts of the Pinguicula Group. Geysers, hot springs, and volcanoes may have been active concurrently, but no record of these possible surficial features remains. Mineralization of Cu, Co, Au and U may have occurred during these stages. Concomitant brecciation has not been documented.

Igneous Rocks

Introduction

Igneous intrusions of Early and Middle Proterozoic ages are present as dykes and stocks, and as clasts in Wernecke Breccia. Three temporally distinct suites of intrusions have been identified, and each represents low to moderate volumes of magmatic activity in the study area. The intrusions are fine- to medium-grained, with rare pegmatitic segregations, and range in composition from mafic to intermediate. The Slab volcanics are probably comagmatic with the oldest intrusive suite; volcanic equivalents of the other suites are not preserved in the study area. Chemical analyses are provided in Table A3-1.

Bonnet Plume River intrusions (EPd)

Numerous small igneous bodies, herein named the Bonnet Plume River intrusions, are present in the Wernecke Supergroup and in zones of Wernecke Breccia (Figs. 31, 32). In the Wernecke Supergroup, the intrusions crosscut sedimentary strata and possibly low-grade schist (the timing of magmatism relative to schist formation remains uncertain). In Wernecke Breccia, the igneous rocks are present as bodies up to tens of metres across.

Crosscutting relations are clear at several localities, including the Porphyry mineral occurrence (Fig. 2) where a small stock of quartz-albite syenite is partly surrounded by Wernecke Breccia. On its eastern side, the stock crosscuts, and is chilled against, siltstone beds of the Fairchild Lake Group.

Bodies of the Bonnet Plume River intrusions are present in Wernecke Breccia in a variety of sizes ranging from a few millimetres to several tens of metres across. The smaller bodies — those up to about 10 m wide — are confidently identified as clasts of the breccia. Small clasts are conspicuous at the southern end of the Porphyry mineral occurrence (Fig. 28), and at the Olympic occurrence (Fig. 29). Some of the largest bodies that can be clearly identified as clasts lie within a breccia zone on the southeastern part of the Slab occurrence. Igneous bodies larger than about 10 m across are present at numerous localities. Some of the largest bodies have exposed areas of up to 0.1 km^2, and may also be megaclasts within Wernecke Breccia (Fig. 31). If so, they must have been displaced in a nearly piston-like manner, moving through the crust in conduits not much wider than themselves, entrained and lubricated by a surging mass of Wernecke Breccia. However, these larger bodies are preferably regarded as stocks which are approximately in situ, and which have been intruded along their margins by hydrothermal fluids and Wernecke Breccia.

The Bonnet Plume River intrusions were solidified prior to engulfment by Wernecke Breccia. This relationship is evident from: (1) the absence of contact metamorphism of

Wernecke Breccia adjacent to the igneous rock; (2) the general absence of chilled margins in the intrusions where they are in contact with the breccia (many clasts show phaneritic textures everywhere along their edges); (3) the absence of chilled, hyaloclastic fragments within the breccia; and (4) the absence of offshoots of igneous material crosscutting Wernecke Breccia.

Four preliminary U-Pb zircon dates (Table A1-1; Fig. 4; J.K. Mortensen, pers. comm., 1995) confirm that the Bonnet Plume River intrusions were intruded by zones of Wernecke Breccia, and not vice versa. Three of the bodies sampled clearly intrude the Fairchild Lake Group. The oldest of these is the quartz-albite syenite at the Porphyry occurrence, dated at 1725 ± 5 Ma. A nearby dioritic dyke with coarse-grained segregations was dated at 1709 ± 20 Ma. At the Slab occurrence, a small gabbroic stock is dated at 1705 ± 1 Ma. These age determinations demonstrate that the Wernecke Supergroup was intruded by mafic to intermediate dykes in the approximate interval 1705-1725 Ma. The fourth date from the Bonnet Plume River intrusions, 1722 ± 20 Ma, was obtained from a rounded, boulder-sized clast of diorite in Wernecke Breccia at the Olympic occurrence (Fig. 31). This date limits the maximum age of Wernecke Breccia at this location to ca. 1720 Ma, which is consistent with the interpreted age of brecciation at ca. 1600 Ma.

Nearly all of the exposures of the Bonnet Plume River intrusions are found within either the Fairchild Lake Group or zones of Wernecke Breccia. Possible exceptions are present at the Olympic mineral occurrence where dioritic dykes tentatively assigned to the Bonnet Plume River intrusions appear to crosscut the Gillespie Lake Group (Thorkelson and Wallace, 1994b). The general absence of Bonnet Plume River intrusions within the overlying Quartet and Gillespie Lake groups may be explained in two ways. In one way, the intrusions may simply not have risen above the top of the Fairchild Lake Group, leaving the overlying Quartet and Gillespie Lake groups unaffected. In the other way, an unconformity exists within or at the top of the Fairchild Lake Group, and the intrusions could have been emplaced sometime during the hiatus. The latter possibility conflicts with all published reports on the Wernecke Supergroup, which describe the formations of the group as entirely conformable (although the possibility of a disconformity or low-angle unconformity cannot be entirely ruled out). Importantly, if the Slab volcanics and the Bonnet Plume River intrusions were co-magmatic, as proposed in this report, then the unconformity model would have difficulty accounting for the preservation of the Slab volcanics only as a megaclast within Wernecke Breccia. If both the intrusions and the volcanic rocks were emplaced during a hiatus below the Quartet Group, then the volcanic rocks should be present at the position of the unconformity. Instead, the volcanic rocks are not found in the Wernecke Supergroup, despite excellent exposure, and the only known succession of the Slab volcanics is a 250-m-thick megaclast within a zone of Wernecke Breccia (at the Slab mineral occurrence). Because the volcanic megaclast was almost certainly derived from above and not within the Wernecke Supergroup, the Bonnet Plume River intrusions, if correlative, would be younger than the entire Wernecke Supergroup.

Most of the Bonnet Plume River intrusions are composed of diorite or gabbro. The bodies are generally fine- to medium-grained, but a few contain phases with coarse-grained or pegmatitic segregations. Only two of the intrusive bodies are known to have compositions other than diorite or gabbro. One is a small stock composed of quartz-albite syenite, located at the Porphyry occurrence. The highly sodic composition of the stock may be partly a result of metasomatism related to Wernecke Breccia formation (see section on Wernecke Breccia). The other intrusion of unusual composition is a megaclast of fine-grained anorthosite in a zone of Wernecke Breccia, at the Olympic mineral occurrence.

Most of the igneous bodies, which lie in or near zones of breccia, have undergone hydrothermal alteration with a "breccia-signature." The hydrothermal effects in the igneous rocks are typified by metasomatic growths of hematite and/or magnetite, and other minerals including dolomite, plagioclase and potassium feldspar, and chlorite. The mineral enrichments generally occur as disseminated grains, clots, fracture-fillings and small veins. Pyrite and chalcopyrite are present locally, and are commonly concentrated along the margins of the igneous bodies, in contact with Wernecke Breccia. Scapolite has replaced plagioclase in dioritic megaclasts at the Slab mineral occurrence. Most of the hydrothermal activity is considered to have occurred at about the same time as breccia formation, at ca. 1.6 Ga. However, minor metasomatic activity is recorded at ca. 1.37 Ga by the U-Pb age of rutile from an anorthosite megaclast at the Olympic occurrence (Table A1-1, Figs. 4, 31).

Lamprophyre (EPl)

Two lamprophyre intrusions of inferred Early Proterozoic age are present in the study area. One is present as a dyke in the Fairchild Lake Group in the central part of the study area, north of the Olympic occurrence. It is approximately 2 m wide and contains phenocrysts of partly chloritized biotite up to 1 cm across. It is crosscut by thin veins and fracture fillings of hematite, a relationship which strongly suggests that the dyke is older than the age of Wernecke Breccia emplacement at ca. 1.6 Ga. The other lamprophyric intrusion, a dyke or small stock, is exposed at the Fairchild occurrence. The intrusion has local spherulitic texture and contains mats of chloritized biotite. It hosts minor Cu mineralization in the form of bornite, chalcopyrite(?) and malachite, and appears to have been metasomatized by fluids moving through an adjacent zone of Wernecke Breccia. As with the lamprophyre dyke, this intrusion probably pre-dates breccia emplacement and is therefore assigned an Early Proterozoic age.

The lamprophyres in the study area are very similar to biotite-phenocryst lamprophyre dykes of uncertain age at the Gremlin mineral occurrence, 20 km northwest of the study area (Delaney, 1981; Hulstein, 1994). Two of those dykes were dated at 552 ± 13 Ma and 613 ± 15 Ma (Delaney, 1981), although whether these dates reflect the age of crystallization or subsequent cooling is uncertain. The Slab volcanics, which also contain biotite, were considered possible extrusive equivalents to the lamprophyre dykes in the study area (Thorkelson and Wallace, 1994a). However, the Slab volcanics are more favourably linked to the chemically similar syenitic stock of the Bonnet Plume River intrusions. Consequently, the lamprophyre intrusions are considered not correlative with any known volcanic succession.

Bear River dykes (MPd)

The Bear River dykes (Figs. 35, 36) are dioritic intrusions of Middle Proterozoic age that crosscut the Gillespie Lake and Quartet groups in the Slats Creek and Fairchild Lake map areas (106D/16 and C/13). Dated at ca. 1.27 Ga, they represent the third and final pulse of magmatism in the study area. The Pinguicula Group, which is interpreted to be older than 1.27 Ga, does not host any of the known Bear River dykes (however, one dyke of unknown age was emplaced into previously folded strata of the Pinguicula Group approximately four km north of the confluence of Kohse Creek and the Bonnet Plume River, in map area 106C/11). An earlier magmatic event to the south and southwest of the study area is recorded by the Hart River sills at 1.38 Ga (Abbott, 1997), but no intrusions of this age have been identified in the study area.

U-Pb isotopic dates were obtained from two Bear River dykes (Table A1-1; Fig. 4; J.K. Mortensen, pers. comm., 1995, 1996). One dyke, located southwest of Bear River, yielded zircon with an isotopic age of 1265 +20/-11 Ma (Fig. 25). The other dyke, located north of Bear River and west of Slats Creek, yielded baddeleyite with an age of ca. 1.27 Ga. Both of these dates are considered to be the ages of dyke emplacement and magma crystallization. It seems likely that a basaltic volcanic succession developed at this time, but has since been removed by erosion. The dyke located north of Bear River has been affected by hydrothermal alteration similar to the metasomatism related to Wernecke Breccia. This relation demonstrates that breccia-style hydrothermal activity was locally active in small amounts until 1.27 Ga or later.

The Bear River dykes are coeval with the Coppermine volcanics, the Muskox intrusion, and the Mackenzie dyke swarm, all of which were emplaced at about 1.27 Ga in the Canadian Shield (LeCheminant and Heaman, 1989). These igneous units represent the Mackenzie igneous event, which was probably caused by uprise and partial melting of a large mantle plume (LeCheminant and Heaman, 1989). The Mackenzie dykes form a huge radiating dyke swarm (Fahrig and West, 1986; Ernst et al., 1995) that extends from Melville Peninsula and Hudson Bay in the east, to the central part of northern Ontario in the south, to the western exposures of the Canadian Shield in the Northwest Territories where they become covered by younger strata. The focal point of the swarm is located beneath what is presently the surface of western Victoria Island (LeCheminant and Heaman, 1989; A.N. LeCheminant, pers. comm., 1994).

If the Mackenzie dykes and the Bear River dykes belong to the same swarm, then the orientation of the Bear River

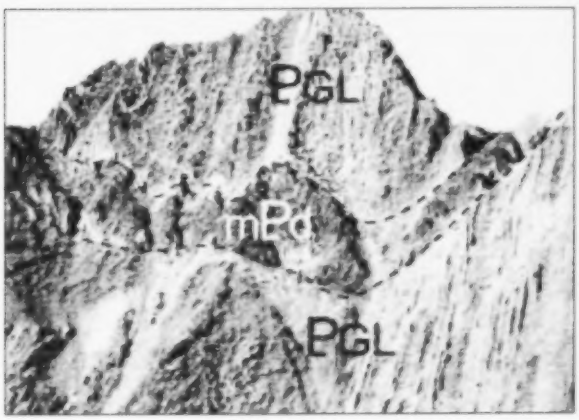

Figure 35. *One of the Bear River mafic dykes (mPd; ca. 1.27 Ga) crosscutting steeply dipping dolostone beds of Gillespie Lake Group (PGL), south of Bear River. Dyke dips steeply away from viewer, and is folded in syncline of interpreted Laramide age to the right of photo (see southeast corner of Fig. 25). View is to the southwest.*

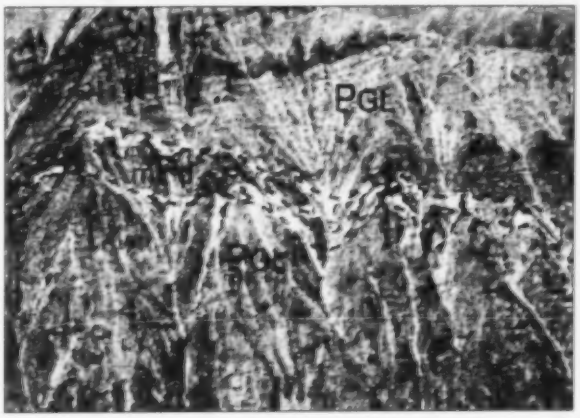

Figure 36. *Two parallel, vertically dipping, dioritic Bear River dykes (ca. 1.27 Ga) crosscutting tilted dolostone of Gillespie Lake Group (PGL), north of Tow mineral occurrence (Fig. 2; southeastern part of Fig. 31). Dykes are bounded by white contact metamorphic aureoles of limestone. Relief of mountainside is approximately 600 m. View is to the north.*

The lamprophyres in the study area are very similar to biotite-phenocryst lamprophyre dykes of uncertain age at the Gremlin mineral occurrence, 20 km northwest of the study area (Delaney, 1981; Hulstein, 1994). Two of those dykes were dated at 552 ± 13 Ma and 613 ± 15 Ma (Delaney, 1981), although whether these dates reflect the age of crystallization or subsequent cooling is uncertain. The Slab volcanics, which also contain biotite, were considered possible extrusive equivalents to the lamprophyre dykes in the study area (Thorkelson and Wallace, 1994a). However, the Slab volcanics are more favourably linked to the chemically similar syenitic stock of the Bonnet Plume River intrusions. Consequently, the lamprophyre intrusions are considered not correlative with any known volcanic succession.

Bear River dykes (MPd)

The Bear River dykes (Figs. 35, 36) are dioritic intrusions of Middle Proterozoic age that crosscut the Gillespie Lake and Quartet groups in the Slats Creek and Fairchild Lake map areas (106D/16 and C/13). Dated at ca. 1.27 Ga, they represent the third and final pulse of magmatism in the study area. The Pinguicula Group, which is interpreted to be older than 1.27 Ga, does not host any of the known Bear River dykes (however, one dyke of unknown age was emplaced into previously folded strata of the Pinguicula Group approximately four km north of the confluence of Kohse Creek and the Bonnet Plume River, in map area 106C/11). An earlier magmatic event to the south and southwest of the study area is recorded by the Hart River sills at 1.38 Ga (Abbott, 1997), but no intrusions of this age have been identified in the study area.

U-Pb isotopic dates were obtained from two Bear River dykes (Table A1-1, Fig. 4; J.K. Mortensen, pers. comm., 1995, 1996). One dyke, located southwest of Bear River, yielded zircon with an isotopic age of 1265 +20/-11 Ma (Fig. 25). The other dyke, located north of Bear River and west of Slats Creek, yielded baddeleyite with an age of ca. 1.27 Ga. Both of these dates are considered to be the ages of dyke emplacement and magma crystallization. It seems likely that a basaltic volcanic succession developed at this time, but has since been removed by erosion. The dyke located north of Bear River has been affected by hydrothermal alteration similar to the metasomatism related to Wernecke Breccia. This relation demonstrates that breccia-style hydrothermal activity was locally active in small amounts until 1.27 Ga or later.

The Bear River dykes are coeval with the Coppermine volcanics, the Muskox intrusion, and the Mackenzie dyke swarm, all of which were emplaced at about 1.27 Ga in the Canadian Shield (LeCheminant and Heaman, 1989). These igneous units represent the Mackenzie igneous event, which was probably caused by uprise and partial melting of a large mantle plume (LeCheminant and Heaman, 1989). The Mackenzie dykes form a huge radiating dyke swarm (Fahrig and West, 1986; Ernst et al., 1995) that extends from Melville Peninsula and Hudson Bay in the east, to the central part of northern Ontario in the south, to the western exposures of the Canadian Shield in the Northwest Territories where they become covered by younger strata. The focal point of the swarm is located beneath what is presently the surface of western Victoria Island (LeCheminant and Heaman, 1989; A.N. LeCheminant, pers. comm., 1994).

If the Mackenzie dykes and the Bear River dykes belong to the same swarm, then the orientation of the Bear River

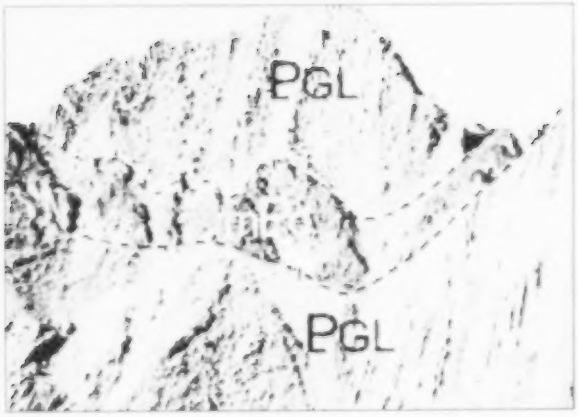

Figure 35. One of the Bear River mafic dykes (mPd, ca. 1.27 Ga) crosscutting steeply dipping dolostone beds of Gillespie Lake Group (PGL), south of Bear River. Dyke dips steeply away from viewer, and is folded in syncline of interpreted Laramide age to the right of photo (see southeast corner of Fig. 25). View is to the southwest.

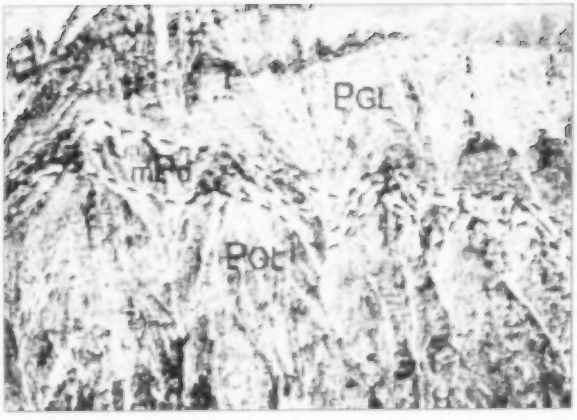

Figure 36. Two parallel, vertically dipping, dioritic Bear River dykes (ca. 1.27 Ga) crosscutting tilted dolostone of Gillespie Lake Group (PGL), north of Tow mineral occurrence (Fig. 2; southeastern part of Fig. 31). Dykes are bounded by white contact metamorphic aureoles of limestone. Relief of mountainside is approximately 600 m. View is to the north.

dykes may be predicted by the location of the study area relative to the focal point (Ernst et al., 1995). Using this method, the predicted orientation of the Bear River dykes is approximately northeast-southwest. The orientation of the Bear River dykes, however, ranges from north-south to east-west (and subvertical in attitude). The lack of parallelism between the predicted and actual orientations may be explained by local stress fields in the study area which controlled the directions of dyke propagation. Alternatively, the Bear River dykes may have been emplaced mainly in the predicted orientation, and subsequently re-oriented during events of Middle Proterozoic to Tertiary deformation. Local modification of dyke orientation during strain is evident south of Bear River where a dyke has been folded in the core of a syncline which probably formed during Mesozoic to Early Tertiary (Laramide) contraction.

Structural History

Introduction

Rock deformation in the study area spanned at least 1.5 billion years and occurred under regimes of contraction, extension, transcurrence, and hydrothermal brecciation. Structural style is dominated by open to tight folds, and steeply to moderately dipping faults. Slaty cleavage is widespread. Schistosity, crenulation cleavage, and kink bands are locally developed in the oldest strata. Fold and fault orientations are highly variable, although certain structural trends are characteristic of specific phases of deformation.

Nine discrete phases of deformation have been recognized, although some may be of local rather than regional importance (Fig. 4). The first six occurred prior to the end of Windermere Supergroup deposition, and are therefore Precambrian in age. Three pulses of contractional deformation have been documented, and are defined by well-exposed angular unconformities (Eisbacher, 1978). From oldest to youngest, they are the Early Proterozoic Racklan Orogeny (Gabrielse, 1967), the Middle Proterozoic Corn Creek Orogeny (named herein but originally recognized by Eisbacher, 1981), and the Cretaceous to Early Tertiary Laramide Orogeny (Norris, 1997). Localized contraction also occurred along the Snake River transcurrent fault in Mesozoic to Tertiary time. Regional importance of the Racklan and Corn Creek orogenies is discussed in the Regional Synthesis. Many structures in the study area cannot be assigned with confidence to a particular phase.

The Fairchild Fault is a prominent structure which bisects the study area along the north-trending Fairchild Lake - Bonnet Plume River corridor (Fig. 2), and may have been active several times from the Early Proterozoic to the Tertiary. The fault is recognized as an east-side-down normal fault, on the basis of contrasting Lower to Middle Proterozoic strata. Minor strike-slip displacement is also considered possible. The preservation of Middle and Late Proterozoic strata beneath the sub-Paleozoic unconformity to the east but not to the west of the fault strongly suggests that normal fault motion occurred in Middle to Late Proterozoic time, during which the western side was elevated and subjected to non-deposition and/or erosion. In this manner, motion along the Fairchild Fault may be responsible for the distribution of Proterozoic and Paleozoic strata, particularly the pronounced unconformity (representing ~1.2 billion years) between Paleozoic sediments (unit CDs) and the Wernecke Supergroup in the western part of the study area. To the north, the Fairchild Fault merges with the Knorr Fault, which is a major strand of the Richardson Fault Array (Figs. 2, 5; Norris, 1981; 1982). The array is currently one of Canada's most seismically active regions. Strands of the array were active in Late Proterozoic and Tertiary times (Norris, 1981) as normal, strike-slip, and thrust faults (Norris, 1981; Hall and Cook, 1998). The central part of the array trends into the Misty Creek Embayment, a sedimentary trough of Early Paleozoic age to the east of the study area (Fig. 5; Cecile, 1982). The embayment was probably generated by extensional faulting related to activity in the Richardson Fault Array (Cecile, 1982) during the Late Proterozoic to Early Paleozoic. Clearly, the Richardson Fault Array and related features may represent a long-lived weak zone in the North American craton. The fault array may even have been active during Early Proterozoic (Racklan) deformation (Fig. 4; J.G. Abbott, pers. comm., 1992), and may have first developed during crustal extension and genesis of the Wernecke basin in Early Proterozoic time. Perhaps the Array marks the location of an Early Proterozoic terrane boundary, which has been repeatedly exploited during successive stages of crustal deformation.

Some important geological events are not included in the following depiction of structural deformation, because there are no known structures or fabrics which mark their development. For example, the origin of the Wernecke basin is inferred to have occurred through crustal extension, and may have involved growth faulting during Wernecke Supergroup sedimentation. However, no specific structures in this regard have been identified. Similarly, uplift and exposure of the Pinguicula Group prior to Hematite Creek Group deposition is implied by karsting of the Pinguicula, and by angular relations in the eastern Ogilvie Mountains (Abbott, 1997), but structures in the study area corresponding to this event have not been identified.

Phase 1: SE-directed contraction (first event of Racklan Orogeny)

The first and second phases of deformation were produced by contraction (Fig. 4). These phases are considered in this report to constitute the Racklan Orogeny, a period of mountain building between deposition of the Wernecke Supergroup and the Pinguicula Group (Wheeler, 1954; Gabrielse, 1967; Eisbacher, 1978). Studies by the author and R.A. Creaser (pers. comm., 1994) have shown that both phases occurred prior to ca. 1.59 Ga when the Wernecke Breccias formed.

The first phase produced northeast- to east-trending folds, slaty cleavage, and schistosity in the Wernecke Supergroup. The folds are inclined to overturned and verge to the southeast (Figs. 2, 8, 7). Stratigraphic conformity among the Fairchild Lake, Quartet and Gillespie Lake groups infers that the folding post-dated deposition of the entire Wernecke Supergroup. Schistosity is preferentially developed in the cores of tight folds, i.e., in the Fairchild Lake Group.

The largest structure of this phase is a south-verging anticline, which spans the Bonnet Plume River valley in the north-central part of the study area (Fig. 2; Delaney, 1981). Petrofabric development is genetically linked to this anticline by the presence of chlorite- and muscovite-bearing schist in a tight parasitic fold on the upright limb of the anticline (cross-section A-D on map 106C/13). Other prominent structures of this phase include overturned folds in the northwestern part of the study area, near Slats Creek (Figs. 2, 7). Smaller folds

sharing the same general orientation are displayed by the white "marker" carbonate of the upper Fairchild Lake Group, about 9 km southwest of the Slab mineral occurrence (Fig. 8).

Phase-one schists are restricted to the Fairchild Lake Group and consist of chloritoid or garnet porphyroblasts in a foliated groundmass dominated by chlorite, muscovite and quartz. The coarsest schist is exposed 0 to 1 kilometres east of the Slab volcanics, but schist is also well developed a few kilometres southwest of the Bonnet Plume River between the Ford and Snowstar mineral occurrences (Fig. 2). Chloritic phyllite, representing the same deformational event as the schist, is best developed: (1) between the Slab and Otter occurrences, west of Fairchild Lake; (2) approximately 2 km northwest of the Snowstar occurrence; and (3) near the Cirque occurrence.

Phase 2: Kink band formation (second event of Racklan Orogeny)

The second phase of deformation produced kink bands in phase-one foliation. Kink bands are well developed in Fairchild Lake Group east of the Slab volcanics, and 8 km southwest of the Slab mineral occurrence (Fig. 2). Kink bands are also well developed in slate of the Fairchild Lake Group at the Julie mineral occurrence, and in chloritic phyllite northwest of the Snowstar occurrence. Localized crenulation cleavage in Quartet and Fairchild Lake shale and siltstone probably also developed during this phase.

The timing of phase-one and phase-two deformation relative to the emplacement of the Bonnet Plume River intrusions is uncertain. Zones of Wernecke Breccia have engulfed most of these intrusions, which have obscured original intrusion morphologies and contact relations. In a few cases, notably on Slab Mountain, intrusions lie within fine-grained schist of the Fairchild Lake Group. The intrusions do not appear to be foliated, inferring that they were emplaced after Racklan deformation. However, precise contacts between the schist and the intrusions were not observed because of overburden. The possibility exists that the margins of these intrusions are foliated, and that the intrusions are pre-Racklan. Additional fieldwork is necessary to clarify the timing of intrusion and deformation.

Phase 3: Explosive brecciation (Wernecke Breccia development)

The third phase of deformation involved fracturing, brecciation, and probably faulting during development and emplacement of Wernecke Breccia (details on the breccias were given previously). Brecciation is considered to have been produced mainly by explosive expansion of hydrothermal fluids. Most breccias consist of granule- to cobble-size clasts of Wernecke Supergroup and dioritic dykes and stocks dated at ca. 1.72 Ga. At the Slab mineral occurrence, breccia also contains a mega-block comprising the Slab volcanics. Most of the brecciation is considered to have occurred during one short interval of time at about 1.6 Ga, when titanite grew from hydrothermal solutions in a Wernecke Breccia zone at the Slab mineral occurrence (Table A1-1, Fig. 4; R.A. Creaser, pers. comm., 1994). Subsequent events of fluid activity in the breccia zones occurred at ca. 1.38 Ga, and at or after 1.27 Ga, as indicated by isotopic dates on hydrothermally precipitated minerals, and crosscutting relations. The amount of brecciation at these times is, however, considered minor.

Petrofabrics indicate the timing of brecciation relative to other deformational events. Two important relations are evident at the Slab and Julie occurrences, where clasts of kinked schist and slate of the Fairchild Lake Group occur with random orientation in Wernecke Breccia. The matrix of the breccia at these locations (and most others) is devoid of secondary petrofabrics, confirming that phase-one dynamothermal metamorphism and phase-two kinking preceded Wernecke brecciation.

In some locations, brittle fabrics are present along faults crosscutting breccia zones, indicating that movement of these faults occurred after breccia development. The clearest examples of this relationship are present at the Pika mineral occurrence (Fig. 34), and in a small breccia zone 5.5 km east of the south end of Fairchild Lake (Fig. 2). In these and other localities, the breccia and nearby country rock is deformed into a fracture cleavage or a set of anastomozing shear planes, both of which differ greatly from the cleavage and kink-bands characteristic of the older (phase one and two) fabrics.

The main phase of brecciation appears to be related to normal or oblique-slip faults, which occur within the Wernecke Supergroup near many of the breccia zones. Some of these faults may represent crustal deformation at the time of breccia genesis, and may have served to localize breccia development (Figs. 32, 31). Although more detailed structural work is required, the possibility of syn-breccia faulting is supported by: (1) faults which bound or "run into" breccia zones; (2) an elongate shape to some breccia zones; and (3) the apparent arrangement of many of the breccia zones in curvilinear arrays which share the trend of some major faults. The most compelling example of breccia zones possibly controlled by fault activity are located west of the Bonnet Plume River near the Olympic and Noranda mineral occurrences (Fig. 2).

Phase 4: Shearing, faulting

In the fourth phase, a foliation consisting of anastomozing fractures developed in Wernecke Breccia at the Pika mineral occurrence (Fig. 34). This fabric is considered to be a result of shear during brittle faulting, and is truncated at the unconformity with the overlying Pinguicula Group. Similar fabrics in a small breccia zone 5 km east of the Fairchild occurrence may also have developed at this time. Whether these textures are manifestations of a set of regional structures, such as a family of steep faults, is unknown. They may represent faults whose motion began during brecciation and continued only shortly thereafter.

Phase 5: West-directed contraction (Corn Creek Orogeny)

The fifth and sixth phases occurred after deposition of the Hematite Creek Group. The fifth phase was contractional, producing westerly to southwesterly verging thrust faults and folds in the Pinguicula and Hematite Creek groups. This deformational event, herein called the Corn Creek Orogeny, was first identified by Eisbacher (1981) who recognized west-verging folds in the eastern part of the study area, and a few kilometres to the south. Additional features belonging to this event have been identified, indicating that the affected region extends throughout the eastern third of the study area, and for at least 25 km to the south.

The definitive structures of the Corn Creek Orogeny are located near Mt. Profeit, in and to the south of the southeastern corner of the study area (Figs. 2, 19). In this area, a thrust fault within the Hematite Creek Group places undivided Hematite Creek strata (PHC) over Corn Creek quartz arenite (PHCC), and is truncated by basal Windermere strata on the western flank of Mount Profeit. A few kilometres southwest of Mount Profeit, overturned folds and related thrust faults are present in the Hematite Creek Group, but the overlying Windermere Supergroup is undeformed by these structures (Figs. 19, 23).

Other west- to southwest-verging thrust faults between Mt. Profeit and the Bonnet Plume River are considered to be additional manifestations of the Corn Creek Orogeny (these structures are located on maps 106C/13 and 106C/14 and cross-section C-D on map 106C/14). Most of these faults occur entirely within the Pinguicula and Hematite Creek groups. However, motion along one reverse fault in the south-central part of 106C/14 has brought rocks of the Gillespie Lake Group over units A, B and C of the Pinguicula Group (a splay of this fault within Pinguicula unit C is shown in Fig. 15). To the north, this fault merges with a large-displacement normal fault of opposite sense within the Wernecke Supergroup. The reverse portion of the fault between the Gillespie and Pinguicula strata is interpreted to be a result of fault reactivation. In this interpretation, a large east-side-down normal fault first developed within the Wernecke Supergroup prior to deposition of the Pinguicula Group. The fault may have been active during emplacement of Wernecke Breccia zones, which are concentrated near the fault. Subsequently, after deposition of the Pinguicula Group, the fault surface was re-used to accommodate east-side-up contraction during the Corn Creek Orogeny. This second event of faulting was sufficient to thrust the Gillespie Lake Group over the Pinguicula Group, but not enough to change the sense of motion to the north along the fault within the Wernecke Supergroup, which retains a net east-side-down sense of displacement.

Structures of the Corn Creek Orogeny confirm the relationship identified by Eisbacher (1981) in which the Hematite Creek and Windermere successions are separated by an angular unconformity representing significant contractional deformation. The regional extent of this orogeny is unknown because exposures of the Hematite Creek Group and correlative strata in Yukon are limited. Structures of the Corn Creek event have not been identified in the Wernecke Supergroup, except for the aforementioned reactivated normal fault. This orogenic event may have been largely thin-skinned above a basement consisting of the Wernecke Supergroup and lower rocks.

Phase 6: Hayhook extension

The sixth phase of deformation was extensional, producing a set of generally west-trending normal faults, some of which truncate phase-five folds and thrust faults of the Corn Creek Orogeny. The faults identified as phase-six structures appear to be syndepositional with the lowest parts of the Windermere Supergroup, and seem to have controlled sedimentary facies in the Sayunei and Twitya formations. The clearest examples of phase-six faulting are located in the eastern half of 106C/14 (Figs. 2, 19, 24, 32). Five km south of Mt. Profeit, a west-southwest-trending normal fault crosscuts the Hematite Creek Group and Corn Creek contractional structures, but is truncated by the Windermere Supergroup. The location of this fault coincides with an abrupt southward thickening of the Sayunei Formation, the basal conglomerate of the Windermere Supergroup. Another normal fault, located two km south of Mt. Profeit, crosscuts Corn Creek structures in the Hematite Creek Group. This fault extends about 1 km into the overlying Windermere Supergroup, and corresponds to the featheredge of a northward-thickening section of Sayunei conglomerate. The present down-to-the-south sense of fault displacement is inconsistent with the northward-thickening conglomerate, but may be a result of fault reactivation as noted in other faults, and described below. A set of faults approximately 5-6 km north of Mt. Profeit also appears to have been active during early Windermere deposition, as it marks the approximate northern limit of a patch of Sayunei conglomerate, and also the pronounced facies boundary between Profeit dolostone and the more basinal shales and siltstones of the Twitya Formation. One of these faults, about 6 km north of Mt. Profeit, shows a different sense of displacement in the Windermere strata than in the underlying Pinguicula and Hematite Creek rocks, suggesting at least two discrete periods of fault activity. Another fault, 16 km north of Mt. Profeit, coincides with local northward thickening of Sayunei conglomerate, and also shows a reversal in its sense of displacement (Fig. 24). That section of Sayunei conglomerate ends 2 km farther to the north, approximately where the basal Windermere succession truncates another west-trending fault in the Pinguicula and Hematite Creek groups (Fig. 24).

When considered together, the set of west-trending faults immediately below (west of) the basal Windermere contact is favourably regarded as products of north-south extension during early Windermere deposition. Their apparent syn-Windermere character connects them to the tectonic episode known as the Hayhook orogeny, or more appropriately, the Hayhook extensional event (Fig. 4; Jefferson and Parrish,

1989). This event is known to have controlled facies of the Windermere Supergroup in the Mackenzie Mountains (Eisbacher, 1981). The history of fault reactivation, described further below, may explain why the current sense of offset is not in accord with the sense of displacement inferred by the variations in thickness of the Sayunei Formation. Thicker successions of the Sayunei would normally be expected to lie on the downthrown block of a synsedimentary normal fault, but subsequent fault reactivation in the opposite sense may account for preservation of thicker deposits preserved on the presently identified upthrown block.

A history of fault reactivation in the area is also indicated in the north-central part of map area 1166 C/14, where a north-trending fault runs along the eastern side of the Blusson mineral occurrence (No. 78 in Fig. 52). It, too, displays a change in the sense of fault displacement, indicating fault reactivation during or after lower Windermere deposition. On the west side of the fault, the Twitya formation sits on Pinguicula Group unit A, whereas on the eastern side of the fault it sits on the Hematite Creek Group. Also, Twitya formation on the west side of the fault is juxtaposed with the Hematite Creek Group. These relations can be explained by down-to-the-east motion prior to Twitya deposition, followed by down-to-the-west displacement after Twitya deposition. Some of these faults may also have been active during deformation phase seven, when the Snake River Fault and related structures were active.

Some strands of the Richardson Fault Array were active in the Late Proterozoic (Norris, 1981). At about the same time, the Snake River Fault may have been active, and may have controlled facies distributions and sediment thickness in the Rapitan Group (Fig. 4, Eisbacher, 1981), although this relationship is not evident from the small section of the Snake River Fault investigated in this report. These Proterozoic motions are probably related, at least in part, to Hayhook extension.

Phase 7: Laramide contraction

Phases seven, eight and nine have been assigned, somewhat arbitrarily, to contraction, transpression and extension, respectively (Fig. 4). The order in which these styles of deformation occurred is not perfectly understood. Uncertainty in chronology exists because each type of deformation may have occurred in more than one event, spanning tens of millions of years. For example, extensional faulting may have occurred as early as Late Proterozoic, and as recently as Eocene. Nevertheless, deformation of these three styles is known to have occurred after deposition of the Upper Proterozoic Windermere Supergroup, and each style is recorded by specific structures within and beyond the study area.

Laramide contractional deformation of Cretaceous to Paleocene age is recognized as a principal cause of orogenesis in western North America. In northern Yukon, effects of Laramide deformation are displayed as prominent fold and thrust belts in the Wernecke, Ogilvie, and Richardson mountain ranges (Norris, 1997). In the study area, however, relatively few structures can be attributed with certainty to Laramide-age deformation. Predominance of Precambrian over Phanerozoic deformation in the study area is revealed by the profound angular unconformity between the Wernecke Supergroup and the overlying succession of Lower Paleozoic carbonate. In several locations, the angular contact between the Paleozoic strata and folded rocks of the Wernecke Supergroup is well exposed (Figs. 25, 26, and frontispiece). Within and immediately southwest of the study area, the Paleozoic strata are exposed mainly as gently tilted homoclinal panels.

Structures assigned to the Laramide orogeny are located in the southwestern corner of the study area, southwest of Bear River. There, a reverse fault places the Gillespie Lake Group over Lower Paleozoic carbonate (Figs. 25, 37). The hanging wall was apparently displaced toward the north or northwest. A few kilometres to the southeast, other thrust faults and a large syncline appear to be kinematically related. The southernmost reverse faults appear to be oversteepened, possibly because more northerly thrusts are younger (cross section A-B on the Slats Creek map). One of the Bear River dykes (ca. 1.27 Ga) has been folded in the core of the large syncline. Folding of the dyke is attributed to Laramide deformation, because (1) dyke emplacement post-dates Racklan orogenesis, and (2) the fold trend is oriented at a high angle to Corn Creek (phase 5) and Snake River Fault (phase 8) structures.

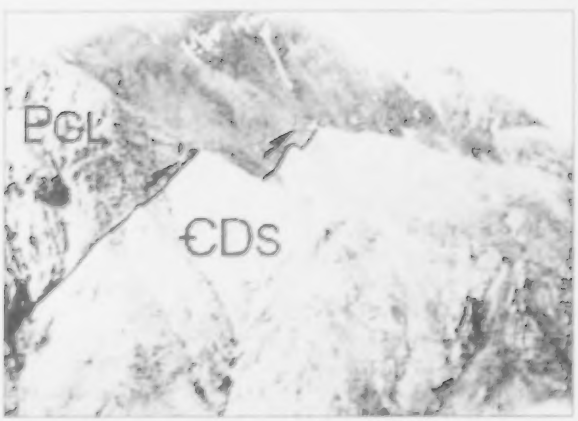

Figure 37. Thrust relationship between Gillespie Lake Group (PGL: hanging wall) and Lower Paleozoic carbonate (CDs), southwest of Bear River (see Fig. 25). View is to the southwest from Bear River.

1989). This event is known to have controlled facies of the Windermere Supergroup in the Mackenzie Mountains (Eisbacher, 1981). The history of fault reactivation, described further below, may explain why the current sense of offset is not in accord with the sense of displacement inferred by the variations in thickness of the Sayunei Formation. Thicker successions of the Sayunei would normally be expected to lie on the downthrown block of a synsedimentary normal fault, but subsequent fault reactivation in the opposite sense may account for preservation of thicker deposits preserved on the presently identified upthrown block.

A history of fault reactivation in the area is also indicated in the north-central part of map area 106C/14, where a north-trending fault runs along the eastern side of the Blusson mineral occurrence (No. 78 in Fig. 32). It, too, displays a change in the sense of fault displacement, indicating fault reactivation during or after lower Windermere deposition. On the west side of the fault, the Twitya formation sits on Pinguicula Group unit A, whereas on the eastern side of the fault it sits on the Hematite Creek Group. Also, Twitya formation on the west side of the fault is juxtaposed with the Hematite Creek Group. These relations can be explained by down-to-the-east motion prior to Twitya deposition, followed by down-to-the-west displacement after Twitya deposition. Some of these faults may also have been active during deformation phase seven, when the Snake River Fault and related structures were active.

Some strands of the Richardson Fault Array were active in the Late Proterozoic (Norris, 1981). At about the same time, the Snake River Fault may have been active, and may have controlled facies distributions and sediment thickness in the Rapitan Group (Fig. 4; Eisbacher, 1981), although this relationship is not evident from the small section of the Snake River Fault investigated in this report. These Proterozoic motions are probably related, at least in part, to Hayhook extension.

Phase 7: Laramide contraction

Phases seven, eight and nine have been assigned, somewhat arbitrarily, to contraction, transpression and extension, respectively (Fig. 4). The order in which these styles of deformation occurred is not perfectly understood. Uncertainty in chronology exists because each type of deformation may have occurred in more than one event, spanning tens of millions of years. For example, extensional faulting may have occurred as early as Late Proterozoic, and as recently as Eocene. Nevertheless, deformation of these three styles is known to have occurred after deposition of the Upper Proterozoic Windermere Supergroup, and each style is recorded by specific structures within and beyond the study area.

Laramide contractional deformation of Cretaceous to Paleocene age is recognized as a principal cause of orogenesis in western North America. In northern Yukon, effects of Laramide deformation are displayed as prominent fold and thrust belts in the Wernecke, Ogilvie, and Richardson mountain ranges (Norris, 1997). In the study area, however, relatively few structures can be attributed with certainty to Laramide-age deformation. Predominance of Precambrian over Phanerozoic deformation in the study area is revealed by the profound angular unconformity between the Wernecke Supergroup and the overlying succession of Lower Paleozoic carbonate. In several locations, the angular contact between the Paleozoic strata and folded rocks of the Wernecke Supergroup is well exposed (Figs. 25, 26, and frontispiece). Within and immediately southwest of the study area, the Paleozoic strata are exposed mainly as gently tilted homoclinal panels.

Structures assigned to the Laramide orogeny are located in the southwestern corner of the study area, southwest of Bear River. There, a reverse fault places the Gillespie Lake Group over Lower Paleozoic carbonate (Figs. 25, 37). The hanging wall was apparently displaced toward the north or northwest. A few kilometres to the southeast, other thrust faults and a large syncline appear to be kinematically related. The southernmost reverse faults appear to be oversteepened, possibly because more northerly thrusts are younger (cross section A-B on the Slats Creek map). One of the Bear River dykes (ca. 1.27 Ga) has been folded in the core of the large syncline. Folding of the dyke is attributed to Laramide deformation, because (1) dyke emplacement post-dates Racklan orogenesis, and (2) the fold trend is oriented at a high angle to Corn Creek (phase 5) and Snake River Fault (phase 8) structures.

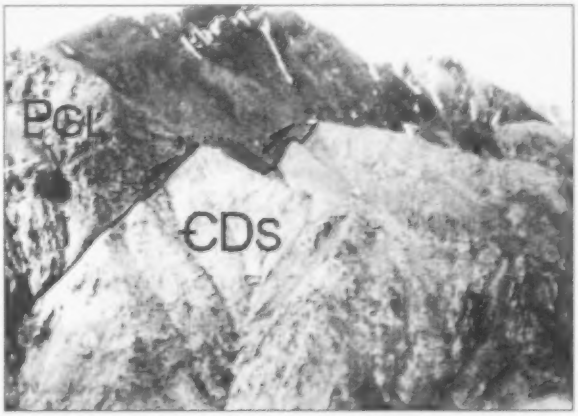

Figure 37. Thrust relationship between Gillespie Lake Group (PGL; hanging wall) and Lower Paleozoic carbonate (CDs), southwest of Bear River (see Fig. 25). View is to the southwest from Bear River.

Phase 8: Transpression along the Snake River Fault system

Phase eight is characterized by southwest-verging thrust faults in the northeastern corner of the study area, southwest of the Snake River (Fig. 24; Thorkelson and Wallace, 1995a, b). These faults superpose imbricate panels of the Upper Proterozoic Windermere Supergroup on younger Proterozoic to Cambrian strata (unit PCs). The faults merge to the southeast with the Snake River Fault, which has been considered as a long-lived strike-slip fault with uncertain timing, sense of displacement, and magnitude of offset (Norris, 1982; Eisbacher, 1983; Cecile, 1984). To the north, the Snake River Fault connects with the Richardson Fault Array, including the Knorr, Deslauriers, and Deception strands which have been identified as post-Paleozoic dextral strike-slip faults (Fig. 5; Norris and Hopkins, 1977; Norris, 1984). Cumulative dextral displacement in the Richardson Fault Array has been estimated at 10-20 km by Cecile (1984) and about 70 km by Norris (1997). The Richardson Fault Array has also been modeled, on the basis of field studies and geophysical data, as a Tertiary, largely contractional feature (Lane, 1996) with up to 33 km of horizontal displacement (Hall and Cook, 1998). However, the relative timing and importance of strike-slip motion vs. contractional motion remains unresolved. If transcurrent and contractional motions were broadly synchronous, then the fault array would be favourably described as a set of oblique-slip faults.

In the study area, the highest and most eastern thrust fault of phase 8 (Fig. 24) is important for two reasons. Firstly, the southeastern end of the fault trends directly down the valley of the Snake River, and appears to be the main strand of the Snake River Fault (which is covered by Quaternary sediments). Consequently, this fault and the other thrusts to the west are considered to be transpressional features possibly generated during dominantly transcurrent motion. Beyond the study area, to the north and northeast, west-verging thrust faults indicated by Norris (1982) may also be a product of transpression during regional dextral strain. Secondly, the fault places a thick succession of Shezal Formation diamictite with a prominent east-trending cleavage over an imbricate Windermere section, in which the Shezal Formation is absent. No Shezal strata are present in the study area to the southwest of the Snake River Fault (if the Shezal were present it would lie between the Sayunei and Twitya formations). The juxtaposition of these two contrasting Windermere successions infers that the fault has considerable offset, probably mainly through strike-slip displacement. The cleavage orientation in the Shezal Formation and the azimuth of the Snake River Fault are consistent with maximum compressive stress oriented approximately north-south.

Phase 9: Extensional block faulting

Some normal faults may be the youngest structures in the study area. This suggestion is based on relationships directly to the north of the Slats Creek map in map area 106E/1 where normal faults of Tertiary age crosscut structures of Laramide age and probably those related to Snake River Fault motion (Norris, 1981, 1982). In the study area, however, none of the faults can actually be shown to post-date motion on the Snake River Fault system. The youngest documented normal faults are located southwest of Bear River where they crosscut both thrust faults and folds assigned to the Laramide Orogeny (Fig. 25). Motion on some of these faults has juxtaposed Lower Paleozoic carbonate and clastic strata with the Wernecke Supergroup. Many other normal faults are present in the study area but constraints on the ages of motion are typically poor. For example, the faults inferred to run along much of the Bonnet Plume River valley may have multiple histories extending from before Wernecke Breccia genesis to after Snake River Fault activity.

Mineral Occurrences

Introduction

The Wernecke Mountains have been a principal region of exploration and claim staking in Yukon since the late 1960s. Exploration for U, Co, Cu, Pb, Zn and coal reached a peak in the late 1970s and early 1980s when about thirty prospects were explored by drilling. Although a few of these occurrences were defined in grade and tonnage, most have not been comprehensively evaluated. Little exploration was undertaken between the early 1980s and about 1992. Since then, the region has been the focus of renewed activity involving claim staking, detailed mapping, systematic geochemical sampling, airborne and ground-based geophysical surveys, and drilling. Most of the recent interest has centred on mineralization related to Wernecke Breccia.

Mineral occurrences in the study area have been organized into three general categories: veins, sedimentary exhalatives (sedex), and those related to Wernecke Breccia (Figs. 2, 38). The veins and breccia-related occurrences are abundant whereas only two sedimentary exhalative occurrences have been discovered. The vein and sedex occurrences are enriched predominantly in Pb and Zn. The Wernecke Breccia-related occurrences are characterized by disseminated grains, stringers, and veins enriched in Cu, Co, Au, Ag, and U. Assays from sites sampled in this program are listed in Table A4-1.

The information on mineral occurrences in this report provides a review of mineralization in the study area. This review is intended to be a companion to Yukon Minfile (1997), which provides systematic information on exploration history, geological descriptions and assay results for all recognized mineral occurrences in Yukon.

Sedimentary exhalative occurrences

Two stratabound Pb-Zn occurrences are present in the Slats Creek and Fairchild Lake map areas (106D/16 and C/13). Both occurrences, the Cord and the Goodfellow, are hosted by the Lower Proterozoic Gillespie Lake Group and are the oldest type of occurrence in the study area. The mineralized rock consists of fine-grained pyrite, sphalerite, galena, siderite and chalcopyrite in shaly beds within a succession dominated by orange-weathering dolostone (Campbell and McClintock, 1980; Hardy and Campbell, 1981; Eaton, 1983).

Mineralization in the Cord occurrence is confined to a siliceous mudstone and siltstone unit within Gillespie Lake dolostone that generally strikes west and dips 10-15° to the south (Hardy and Campbell, 1981). Diamond drilling was carried out in 1981. Four holes totaling 366 m were drilled, but only one reached the desired depth. Stratiform mineralization in drill core consists of thinly laminated pyrite and/or pyrrhotite with lesser amounts of chalcopyrite, sphalerite, and galena, within 0.5-4 m beds of siliceous mudstone. Mineralization also occurs as veinlets and coarsely crystalline "disturbed sulphides" consisting of pyrite, pyrrhotite, with minor chalcopyrite, sphalerite, and galena. The best grades obtained in drill core were 0.50% Pb, 0.63% Zn, and 0.05% Cu over 2.0 m (Hardy and Campbell, 1981). The Goodfellow occurrence is located approximately 8 km east-southeast of the Cord. Mineralization occurs as both stratabound disseminated mineralization and veins. The veins are 1-2 m wide and contain coarse-grained pyrite, galena, and sphalerite in calcite, dolomite or quartz gangue. An assay from the Goodfellow is given in Table A4-1.

No occurrences correlative with the Cord and Goodfellow are known. The Middle Proterozoic Hart River deposit, 140 km to the southwest, was previously considered to be the same age and type of deposit (Thorkelson and Wallace, 1994a). However, the Hart River deposit is now known to be younger, and crosscutting instead of stratiform (Abbott, 1997). Lead isotopic ratios in galena from the Goodfellow and Cord occurrences are very similar to those from other Proterozoic occurrences, including the Hart River deposit, and the Middle Proterozoic Sullivan mine, a large Pb-Zn deposit in mid-Proterozoic sedimentary strata in southeastern British Columbia (Godwin et al., 1988; J.K. Mortensen, pers. comm., 1994; Abbott, 1997).

Wernecke Breccia-related occurrences

Wernecke Breccia is a collective term for numerous breccia zones in the Wernecke Supergroup (Figs. 2, 5). Breccia zones generally range from 0.1 to 10 km^2 and crop out in curvilinear arrays over a large area (3500 km^2) in the Wernecke Mountains (Bell, 1986a; Wheeler and McFeely, 1991; Thorkelson and Wallace, 1993b). Correlative breccia zones in the Ogilvie Mountains were called Ogilvie Mountains breccias by Lane (1990). Considerable mineralization of Cu, Co, Au, Ag and U, and rare Mo in and around the breccia zones, has been an intermittent focus of mineral exploration over the past few decades. Large exploration projects were undertaken in the late 1970s and the mid-1990s. Bell (1989), Gandhi and Bell (1990), and Hitzman et al. (1992) noted similarities between Wernecke Breccia and other breccias of similar age and environment. A strong connection was drawn with breccias of the Olympic Dam mine in Australia on the basis of similar physical and mineralogical characteristics.

Details of field relations, age and petrology are provided in the section on Wernecke Breccia. A summary of observations and interpretations is given here. Forceful explosions of volatile-rich fluids within the crust generated the breccia zones. The source of the fluids is uncertain, but may be related to igneous intrusions at depth. Rapid expansion of the fluids shattered large volumes of country rock, mainly sedimentary rocks of the Wernecke Supergroup, but also dioritic to syenitic rocks of the Bonnet Plume River intrusions. In the central parts of the brecciated rock, fragments underwent considerable motion, and in some cases became rounded from abrasion. Venting of brecciated rock and fluid is considered likely, but surface deposits are nowhere preserved. At "Slab Mountain," large blocks of country rock

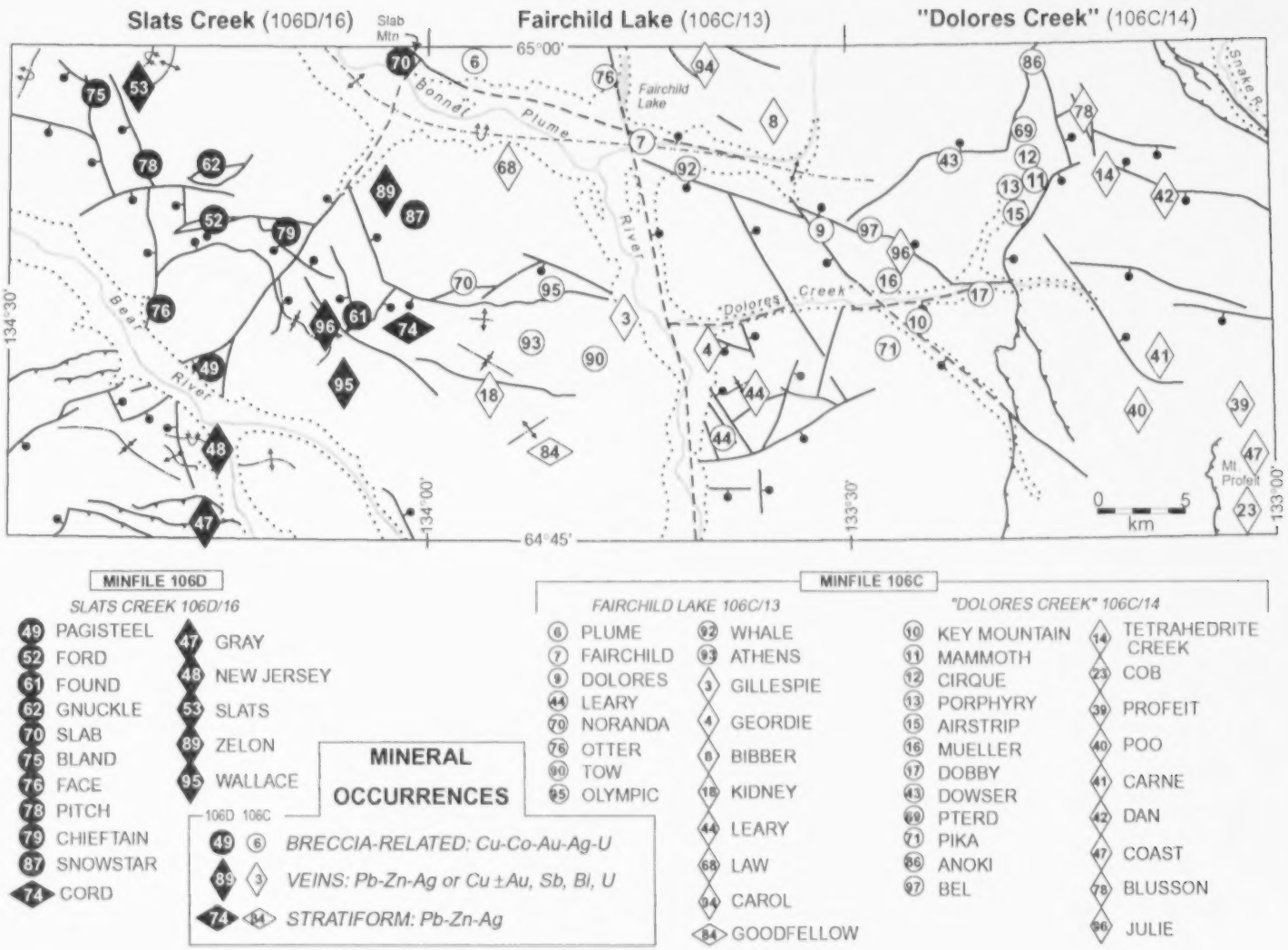

Figure 38. Mineral occurrences (Yukon Minfile, 1997) in the study area relative to major geological structures.

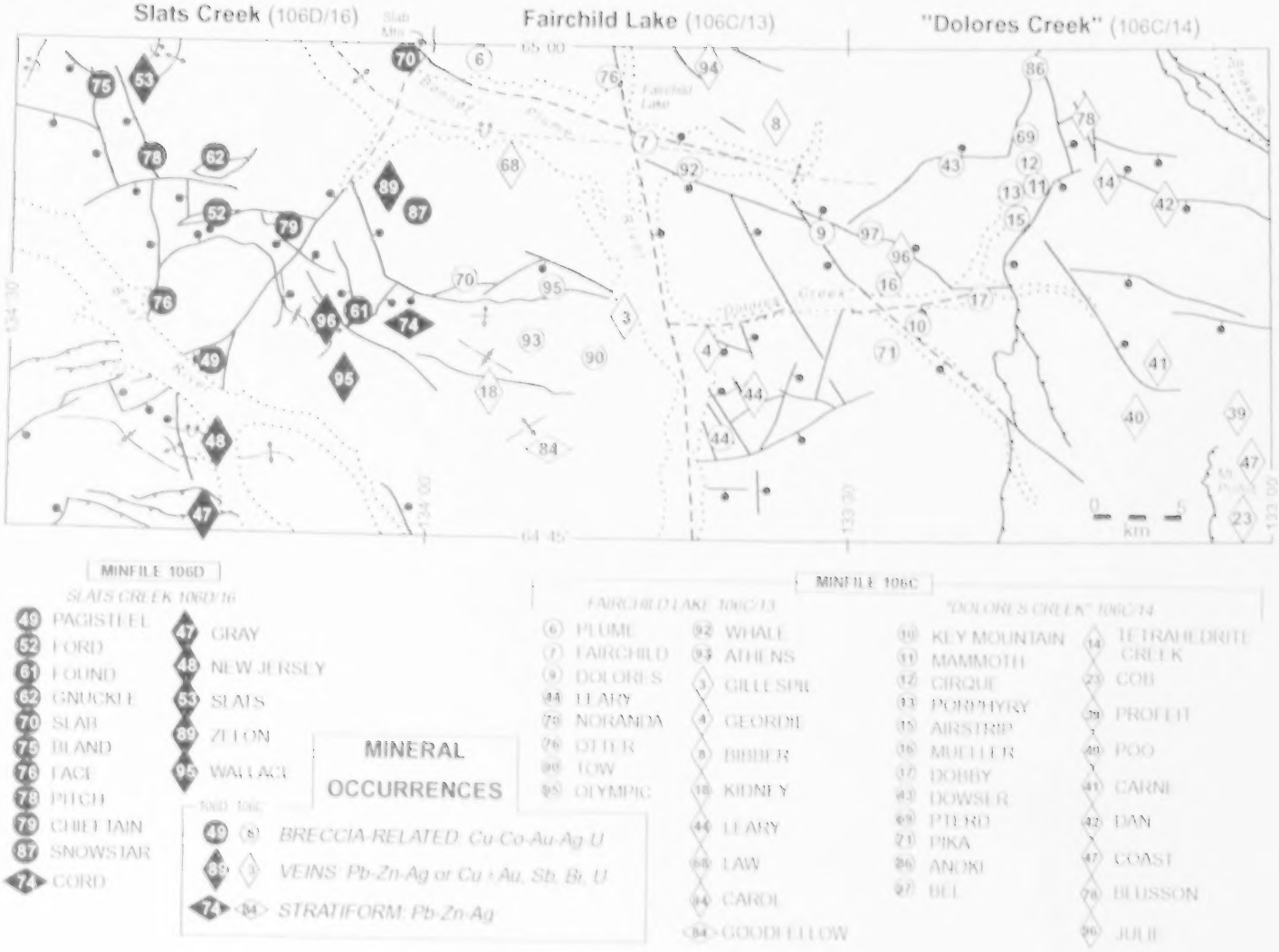

Figure 38. Mineral occurrences (Yukon Minfile, 1997) in the study area relative to major geological structures.

foundered into open space at the top of a breccia zone, forming a fallback megabreccia. Faulting may have been active concurrently. The hydrothermal fluids flowed through the brecciated rock. Minerals of various types including hematite, quartz, carbonate, chlorite, feldspar and mica precipitated among the fragments, cementing them together. In most cases, clasts and wallrocks were hydrothermally altered, leading to metasomatic growth of secondary minerals (for example, flecks of hematite or rhombs of dolomite). Widely disseminated earthy hematite and local potassic alteration in the breccia clasts have resulted in colour changes from original drab hues to striking pink, red and green. Clasts with embayments rimmed with secondary minerals, such as specular hematite, infer dissolution of clasts or their diagenetic cements by the hydrothermal fluids. Multiple events of brecciation and hydrothermal activity are evident. The main phase of brecciation and metasomatism occurred at ca. 1.6 Ga. Minor surges of hydrothermal activity related to emplacement of the Hart River intrusions and Bear River dykes occurred at ca. 1.38 and 1.27 Ga, respectively.

Mineral enrichments

Enrichments of Cu, Co, Au, Ag, Mo and U are localized within breccia zones and adjacent metasomatized country rock. The mineralizing events occurred chiefly in the main period of breccia formation and metasomatism. The absence of Fe-Cu-Co-Au-Ag-U enrichments in the Pinguicula Group, which was unconformably deposited on the breccia and its host rocks at ca. 1.38 Ga, is strong evidence that the vast majority of "breccia-related" mineralization occurred in the main stage of fluid flux, at ca. 1.6 Ga. Copper occurs as chalcopyrite, malachite, and rarely as bornite and chalcocite; cobalt occurs as cobaltite and erythrite; and uranium occurs as brannerite, uraninite, and related secondary minerals. Molybdenum occurs as molybdenite. Gold and silver concentrations are generally dependent on copper abundances.

The metasomatic alteration, which is so characteristic of the breccia zones, did not produce significant increases in the background concentrations of metals. Low background levels in Wernecke Breccia were established by Thorkelson and Wallace (1993a). Concentrations of Pb, Zn, Cu, Ni, Co, Cr, Sn, Sb, U, Th, Au and FeO in four hematitic breccia samples from the western part of the study area (106D/16) were normalized to average sedimentary rock (Fig. 39). All of the samples contain sedimentary clasts that are highly reddened, probably from hematitic and possibly potassic alteration, but none had visible enrichments of base or precious metals other than Fe. None of the samples have concentrations of any element greater than ten times the sedimentary normalizing values. In contrast, the strongly mineralized parts of the breccias commonly contain enrichments of Cu, Co, U, or Au which are hundreds or thousands of times higher than normal "background" levels (see Appendix 4). These data indicate that breccia-related hydrothermal alteration did not ubiquitously raise the concentrations of metallic elements. Local variations in country rock or perturbations in hydrothermal activity are likely to have controlled the distribution of Cu, Co, U and Au mineralization. The timing and compositional characteristics of mineralization relative to the more widespread iron-alkali-carbonate-silica alteration has not been determined. Preliminary studies of mineral paragenesis suggest that the mineralization occurred late in the history of initial hydrothermal activity (A. Conly and R.P Taylor, pers. comm., 1994). As discussed below, mineralization may have occurred in at least two pulses, spanning hundreds of millions of years.

The presence of igneous rock in and near the breccia zones has locally enhanced Cu mineralization. This relationship is established at the Porphyry, Olympic, Fairchild, Dolores and Pika occurrences (e.g., Fig. 34), where Cu showings commonly occur within or adjacent to bodies of diorite, quartz syenite or biotitic andesite mainly of the Bonnet Plume River intrusions. Apparently, the composition of these igneous bodies was particularly suitable for deposition of Cu from mineralizing fluids.

Some of the Cu in these occurrences may represent local redistribution of Cu within the intrusions (Laznicka and Edwards, 1979). However, some of the Cu was probably also derived from the hydrothermal fluids. This contention is supported by strong Cu enrichments in areas of breccia apparently distal from igneous rock. At the Tow occurrence,

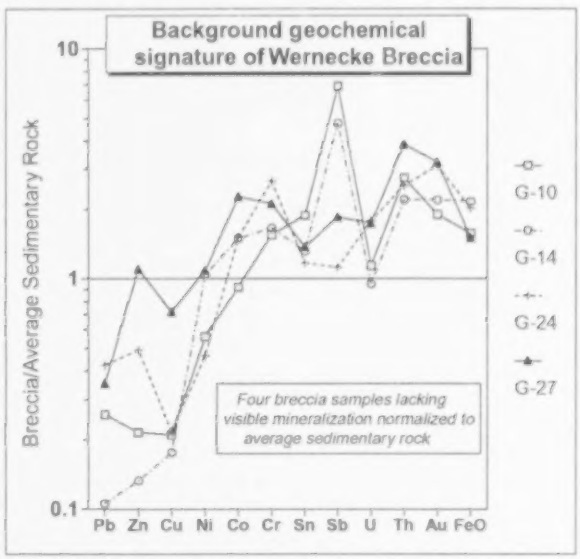

Figure 39. *Background metal concentrations in metasomatized but visibly non-mineralized samples of Wernecke Breccia. Concentrations in breccia samples are divided by those in worldwide-average sedimentary rock, taken from various sources. Normalizing values: 12 ppm Pb, 44 ppm Zn, 18 ppm Cu, 30 ppm Ni, 6.5 ppm Co, 45 ppm Cr, 2.3 ppm Sn, 0.58 ppm Sb, 2.1 ppm U, 5.1 ppm Th, 10 ppb Au, 4% FeO (total Fe as FeO).*

for example, no igneous rocks are exposed, and chalcopyrite is abundant as disseminated grains within siliceous breccia matrix. The source of Cu in the hydrothermal fluids responsible for this mineralization is unknown. Possibly, Cu was leached from igneous intrusions at depth. The source of Cu and other elements in Wernecke Breccia may be principally of igneous origin or derivation. This possibility is supported by the common spatial association between breccia bodies and igneous intrusions (Laznicka and Gaboury, 1988; Lane, 1990), which suggests that many of the breccias developed in zones of crustal weakness previously intruded by stocks and dykes.

Crude zonation of alteration has been documented at the Porphyry and Igor (106F/2) occurrences (Hitzman et al., 1992; Laznicka and Edwards, 1979). At the Porphyry occurrence, albitized rock in the centre of the aureole progressively gives way to rock enriched in quartz and sericite, and farther out, to rock enriched in quartz and carbonate. Additional studies are necessary to determine if these trends are generally true for other zones of Wernecke Breccia.

Weak supergene enrichment appears to have occurred at the Pika mineral occurrence beneath the angular unconformity separating Pinguicula Group from Gillespie Lake Group (Fig. 34). A thin zone of Cu enrichment in the form of malachite staining was observed below the unconformity at the base of a leached zone. The malachite-rich horizon is interpreted as a thin supergene-oxide zone, which resulted from downward migration and redeposition of Cu at the base of the leached zone. Hypogene mineralization of Cu occurs in breccia, dolostone and diorite beneath the malachite-rich layer.

Characteristics of selected occurrences

Disseminated chalcopyrite is concentrated in a quartz syenite stock at the Porphyry occurrence. The stock has been altered by sodic and ferric metasomatism, and is nearly surrounded by Wernecke Breccia. The stock crosscuts the Fairchild Lake Group on its eastern side, and was dated at ca. 1725 Ma. The occurrence was modestly explored in 1969, receiving 7 drill holes totaling 600 m (Yukon Minfile, 1997). It hosts disseminated chalcopyrite and yields enrichments of Cu averaging about 0.7%. Copper mineralization may be related to emplacement of the stock, to development of an adjacent breccia zone, or to both. The concentration of Cu in the stock rather than the country rock is consistent with Cu distribution at other igneous-breccia-related occurrences in the region.

The Bel is a group of chalcopyrite-malachite showings in fractured and brecciated siltstone of the Fairchild Lake Group, and in veined, metasomatized diorite of the Bonnet Plume River intrusions. It was previously identified but not described by Bell (1986a). The showings occur over a 1 x 0.5 km area. The diorite crops out along the banks of two small creeks in exposures up to 0.1 km^2, and appears to form the roof of a stock or a large mega-clast. The diorite hosts veinlet and disseminated secondary specularite, potassium feldspar, and locally, chalcopyrite. The best assay result, 0.8% Cu, came from a selected hand-specimen from a showing in brecciated siltstone (Table A4-1).

Chalcopyrite occurs as veinlets and disseminated grains in and around zones of Wernecke Breccia at the Mammoth, Dowser, Key Mountain and Airstrip occurrences (Yukon Minfile, 1997). Similar mineralization at the Mueller occurrence is over 1 km south of the nearest identified breccia. At the Cirque occurrence, chalcopyrite and cobaltite are disseminated and occur in siderite-quartz-bearing stringers sealing fractures. Chip samples reported from exploration in 1981 averaged 0.2% Cu and 0.02% Co (Yukon Minfile, 1997).

Uranium occurs along with Cu in the Anoki, Tetrahedrite Creek, Dobby, and Pterd breccia-related occurrences. At the Anoki occurrence, fracture zones related to faults contain uraninite, brannerite and chalcopyrite (Yeager and Ikona, 1979). Concentrations of 0.6% U_3O_8 and 1% Cu were reported over a 1 m interval (Stammers and Ikona, 1977). At the Pterd occurrence, fracture fillings in altered sedimentary rock contain pitchblende and chalcopyrite. At the Tetrahedrite Creek occurrence, a breccia body and adjacent 'skarn' in metasomatized siltstone host veinlets and disseminated grains of chalcopyrite, tetrahedrite and brannerite. Nearby vein mineralization is also included in this occurrence.

At the Pika occurrence, enrichments of Cu (chalcopyrite) and Au occur in breccia and country rock. Copper mineralization is concentrated along contacts between breccia and metasomatized diorite. Minor supergene-oxide enrichment of Cu and Ag occurs in a malachite-bearing horizon at the base of a leached zone beneath the overlying Pinguicula Group (Thorkelson and Wallace, 1994a). A sample from the malachite-bearing horizon contained 0.2% Cu, and 2.9 ppm Ag. One sample from a conspicuous zone of disseminated sulphides in the underlying hypogene zone contained 2% Cu and 1.5 ppm Ag.

Chalcopyrite, pyrite, barite, brannerite, cobaltite and rare molybdenite are present as fracture-fillings in altered sedimentary rock of the Fairchild Lake Group at the Slab occurrence. Nearby Wernecke Breccia is not mineralized and appears to have been emplaced after the fracturing and mineralization. The mineralization may have occurred during emplacement of adjacent stocks and dykes of the Bonnet Plume River intrusions, or during a phase of breccia-related hydrothermal activity, which preceded the emplacement of breccia at this locality.

Massive specular hematite is present at the Pagisteel occurrence in a breccia body, which crops out on both sides of the Bear River valley near an airstrip. Drilling has outlined approximately 1 million tonnes of 29.3% soluble iron.

Significant precious metal enrichments were noted at the Leary occurrence, where breccia contains up to 1.34% Cu, 311 ppm Bi, 1.2 ppm Ag, and 1.4 ppm Au. At the Sihota occurrence, about 30 km west of the study area, one sample of breccia adjacent to a highly metasomatized body of diorite yielded about 1.5 ppm Au.

Vein occurrences

Two main types of vein occurrences are present in the study area. One type consists of veins and associated pods enriched mainly in Pb, Zn and Ag. The other type consists of mainly Cu enrichments with local Sb, Bi and Au.

The Pb-Zn-Ag vein occurrences are most abundant in the southeastern part of the study area (Fig. 38), where the Cob, Coast, Profeit and Dan define a north-northwest trend and are hosted by Upper Proterozoic Profeit dolostone. The nearby Carne and Poo occurrences, which are located a few km to the west, share the same metallic signature but are hosted in dolostone of Pinguicula Group Unit C. The Profeit occurrence is the best known and was explored by five drill holes totaling 200 m. It includes several showings in a 1200-m-long zone within Profeit dolostone. Galena, sphalerite, tetrahedrite, pyrite, marcasite and minor chalcopyrite form massive pods, vug fillings, and veinlets. Replacement and open-space filling appear to have been important controls on mineralization. The largest pod of massive sulphides, 9 m long x 8 m wide, assayed 17% Zn, 47% Pb, and 580 g/t Ag (Yukon Minfile, 1997). At the nearby Cob occurrence, Zn/Pb ratios are higher, and a sulphide-rich vein assayed 42% Zn, 20% Pb, and 600 g/t Ag (Yukon Minfile, 1997). The Coast, Poo, Dan and Carne occurrences have similar metal signatures but lower grades. A newly discovered lens of sphalerite and galena, about 700 m east of the Dan, is considered part of that Minfile occurrence. The Tetrahedrite Creek occurrence lies at the north end of the "Profeit belt" of Pb-Zn-Ag occurrences. It is hosted by the Early Proterozoic Gillespie Lake Group, and consists of native Au, with tetrahedrite, galena, and sphalerite in quartz-carbonate veins. Selected samples yielded assays up to 410 g/t Au, 82 g/t Ag, 6% Cu, 5.5% Zn, and 21% Pb (Yukon Minfile, 1997). Lead-zinc-silver veins are also present in the central part of the study area.

The Geordie, Gillespie and Leary occurrences cluster near the confluence of Dolores Creek and the Bonnet Plume River (Fig. 38). They are hosted by dolostone of the Gillespie Lake Group. Mineralization in the Gillespie occurs as open-space fillings in brecciated dolostone. Samples collected from the Gillespie contain up to 3.0% Zn and 0.7% Pb (Dean, 1975). In the nearby and probably related Geordie occurrence, pyrite, galena, and sphalerite were found within a 77-m-wide easterly trending fracture zone which grades up to 1.1% Zn and 7.5 ppm Ag (Yukon Minfile, 1997). The Leary occurrence consists of stockwork hosting pyrite, galena and sphalerite along a 310-m-wide zone of fracturing. The best assays from channel samples on the Leary were 1.74% Zn and 0.24% Pb across 6.2 m (Alsen and Leary, 1975).

The eastern belt of the Pb-Zn-Ag occurrences extends from the Cob, at the southern edge of the study area, southward for at least 60 km to the Spectroair, Frigstad, Corn, Canwex, McKelvie, and several other occurrences. These occurrences are classified in Yukon Minfile (1997) as Mississippi Valley-type, an interpretation which draws attention to the genetic processes involved in the Profeit and other "vein" occurrences in the study area. Indeed, the pod-like aspect of some of the occurrences in the study area is suggestive of vug filling and replacement rather than crosscutting veining. Furthermore, all of the Pb-Zn-Ag occurrences in the study area occur within dolostone. The degree to which Mississippi Valley-type (low temperature) and vein-type (medium-high temperature) processes were involved in the Pb-Zn-Ag mineralization, within and to the south of the study area, remains unresolved.

The vein occurrences that are enriched in Cu ± other metals are hosted almost exclusively by the Wernecke Supergroup. Some may be related to Wernecke Breccia-type enrichments, which are also Cu-rich. In the eastern part of the study area, the Blusson occurrence lies north of the "Profeit belt" of Pb-Zn-Ag occurrences (Fig. 38), within Pinguicula Group unit A. The Blusson is a weak showing of scattered, thin veinlets of chalcopyrite and malachite. Along with the Au-rich Tetrahedrite Creek occurrence, the Blusson differs mineralogically from the "Profeit belt." Despite the mineralogical differences, all of these occurrences may have been produced by the same mineralizing event. The Au and Cu enrichments in the Tetrahedrite Creek and Blusson occurrences may have been caused by remobilization of nearby Wernecke Breccia-type enrichments during flux of mainly Zn-, Pb- and Ag-bearing fluids.

The Julie occurrence, north of Dolores Creek (Fig. 38), may also be related to Wernecke-breccia mineralization. The Julie consists of quartz-dolomite-pyrite-chalcopyrite veins hosted by slate of the Fairchild Lake Group. Two zones of veining about 5 m wide within the Fairchild Lake Group occur near the base of a cirque headwall less than 100 m from a zone of Wernecke Breccia. Abundant vein float suggests that additional veins may crop out higher on the cirque walls. The two best assays from vein material were 1.8% Cu, 0.42 g/t Au; and 0.02% Cu, 0.23 g/t Au. Other occurrences in which Cu is a principal metal include the Bibber (Cu), Kidney (Cu-U), Carol (Cu), New Jersey (Cu), Gray (Cu), Slats (Cu) and Zelon (Cu-Co-U). The metallic signature of the Zelon, in particular, resembles that of mineral occurrences in Wernecke Breccia. On the Bibber, chalcopyrite occurs in quartz veins up to 3.6 m wide within the Quartet Group, similar to the Julie. The Kidney occurrence contains U-minerals and chalcopyrite in narrow veinlets associated with two closely spaced faults in the Gillespie Lake Group.

The Wallace occurrence consist of polymetallic veins crosscutting the basal part of the Gillespie Lake Group. Its metal content differs from that of Wernecke Breccia-related occurrences, and from most other vein occurrences in the study area. One sample yielded 5.1% Cu, 2500 ppm Sb and 700 ppm Bi (Thorkelson and Wallace, 1994a). The veins at the Wallace may extend toward the Reid occurrence, 6 km to the north, which hosts north-trending veins of similar metallic signature.

Regional Synthesis

Introduction

Regional mapping and geochronology in the Wernecke and Ogilvie mountains of Yukon (Figs. 2, 5) has clarified the Lower and Middle Proterozoic geological evolution of northwestern Canada. The chronology of events and the correlation of units described in this report differ significantly from depictions presented a few years earlier (e.g., Aitken and McMechan, 1992; McMechan and Price, 1982; Young et al., 1979). Many of the new findings have been described by Thorkelson and Wallace (1994a; 1995a), Rainbird et al. (1997), Abbott et al. (1997), Abbott (1997), and Thorkelson et al. (1998). However, this report is the first to summarize all the salient data — both old and new — in a succinct geological history with accompanying documentation.

The chronology of events given below shows how the geological processes which shaped Yukon in Precambrian time are reflected in equivalent events in the Mackenzie Mountains and proximal parts of the Northwest Territories. The geological events are presented numerically, from first to last, and are grouped into specific intervals of time bounded by important igneous or metasomatic events.

Geological history

The timing of the following geological events is shown on a regional stratigraphic correlation diagram (Fig. 12). Major events pertaining to the study area are also indicated in a time-statigraphic diagram (Fig. 4).

>1.73 Ga

1. Formation of continental basement. The cratonic basement of Yukon is not exposed, and its age and nature are unknown. It may consist of rocks of Archean to Early Proterozoic age. The nearest cratonic constituent is the Nahanni domain, which is restricted to the subsurface and extends from the western Northwest Territories to southeastern Yukon and northeastern British Columbia. Hoffman (1989) distinguished the Nahanni domain from the Fort Simpson domain to the east on the basis of aeromagnetic character. Whether the Nahanni domain extends westward beneath the Ogilvie and Wernecke mountains is unknown. The Fort Simpson domain contains granitic rocks as young as 1.845 Ga, and may be a subduction-generated magmatic arc or collisional welt built on the eastern edge of the Nahanni domain (Villeneuve et al., 1991).

2. Rifting and formation of the Wernecke basin, probably after ca. 1.84 Ga Fort Simpson magmatism. Attenuation of the basement is implied by the 14 km thickness of the overlying Wernecke Supergroup (Delaney, 1981). Rifting may have separated or partially separated North America from another continent, perhaps Australia. Syn-rift igneous rocks are not exposed, inferring that the main axis of extension lay to the west of the present Wernecke basin.

3. Wernecke Supergroup sedimentation from (?)1.84 Ga to 1.73 Ga. Three regionally extensive groups were deposited, forming two clastic-to-carbonate grand cycles (Delaney, 1981). An event of syndepositional rifting is likely to have initiated the second grand cycle, as indicated by an abrupt transition from dolostone to pyritic shale at the top of the Fairchild Lake Group. Minor Pb-Zn sedimentary exhalations occurred toward the top of the Wernecke Supergroup. Deposition of the Supergroup was probably concurrent with accumulation of thinner, more platformal sedimentary strata of the lower Hornby Bay Group (East River and Lady Nye formations; Kerans et al., 1981; Cook and Maclean, 1995).

1.73-1.59 Ga

The relative timing of the Racklan Orogeny and the emplacement of the Bonnet Plume River intrusions is uncertain (see discussion under Phase 2 in the Structural History section). Correlation of the Slab volcanics with the Bonnet Plume River intrusions is speculative (Figs. 4, 12). Thus, the order of geological events 4 and 5, given below, remains unknown.

4. Intrusion of mainly mafic igneous magmas from 1.73-1.71 Ga (Bonnet Plume River intrusions; J.K. Mortensen, pers. comm., 1994). Magmatism was probably related to mantle plume activity and/or extensional tectonism. Local Cu-Au-Co enrichments at the Slab and possibly other mineral occurrences may have been generated during emplacement of local intrusions. The Slab volcanics, which are remnants of an undated shield volcano engulfed by 1.59 Ga Wernecke Breccia, may have been co-magmatic with the Bonnet Plume River intrusions, as speculatively indicated on Figs. 4 and 12.

5. Racklan Orogeny: east- to southeast-directed deformation producing folds, schistosity and kink bands in the Wernecke Supergroup. Deformation occurred after deposition of the Wernecke Supergroup, and before 1.6 Ga development of Wernecke Breccia (Thorkelson and Wallace, 1994a; Abbott et al., 1997). However, it is unclear whether deformation occurred before or after 1.71 Ga dyking, and eruption of the Slab volcanics, whose age has yet to be determined. Racklan deformation is probably equivalent to the Forward Orogeny (ca. 1.66 Ga) in the Northwest Territories (Bowring and Ross, 1985; Cook and Maclean, 1995). It is much older than deformation described from the subsurface and the Coppermine Homocline by Cook (1992). Concurrent deformation in west and south Australia may be represented by the Isan or Kimban orogenies.

6. Possible plutonism and volcanism at about 1.6 Ga. Plutonic activity in the region is inferred from a ca. 1.6 Ga inherited zircon component in a granitic diatreme clast from the Mackenzie Mountains (Jefferson and Parrish, 1989). Concurrent volcanism may or may not be represented by the Slab volcanics, a remnant of an undated shield volcano in the Wernecke Mountains that is engulfed by 1.59 Ga Wernecke Breccia. Undated biotite lamprophyre dykes, which are crosscut by hematite veinlets, may belong to the suggested

1.6 Ga magmatism. Possible correlatives in South Australia include the Gawler Range volcanics and the Hiltaba plutonic suite, both of which are about 1.6 Ga.

7. Surges of hydrothermal activity and phreatic explosions at about 1.59 Ga, producing zones of hematitic breccia (Wernecke Breccia) and enrichments of Cu, Au, Co, and U (Thorkelson and Wallace, 1994a; Abbott et al., 1997). Brecciation was probably accompanied by explosive venting and maar formation above the Slab volcanics, and by normal faulting. The mega-clast of the Slab volcanics was incorporated in the breccia, apparently during clastic fallback after diatreme-like venting. The hydrothermal activity may have been generated during emplacement and cooling of the 1.6 Ga intrusions. Time-equivalent breccias of similar lithology and mineralogy were generated at the Olympic Dam mine in South Australia (Bell and Jefferson, 1987; Hitzman et al., 1992; Creaser and Cooper, 1993).

1.59-1.27 Ga

8. Faulting in the Wernecke Mountains producing shear fabrics in Wernecke Breccia that are truncated by the Pinguicula Group.

9. Deep weathering of the Wernecke Supergroup and Wernecke Breccia during the interval 1.59-1.38 Ga. Local supergene enrichment of mineralized rock (Thorkelson and Wallace, 1994a).

10. Rifting, mafic magmatism, and deposition of the basal Pinguicula and Fifteenmile groups at ca. 1.38 Ga. Rifting is implied by development of the Pinguicula basin, which accommodated >3 km of basinal clastic to platformal carbonate deposits (Eisbacher, 1981). The time of rifting is known from the ca. 1.38 Ga Hart River sills. One of the sills lies unconformably beneath the Pinguicula Group, and another intrudes the base of the Pinguicula Group (Abbott, 1997; Thorkelson and Mortensen, unpublished). The undated Hart River volcanics, which sit below the Pinguicula Group, are considered co-magmatic with the Hart River sills. Listric-normal faulting and rifting accompanied deposition of the basal lower Fifteenmile Group in the western Ogilvie Mountains (Thompson, 1995; Abbott, 1997). Hydrothermal activity during rifting is indicated by: (1) rutile dated at ca. 1.38 Ga from the Slab volcanics (Thorkelson and Mortensen, unpublished); and (2) the Hart River polymetallic massive sulphide deposit which crosscuts the Hart River volcanics but not the overlying Pinguicula Group (Abbott, 1997). The lower Pinguicula Group (units A-C) and units R1-4 of the Lower Fifteenmile Group are correlated with the Dismal Lakes Group of the Northwest Territories. The 1.38 Ga rift event is approximately time equivalent to the East Kootenay orogeny in southern British Columbia (McMechan and Price, 1982; Doughty and Chamberlin, 1996).

11. Emplacement of the Bear River dykes, and probable eruption of mafic lavas, at ca. 1.27 Ga (Thorkelson and Mortensen, unpublished). Igneous intrusions of this age probably extend northward into the Richardson Mountains where hydrothermal alteration is recorded by 1.27 Ga monazite (Parrish and Bell, 1987). Hematitic alteration of a Bear River dyke in the Wernecke Mountains was probably part of this magma-fluid event. Bear River magmatism is considered part of the huge Mackenzie igneous event in the Canadian Shield, including emplacement of the Mackenzie dyke swarm and the Muskox intrusion, and eruption of the Coppermine Lavas (LeCheminant and Heaman, 1989).

1.27-0.8 Ga

12. Minor plutonism in the crust beneath the Mackenzie Mountains at approximately 1.15 Ga, as indicated by the age of a granite clast in a diatreme (Jefferson and Parrish, 1989). This igneous event may be tied to weak Grenville-age orogenesis, which extended through Australia and into western Canada (Ross et al., 1992).

13. From 1.27-1.1 Ga, complete erosion of all volcanic strata inferred to have been deposited during the 1.27 Ga and (?)1.15 Ga igneous events. Uplift, karsting, and local deformation of the Pinguicula Group probably occurred in this interval.

14. Deposition of the Hematite Creek Group and the lower Upper part of the Fifteenmile Group (unit R5) as epicontinental clastic and carbonate deposits. Deposition, which was probably restricted to the interval 1.1-0.9 Ga, occurred on a terrain of locally karsted and tilted carbonate strata of the lower Pinguicula Group in the Wernecke Mountains, and with angular unconformity on rocks as old as the Wernecke Supergroup and Wernecke Breccia in the western Ogilvie Mountains. Sandstone beds contain Grenville-age zircon and muscovite grains (Rainbird et al., 1997; Thorkelson and Villeneuve, unpublished). Apparently, sediment was shed from the Grenville orogen and transported northwestward across the continent by major river systems (Rainbird et al., 1997). The Hematite Creek Group and correlative parts of the Fifteenmile group are two of several successions that formed during widespread subsidence of western and northern Canada. Subsidence was in response to Grenville orogenesis along the eastern and southern parts of ancestral North America. Other successions with equivalent sedimentological characteristics include the Katherine Group and possibly other parts of the Mackenzie Mountains Supergroup, and the Shaler Supergroup in the western Canadian Arctic. The unconformity separating the Pinguicula Group (and correlative strata) from the Hematite Creek Group (and correlative strata) may reflect wholly or in part the 1.27 Ga igneous event and associated uplift and rifting documented in the Coppermine homocline (reviewed in Cook, 1992).

15. Corn Creek Orogeny: west-directed folding and thrust-faulting of the Hematite Creek Group, the Pinguicula Group (Eisbacher, 1981) and, locally, the Wernecke Supergroup (Thorkelson and Wallace, 1995a). The timing and regional extent of this orogenic event (named herein) are not well understood. The orogeny is best displayed in the Wernecke Mountains where overturned folds and thrust faults

in the Group are truncated by the Sayunei Formation of the Windermere Supergroup (Eisbacher, 1981). This relationship constrains the timing of Corn Creek deformation to the interval between the end of Hematite Creek Group deposition (<1.0 Ga) and the onset of Sayunei deposition (<0.75 Ga). If the Corn Creek Orogeny occurred early in this interval, it could be regarded as a "late Grenville" event. Despite unequivocal evidence for deformation in the Wernecke Mountains, the expression of orogenesis in other areas is unclear, and the timing and cause of contraction is problematic. Contraction may have been related to an early history of motion on the Snake River. It is possible that the Corn Creek Orogeny occurred after deposition of the Callison Lake dolostone and related units (described below)

16. Deposition of Callison Lake dolostone and units F1-F3 (mainly carbonate) of the upper Fifteenmile Group, in the Ogilvie Mountains. Sedimentation occurred before Windermere Supergroup deposition, probably in the interval 900-800 Ma. The Callison Lake-upper Fifteenmile strata are bounded by unconformities, one of which may correspond to the Corn Creek Orogeny. The Little Dal Group, and possibly only the upper Little Dal carbonate, are probable correlative units in the Mackenzie Mountains (Abbott, 1997).

800-550 Ma

17. Rifting, and deposition of the Mount Harper Group in the western Ogilvie Mountains. Deposition began with coarse clastic rocks, and continued with mainly mafic volcanism at ca. 750 Ma (Mustard and Roots, 1997). The rifting may be considered the first part of the Hayhook tectonic event during which the crust in the Mackenzie Mountains and adjacent areas was extended (Young et al., 1979; Jefferson and Parrish, 1989; Norris and Dyke, 1997), and the basal Windermere Supergroup was deposited (Mustard and Roots, 1997). In the Mackenzie Mountains, magmatism broadly coeval with Mount Harper volcanism occurred as a quartz diorite stock (ca. 778 Ma; Jefferson and Parrish, 1989) and the Tsezotene sills (ca. 779 Ma; Heaman et al., 1992). The nearby and chemically similar Little Dal basalts probably erupted at this time (Dudas and Lustwerk, 1997; Mustard and Roots, 1997). Consequently, the Coates Lake Group should also be considered part of the basal Windermere Supergroup (Aitken, 1981).

18. Deposition of the Rapitan Group and higher parts of the Windermere Supergroup. Sedimentation began sometime after ca. 755 Ma, which is the age of a granite clast in basal Windermere conglomerate (Ross and Villeneuve, 1997). Deposition involved a wide range of sediment types, with conglomerate and glacial diamictite dominant near the bottom, and sandstone, shale, and carbonate dominant toward the top (Eisbacher, 1981; Jefferson and Parrish, 1989). Banded iron formation of the Crest mineral occurrence was deposited early in Windermere time (Yeo, 1981). Ediacaran fauna is preserved in the top half up the Windermere succession (Narbonne and Hoffman, 1987). In the Wernecke Mountains and possibly elsewhere, the Rapitan Group is separated from younger Windermere strata by a lacuna of perhaps 50 million years. Syn-sedimentary block faulting occurred during protracted extension of the Hayhook event. This event and subsequent Early Paleozoic rifting and subsidence may record complete, oceanic separation of Australia from western North America (Ross, 1991; Dalziel, 1991).

19. Complete erosion of the Pinguicula Group, Hematite Creek Group, Windermere Supergroup, and Unit PCs, west of the Fairchild Fault. Erosion was followed by widespread deposition of unit CDs, which correlates with the Lower Paleozoic Slats Creek, Franklin Mountain and Mount Kindle formations (Green, 1972; Cecile, 1982). These strata, dominated by resistant, grey-weathering dolostone, characterize Mackenzie Platform and separate it from mainly clastic rocks of Selwyn Basin to the south, and Richardson Trough to the north.

References

Abbott, J.G., 1993. Revised stratigraphy and new exploration targets in the Hart River area (NTS 116A/10, 116A/11), southeastern Yukon. *In:* Yukon Exploration and Geology 1992, Exploration and Geological Services Division, Yukon, Indian and Northern Affairs Canada, p. 13-23.

Abbott, J.G., 1997. Geology of the upper Hart River area, eastern Ogilvie Mountains, Yukon Territory (116A/10, 116A/11). Exploration and Geological Services Division, Yukon, Indian and Northern Affairs Canada, Bulletin 9, 76 p.

Abbott, G., Thorkelson, D., Creaser, R., Bevier, M.L., and Mortensen, J., 1997. New correlations among Proterozoic successions and intrusive breccias in the Ogilvie and Wernecke mountains, Yukon. *In:* Lithoprobe Report No. 56, p. 188-197.

Aitken, J.D., 1981. Stratigraphy and sedimentology of the Upper Proterozoic Little Dal Group, Mackenzie Mountains, Northwest Territories. *In:* Proterozoic Basins of Canada, F.H.A. Campbell (ed.), Geological Survey of Canada, Paper 81-10, p. 47-72.

Aitken, J.D., 1991. The Ice Brook Formation and post-Rapitan, Late Proterozoic glaciation, Mackenzie Mountains, Northwest Territories. Geological Survey of Canada, Bulletin 404, 43 p.

Aitken, J.D., and McMechan, M.E., 1992. Middle Proterozoic assemblages, Chapter 5. *In:* H. Gabrielse and C.J. Yorath (eds.), Geological Survey of Canada, Geology of the Cordilleran Orogen in Canada, no. 4, p. 97-124.

Aleinikoff, J.N., Evans, K.V., Fanning, C.M., Obradovish, J.D., Ruppel, E.T., Zeig, J.A. and Steinmetz, J.C., 1996. SHRIMP U-Pb ages of felsic igneous rocks, Belt Supergroup, western Montana. Geological Society of America, Program with Abstracts, vol. 28, p. A376.

Alsen, J.B. and Leary, G.M., 1975. Dolores Creek Pb-Zn Property DTG 1-144 Claims. Mineral Resources Directorate, Yukon, Indian and Northern Affairs Canada, Assessment Report #090061.

Anderson, H.E. and Davis, D.W., 1995. U-Pb geochronology of the Moyie sills, Purcell Supergroup, southeastern British Columbia: Implications for the Mesoproterozoic geological history of the Purcell (Belt) basin. Canadian Journal of Earth Sciences, vol. 32, p. 1180-1193.

Anderson, J.L. and Morrison, J., 1992. The role of anorogenic granites in the Proterozoic crustal development of North America. *In:* Proterozoic Crustal Evolution, K.C. Condie (ed.), Elsevier Science Publishers B.V., Amsterdam, p. 263-299.

Archer, A., Bell, R.T. and Thorpe, R.I., 1986. Age relationships from U-Th-Pb isotope studies of uranium mineralization in Wernecke Breccias, Yukon Territory. *In:* Current Research, Part A, Geological Survey of Canada, Paper 86-1A, p. 385-391.

Archer, A. and Schmidt, U., 1978. Mineralized breccias of early Proterozoic age, Bonnet Plume River district, Yukon Territory. Canadian Mining and Metallurgy Bulletin, vol. 71, no. 796, p. 53-58.

Bell, R.T., 1968. Proterozoic stratigraphy of northeastern British Columbia. Geological Survey of Canada, Paper 67-68, 75 p.

Bell, R.T., 1978. Breccias and uranium mineralization in the Wernecke Mountains, Yukon - A progress report. *In:* Current Research, Geological Survey of Canada, Paper 78-1A, p. 317-322.

Bell, R.T., 1986a. Geological map of northeastern Wernecke Mountains, Yukon Territory. Geological Survey of Canada, Open File 1207.

Bell, R.T., 1986b. Megabreccias in northeastern Wernecke Mountains, Yukon Territory. *In:* Current Research, Part A, Geological Survey of Canada, Paper 1986-1A, p. 375-384.

Bell, R.T., 1989. A conceptual model for development of megabreccias and associated mineral deposits in Wernecke Mountains, Canada, Copperbelt, Zaire, and Flinders Range, Australia. *In:* Uranium Resources and Geology of North America; Proceedings of a technical committee meeting organized by the International Atomic Energy Agency and held in Saskatoon, Canada (1987), p. 149-169.

Bell, R.T. and Delaney, G.D., 1977. Geology of some uranium occurrences in Yukon Territory. *In:* Current Research, Part A. Geological Survey of Canada, Paper 77-1A, p. 33-37.

Bell, R.T. and Jefferson, C.W., 1987. A hypothesis for an Australian-Canadian connection in the late Proterozoic and the birth of the Pacific Ocean. *In:* Pacific Rim Congress '87, Parkville, Victoria, p. 39-50.

Blusson, S.L., 1974. Geology of Nadaleen River, Lansing, Niddery Lake, Bonnet Plume Lake, and Mount Eduni map areas, Yukon Territory. Geological Survey of Canada, Open File 205, 1:250 000 scale.

Bowring, S.A. and Ross, G.M., 1985. Geochronology of the Narakay Volcanic Complex: Implications for the age of the Coppermine Homocline and Mackenzie igneous events. Canadian Journal of Earth Sciences, vol. 22, p. 774-781.

Campbell, C. and McClintock, J., 1980. Cord Claims Geology and Geophysics 1980. Mineral Resources Directorate, Yukon, Indian and Northern Affairs Canada, Assessment Report #090759.

Cecile, M.P., 1982. The lower Paleozoic Misty Creek Embayment, Selwyn Basin, Yukon and Northwest Territories. Geological Survey of Canada, Bulletin 335, 78 p.

Cecile, M.P., 1984. Evidence against large-scale strike-slip separation of Paleozoic strata along the Richardson-Hess fault system, northern Canadian Cordillera. Geology, vol. 12, p. 403-407.

Conly, A.G., 1993. Mineralogy and mineral chemistry of hydrothermal alteration of Wernecke Breccia from the Slats Creek (NTS 106D/16) map area, Wernecke Mountains, Yukon. Unpublished report, Carleton University, 60 p.

Cook, D.G. and MacLean, B.C., 1995. The intracratonic Forward orogeny, and implications for regional correlations, Northwest Territories, Canada. Canadian Journal of Earth Sciences, vol. 32, p. 1991-2008.

Cook, D.G. and MacLean, B.C., 1999. The Imperial anticline, a fault-bend fold above a bedding-parallel thrust ramp, Northwest Territories, Canada. Journal of Structural Geology, vol. 21, p. 215-228.

Cook, F.A., 1992. Racklan orogen. Canadian Journal of Earth Sciences, vol. 29, p. 2490-2496.

Cook, F.A., Dredge, M. and Clark, E.A., 1992. The Proterozoic Fort Simpson structural trend in northwestern Canada. *In:* Geological Society of America Bulletin, vol. 104, p. 1121-1137.

Cook, F.A., van der Velden, A.J., Hall, K.W. and Roberts, B.J., 1998. Tectonic delamination of the Precambrian lithosphere in northwestern Canada mapped by LITHOPROBE. *In:* Cook, F. and P. Erdmer (compilers), 1998, Slave-Northern Cordillera Lithospheric Evolution (SNORCLE) Transect and Cordilleran Tectonics Workshop Meeting (March 6-8), Simon Fraser University, Lithoprobe Report No. 64, p. 58-69.

Cook, F.A., Varsek, J.L. and Clark, E.A., 1991. Proterozoic craton to basin crustal transition in western Canada and its influence on the evolution of the Cordillera. Canadian Journal of Earth Sciences, vol. 28, p. 1148-1158.

Creaser, R.A., 1995. Neodymium isotopic constraints for the origin of Mesoproterozoic felsic magmatism, Gawler Craton, South Australia. Canadian Journal of Earth Sciences, vol. 32, p. 460-471.

Creaser, R.A. and Cooper, J.A., 1993. U-Pb geochronology of Middle Proterozoic felsic magmatism surrounding the Olympic Dam Cu-U-Au-Ag and Moonta Cu-Au-Ag deposits, South Australia. Economic Geology, vol. 88, p. 186-197.

Dalziel, I.W.D., 1991. Pacific margins of Laurentia and east Antarctica-Australia as a conjugate rift pair: Evidence and implications for an Eocambrian supercontinent. Geology, vol. 19, p. 598-601.

Dean, P., 1975. 1975 Exploration Report Ape Mineral Claim Group. Mineral Resources Directorate, Yukon, Indian and Northern Affairs Canada, Assessment Report #090053.

Delaney, G.D., 1981. The mid-Proterozoic Wernecke Supergroup, Wernecke Mountains, Yukon Territory. *In:* Proterozoic Basins of Canada, F.H.A. Campbell (ed.), Geological Survey of Canada, Paper 81-10, 23 p.

Doughty, P.T. and Chamberlin, K.R., 1996. Salmon River Arch: New evidence for rifting near the end of deposition in the Middle Proterozoic Belt basin. Canadian Journal of Earth Sciences, vol. 33, p.1037-1052.

Doughty, P.T., Price, R.A. and Parrish, R.R., 1998. Geology and U-Pb geochronology of Archean basement and Proterozoic cover in the Priest River complex, northwestern United States, and their implications for Cordilleran structure and Precambrian continent reconstructions. Canadian Journal of Earth Sciences, vol. 35, p. 39-54.

Dredge Mitchelmore, M. and Cook, F.A., 1994. Inversion of the Proterozoic Wernecke basin during tectonic development of the Racklan Orogen, northwest Canada. Canadian Journal of Earth Sciences, vol. 31, p. 447-457.

Dudas, F.O. and Lustwerk, R.L., 1997. Geochemistry of the Little Dal basalts: Continental tholeiites from the Mackenzie Mountains, Northwest Territories, Canada. Canadian Journal of Earth Sciences, vol. 34, p. 50-58.

Eaton, W.D., 1983. Wernecke Joint Venture Geological and Geochemical Report Jolly 1-10 Claims. Mineral Resources Directorate, Yukon, Indian and Northern Affairs Canada, Assessment Report #091442.

Eisbacher, G.H., 1978. Two major Proterozoic unconformities, Northern Cordillera. *In:* Current Research, Part A, Geological Survey of Canada, Paper 78-1A, p. 53-58.

Eisbacher, G.H., 1981. Sedimentary tectonics and glacial record in the Windermere Supergroup, Mackenzie Mountains, northwestern Canada. Geological Survey of Canada, Paper 80-27, 40 p.

Eisbacher, G.H., 1983. Devonian-Mississippian sinistral transcurrent faulting along the cratonic margin of western North America: A hypothesis. Geology, vol. 11, p. 7-10.

Eisbacher, G.H., 1985. Late Proterozoic rifting, glacial sedimentation, and sedimentary cycles in the light of Windermere deposition, western Canada. Palaeogeography, Palaeoclimatology, Palaeoecology, vol. 51, p. 231-254.

Ernst, R.E., Head, J.W., Parfitt, E., Grosfils, E. and Wilson, L., 1995. Giant radiating dyke swarms on Earth and Venus. Earth-Science Reviews, vol. 39, p. 1-58.

Fahrig, W.F. and West, T.D., 1986. Diabase dyke swarms of the Canadian Shield. Geological Survey of Canada, Map 1627 A, 1:4 873 900 scale.

Francis, D., 1994. Chemical interaction between picritic magmas and upper crust along the margins of the Muskox intrusion, Northwest Territories. Geological Survey of Canada, Paper 92-12, 94 p.

Fritz, W.H., 1997. Chapter 5: Cambrian. *In:* Geology and Mineral and Hydrocarbon Potential of Northern Yukon Territory and Northwestern District of Mackenzie, D.K. Norris (ed.), p. 84-117.

Fritz, W.H., Narbonne, G.M. and Gordey, S.P., 1983. Strata and trace fossils near the Precambrian-Cambrian boundary, Mackenzie, Selwyn and Wernecke mountains, Yukon and Northwest Territories. *In:* Current Research, Part B, Geological Survey of Canada, Paper 83-1B, p. 365-375.

Gabrielse, H., 1967. Tectonic evolution of the northern Canadian Cordillera. Canadian Journal of Earth Sciences, vol. 4, p. 271-298.

Gabrielse, H., 1972. Younger Precambrian of the Canadian Cordillera. American Journal of Science, vol. 272, p. 521-536.

Gabrielse, H. and Campbell, R.B., 1991. Chapter 6: Upper Proterozoic assemblages. *In:* Geology of the Cordilleran Orogen in Canada, Geology of North America, vol. G-2, Geology of Canada, No. 4, p. 127-150.

Gandhi, S.S. and Bell, R.T., 1990. Metallogenic concepts to aid exploration for the giant Olympic Dam-type deposits and their possible derivatives. *In:* Proceedings of the Eighth Quadrennial IAGOD Symposium, Ottawa, Canada, 1990, p. 787-802.

Godwin, C.I., Gabites, J.E. and Andrew, A., 1988. Leadtable: A galena lead isotope data base for the Canadian Cordillera. British Columbia Geological Survey Branch, Paper 1988-4, 188 p.

Gordey, S.P. and Anderson, R.G. 1993. Evolution of the northern Cordilleran miogeocline, Nahanni map area (105I), Yukon and Northwest Territories. Geological Survey of Canada, Memoir 428, 214 p.

Green, L.H., 1972. Geology of Nash Creek, Larsen Creek, and Dawson Creek map-areas, Yukon Territory. Geological Survey of Canada, Memoir 364, 157 p.

Hall, K.W. and Cook, F.A., 1998. Geophysical transect of the Eagle Plains foldbelt and Richardson Mountains anticlinorium, northwestern Canada. Geological Society of America Bulletin, vol. 110, no. 3, p. 311-325.

Hardy, J.L. and Campbell, C.J., 1981. Cord Group (Snakehead Property) Geophysics and Diamond Drilling. Mineral Resources Directorate, Yukon, Indian and Northern Affairs Canada, Assessment Report #090996.

Heaman, L.M., LeCheminant, A.N. and Rainbird, R.H., 1992. Nature and timing of Franklin igneous events, Canada: Implications for a Late Proterozoic mantle plume and the break-up of Laurentia. Earth and Planetary Science Letters, vol. 109, p. 117-131.

Hitzman, M.W., Oreskes, N. and Einaudi, M.T., 1992. Geological characteristics and tectonic setting of Proterozoic iron oxide (Cu-U-Au-REE) deposits. *In:* Precambrian Metallogeny Related to Plate Tectonics, G. Gall and K. Schulz (eds.), Precambrian Research, vol. 58, p. 241-287.

Hoffman, P., 1989. Precambrian geology and tectonic history of North America. *In:* The Geology of North America – An Overview, A.W. Bally and A.R. Palmer (eds.), Geological Society of America, Geology of North America, vol. A., p. 447-512.

Hofmann, H.J., Narbonne, G.M. and Aitken, J.D., 1990. Ediacaran remains from intertillite beds in northwestern Canada. Geology, vol. 18, p. 1199-1202.

Hulstein, R., 1994. Assessment Report on the 1993 Geological and Geochemical Investigation of the Kiwi Property, Kennecott Canada, Inc., Mayo Mining District, Yukon Territory, NTS map area 105E/2E. Mineral Resources Directorate, Yukon, Indian and Northern Affairs Canada, Assessment Report, 23 p.

Jefferson, C.W. and Parrish, R.R., 1989. Late Proterozoic stratigraphy, U-Pb zircon ages, and rift tectonics, Mackenzie Mountains, northwestern Canada. Canadian Journal of Earth Sciences, vol. 26, p. 1784-1801.

Kerans, C., Ross, G.M., Donaldson, J.A. and Geldsetzer, H.J., 1981. Tectonism and depositional history of the Helikian Hornby Bay and Dismal Lakes groups, District of Mackenzie. *In:* Proterozoic Basins of Canada, F.H.A. Campbell (ed.), Geological Survey of Canada, Paper 81-10, p. 157-182.

Lane, L.L., 1996. Geometry and tectonics of early Tertiary triangle zones, northeastern Eagle Plain, Yukon Territory. Canadian Society of Petroleum Geologists Bulletin, vol. 44, p. 337-348.

Lane, R.A., 1990. Geologic setting and petrology of the Proterozoic Ogilvie Mountains Breccia of the Coal Creek inlier, southern Ogilvie Mountains, Yukon Territory. Unpublished M.Sc. thesis, University of British Columbia, Vancouver, B.C., 223 p.

Laznicka, P. and Edwards, R.J., 1979. Dolores Creek, Yukon - a disseminated copper mineralization in sodic metasomatites. Economic Geology, vol. 74, p. 1352-1370.

Laznicka, P. and Gaboury, D., 1988. Wernecke Breccias and Fe, Cu, U mineralization: Quartet Mountain-Igor area (NTS 106E). *In:* Yukon Geology, Volume 2, J.G. Abbott (ed.), Exploration and Geological Services Division, Yukon, Indian and Northern Affairs Canada, p. 42-50.

LeCheminant, A.N. and Heaman, L.M., 1989. Mackenzie igneous events, Canada: Middle Proterozoic hotspot magmatism associated with ocean opening. Earth and Planetary Science Letters, vol. 96, p. 38-48.

McMechan, M.E. and Price, R.A., 1982. Superimposed low-grade metamorphism in the Mount Fisher area, southeastern British Columbia – implications for the east Kootenay Orogeny. Canadian Journal of Earth Sciences, vol. 19, p. 476-489.

Mitchell, R.H., 1991. Kimberlites and lamproites: Primary sources of diamond. Geoscience Canada, vol. 18, p. 1-16.

Moores, E.M., 1991. Southwest U.S. - East Antarctic (SWEAT) connection: A hypothesis. Geology, vol. 19, p. 425-428.

Mortensen, J.K. and Colpron, M., 1998. Geochronological and geochemical studies of the Coates Lake Diatreme, southern Mackenzie Mountains, western N.W.T. *In:* Lithoprobe, Report No. 64, p. 278.

Mustard, P.S. and Roots, C.F., 1997. Rift-related volcanism, sedimentation, and tectonic setting of the Mount Harper Group, Ogilvie Mountains, Yukon Territory. Geological Survey of Canada, Bulletin 492, 92 p.

Mustard, P.S., Roots, C.F., and Donaldson, J.A., 1990. Stratigraphy of the Middle Proterozoic Gillespie Lake Group in the southern Wernecke Mountains, Yukon. *In:* Current Research, Part E, Geological Survey of Canada, Paper 90-1E, p. 43-53.

Narbonne, G.M. and Aitken, J.D., 1995. Neoproterozoic of the Mackenzie Mountains, northwestern Canada. Precambrian Research, vol. 73, p. 101-121.

Narbonne, G.M. and Hofmann, H.J., 1987. Ediacaran biota of the Wernecke Mountains, Yukon, Canada. Paleontology, vol. 30, p. 647-676.

Narbonne, G.M., Hofmann, H.J. and Aitken, J.D., 1985. Precambrian-Cambrian boundary sequence, Wernecke Mountains, Yukon Territory. *In:* Current Research, Part A, Geological Survey of Canada, Paper 85-1A, p. 603-608.

Norford, B.S., 1997. Chapter 6: Ordovician and Silurian. *In:* The Geology, Mineral and Hydrocarbon Potential of Northern Yukon Territory and Northwestern District of Mackenzie, D.K. Norris (ed.), Geological Survey of Canada, Bulletin 422, p. 119-162.

Norris, D.K., 1972. En echelon folding in the northern Cordillera of Canada. Bulletin of Canadian Petroleum Geology, vol. 20, p. 634-642.

Norris, D.K., 1981. Wind River. Geological Survey of Canada, Map 1528A, 1:250 000 scale.

Norris, D.K., 1982. Snake River. Geological Survey of Canada, Map 1529A, 1:250 000 scale.

Norris, D.K., 1984. Geology of the northern Yukon and northwestern District of Mackenzie. Geological Survey of Canada, Map 1581A, 1:500 000 scale.

Norris, D.K., 1997. Chapter 3: Geological setting. *In:* The Geology, Mineral and Hydrocarbon Potential of Northern Yukon Territory and Northwestern District of Mackenzie, D.K. Norris (ed.), Geological Survey of Canada, Bulletin 422, p. 21-64.

Norris, D.K. and Dyke, L.D., 1997. Chapter 4: Proterozoic. *In:* The Geology, Mineral and Hydrocarbon Potential of Northern Yukon Territory and Northwestern District of Mackenzie, D.K. Norris (ed.), Geological Survey of Canada, Bulletin 422, p. 65-84.

Norris, D.K. and Hopkins, W.S. Jr., 1977. The geology of the Bonnet Plume Basin, Yukon Territory. Geological Survey of Canada, Paper 76-8, 20 p.

Oreskes, N., and Einaudi, M.T., 1992. Origin of hydrothermal fluids at Olympic Dam: Preliminary results from fluid inclusions and stable isotopes. Economic Geology, vol. 87, p. 64-90.

Parrish, R.R., and Bell, R.T., 1987. Age of the Nor breccia pipe, Wernecke Supergroup, Yukon Territory. *In:* Radiogenic Age and Isotopic Studies: Report 1, Geological Survey of Canada, Paper 87-2, p. 39-42.

Rainbird, R.H., Heaman, L.M. and Young, G.M., 1992. Sampling Laurentia: Detrital zircon geochronology offers evidence for an extensive Neoproterozoic river system originating from Grenville orogen. Geology, vol. 20, p. 351-354.

Rainbird, R.H., Jefferson, C.W., and Young, G.M., 1996. The early Neoproterozoic sedimentary Succession B of northwestern Laurentia: Correlations and paleogeographic significance. Geological Society of America Bulletin, vol. 108, no. 4, p. 454-470.

Rainbird, R.H., McNicoll V.J., Theriault, R.J., Heaman, L.M., Abbott, J.G., Long, D.G.F. and Thorkelson, D.J., 1997. Pan-continental river system draining Grenville orogen recorded by U-Pb and Sm-Nd geochronology of Neoproterozoic quartzites and mudrocks, northwestern Canada. Journal of Geology, vol. 105, p. 1-17.

Rogers, J.J.W., 1996. A history of continents in the past three billion years. Journal of Geology, vol. 104, p. 91-107.

Roots, C.F. and Thompson, R.I., 1988. Long-lived basement weak zones and their role in extensional magmatism in the Ogilvie Mountains, Yukon Territory. *In:* Proceedings of the International Conference on Basement Tectonics, M.J. Bartholomew, D.W. Hyndman, D.W. Mogk, and R. Mason, (eds.), vol. 8, p. 359-372.

Ross, G.M., 1991. Tectonic setting of the Windermere Supergroup revisited. Geology, vol. 19, p. 1125-1128.

Ross, G.M. and Donaldson, J.A., 1989. Reef development and facies geometry on a high-energy Early Proterozoic carbonate shelf (Hornby Bay, Northwest Territories, Canada). *In:* Reefs, Canada and Adjacent Areas, H.H.J. Geldsetzer, N.P. James and G.E. Tebbutt (eds.), Canadian Society of Petroleum Geologists, Memoir 13, p. 120-128.

Ross, G.M. and Villeneuve, M.E., 1997. U-Pb geochronology of stranger stones in Neoproterozoic diamictites, Canadian Cordillera: Implications for provenance and ages of deposition. *In:* Radiogenic Age and Isotopic Studies: Report 10, Geological Survey of Canada, Current Research 1997-F, p. 141-155.

Ross, G.M., Parrish, R.R. and Winston, D., 1992. Provenance and U-Pb geochronology of the Mesoproterozoic Belt Supergroup (northwestern United States): Implications for age of deposition and pre-Panthalassa plate reconstructions. Earth and Planetary Science Letters, vol. 113, p. 57-76.

Stammers, M.A. and Ikona, C., 1977. Geologic Report on the Ram 1-48 Mineral Claims. Mineral Resources Directorate, Yukon, Indian and Northern Affairs Canada, Assessment Report #090284.

Tempelman-Kluit, D.J., 1981. Nor, summary of assessment work and description of mineral properties. *In:* Yukon Geology and Exploration, 1979-1980, Exploration and Geological Services Division, Yukon, Indian and Northern Affairs Canada, p. 300-301.

Thompson, R.I., 1995. Geological compilation (1:250 000) of Dawson map area (northeast of Tintina Trench). Geological Survey of Canada, Open File 3223.

Thorkelson, D.J., Abbott, J.G., Mortensen, J.K., Creaser, R.A. and Villeneuve, M.E., 1998. Proterozoic sedimentation, magmatism, metasomatism and deformation in the Wernecke and Ogilvie Mountains, Yukon. *In:* Slave-Northern Cordillera Lithospheric Evolution (SNORCLE) Transect and Cordilleran Tectonics Workshop Meeting (March 6-8), Simon Fraser University, F. Cook and P. Erdmer (compilers), 1998, Lithoprobe Report No. 64, p. 110-119.

Thorkelson, D.J. and Wallace, C.A., 1993a. Development of Wernecke Breccias in Slats Creek (106D/16) map area, Wernecke Mountains, Yukon. *In:* Yukon Exploration and Geology, 1992, Exploration and Geological Services Division, Yukon, Indian and Northern Affairs Canada, p. 19-30.

Thorkelson, D.J. and Wallace, C.A., 1993b. Geological map of Slats Creek (106D/16) map area, Wernecke mountains, Yukon. Exploration and Geological Services Division, Yukon, Indian and Northern Affairs Canada, Open File 1993-2-G, 1:50 000 scale.

Thorkelson, D.J. and Wallace, C.A., 1994a. Geological setting of mineral occurrences in Fairchild Lake map area (106C/13), Wernecke Mountains, Yukon. *In:* Yukon Exploration and Geology;, 1993, Exploration and Geological Services Division, Yukon, Indian and Northern Affairs Canada, p. 79-92.

Thorkelson, D.J., and Wallace, C.A., 1994b. Geological map of Fairchild Lake map area (106C/13), Wernecke Mountains, Yukon. Exploration and Geological Services Division, Yukon, Indian and Northern Affairs Canada, Open File 1994-6, 1:50 000 scale.

Thorkelson, D.J., and Wallace, C.A., 1995a. Geology and mineral occurrences of the Dolores Creek map area (106C/14), Wernecke Mountains, northeastern Yukon. *In:* Yukon Exploration and Geology, 1994, Exploration and Geological Services Division, Yukon, Indian and Northern Affairs Canada, p. 19-30.

Thorkelson, D.J., and Wallace, C.A., 1995b. Geological map of the Dolores Creek map area (106C/14), Wernecke Mountains, northeastern Yukon. Exploration and Geological Services Division, Yukon, Indian and Northern Affairs Canada, Open File 1995-6, 1:50 000 scale.

Thorkelson, D.J., and Wallace, C.W., 1998a. Geological map of Slats Creek area, Wernecke Mountains, Yukon (106D/16). Exploration and Geological Services Division, Yukon, Indian and Northern Affairs Canada, Geoscience Map 1998-9, 1:50 000 scale.

Thorkelson, D.J. and Wallace, C.W., 1998b. Geological map of Fairchild Lake area, Wernecke Mountains, Yukon (106C/13). Exploration and Geological Services Division, Yukon Indian and Northern Affairs Canada, Geoscience Map 1998-10, 1:50 000 scale.

Thorkelson, D.J. and Wallace, C.W., 1998c. Geological map of Dolores Creek area, Wernecke Mountains, Yukon (106C/14). Exploration and Geological Services Division, Yukon, Indian and Northern Affairs Canada, Geoscience Map 1998-11, 1:50 000 scale.

Thorkelson, D.J. and Wallace, C.A., 1999. New geological maps of the Wernecke Mountains, Yukon Territory (106D/16, 106C/13, 106C/14). *In:* Slave-Northern Cordillera Lithospheric Evolution (SNORCLE) Transect and Cordilleran Tectonics Workshop Meeting (March 5-7), 1999, University of Calgary, F. Cook and P. Erdmer (compilers), Lithoprobe Report No. 69, p. 320-323.

Villeneuve, M.E., Butterfield, N.J., Cook, D.G., MacLean, B.C. and Rainbird, R.H., 1998. Age of the Cap Mountain (Northwest Territories) Proterozoic section, sequence B, based on detrital zircon ages. *In:* Radiogenic Age and Isotope Studies, Report 11, Geological Survey of Canada, p. 117-127.

Villeneuve, M.E., Theriault, R.J. and Ross, G.M., 1991. U-Pb ages and Sm-Nd signature of two subsurface granites from the Fort Simpson magnetic high, northwest Canada. Canadian Journal of Earth Sciences, vol. 28, p. 1003-1008.

Wallace, M.W., Both, R.A., Ruano, S.M., Hach-all, P.F., and Lees, T., 1994. Zebra textures from carbonate-hosted sulfide deposits: Sheet cavity networks produced by fracture and solution enlargement. Economic Geology, vol. 89, p. 1183-1191.

Wernicke, B., 1985. Uniform-sense normal simple shear of the continental lithosphere. Canadian Journal of Earth Sciences, vol. 22, p. 108-125.

Wheeler, J.O., 1954. A geological reconnaissance of the northern Selwyn Mountains Region, Yukon and Northwest Territories. Geological Survey of Canada, Paper 53-7, 42 p.

Wheeler, J.O. and McFeely, P., 1991. Tectonic assemblage map of the Canadian Cordillera and adjacent parts of the United States of America. Geological Survey of Canada, Map 1712A, 1:2 000 000 scale.

Yeager, D., and Ikona, C., 1979. Geological and geochemical report on the Elk 1-90 mineral claims. Mineral Resources Directorate, Yukon, Indian and Northern Affairs Canada, Assessment Report #090424.

Yeo, G., 1981. The late Proterozoic Rapitan glaciation in the northern Cordillera. *In:* Proterozoic Basins of Canada, F.H.A. Campbell (ed.), Geological Survey of Canada Paper 81-10, p. 25-46.

Yeo, G.M., 1986. Iron-formation in the Late Proterozoic Rapitan Group, Yukon and N.W.T. *In:* Mineral Deposits of Northern Cordillera, J.A. Morin (ed.), Canadian Institute of Mining and Metallurgy, Special Volume 37, p. 142-143.

Yeo, G.M., Delaney, G.D. and Jefferson, C.W., 1978. Two major Proterozoic unconformities, northern Cordillera: Discussion. *In:* Current Research, Part B, Geological Survey of Canada, Paper 78-1B, p. 225-230.

Young, G.M., 1992. Late Proterozoic stratigraphy and the Canada-Australia connection. Geology, vol. 20, p. 215-218.

Young, G.M., 1995. Are Neoproterozoic glacial deposits preserved on the margins of Laurentia related to the fragmentation of two supercontinents? Geology, vol. 23, p. 153-156.

Young, G. M., Jefferson, C.W., Long, D.G.F., Delaney, G.D. and Yeo, G.M., 1979. Middle and Late Proterozoic evolution of the northern Canadian Cordillera and Shield. Geology, vol. 7, p. 125-128.

Yukon Minfile, 1997. Exploration and Geological Services Division, Yukon, Indian and Northern Affairs Canada. Also available from Hyperborean Productions, Whitehorse, Yukon.

Appendices

Appendix 1: Age determinations

Isotopic age determinations were obtained from several laboratories using either the U-Pb method or the Ar-Ar ($^{40}Ar/^{39}Ar$) method, on several mineral types. The determinations are listed in Table A1-1, and are considered preliminary because they have not yet been critically evaluated by peer review. The data are grouped according to the interpreted significance of the isotopic date, i.e., igneous crystallization, hydrothermal precipitation, cooling, or detrital mineral age.

Appendix 2: Neodymium model ages

Neodymium-Samarium isotopic studies were carried out on several samples ranging in age from Early to Middle Proterozoic. Nd model ages for derivation from a depleted mantle source, and other information, is provided in Table A2-1. Mineral occurrences located near to geochemical sampling sites are indicated in the Field Relations column (in upper case letters).

Unit abbreviations

See Appendix 1 and as below.
PGL: Gillespie Lake Group
PQ: Quartet Group

Appendix 3: Geochemical analyses

Geochemical analyses were obtained on a wide variety of rock types in the study area. The analyses and corresponding information are listed in Table A3-1. Mineral occurrences located near to geochemical sampling sites are indicated in the Field Relations column (in upper case letters). The analyses are grouped according to geological unit. Within each group of igneous rocks, samples are arranged by MgO concentration. Within Wernecke Breccia and units of sedimentary rock, samples are arranged by UTM Easting. Major elements have been recalculated from the original analyses on a volatile-free basis. Concentrations of Cr obtained in 1992 have been reduced by 17 ppm to account for the average value of Cr contamination.

Major oxides were measured at X-ray Assay Laboratories by X-ray fluorescence spectrometry. Trace element analysis was carried out at the University of Saskatchewan by inductively coupled plasma mass spectrometry. Sample pulverization was performed at either the University of Saskatchewan or X-ray Assay Laboratories except for those submitted in 1992 which were prepared at Northern Analytical Laboratories.

Unit abbreviations

See accompanying maps and Figures 3 and 25.
na: not available
negative values: below detection limit

Appendix 4: Assays

Assays were obtained from rock samples taken from selected sites throughout the study area. Some samples showed visible mineral enrichments, while others did not. The analyses and corresponding information are listed in Table A4-1. Analyses are arranged by increasing UTM Easting of sample location. Element concentrations were determined mainly at International Plasma Laboratories and Bondar-Clegg and Company. Northern Analytical Laboratories provided some of the gold assays.

In Table A4-1, na = not analyzed; nd = not determined (below determination limit); -5 = below detection limit of 5 ppm; +2000 = above determination maximum of 2000 ppm.

Appendix 1: Age Determinations Table A1-1

Ref. no.	Sample no.	Geological Unit	Rock type	Location NTS	UTM E	UTM N	Geo.	Method	Mineral	Age (Ma) (preliminary)
				Igneous Crystallization Ages						
1	DT-93-52-1C	Bonnet P. R. intr. (EPd)	syenite	106C/14	580700	7201000	JM	U-Pb	zircon	1725 ± 5
2	DT-93-25-1C	Bonnet P. R. intr. (EPd)	diorite	106C/13	554700	7194800	JM	U-Pb	zircon	1722 ± 20
3	DT-94-22-1C	Bonnet P. R. intr. (EPd)	diorite	106C/14	580900	7202600	JM	U-Pb	zircon	1709 ± 10
4	DT-94-20-1C	Bonnet P. R. intr. (EPd)	diorite	106D/16	546100	7208100	JM	U-Pb	zircon	1705 ± 1
5	TOA-96-6-4-2B	Hart River intrusion	diorite	106C/11	573900	7160000	JM	U-Pb	zircon	ca. 1382
6	TOA- 96-6-7-1C	Bear River dyke (MPd)	diorite	106D/16	528050	7203300	JM	U-Pb	baddeleyite	ca.1270
7	DT-95-1	Bear River dyke (MPd)	diorite	106D/16	531900	7187000	JM	U-Pb	zircon	1265 +20/-11
				Hydrothermal Precipitation Ages						
8	DT-93-7-1B	Wernecke Bx. (PWb)	breccia	106D/16	546100	7207950	RC	U-Pb	titanite	1595 +8/-5
9	DT-94-21-1C	Slab volcanics (PSv)	mafic lava	106D/16	546000	7207500	JM	U-Pb	rutile	1382 ± 8.4
10	DT-93-25-2C	Bonnet P.R. intr. (EPd)	anorthosite	106C/13	554700	7194800	JM	U-Pb	rutile	ca. 1370 Ma
				Cooling Ages						
11	DT-93-151-1C	Slab volcanics (PSv)	mafic lava	106D/16	552700	7197500	MV	Ar-Ar	biotite	522 ± 5
12	DT-95-2-1B	Fairchild L. Gp. (PFL)	schist	106D/16	546200	7208350	PL	Ar-Ar	muscovite	980 ± 15
13	DT-93-22-1	Fairchild L. Gp. (PFL)	schist	106C/13	552800	7208200	PL	Ar-Ar	muscovite	833 ± 17
				Detrital Mineral Ages						**Range of Ages**
14	DT-93-153-1B	Pinguicula unit a (PPa)	sandstone	106C/14	571400	7191000	VM	U-Pb	zircon	1841-3078
15	DT-93-168-1B	Corn Ck qtz. ar. (PHCC)	sandstone	106C/11	577800	7180000	VM	U-Pb	zircon	1271-1650
16	DT-95-11-1B	Corn Ck qtz. ar. (PHCC)	sandstone	106C/14	589400	7192500	MV	Ar-Ar	muscovite	1033-2411

Geochronologists
(listed in above under Geo heading)

RC = Robert Creaser — University of Alberta
PL = Paul Layer — University of Alaska
VM = Vicki McNicoll — Geological Survey of Canada
JM = James Mortensen — University of British Columbia
MV = Michael Villeneuve — Geological Survey of Canada

Appendix 2: Neodymium model ages Table A2-1

Geol	Yr	Sample Number	Unit	NTS	UTM E	UTM N	Field Relations	Nd T_{dm} (Ga)
DT	93	163-1b	EPd	106C/14	573540	7191370		
		Diorite with specular hematite veins					Large breccia zone (PIKA)	6.67
DT	94	20-1b	EPd	106D/16	546200	7208200		
		Medium-grained diorite, little alteration					Small stock intrudes PFL; crosscut by PWb (SLAB)	2.29
DT	94	22-1b	EPd	106C/14	508850	7202700		
		Locally pegmatitic diorite, little alteration					Dyke intrudes PFL; crosscut by PWb (COBALT CIRQUE)	2.42
DT	93	52-1b	EPd	106C/14	580700	7200900		
		Quartz albite syenite					Small stock intrudes PFL; crosscut by PWb (PORPHYRY)	2.57
DT	94	9-2	EPd	106C/14	580700	7200900		
		Quartz albite syenite, sulphide-rich					Small stock intrudes PFL; crosscut by PWb (PORPHYRY)	2.37
CW	93	19-1b	MPd	106C/13	556900	7192900		
		Fine-grained diorite					Dyke intrudes PGL north of TOW	2.09
DT	92	11-1b	MPd	106D/16	532000	7186800		
		Fine-grained diorite					Dyke intrudes PGL south of Bear River	2.69
DT	93	72-1b	MPd	106C/13	569600	7196900		
		Fine-grained diorite					Dyke intrudes PGL southwest of "Glacier Lake"	2.13
TOA	96	6-7-2b	MPd	106D/16	527600	7203300		
		Fine-grained diorite					Dyke intrudes PGL north of Bear River	2.72
DT	92	160-4b	PSv	106D/16	546100	7207600		
		Aphyric basalt					Lava flow of volcanic megaclast in Wernecke Breccia (SLAB)	3.00
DT	92	126-1	PFL	106D/16	544800	7200900		
		Siltstone					Lower Fairchild Lake Group	2.69
DT	92	129-1	PFL	106D/16	545600	7198100		
		Chloritic phyllite with crenulations					Locally deformed zone in Lower Fairchild Lake Group	2.48
DT	92	132-7	PFL	106D/16	546100	7197200		
		Siltstone					Lower Fairchild Lake Group	2.53
DT	92	27-2	PQ	106D/16	536300	7204050		
		Siltstone					Middle part of Quartet succession	2.64
DT	92	55-1b	PQ	106D/16	532400	7203200		
		Siltstone					Low in PQ succession	2.45
DT	92	80-1b	PGL	106D/16	532050	7197300		
		Black shale					10 m interbed in PGL dolostone	2.28
DT	92	99-1	PGL	106D/16	545800	7192250		
		Dolostone					Uncertain stratigraphic position above basal PGL	3.35
DT	93	129-1b	PGL	106C/13	555400	7195300		
		Siltstone					From enclave in large breccia zone of PWb	2.47
DT	93	129-2b	PGL	106C/13	555400	7195300		
		Dolostone					From enclave in large breccia zone of PWb	4.21
DT	92	160-3b	PWb	106D/16	546100	7207600		
		Granular matrix of grey, hematite-poor breccia					Contains kinked phyllite clasts (SLAB)	2.96
DT	92	77-1b	PWb	106D/16	533050	7200450		
		Matrix of red-clast breccia					Granular; between diorite megaclast and breccia	2.42
DT	93	107-2b	PWb	106C/13	557900	7191700		
		Breccia matrix; with disseminated chalcopyrite					Collected from float below breccia outcrops (TOW)	2.45
DT	93	11-3b	PWb	106D/16	534400	7201800		
		Breccia with 85% matrix					Clasts and matrix appear weakly metasomatized	2.85
DT	93	126-1b	PWb	106C/13	555500	7194900		
		Breccia, matrix-rich with pink and red clasts					Near contact where breccia faulted against PGL (OLYMPIC)	2.69
DT	94	13-1	PWb	106C/14	571500	7199300		
		Chalcopyrite-rich breccia					In large breccia zone associated with large bodies of EPd	2.36

Appendix 1: Age Determinations (table A1-1)

Ref. no.	Sample no.	Geological Unit	Rock type	Location NTS	UTM E	UTM N	Geo	Method	Mineral	±	Age (Ma) (preliminary)
				Igneous Crystallization Ages							
				Hydrothermal Precipitation Ages							
				Cooling Ages							
				Detrital Mineral Ages							Range of Ages

Appendix 2: Neodymium model ages Table A2-1

Geol	Yr	Sample Number	Rock Type	Unit	NTS	UTM E	UTM N	Field Relations	Nd T_{dm} (Ga)
[illegible]	[illegible]	[illegible]	[illegible]	[illegible]	[illegible]	[illegible]	[illegible]	[illegible]	[illegible]
[illegible]	[illegible]	[illegible]	[illegible]	[illegible]	[illegible]	[illegible]	[illegible]	Lower Swayze suite; PSKA	3.07
[illegible]	[illegible]	[illegible]	[illegible]	[illegible]	[illegible]	[illegible]	[illegible]	Small stock intrudes PEL; crosscut by PWb (SLAb)	2.29
[illegible]	[illegible]	[illegible]	[illegible]	[illegible]	[illegible]	[illegible]	[illegible]	Dyke intrudes PEL; crosscut by PWb (UBALLYARGLE)	2.42
[illegible]	[illegible]	[illegible]	[illegible]	[illegible]	[illegible]	[illegible]	[illegible]	Small stock intrudes PEL; crosscut by PWb (PORPHYRY)	2.65
[illegible]	[illegible]	[illegible]	[illegible]	[illegible]	[illegible]	[illegible]	[illegible]	Small stock intrudes PEL; crosscut by PWb (PORPHYRY)	2.57
CW	83	[illegible]	MM	[illegible]	[illegible]	[illegible]	[illegible]	Dyke intrudes PEL north of DW	2.59
[illegible]	[illegible]	[illegible]	MM	[illegible]	[illegible]	[illegible]	[illegible]	Dyke intrudes PEL north of Bear River	2.69
[illegible]	[illegible]	[illegible]	MM	[illegible]	[illegible]	[illegible]	[illegible]	Dyke intrudes PEL southwest of Clearing Lake	2.53
[illegible]	[illegible]	[illegible]	MM	[illegible]	[illegible]	[illegible]	[illegible]	Dyke intrudes PEL north of Bear River	2.72
[illegible]	[illegible]	[illegible]	PW	[illegible]	[illegible]	[illegible]	[illegible]	Lava flow of volcanic megaclast in Wawaskie Intrusion (SLAb)	3.01
[illegible]	[illegible]	[illegible]	[illegible]	[illegible]	[illegible]	[illegible]	[illegible]	Unnamed unit west Lake Group	2.99
[illegible]	[illegible]	[illegible]	[illegible]	[illegible]	[illegible]	[illegible]	[illegible]	Lapilli-dominated gneiss in Lower Fawnhill Lake Group	2.48
[illegible]	[illegible]	[illegible]	[illegible]	[illegible]	[illegible]	[illegible]	[illegible]	Lower Fawnhill Lake Group	2.53
[illegible]	[illegible]	[illegible]	[illegible]	[illegible]	[illegible]	[illegible]	[illegible]	Mafic part of gneissic succession	2.64
[illegible]	[illegible]	[illegible]	[illegible]	[illegible]	[illegible]	[illegible]	[illegible]	Unit in PEL succession	2.45
[illegible]	[illegible]	[illegible]	[illegible]	[illegible]	[illegible]	[illegible]	[illegible]	Tonalite intrusion in PEL dacite/rhyolite	2.28
[illegible]	[illegible]	[illegible]	[illegible]	[illegible]	[illegible]	[illegible]	[illegible]	Unnamed metasedimentary gneissic unit in PEL	3.35
[illegible]	[illegible]	[illegible]	[illegible]	[illegible]	[illegible]	[illegible]	[illegible]	Trondhjemite to felsic monzogranite sill in PWb	2.47
[illegible]	[illegible]	[illegible]	[illegible]	[illegible]	[illegible]	[illegible]	[illegible]	Trondhjemite to felsic monzogranite sill in PWb	3.21
[illegible]	[illegible]	[illegible]	[illegible]	[illegible]	[illegible]	[illegible]	[illegible]	Coarse-banded pyroclast clasts (SLAb)	2.99
[illegible]	[illegible]	[illegible]	[illegible]	[illegible]	[illegible]	[illegible]	[illegible]	Granodiorite/monzogranite sill in PWb	2.92
[illegible]	[illegible]	[illegible]	[illegible]	[illegible]	[illegible]	[illegible]	[illegible]	Clast(s) from fine-tuffaceous interval in PEL (DW)	2.45
[illegible]	[illegible]	[illegible]	[illegible]	[illegible]	[illegible]	[illegible]	[illegible]	Clast(s) from fine-tuffaceous interval in PEL (DW)	2.85
[illegible]	[illegible]	[illegible]	[illegible]	[illegible]	[illegible]	[illegible]	[illegible]	Basal contact with PEL (DW)	2.59
[illegible]	[illegible]	[illegible]	[illegible]	[illegible]	[illegible]	[illegible]	[illegible]	Clast(s) from fine-tuffaceous interval in PEL (DW)	2.53

Appendix 3

See 2 foldout pages to the right.

page 67a

APPENDIX 3: GEOCHEMICAL ANALYSES Table A3-1: Left side

Geol	Yr	Sample no. Number	Lab Sample #	Rock Type	Field Relations	NTS	UTM E	UTM N	SiO_2 wt %	T v
				Bonnet Plume River intrusions; Early Proterozoic diorite (EPd)						
DT	92	132-5b	G-12	Aphanitic dense basalt	Dyke cuts PFL; crosscut by PWb (SNOWSTAR)	106D/16	546150	7197250	47.2	2
DT*	93	167-1b	G-124	Fine-grained diorite	Body of diorite crosscut by PWb (PIKA)	106C/14	572900	7191600	52.3	1
DT	92	139-5b	G-16	Fine-grained diorite	Crosscut by PWb (SIHOTA)	106D/14	497200	7188650	48.4	1
DT	92	53-6b	G-5	Fine-grained diorite, some pyrite	Crosscut by shale-clast PWb (GNUCKLE)	106D/16	534800	7201850	50.8	2
DT	93	113-1b	G-116	Fine-grained diorite, hematitic	Rounded clast in PWb (OLYMPIC)	106C/13	554700	7195300	48.5	1
DT	92	76-6b	G-9	Fine-grained diorite	Surrounded by PWb (PITCH)	106D/16	533450	7200550	50.5	1
CW	93	101-1a	G-126	Fine-grained diorite (reddened)	Body of diorite crosscut by PWb (PIKA)	106C/14	572800	7191700	46.1	2
DT	94	20-1b	G-205	Medium-grained diorite, little alteration (SLAB)	Small stock intrudes PFL; crosscut by PWb (SLAB)	106D/16	546200	7208200	48.6	2
DT	92	139-6b	G-17	Fine-grained diorite with red metasomatic clots	Crosscut by PWb (SIHOTA)	106D/14	497200	7188650	50.4	C
DT	93	78-1b	G-113	Fine to medium-grained diorite	Dyke intrudes PFL; crosscut by PWb (DOLORES)	106C/13	570100	7197400	51.6	1
DT	93	25-1b	G-106	Fine-grained diorite	Rounded clast in PWb (OLYMPIC)	106C/13	554700	7194800	52.2	C
DT	94	16-1b	G-203	Diorite with minor specularite and epidote	Body of diorite crosscut by PWb (BEL)	106C/14	572500	7199550	50.9	2
DT	93	11-1b	G-103	Fine-grained diorite	Crosscut by shale-clast PWb (GNUCKLE)	106D/16	534400	7201800	50.1	1
DT	92	158-5b	G-30	Fine-grained diorite	Megaclast (6x9 m) in PWb (SLAB)	106D/16	545800	7207800	51.0	1
DT	92	135-4b	G-13	Fine-grained diorite	Along with coarse-grained diorite, cuts PFL (SLAB)	106D/16	546100	7208250	50.8	1
DT	93	11-2b	G-104	Reddened fine-grained diorite	Crosscut by shale-clast PWb (GNUCKLE)	106D/16	534400	7201800	50.2	1
DT	92	53-2b	G-4	Fine-grained diorite, hematitic	Crosscut by shale-clast PWb (GNUCKLE)	106D/16	534800	7201850	52.6	1
DT	93	120-1b	G-117	Fine to medium-grained diorite	Megaclast in PWb (OLYMPIC)	106C/13	556300	7195000	48.0	C
DT	93	163-1b	G-123	Diorite with specular hematite veining	Large breccia zone (PIKA)	106C/14	573540	7191370	53.6	2
DT	94	15-2b	G-202	Fine-grained diorite	5 cm from contact with PWb (BEL)	106C/14	572550	7199600	52.0	1
CW	93	101-2a	G-127	Fine-grained diorite (visibly unaltered)	Body of diorite crosscut by PWb (PIKA)	106C/14	572800	7191700	45.7	2
DT	93	25-2b	G-107	Fine-grained anorthosite, hematitic	Megaclast in PWb (OLYMPIC)	106C/13	554700	7194800	51.9	2
DT	94	22-1b	G-207	Locally pegmatitic diorite, little alteration	Dyke intrudes PFL; crosscut by PWb (COBALT CIRQUE)	106C/14	508850	7202700	56.8	2
DT	93	52-1b	G-110	Quartz albite syenite	Small stock intrudes PFL; crosscut by PWb (PORPHYRY)	106C/14	580700	7200900	59.1	2
DT	94	16-2b	G-204	Diorite, reddened, with specularite +/- magnetite	Body of diorite crosscut by PWb (BEL)	106C/14	572500	7199550	54.8	C
				Slab volcanics (PSV)						
DT	94	21-1b	G-206	Aphyric basalt	Lava flow of volcanic megaclast in Wernecke Breccia (SLAB)	106D/16	546050	7207500	51.9	1
DT	93	9-1b	G-101	Aphyric basalt	Lava flow of volcanic megaclast in Wernecke Breccia (SLAB)	106D/16	546100	7207500	52.7	2
DT	92	160-4b	G-32	Aphyric basalt	Lava flow of volcanic megaclast in Wernecke Breccia (SLAB)	106D/16	546100	7207600	53.5	1
				Middle Proterozoic lamprophyre (MPl)						
DT	93	151-1b	G-108	Biotitic basalt dyke	Intrudes PFL; crosscut by hematite veins near sample site	106C/13	552700	7197500	39.4	3
				Bear River intrusions; Middle Proterozoic diorite (MPd)						
TOA	96	6-7-2b	6-7-2b	Fine-grained diorite	Dyke intrudes PGL north of Bear River	106D/16	527600	7203300	na	r
DT	92	11-1b	G-2	Fine-grained diorite	Dyke intrudes PGL south of Bear River	106D/16	532000	7186800	53.5	1
CW	93	19-1b	G-125	Fine-grained diorite	Dyke intrudes PGL north of TOW	106C/13	556900	7192900	48.8	1
DT	93	72-1b	G-112	Fine-grained diorite	Dyke intrudes PGL southwest of "Glacier Lake"	106C/13	569600	7196900	51.9	2
				Wernecke Supergroup (PFL, PQ, PGL) and Pinguicula Group (PP)						
DT	92	80-1b	G-11	Black shale (PGL)	10 m interbed in PGL dolostone	106D/16	532050	7197300	58.8	C
DT	92	55-1b	G-6	Siltstone (PQ)	Low in PQ succession	106D/16	532400	7203200	66.2	C
DT	92	169-1b	G-33	Laminated pink-green siltstone (PFL)	Intermediate stratigraphic position in PFL	106D/16	546100	7198850	63.7	C
DT	93	129-1b	G-119	Siltstone (PGLb)	From enclave in large breccia zone of PWb	106C/13	555400	7195300	82.5	C
DT	93	129-2b	G-120	Dolostone (PGLb)	From enclave in large breccia zone of PWb	106C/13	555400	7195300	36.9	C
DT	94	36-6b	G-213	Basal sandstone of PPa	20 cm above unconformity with PWb	106C/14	582950	7207350	87.2	C
				Wernecke Breccia and related metasomatic rocks (PWb)						
DT	92	138-1b	G-14	Breccia with red, altered siltstone and diorite clasts	Breccia body, Royal Creek area (SIHOTA)	106D/14	497200	7188500	60.9	C
DT	92	149-8b	G-28	Jasperized band of altered siltstone (PQ) near breccia	Large breccia zone; northwest of BLAND	106E/1	525850	7208500	70.8	C
DT	92	149-7b	G-27	Breccia, pale in colour and with abundant matrix, in PQ	Large breccia zone; northwest of BLAND	106E/1	525850	7208500	54.3	C
DT	92	149-6b	G-25	Breccia, close-packed with abundant specularite	Large breccia zone; northwest of BLAND	106E/1	525850	7208500	50.2	C
DT	92	149-5b	G-24	Slightly altered (brown) siltstone of PQ	Large breccia zone; northwest of BLAND	106E/1	525850	7208500	58.0	C
DT	92	143-1b	G-23	Altered siltstone of PQ or PGL, with red banding	Margin of large bx zone in PGL and PQ (BLAND)	106D/16	527650	7207050	63.4	C
DT	92	142-5b	G-22	Altered siltstone of PQ or PGL	Altered siltstone grades into red clast bx (BLAND)	106D/16	527700	7206550	62.2	C
DT	92	52-4b	G-3	Altered siltstone of PQ or PGL	Clast from breccia zone	106D/16	528250	7205150	54.8	C
DT	92	62-2b	G-7	Hematitic breccia	Intrudes phyllite of PFL	106D/16	529200	7207400	54.3	C
DT	92	77-1b	G-10	Matrix of red-clast breccia	Granular; between diorite megaclast and breccia	106D/16	533050	7200450	53.3	C
DT	93	11-3b	G-105	Breccia with 85% matrix	Breccia and clasts appear less metasomatized than normal	106D/16	534400	7201800	73.0	C
DT	93	10-1b	G-102	Massive hematite with limonite and calcite	Metallic zone in breccia	106D/16	535150	7201300	19.1	C
DT	92	160-3b	G-31	Granular matrix of grey, hematite-poor breccia	Contains kinked phyllite clasts (SLAB)	106D/16	546100	7207600	56.5	C
DT	93	7-1c	G-100	Matrix of poorly indurated, grey breccia	Contains kinked phyllite clasts (SLAB)	106D/16	546150	7207950	55.1	C
DT	93	126-1b	G-118	Breccia, matrix-rich with pink and red clasts	Near contact where breccia faulted against PGL (OLYMPIC)	106C/13	555500	7194900	56.9	C
DT	93	57-1b	G-111	Breccia with granular, pale matrix	Small breccia zone near OTTER	106C/13	557000	7207600	55.6	C
DT	93	49-1b	G-109	Breccia, matrix-rich	In long, narrow breccia zone in PGL (TOW)	106C/13	557200	7190800	56.6	C
DT	93	107-2b	G-115	Breccia matrix; with disseminated chalcopyrite	Collected from float below breccia outcrops (TOW)	106C/13	557900	7191700	50.8	1
DT	93	94-1b	G-114	Vein of hematite in PGL	Not associated with exposure of breccia	106C/13	567800	7189800	48.7	C
DT	94	15-1b	G-201	Typical red-clast breccia	5 cm from contact with large body of diorite (BEL)	106C/14	572550	7199600	55.3	C
DT	93	159-1b	G-121	Altered siltstone clasts	Large breccia zone (PIKA)	106C/14	572920	7191390	65.7	C
DT	93	159-3b	G-122	Breccia with 60% matrix	Large breccia zone (PIKA)	106C/14	572920	7191390	64.1	C
DT	94	36-1b	G-210	Chlorite-matrix red-clast Wernecke Breccia	16 m below unconformity with Pinguicula Group (ANOKI)	106C/14	582950	7207350	56.9	C
DT	94	36-2	G-208	Chlorite-matrix red-clast Wernecke Breccia	11 m below unconformity with Pinguicula Group (ANOKI)	106C/14	582950	7207350	55.4	C
DT	94	36-3b	G-211	Brownish Wernecke Breccia	7 m below unconformity with Pinguicula Group (ANOKI)	106C/14	582950	7207350	56.6	C
DT	94	36-4	G-209	Brownish yellow Wernecke Breccia	3 m below unconformity with Pinguicula Group (ANOKI)	106C/14	582950	7207350	56.8	C
DT	94	36-5b	G-212	Yellow, friable breccia	10-30 cm below unconformity with Pinguicula Group (ANOKI)	106C/14	582950	7207350	54.5	C

page 67a

APPENDIX 3: GEOCHEMICAL ANALYSES Table A3-1: Left side

Geol	Sample no. Yr	Number	Lab Sample #	Rock Type	Field Relations	NTS	UTM E	UTM N	SiO_2 wt %	T
				Bonnet Plume River intrusions; Early Proterozoic diorite (EPd)						
DT	92	132-5b	G-12	Aphanitic dense basalt	Dyke cuts PFL; crosscut by PWb (SNOWSTAR)	106D/16	546150	7197250	47.2	2
DT*	93	167-1b	G-124	Fine-grained diorite	Body of diorite crosscut by PWb (PIKA)	106C/14	572900	7191600	52.3	1
DT	92	139-5b	G-16	Fine-grained diorite	Crosscut by PWb (SIHOTA)	106D/14	497200	7188650	48.4	1
DT	92	53-6b	G-5	Fine-grained diorite, some pyrite	Crosscut by shale-clast PWb (GNUCKLE)	106D/16	534800	7201850	50.8	2
DT	93	113-1b	G-116	Fine-grained diorite, hematitic	Rounded clast in PWb (OLYMPIC)	106C/13	554700	7195300	48.5	1
DT	92	76-6b	G-9	Fine-grained diorite	Surrounded by PWb (PITCH)	106D/16	533450	7200550	50.5	1
CW	93	101-1a	G-126	Fine-grained diorite (reddened)	Body of diorite crosscut by PWb (PIKA)	106C/14	572800	7191700	46.1	2
DT	94	20-1b	G-205	Medium-grained diorite, little alteration (SLAB)	Small stock intrudes PFL; crosscut by PWb (SLAB)	106D/16	546200	7208200	48.6	2
DT	92	139-6b	G-17	Fine-grained diorite with red metasomatic clots	Crosscut by PWb (SIHOTA)	106D/14	497200	7188650	50.4	0
DT	93	78-1b	G-113	Fine to medium-grained diorite	Dyke intrudes PFL; crosscut by PWb (DOLORES)	106C/13	570100	7197400	51.6	1
DT	93	25-1b	G-106	Fine-grained diorite	Rounded clast in PWb (OLYMPIC)	106C/13	554700	7194800	52.2	0
DT	94	16-1b	G-203	Diorite with minor specularite and epidote	Body of diorite crosscut by PWb (BEL)	106C/14	572500	7199550	50.9	2
DT	93	11-1b	G-103	Fine-grained diorite	Crosscut by shale-clast PWb (GNUCKLE)	106D/16	534400	7201800	50.1	1
DT	92	158-5b	G-30	Fine-grained diorite	Megaclast (6x9 m) in PWb (SLAB)	106D/16	545800	7207800	51.0	1
DT	92	135-4b	G-13	Fine-grained diorite	Along with coarse-grained diorite, cuts PFL (SLAB)	106D/16	546100	7208250	50.8	1
DT	93	11-2b	G-104	Reddened fine-grained diorite	Crosscut by shale-clast PWb (GNUCKLE)	106D/16	534400	7201800	50.2	1
DT	92	53-2b	G-4	Fine-grained diorite, hematitic	Crosscut by shale-clast PWb (GNUCKLE)	106D/16	534800	7201850	52.6	1
DT	93	120-1b	G-117	Fine to medium-grained diorite	Megaclast in PWb (OLYMPIC)	106C/13	556300	7195000	48.0	0
DT	93	163-1b	G-123	Diorite with specular hematite veining	Large breccia zone (PIKA)	106C/14	573540	7191370	53.6	2
DT	94	15-2b	G-202	Fine-grained diorite	5 cm from contact with PWb (BEL)	106C/14	572550	7199600	52.0	1
CW	93	101-2a	G-127	Fine-grained diorite (visibly unaltered)	Body of diorite crosscut by PWb (PIKA)	106C/14	572800	7191700	45.7	2
DT	93	25-2b	G-107	Fine-grained anorthosite, hematitic	Megaclast in PWb (OLYMPIC)	106C/13	554700	7194800	51.9	2
DT	94	22-1b	G-207	Locally pegmatitic diorite, little alteration	Dyke intrudes PFL; crosscut by PWb (COBALT CIRQUE)	106C/14	508850	7202700	56.8	2
DT	93	52-1b	G-110	Quartz albite syenite	Small stock intrudes PFL; crosscut by PWb (PORPHYRY)	106C/14	580700	7200900	59.1	2
DT	94	16-2b	G-204	Diorite, reddened, with specularite +/- magnetite	Body of diorite crosscut by PWb (BEL)	106C/14	572500	7199550	54.8	0
				Slab volcanics (PSV)						
DT	94	21-1b	G-206	Aphyric basalt	Lava flow of volcanic megaclast in Wernecke Breccia (SLAB)	106D/16	546050	7207500	51.9	1
DT	93	9-1b	G-101	Aphyric basalt	Lava flow of volcanic megaclast in Wernecke Breccia (SLAB)	106D/16	546100	7207500	52.7	2
DT	92	160-4b	G-32	Aphyric basalt	Lava flow of volcanic megaclast in Wernecke Breccia (SLAB)	106D/16	546100	7207600	53.5	1
				Middle Proterozoic lamprophyre (MPl)						
DT	93	151-1b	G-108	Biotitic basalt dyke	Intrudes PFL; crosscut by hematite veins near sample site	106C/13	552700	7197500	39.4	3
				Bear River intrusions; Middle Proterozoic diorite (MPd)						
TOA	96	6-7-2b	6-7-2b	Fine-grained diorite	Dyke intrudes PGL north of Bear River	106D/16	527600	7203300	na	n
DT	92	11-1b	G-2	Fine-grained diorite	Dyke intrudes PGL south of Bear River	106D/16	532000	7186800	53.5	1
CW	93	19-1b	G-125	Fine-grained diorite	Dyke intrudes PGL north of TOW	106C/13	556900	7192900	48.8	1
DT	93	72-1b	G-112	Fine-grained diorite	Dyke intrudes PGL southwest of "Glacier Lake"	106C/13	569600	7196900	51.9	2
				Wernecke Supergroup (PFL, PQ, PGL) and Pinguicula Group (PP)						
DT	92	80-1b	G-11	Black shale (PGL)	10 m interbed in PGL dolostone	106D/16	532050	7197300	58.8	0
DT	92	55-1b	G-6	Siltstone (PQ)	Low in PQ succession	106D/16	532400	7203200	66.2	0
DT	92	169-1b	G-33	Laminated pink green siltstone (PFL)	Intermediate stratigraphic position in PFL	106D/16	546100	7198850	63.7	0
DT	93	129-1b	G-119	Siltstone (PGLb)	From enclave in large breccia zone of PWb	106C/13	555400	7195300	82.5	0
DT	93	129-2b	G-120	Dolostone (PGLb)	From enclave in large breccia zone of PWb	106C/13	555400	7195300	36.9	0
DT	94	36-6b	G-213	Basal sandstone of PPa	20 cm above unconformity with PWb	106C/14	582950	7207350	87.2	0
				Wernecke Breccia and related metasomatic rocks (PWb)						
DT	92	138-1b	G-14	Breccia with red, altered siltstone and diorite clasts	Breccia body, Royal Creek area (SIHOTA)	106D/14	497200	7188500	60.9	0
DT	92	149-8b	G-28	Jasperized band of altered siltstone (PQ) near breccia	Large breccia zone; northwest of BLAND	106E/1	525850	7208500	70.8	0
DT	92	149-7b	G-27	Breccia, pale in colour and with abundant matrix, in PQ	Large breccia zone; northwest of BLAND	106E/1	525850	7208500	54.3	0
DT	92	149-6b	G-25	Breccia, close-packed with abundant specularite	Large breccia zone; northwest of BLAND	106E/1	525850	7208500	50.2	0
DT	92	149-5b	G-24	Slightly altered (brown) siltstone of PQ	Large breccia zone; northwest of BLAND	106E/1	525850	7208500	58.0	0
DT	92	143-1b	G-23	Altered siltstone of PQ or PGL, with red banding	Margin of large bx zone in PGL and PQ (BLAND)	106D/16	527650	7207050	63.4	0
DT	92	142-5b	G-22	Altered siltstone of PQ or PGL	Altered siltstone grades into red clast bx (BLAND)	106D/16	527700	7206550	62.2	0
DT	92	52-4b	G-3	Altered siltstone of PQ or PGL	Clast from breccia zone	106D/16	528250	7205150	54.8	0
DT	92	62-2b	G-7	Hematitic breccia	Intrudes phyllite of PFL	106D/16	529200	7207400	54.3	0
DT	92	77-1b	G-10	Matrix of red-clast breccia	Granular; between diorite megaclast and breccia	106D/16	533050	7200450	53.3	0
DT	93	11-3b	G-105	Breccia with 85% matrix	Breccia and clasts appear less metasomatized than normal	106D/16	534400	7201800	73.0	0
DT	93	10-1b	G-102	Massive hematite with limonite and calcite	Metallic zone in breccia	106D/16	535150	7201300	19.1	0
DT	92	160-3b	G-31	Granular matrix of grey, hematite-poor breccia	Contains kinked phyllite clasts (SLAB)	106D/16	546100	7207600	56.5	0
DT	93	7-1c	G-100	Matrix of poorly indurated, grey breccia	Contains kinked phyllite clasts (SLAB)	106D/16	546150	7207950	55.1	0
DT	93	126-1b	G-118	Breccia, matrix-rich with pink and red clasts	Near contact where breccia faulted against PGL (OLYMPIC)	106C/13	555500	7194900	56.9	0
DT	93	57-1b	G-111	Breccia with granular, pale matrix	Small breccia zone near OTTER	106C/13	557000	7207600	55.6	0
DT	93	49-1b	G-109	Breccia, matrix-rich	In long, narrow breccia zone in PGL (TOW)	106C/13	557200	7190800	56.6	0
DT	93	107-2b	G-115	Breccia matrix; with disseminated chalcopyrite	Collected from float below breccia outcrops (TOW)	106C/13	557900	7191700	50.8	1
DT	93	94-1b	G-114	Vein of hematite in PGL	Not associated with exposure of breccia	106C/13	567800	7189800	48.7	0
DT	94	15-1b	G-201	Typical red-clast breccia	5 cm from contact with large body of diorite (BEL)	106C/14	572550	7199600	55.3	0
DT	93	159-1b	G-121	Altered siltstone clasts	Large breccia zone (PIKA)	106C/14	572920	7191390	65.7	0
DT	93	159-3b	G-122	Breccia with 60% matrix	Large breccia zone (PIKA)	106C/14	572920	7191390	64.1	0
DT	94	36-1b	G-210	Chlorite-matrix red clast Wernecke Breccia	16 m below unconformity with Pinguicula Group (ANOKI)	106C/14	582950	7207350	56.9	0
DT	94	36-2	G-208	Chlorite-matrix red-clast Wernecke Breccia	11 m below unconformity with Pinguicula Group (ANOKI)	106C/14	582950	7207350	55.4	0
DT	94	36-3b	G-211	Brownish Wernecke Breccia	7 m below unconformity with Pinguicula Group (ANOKI)	106C/14	582950	7207350	56.6	0
DT	94	36-4	G-209	Brownish yellow Wernecke Breccia	3 m below unconformity with Pinguicula Group (ANOKI)	106C/14	582950	7207350	56.8	0
DT	94	36-5b	G-212	Yellow, friable breccia	10-30 cm below unconformity with Pinguicula Group (ANOKI)	106C/14	582950	7207350	54.5	0

N	SiO_2 wt %	TiO_2 wt %	Al_2O_3 wt %	FeO* wt %	MnO wt %	MgO wt %	CaO wt %	Na_2O wt %	K_2O wt %	P_2O_5 wt %	Li ppm	Be ppm	Sc ppm	V ppm	Rb ppm	Sr ppm	Y ppm	Zr ppm	Nb ppm	Cs ppm
7250	47.2	2.51	16.2	20.8	0.26	11.48	0.48	0.75	0.10	0.17	142.91	1.14	21.21	270.61	1.47	6.83	10.53	41.36	19.53	0.95
1600	52.3	1.67	12.1	18.7	0.09	9.61	1.43	0.23	3.66	0.22	76.05	2.76	25.64	295.03	56.71	11.76	28.28	142.67	16.58	0.63
3650	48.4	1.23	14.7	15.7	0.32	9.49	6.98	0.09	3.00	0.10	56.03	1.98	43.02	323.93	143.70	58.48	10.44	18.68	3.45	3.11
1850	50.8	2.44	16.2	16.5	0.21	9.19	2.41	0.01	2.05	0.18	41.25	2.01	35.77	509.17	67.07	6.04	16.20	77.09	10.32	2.67
3300	48.5	1.03	15.7	20.4	0.13	8.66	0.32	2.95	2.19	0.10	46.80	1.11	33.16	273.58	45.23	17.76	8.05	22.12	4.69	0.89
3550	50.5	1.91	16.3	18.5	0.19	7.29	1.13	0.81	3.25	0.20	109.04	3.82	32.44	381.30	97.96	7.26	23.07	104.07	11.94	6.27
1700	46.1	2.39	12.5	23.1	0.16	7.28	3.35	2.10	2.78	0.24	49.52	0.77	32.25	477.30	63.82	112.99	34.00	183.97	18.17	0.59
3200	48.6	2.15	16.7	8.1	0.22	7.27	12.26	3.44	1.18	0.17	17.40	na	46	216.00	56.10	512.00	21.10	46.60	24.20	1.70
3650	50.4	0.60	17.3	8.4	0.41	6.97	5.59	0.15	9.97	0.20	42.20	1.43	15.88	95.46	181.32	33.86	11.43	58.86	13.30	1.62
7400	51.6	1.76	14.0	11.8	0.26	6.82	8.93	3.92	0.79	0.17	11.14	3.86	47.69	371.88	31.09	244.52	25.25	66.68	9.95	0.86
4800	52.2	0.92	16.8	11.5	0.19	6.80	6.91	2.43	2.12	0.07	27.12	1.75	32.76	269.24	50.85	146.18	10.90	18.23	3.23	0.76
3550	50.9	2.31	15.3	11.0	0.19	6.65	5.49	2.27	5.61	0.19	19.50	na	na	358.00	128.90	170.60	28.60	24.70	12.50	1.30
1800	50.1	1.54	14.9	12.7	0.15	6.06	8.56	4.13	1.55	0.29	14.76	2.24	28.41	335.98	45.23	259.27	29.53	138.80	18.98	9.71
7800	51.0	1.47	14.1	11.5	0.13	6.06	9.76	4.90	0.96	0.15	8.05	2.02	40.83	315.03	19.89	223.13	24.96	41.76	9.69	1.18
4250	50.8	1.82	14.0	12.8	0.14	5.95	9.01	5.04	0.39	0.17	4.63	1.25	38.52	362.33	4.44	235.98	28.31	48.42	10.50	2.74
1800	50.2	1.82	13.4	15.1	0.22	5.78	5.79	1.78	5.71	0.13	29.21	1.93	34.14	373.86	114.29	185.73	29.50	126.75	12.00	0.62
1850	52.6	1.68	14.1	15.0	0.20	5.62	3.13	1.55	5.88	0.16	31.95	0.88	39.23	330.93	123.02	45.60	23.11	42.69	9.90	2.29
5000	48.0	0.95	15.0	18.6	0.34	5.59	6.61	2.40	2.40	0.09	19.60	1.52	34.72	344.02	76.46	119.61	18.35	53.79	3.89	0.58
1370	53.6	2.01	11.4	21.1	0.13	5.08	1.19	0.64	4.48	0.28	39.08	1.55	33.69	636.75	65.40	68.41	14.52	68.69	6.40	0.59
3600	52.0	1.02	14.5	13.8	0.24	4.71	6.67	5.96	0.96	0.18	18.00	na	na	224.00	20.50	49.30	22.40	50.90	12.90	0.62
1700	45.7	2.37	13.2	19.0	0.18	3.87	8.35	3.08	3.96	0.25	33.19	2.64	33.41	460.00	77.89	132.83	36.57	167.91	18.51	0.55
4800	51.9	2.41	15.1	11.2	0.47	3.30	7.08	7.58	0.41	0.48	1.01	0.57	23.57	288.97	15.23	75.82	26.52	298.22	30.96	0.29
2700	56.8	2.05	14.3	10.6	0.16	2.95	5.27	6.04	1.00	0.74	12.10	na	13	104.00	19.70	63.90	81.40	282.90	73.50	0.74
3900	59.1	2.00	12.1	12.6	0.07	2.12	5.16	6.07	0.08	0.72	5.98	0.69	16.44	27.38	2.51	49.41	108.09	508.36	66.03	0.18
4550	54.8	0.62	16.5	9.4	0.17	1.56	6.39	6.03	4.30	0.22	11.20	na	na	82.00	78.90	47.20	8.00	49.80	16.40	0.63
7500	51.9	1.83	14.5	12.4	0.11	4.09	5.58	6.81	2.40	0.35	16.80	na	na	275.00	146.50	44.40	37.80	100.00	31.60	3.10
7500	52.7	2.08	14.2	14.2	0.11	3.15	4.49	6.34	2.06	0.55	14.27	1.50	22.30	218.90	119.95	54.31	52.63	240.14	49.02	2.89
7600	53.5	1.82	14.6	15.4	0.07	2.82	2.51	6.91	1.94	0.43	16.00	1.04	11.77	194.97	115.87	24.26	47.56	142.07	37.96	3.31
7500	39.4	3.69	7.0	20.5	0.46	16.85	9.69	0.48	1.06	0.91	103.45	0.75	23.84	321.73	38.31	845.83	24.64	317.77	122.42	3.12
3300	na	na	na	na	na	na	na	na	na	na	na	na	na	263.00	76.02	145.52	21.00	99.56	7.70	1.89
5800	53.5	1.09	13.4	11.4	0.15	8.05	6.74	2.21	3.24	0.12	32.06	0.54	31.34	284.00	164.65	102.85	15.46	73.22	6.44	5.72
2900	48.8	1.30	12.7	17.0	0.16	6.19	9.48	1.61	2.65	0.14	27.33	0.54	25.77	238.15	35.31	294.48	19.20	113.41	15.01	0.90
5900	51.9	2.28	13.1	14.0	0.23	5.89	8.34	2.91	1.11	0.23	17.36	1.50	28.21	418.92	25.19	256.01	23.44	136.85	10.30	2.57
7300	58.8	0.77	16.3	2.9	0.02	19.73	0.14	0.01	1.05	0.23	na	na	na	na	na	24.75	30.05	229.06	12.77	na
3200	66.2	0.98	20.3	6.0	0.06	1.85	0.10	0.71	3.59	0.07	na	na	na	na	na	64.51	24.82	157.19	14.65	na
8850	63.7	0.72	22.9	3.6	0.06	1.21	0.35	0.24	7.07	0.13	20.12	4.19	15.62	80.92	361.47	15.62	22.75	134.35	19.22	8.03
5300	82.5	0.27	6.8	2.1	0.18	2.07	2.96	0.22	2.94	0.05	4.52	0.69	3.66	17.94	92.73	18.27	7.54	103.36	5.38	2.21
5300	36.9	0.09	3.5	12.7	1.56	15.71	27.73	0.23	1.52	0.05	15.98	0.99	1.49	5.71	36.25	57.91	9.39	27.46	1.92	0.58
7350	87.2	0.32	5.5	2.6	0.10	1.00	1.33	0.00	1.86	0.03	5.10	na	na	43.00	77.10	12.20	10.60	53.90	6.20	2.50
8500	60.9	0.56	11.9	8.1	0.60	4.30	6.77	2.00	4.81	0.18	13.21	0.33	12.09	65.00	97.26	54.90	11.18	47.71	11.01	1.23
8500	70.8	0.43	9.2	4.3	0.19	2.72	4.87	0.15	7.26	0.15	3.02	1.15	6.51	32.18	117.52	297.58	5.54	51.71	7.11	0.83
8500	54.3	0.54	14.0	8.7	0.48	5.71	9.68	0.04	6.44	0.19	18.69	2.84	10.64	58.41	186.23	207.18	12.25	74.53	11.07	1.54
8500	50.2	0.51	14.2	9.9	0.47	5.27	9.34	0.09	9.83	0.22	5.97	1.21	9.16	54.34	197.65	64.32	11.02	63.08	10.91	1.24
8500	58.0	0.69	14.7	6.3	0.28	4.35	7.10	0.83	7.58	0.19	7.23	1.23	9.63	66.77	163.82	41.68	7.57	90.00	13.43	2.23
7050	63.4	0.61	17.3	0.7	0.05	1.24	1.71	0.05	14.78	0.22	3.56	0.35	10.30	44.45	298.54	27.16	6.09	91.34	9.10	2.25
6550	62.2	0.61	15.5	1.2	0.06	3.11	3.85	0.12	13.13	0.23	5.44	0.30	9.44	51.63	237.12	23.08	7.09	82.24	10.11	2.16
5150	54.8	0.52	15.0	12.3	0.11	1.83	2.70	0.07	12.45	0.22	8.13	0.41	16.88	77.65	219.68	16.33	11.91	85.14	10.35	1.02
7400	54.3	0.47	13.1	9.7	0.23	4.61	7.32	0.01	10.17	0.19	1.82	0.24	9.31	45.89	167.04	18.31	12.60	63.69	8.38	0.41
0450	53.3	0.65	15.4	6.0	0.48	6.61	9.13	6.02	1.68	0.72	21.41	1.44	13.04	123.78	22.25	34.57	23.97	101.03	10.87	0.41
1800	73.0	0.53	10.9	7.1	0.06	6.41	0.74	0.15	0.90	0.19	52.99	0.24	9.23	97.37	20.28	24.79	4.23	84.74	12.33	2.02
1300	19.1	0.11	1.8	71.6	0.30	1.49	3.74	0.37	0.87	0.61	6.94	0.74	1.58	846.33	19.54	12.29	17.51	10.77	46.41	0.13
7600	56.5	0.80	13.9	7.6	0.14	3.61	8.82	4.54	3.84	0.27	29.07	2.76	15.99	108.16	89.71	42.50	27.19	33.58	13.13	1.75
7950	55.1	0.76	13.9	10.1	0.17	4.09	7.74	4.72	3.29	0.17	21.76	3.17	15.08	105.52	106.27	41.08	19.44	41.51	11.84	1.47
4900	56.9	0.64	12.8	12.2	0.32	3.06	4.98	0.39	8.45	0.24	3.59	0.19	11.06	96.89	160.02	21.94	9.56	75.32	12.28	1.24
7600	55.6	0.52	14.2	5.8	0.54	2.29	12.90	7.79	0.12	0.21	6.52	0.92	15.25	28.38	4.61	111.26	20.93	78.11	7.96	0.33
0800	56.6	0.47	11.7	9.8	0.21	4.70	7.20	0.29	8.91	0.19	8.58	1.83	9.40	56.23	165.55	151.36	11.11	49.86	9.90	2.12
1700	50.8	1.80	13.7	12.7	0.36	2.84	5.45	0.24	11.97	0.24	0.99	0.34	22.87	252.07	184.19	27.07	21.32	118.52	12.02	0.64
9800	48.7	0.07	2.5	43.6	0.04	1.90	1.99	0.26	0.85	0.10	9.17	0.85	0.57	43.36	8.42	11.07	4.72	25.54	1.63	0.31
9600	55.3	0.56	12.3	11.7	0.24	1.81	10.05	3.80	4.06	0.19	5.60	na	na	89.00	53.10	57.20	15.40	40.40	12.00	0.27
1390	65.7	0.59	12.2	5.0	0.11	2.15	3.18	0.28	10.54	0.19	2.72	0.36	6.56	42.18	138.74	18.87	4.66	146.41	14.81	0.50
1390	64.1	0.56	13.8	9.4	0.07	0.40	0.63	0.25	10.54	0.26	4.21	1.08	11.48	94.44	144.69	13.16	12.85	116.36	14.93	1.20
7350	56.9	0.57	14.5	11.4	0.12	3.76	2.48	0.15	9.93	0.23	29.90	na	na	78.00	214.50	18.30	8.40	32.60	14.50	1.20
7350	55.4	0.57	13.9	12.0	0.17	5.03	3.60	0.14	8.87	0.26	36.90	na	na	80.00	188.60	18.80	13.70	37.70	12.50	1.30
7350	56.6	0.55	13.3	11.0	0.27	5.23	5.96	0.07	6.89	0.18	20.50	na	na	80.00	221.20	40.40	10.90	28.40	10.90	4.50
7350	56.8	0.61	15.5	9.1	0.42	4.91	6.16	0.12	6.11	0.23	11.20	na	na	87.00	262.90	31.60	11.60	64.80	13.30	3.00
7350	54.5	0.52	12.4	6.9	0.61	7.10	13.28	0.02	4.46	0.26	11.20	na	na	60.00	210.40	47.70	16.60	56.60	8.10	2.70

APPENDIX 3: GEOCHEMICAL ANALYSES Table A3-1: Right side

Sample no. Geol	Yr	Number	Lab Sample#	Ba ppm	La ppm	Ce ppm	Pr ppm	Nd ppm	Sm ppm	Eu ppm	Gd ppm	Tb ppm	Dy ppm	Ho ppm	Er ppm	Tm ppm	Yb ppm	Lu ppm	Hf ppm	Ta ppm
				...Bonnet Plume River intrusions; Early Proterozoic diorite (EPd)																
DT	92	132-5b	G-12	8.12	7.35	12.94	1.50	5.82	1.69	0.79	2.59	0.52	3.41	0.61	1.92	0.26	1.65	0.22	1.39	1.30
DT	93	167-1b	G-124	550.37	37.60	70.28	7.81	27.61	5.38	1.46	5.17	0.84	5.82	1.22	3.71	0.57	3.81	0.58	4.34	1.16
DT	92	139-5b	G-16	133.48	8.96	18.24	2.23	9.38	2.18	0.60	2.35	0.35	2.22	0.42	1.22	0.18	1.06	0.15	0.73	0.37
DT	92	53-6b	G-5	112.18	14.71	29.79	3.58	14.68	3.30	1.01	3.55	0.56	3.86	0.81	2.54	0.41	2.81	0.42	2.50	0.84
DT	93	113-1b	G-116	307.30	15.59	31.06	3.43	11.99	2.16	0.61	1.92	0.28	1.89	0.43	1.29	0.20	1.25	0.16	0.70	0.30
DT	92	76-6b	G-9	199.48	24.60	51.05	5.96	21.30	4.21	1.07	4.42	0.73	5.54	1.24	4.29	0.67	4.35	0.66	3.35	0.93
CW	93	101-1a	G-126	1726.94	21.43	50.86	6.84	27.70	6.67	1.72	6.95	1.12	7.12	1.47	4.28	0.65	3.96	0.64	5.27	1.25
DT	94	20-1b	G-205	295.60	20.70	44.70	5.80	24.40	5.60	2.00	5.40	0.75	4.50	0.86	2.30	0.30	1.80	0.27	2.00	1
DT	92	139-6b	G-17	301.62	9.51	19.25	2.33	9.61	2.45	0.68	2.33	0.35	2.10	0.39	1.19	0.21	1.50	0.24	1.65	1.03
DT	93	78-1b	G-113	171.61	14.32	32.55	4.42	18.40	4.58	1.42	5.30	0.81	5.29	1.03	2.94	0.41	2.46	0.36	2.01	0.71
DT	93	25-1b	G-106	211.60	5.22	13.17	1.74	7.72	1.93	0.62	2.44	0.38	2.59	0.55	1.62	0.23	1.50	0.20	0.78	0.26
DT	94	16-1b	G-203	2477.00	9.00	22.80	3.30	15.20	4.80	1.40	5.90	0.98	6.20	1.20	3.50	0.49	2.70	0.34	1.20	1
DT	93	11-1b	G-103	1564.98	22.33	49.08	6.05	23.99	5.43	1.56	6.38	0.91	6.15	1.26	3.49	0.54	3.46	0.51	3.69	1.19
DT	92	158-5b	G-30	77.02	18.25	40.61	5.00	20.35	4.71	1.40	5.01	0.75	5.11	1.05	3.13	0.44	2.93	0.43	1.59	0.82
DT	92	135-4b	G-13	70.35	25.04	50.89	5.96	23.44	5.17	1.44	5.65	0.86	5.75	1.13	3.33	0.50	3.18	0.45	1.74	0.82
DT	93	11-2b	G-104	433.43	18.16	39.72	5.16	20.91	5.02	1.34	5.77	0.84	6.04	1.17	3.53	0.53	3.51	0.51	3.48	0.79
DT	92	53-2b	G-4	1293.45	8.28	19.38	2.71	12.44	3.54	1.08	4.34	0.70	4.78	1.00	2.93	0.44	2.98	0.40	1.60	0.80
DT	93	120-1b	G-117	170.26	3.32	10.06	1.34	6.70	2.06	0.80	3.03	0.49	3.64	0.75	2.11	0.32	2.01	0.27	1.47	0.24
DT	93	163-1b	G-123	612.91	3.44	7.36	1.00	4.03	1.35	0.59	2.27	0.42	2.82	0.57	1.61	0.23	1.35	0.21	2.02	0.42
DT	94	15-2b	G-202	136.00	7.90	16.00	2.00	9.50	3.20	1.20	4.00	0.68	4.10	0.85	2.50	0.32	2.20	0.30	1.70	1
CW	93	101-2a	G-127	1196.62	24.57	55.28	7.29	29.74	7.39	2.03	8.43	1.25	7.70	1.48	4.14	0.60	3.68	0.58	4.71	1.22
DT	93	25-2b	G-107	50.04	55.59	111.30	13.35	49.63	9.38	2.10	7.83	0.96	5.58	1.08	3.57	0.60	4.34	0.74	7.49	1.95
DT	94	22-1b	G-207	176.80	83.30	180.80	20.80	78.60	16.70	3.50	15.60	2.50	15.40	3.20	9.20	1.30	8.00	1.00	6.70	5
DT	93	52-1b	G-110	130.76	59.49	144.66	19.31	80.80	18.77	4.52	20.76	3.16	21.15	4.28	12.68	1.88	12.07	1.86	13.25	4.04
DT	94	16-2b	G-204	750.40	19.80	37.10	4.10	15.40	2.90	0.81	2.10	0.30	1.80	0.33	1.00	0.17	1.20	0.21	1.60	1
				...Slab volcanics (PSV)																
DT	94	21-1b	G-206	126.30	28.90	73.20	9.00	36.30	8.10	2.30	7.70	1.20	7.20	1.50	4.60	0.64	4.30	0.63	2.60	2
DT	93	9-1b	G-101	92.28	24.84	75.54	11.06	48.72	12.34	2.94	12.88	1.90	12.02	2.19	6.26	0.93	5.99	0.89	6.14	2.53
DT	92	160-4b	G-32	72.04	23.85	83.58	14.76	70.99	19.61	3.97	15.67	2.13	12.26	2.11	5.47	0.88	5.43	0.70	3.87	2.13
				...Middle Proterozoic lamprophyre (MPl)																
DT	93	151-1b	G-108	4262.82	66.78	134.02	16.21	64.24	12.12	3.18	11.11	1.23	6.53	1.03	2.26	0.30	1.44	0.19	7.59	5.94
				...Bear River intrusions; Middle Proterozoic diorite (MPd)																
TOA	96	6-7-2b	6-7-2b	386.75	15.08	32.69	3.34	15.34	3.47	1.09	3.80	0.66	3.69	0.72	2.20	0.29	2.15	0.32	2.94	0.47
DT	92	11-1b	G-2	267.85	12.98	27.29	3.25	13.79	3.15	0.96	3.50	0.50	3.36	0.62	1.86	0.25	1.63	0.24	2.22	0.52
CW	93	19-1b	G-125	430.71	21.93	49.31	5.95	22.26	4.77	1.43	4.78	0.71	4.26	0.84	2.20	0.31	2.04	0.29	3.55	1.09
DT	93	72-1b	G-112	331.84	12.51	31.62	4.42	20.19	5.28	1.84	6.18	0.86	5.23	0.97	2.58	0.37	2.05	0.29	3.82	0.59
				...Wernecke Supergroup (PFL, PQ, PGL) and Pinguicula Group (PP)																
DT	92	80-1b	G-11	66.49	91.98	141.82	16.10	55.78	na	1.33	6.46	0.80	5.13	1.04	3.25	0.52	3.70	0.57	6.24	0.99
DT	92	55-1b	G-6	676.72	51.98	105.09	11.96	43.31	na	1.40	6.24	0.84	5.03	0.98	2.75	0.42	2.64	0.38	4.48	1.20
DT	92	169-1b	G-33	930.02	76.83	151.98	16.75	59.63	10.32	1.76	7.20	0.90	5.16	0.92	2.61	0.41	2.77	0.45	3.95	1.53
DT	93	129-1b	G-119	294.87	17.77	37.90	4.28	15.15	2.57	0.48	1.98	0.23	1.49	0.30	0.92	0.15	0.95	0.16	3.03	0.40
DT	93	129-2b	G-120	79.67	8.07	16.86	2.11	8.22	2.43	0.63	2.90	0.40	2.13	0.36	1.03	0.12	0.86	0.14	0.94	0.12
DT	94	36-6b	G-213	76.50	43.30	99.80	10.70	38.50	6.20	0.95	3.00	0.41	2.30	0.44	1.30	0.18	1.10	0.17	1.60	0.45
				...Wernecke Breccia and related metasomatic rocks (PWb)																
DT	92	138-1b	G-14	295.92	12.45	23.66	2.88	10.76	2.46	0.62	2.46	0.34	2.20	0.45	1.37	0.21	1.61	0.23	1.60	1.05
DT	92	149-8b	G-28	9918.37	8.36	17.34	1.97	7.40	1.77	0.42	2.72	0.22	1.25	0.23	0.67	0.11	0.85	0.12	1.59	0.59
DT	92	149-7b	G-27	9060.87	17.94	35.39	4.00	14.54	4.01	1.11	5.86	0.55	3.01	0.49	1.45	0.24	1.77	0.26	2.43	0.92
DT	92	149-6b	G-25	4583.97	11.77	20.57	2.22	8.37	2.16	0.55	2.95	0.39	2.41	0.43	1.27	0.20	1.45	0.23	1.93	0.97
DT	92	149-5b	G-24	632.34	4.39	8.63	1.09	4.58	1.55	0.43	1.90	0.27	1.63	0.30	1.02	0.17	1.32	0.20	2.77	1.18
DT	92	143-1b	G-23	1592.15	2.17	5.80	0.78	3.31	0.85	0.28	1.01	0.18	1.18	0.25	0.87	0.13	0.97	0.16	2.75	0.85
DT	92	142-5b	G-22	1080.13	3.04	7.54	0.97	4.11	1.12	0.34	1.32	0.21	1.49	0.31	0.88	0.15	1.08	0.16	2.69	0.93
DT	92	52-4b	G-3	1730.51	72.90	116.48	11.79	40.21	6.44	1.55	5.09	0.53	2.68	0.47	1.31	0.22	1.48	0.24	2.64	0.91
DT	92	62-2b	G-7	706.15	57.61	99.46	10.48	37.32	6.37	1.51	4.76	0.50	2.71	0.47	1.35	0.20	1.36	0.21	2.04	0.80
DT	92	77-1b	G-10	239.36	31.61	72.33	8.93	34.05	6.76	1.57	6.04	0.82	4.93	0.93	2.68	0.38	2.52	0.36	3.12	1.23
DT	93	11-3b	G-105	962.47	18.24	33.92	3.90	14.01	2.69	0.68	2.34	0.20	0.94	0.17	0.47	0.08	0.54	0.11	2.51	0.89
DT	93	10-1b	G-102	120.08	394.67	644.18	70.80	234.36	35.01	9.60	25.12	1.90	6.44	0.72	1.34	0.14	0.85	0.12	0.31	0.64
DT	92	160-3b	G-31	481.40	37.05	72.54	8.23	32.00	6.61	1.64	6.30	0.85	5.44	1.06	2.96	0.43	2.69	0.39	1.03	1.14
DT	93	7-1c	G-100	440.96	40.65	80.67	8.83	31.39	5.59	1.25	5.41	0.71	4.25	0.82	2.28	0.33	2.09	0.31	1.51	0.91
DT	93	126-1b	G-118	1379.78	73.73	128.12	13.89	46.81	6.98	1.75	5.05	0.51	2.41	0.41	1.27	0.20	1.41	0.22	2.48	0.96
DT	93	57-1b	G-111	60.90	145.87	281.42	32.64	115.95	19.73	3.89	12.94	1.21	5.45	0.88	2.34	0.34	2.32	0.40	2.48	0.80
DT	93	49-1b	G-109	28510.00	36.76	62.99	6.59	22.17	4.15	2.20	6.75	0.42	2.42	0.45	1.25	0.19	1.17	0.19	1.66	0.70
DT	93	107-2b	G-115	983.45	23.28	40.17	4.58	16.51	3.59	1.12	4.13	0.60	4.22	0.87	2.60	0.40	2.63	0.39	3.55	0.78
DT	93	94-1b	G-114	65.00	5.27	11.94	1.49	5.53	1.26	0.28	1.23	0.16	1.00	0.17	0.45	0.06	0.38	0.06	0.48	0.09
DT	94	15-1b	G-201	550.20	54.10	98.60	10.30	36.20	5.80	1.30	4.10	0.56	3.10	0.59	1.70	0.24	1.50	0.21	1.30	0.87
DT	93	159-1b	G-121	665.09	14.90	29.41	3.28	11.01	2.04	0.43	1.50	0.20	1.01	0.20	0.61	0.11	0.87	0.18	4.55	1.25
DT	93	159-3b	G-122	1052.41	35.25	71.72	7.63	26.23	5.28	1.40	4.33	0.57	3.16	0.63	1.73	0.28	1.83	0.30	4.04	1.35
DT	94	36-1b	G-210	953.00	105.70	185.00	18.80	64.10	10.40	2.20	6.40	0.60	2.40	0.36	0.95	0.14	0.73	0.14	1.00	1.10
DT	94	36-2	G-208	842.20	219.90	403.10	41.90	142.80	24.40	5.40	15.50	1.40	4.70	0.62	1.50	0.19	0.92	0.20	1.20	1.00
DT	94	36-3b	G-211	981.40	26.40	49.60	5.20	18.30	3.20	0.81	2.70	0.40	2.40	0.46	1.40	0.22	1.40	0.22	0.86	0.73
DT	94	36-4	G-209	263.00	25.30	45.60	4.70	16.70	3.00	0.90	2.60	0.38	2.40	0.46	1.40	0.21	1.40	0.22	2.00	0.89
DT	94	36-5b	G-212	167.10	25.90	55.00	6.30	23.20	4.60	0.99	3.70	0.56	3.30	0.65	2.00	0.28	1.70	0.26	1.60	0.61

page 68b

Hf ppm	Ta ppm	Tl ppm	Pb ppm	Bi ppm	Th ppm	U ppm	Cr ppm	Co ppm	Ni ppm	Cu ppm	Zn ppm	Ag ppm	Sn ppm	Sb ppm	K ppm	Mn ppm	P ppm	Ti ppm	Nd T_{dm} (Ga)
1.39	1.30	0.26	1.05	0.05	2.17	0.88	936	84	234.07	8.03	90.85	0.01	2.06	6.28	816	2033	762	15083	na
4.34	1.16	0.19	2.82	0.18	8.88	4.39	69	46	73.03	58.57	70.44	1.56	2.98	1.78	30368	707	972	10034	na
0.73	0.37	0.64	3.17	0.09	1.24	0.35	173	82	131.62	8.42	71.65	0.31	0.43	0.98	24903	2507	438	7361	na
2.50	0.84	0.13	5.18	0.50	3.31	1.94	49	35	81.47	14.03	39.72	0.70	8.14	2.87	17050	1626	770	14644	na
0.70	0.30	0.17	2.21	0.24	1.12	1.89	173	61	130.92	20.59	143.61	na	1.69	4.95	18182	1012	438	6210	na
3.35	0.93	0.27	4.73	0.28	5.42	2.93	138	82	102.99	53.25	189.93	1.22	2.43	10.61	27005	1448	863	11476	na
5.27	1.25	0.24	5.84	0.22	7.61	2.50	51	75	35.53	120.94	112.21	2.02	2.24	1.07	23114	1238	1044	14313	na
2.00	1	0.11	6.50	0.08	2.50	0.52	165	32	75.00	na	52.00	na	na	na	9780	1712	734	12877	2.29
1.65	1.03	0.72	3.36	0.00	11.88	2.48	58	18	35.60	2.73	28.01	0.17	1.85	0.39	82792	3199	876	3615	na
2.01	0.71	0.14	2.19	0.38	3.59	0.71	71	37	57.57	21.86	178.89	0.12	1.36	1.50	6529	2032	732	10573	na
0.78	0.26	0.14	1.82	0.15	0.77	0.29	490	47	67.98	13.96	51.11	0.03	1.11	4.27	17559	1491	326	5539	na
1.20	1	0.47	2.30	0.13	2.80	0.61	30	48	68.00	na	115.00	na	na	na	46599	1489	838	13833	na
3.69	1.19	0.37	6.47	0.11	8.81	1.63	117	51	89.37	167.61	39.74	0.51	2.16	1.39	12839	1150	1247	9217	na
1.59	0.82	0.06	5.78	0.16	4.24	1.15	211	36	43.82	113.00	33.02	0.72	2.21	1.48	7969	981	644	8800	na
1.74	0.82	0.01	2.73	0.10	4.14	1.87	119	35	41.11	46.09	41.21	0.79	2.15	1.49	3227	1059	733	10907	na
3.48	0.79	0.30	3.02	0.07	4.98	1.93	92	39	56.92	14.31	90.86	0.43	1.37	0.87	47362	1723	554	10926	na
1.60	0.80	0.52	5.27	0.45	3.43	1.31	120	46	53.79	16.77	68.05	0.31	2.38	2.26	48836	1575	700	10077	na
1.47	0.24	0.24	4.19	0.29	0.56	6.59	121	52	81.12	129.45	196.85	0.15	0.94	5.15	19900	2644	382	5707	na
2.02	0.42	0.36	2.82	0.08	2.27	0.79	59	34	37.16	37.33	61.98	0.74	2.11	2.50	37180	980	1241	12079	6.67
1.70	1	0.10	2.60	0.27	10.30	4.30	69	21	47.00	na	89.00	na	na	na	7949	1877	768	6143	na
4.71	1.22	0.42	5.06	0.07	6.50	1.70	48	56	32.17	127.77	125.38	1.74	1.81	1.65	32903	1422	1111	14247	na
7.49	1.95	0.07	2.89	0.15	18.71	4.69	46	65	10.28	13.76	19.94	1.02	2.29	4.99	3420	3625	2088	14434	na
6.70	5	0.09	7.00	0.22	49.80	4.20	12	33	10.00	na	114.00	na	na	na	8308	1251	3238	12270	2.42
13.25	4.04	0.00	6.26	0.22	34.52	5.93	49	39	2.18	2124.00	53.58	2.67	3.15	0.54	698	570	3118	11988	2.57
1.60	1	0.22	4.90	0.22	3.30	3.30	87	13	43.00	na	49.00	na	na	na	35652	1345	946	3710	na
2.60	2	0.17	3.00	0.05	13.40	3.40	12	30	22.00	na	28.00	na	na	na	19896	841	1513	10999	na
6.14	2.53	0.16	3.65	0.05	20.20	4.82	64	34	10.86	11.63	29.28	0.82	3.31	0.60	17073	818	2392	12469	na
3.87	2.13	0.14	2.20	0.02	20.10	4.84	54	37	14.64	10.25	24.82	1.37	3.26	0.79	16117	560	1891	10907	3.00
7.59	5.94	0.15	6.38	0.07	8.74	2.42	851	84	591.37	19.37	408.04	1.23	3.14	1.61	8826	3590	3948	22111	na
2.94	0.47	0.35	5.00	0.81	4.08	0.87	357	70	162.00	122.00	50.00	0.50	0.80	2.09	na	na	na	na	2.72
2.22	0.52	0.62	21.69	0.26	2.81	0.68	479	41	151.18	141.92	102.00	0.66	35.58	7.39	26921	1139	503	6550	2.69
3.55	1.09	0.30	15.73	0.05	4.36	1.93	208	34	81.90	69.53	120.57	1.44	1.95	2.40	21989	1203	592	7802	2.09
3.82	0.59	0.19	22.94	0.05	1.81	1.04	109	46	78.24	370.56	156.45	0.95	1.66	1.19	9222	1770	996	13706	2.13
6.24	0.99	na	na	na	13.96	na	na	na	na	na	na	na	na	na	8696	173	1020	4607	2.28
4.48	1.20	na	na	na	16.13	na	na	na	na	na	na	na	na	na	29819	493	323	5882	2.45
3.95	1.53	1.31	2.30	0.06	24.86	7.51	74	12	36.27	4.00	8.88	0.98	4.34	1.36	58687	481	586	4298	na
3.03	0.40	0.26	4.19	0.19	6.14	1.21	35	2	4.41	11.09	8.24	0.27	0.70	0.58	24435	1375	228	1647	2.47
0.94	0.12	0.00	2.38	0.01	2.71	0.67	27	5	10.70	1.94	17.25	0.30	0.81	0.23	12587	12071	238	557	4.21
1.60	0.45	0.41	15.70	0.36	8.10	25.70	53	13	84.00	na	9.00	na	na	na	15451	738	138	1904	na
1.60	1.05	0.31	5.06	0.04	13.03	3.78	103	10	13.88	3.89	21.42	0.14	2.73	0.65	39928	4639	773	3379	na
1.59	0.59	0.35	2.44	0.08	9.85	2.04	97	4	12.49	4.53	6.75	0.36	1.83	3.52	60272	1445	670	2560	na
2.43	0.92	0.45	1.27	0.04	11.33	2.01	58	10	31.17	3.17	5.82	0.53	3.07	2.77	53471	3705	834	3256	na
1.93	0.97	0.17	2.26	0.03	11.50	3.15	69	10	27.93	3.45	6.91	0.43	2.25	3.76	81551	3673	958	3066	na
2.77	1.18	0.34	3.08	0.05	14.06	2.41	53	6	16.70	3.76	9.36	0.61	4.40	4.01	62944	2174	832	4126	na
2.75	0.85	1.11	7.92	0.42	13.79	3.81	53	5	8.83	12.01	6.22	1.05	1.38	1.20	122705	409	967	3662	na
2.69	0.93	1.03	5.40	0.42	11.46	2.89	83	2	6.50	8.98	7.10	0.61	1.02	0.53	108949	496	1024	3650	na
2.64	0.91	0.42	5.21	0.41	18.49	2.49	69	38	8.65	54.19	8.87	0.43	6.08	1.63	103353	818	966	3134	na
2.04	0.80	0.29	1.55	0.10	8.64	2.85	36	7	4.80	4.43	3.54	0.25	2.41	1.31	84426	1821	829	2793	na
3.12	1.23	0.01	4.21	0.02	19.70	3.68	79	15	32.45	12.87	47.96	0.46	3.20	1.08	13904	3709	3130	3897	2.42
2.51	0.89	0.08	1.80	0.06	13.51	6.42	94	11	62.37	4.17	20.53	0.25	4.06	1.27	7434	490	827	3168	2.85
0.31	0.64	0.06	4.76	0.16	6.17	4.79	220	94	53.92	3.01	9.25	1.19	44.60	2.92	7200	2327	2667	641	na
1.03	1.14	0.28	2.24	0.06	13.60	3.15	75	21	33.40	124.57	16.85	0.52	2.73	0.52	31835	1095	1184	4818	2.96
1.51	0.91	0.32	2.36	0.07	11.96	2.89	87	21	40.28	21.69	23.66	0.24	3.00	0.52	27267	1282	721	4584	na
2.48	0.96	0.51	2.50	0.08	13.18	3.40	98	25	12.16	5.32	12.89	0.45	3.90	1.66	70148	2516	1038	3837	2.69
2.48	0.80	0.09	2.19	0.05	12.63	1.31	82	8	11.46	12.12	10.48	0.24	2.75	1.85	1015	4223	921	3142	na
1.66	0.70	0.55	5.18	0.15	8.63	2.54	85	12	13.57	6.58	20.55	0.25	2.98	1.54	73956	1657	829	2844	na
3.55	0.78	0.37	3.09	0.26	6.35	5.37	96	21	23.22	2142.35	16.99	0.67	1.94	4.83	99312	2757	1034	10801	2.45
0.48	0.09	0.12	71.93	0.42	1.47	4.28	172	2	14.10	2.91	87.05	0.09	1.31	30.83	7056	334	422	426	na
1.30	0.87	0.18	2.20	0.52	12.10	4.90	67	75	27.00	na	37.00	na	na	na	33702	1826	831	3365	na
4.55	1.25	0.51	3.52	0.12	17.01	1.49	77	3	8.66	3.32	10.38	1.34	2.16	0.99	87466	889	819	3568	na
4.04	1.35	0.76	3.75	0.06	17.25	2.42	94	3	6.25	10.22	10.07	1.14	4.21	2.93	87489	555	1115	3359	na
1.00	1.10	0.63	2.70	0.19	14.40	2.00	73	24	47.00	na	31.00	na	na	na	82459	924	992	3445	na
1.20	1.00	0.56	2.70	0.48	14.00	2.40	97	32	50.00	na	36.00	na	na	na	73599	1292	1114	3400	na
0.86	0.73	0.71	1.50	0.06	11.70	1.60	54	12	29.00	na	17.00	na	na	na	57224	2059	806	3326	na
2.00	0.89	0.73	4.70	5.00	12.20	4.00	84	11	34.00	na	18.00	na	na	na	50741	3261	1019	3647	na
1.60	0.61	0.57	9.00	0.36	11.50	25.70	63	7	199.00	na	15.00	na	na	na	37030	4733	1141	3140	na

Appendix 4: Assays Table A4-1 (top left side)

Assays arranged from west to east

Sample no. Geol	Yr.	Number	Lab Sample	UTM E	N	Map NTS	Nearest Relevant Mineral Occurrence	Lithologic Description	Au ppb	Ag ppm	Cu ppm	Pb ppm	Zn ppm	As ppm	Sb ppm	Hg ppm	Mo ppm	Tl ppm
DT	92	138-1b	G-14	497200	7188600	106D/14	SIHOTA	Wernecke Breccia	31	na	na	na	na	na	na	na	na	na
DT	92	139-5b	G-16	497200	7188650	106D/14	SIHOTA	Dioritic dyke adjacent Wernecke Breccia	19	na	na	na	na	na	na	na	na	na
DT	92	139-6b	G-17	497200	7188650	106D/14	SIHOTA	Reddened dioritic dyke adjacent Wernecke Bx	1494	na	na	na	na	na	na	na	na	na
DT	92	149-6b	G-25	525850	7208600	106E/1	BLAND	Wernecke breccia with specularite	23	na	na	na	na	na	na	na	na	na
DT	92	149-8b	G-29	525850	7208500	106E/1	BLAND	Altered siltstone clast in Wernecke Breccia	26	na	na	na	na	na	na	na	na	na
DT	92	149-5b	G-24	525850	7208500	106E/1	BLAND	Slightly altered (brown) siltstone (P?)	19	na	na	na	na	na	na	na	na	na
DT	92	149-7b	G-27	525850	7208500	106E/1	BLAND	Wernecke Breccia, pinkish matrix rich	22	na	na	na	na	na	na	na	na	na
DT	92	143-1b	G-23	527650	7207050	106D/16	BLAND	Red banded altered siltstone	37	na	na	na	na	na	na	na	na	na
DT	92	142-5b	G-22	527700	7206550	106D/16	BLAND	Altered siltstone	21	na	na	na	na	na	na	na	na	na
DT	92	77-1b	G-10	533050	7200450	106D/16	PITCH	Matrix of Wernecke Breccia	32	na	na	na	na	na	na	na	na	na
DT	92	53-2b	G-4	534500	7201850	106D/16	CRUICKLE	Micro-granodioritic hematitic	26	na	na	na	na	na	na	na	na	na
CW	92	45-1b	G-200	541100	7190700	106D/16	WALLACE	Metalliferous vein in Gillespie Lake Group	na	26.0	5.1%	11	196	1.7%	2503	7	2	nd
DT	93	30-1b	G-139	549700	7199300	106C/13	NORANDA	Wernecke Breccia	na	0.2	6900	9	46	nd	nd	nd	124	nd
DT	93	113-2	G-138	554700	7195300	106C/13	OLYMPIC	Mafic dyke	na	0.1	2044	12	102	nd	nd	nd	3	nd
DT	93	25-5	G-140	554700	7194900	106C/13	OLYMPIC	Malachite-stained Wernecke Breccia	na	0.1	2986	11	49	nd	nd	nd	6	nd
CW	93	66-1b	G-142	555300	7197200	106C/13	ATHENS	Dolostone, Gillespie Lake Group	na	0.2	458	12	23	nd	nd	nd	5	nd
DT	93	129-2b	G-126	555400	7195300	106C/13	OLYMPIC	Dolostone, Gillespie Lake Group	-5	na	na	na	na	na	na	na	na	na
DT	93	126-2b	G-132	555500	7194900	106C/13	OLYMPIC	Cu-stained Wernecke Breccia	na	0.4	6893	13	165	15	nd	nd	3	nd
CW	93	31-1	G-145	555700	7186600	106C/13	GOODFELLOW	Gossan vein in Gillespie Lake Group	na	3.3	162	357	991	49	nd	nd	5	nd
DT	93	120-1b	G-117	556300	7195000	106C/13	OLYMPIC	Boxwell Plume River diorite, in breccia	-5	na	na	na	na	na	na	na	na	na
CW	93	46-1	G-141	563200	7201600	106C/13	CAROL	Calcareous siltstone, upper Fairchild L. Gp.	238	3.3	4.3%	12	65	166	nd	nd	16	nd
CW	93	86-1b	G-144	564000	7187000	106C/13	LEARY	Wernecke Breccia, purplish	1180	19.6	31343	15	28	6	nd	nd	16	nd
CW	93	85-1b	G-143	564300	7187400	106C/13	LEARY	Wernecke Breccia, purplish	na	0.6	3390	8	10	125	nd	nd	10	nd
DT	94	13-4	G-226	571500	7199300	106C/14	BEL	Diorite with pyrite and magnetite	-5	0.2	3	5	25	-5	-5	na	-1	na
DT	94	13-10	G-232	571500	7199300	106C/14	BEL	Light grey Wernecke Breccia	16	0.2	27	11	4	-5	-5	na	15	na
DT	94	13-7	G-229	571500	7199300	106C/14	BEL	Silicified Wernecke Breccia	-5	0.2	1	5	2	-5	-5	na	1	na
DT	94	13-6	G-228	571500	7199300	106C/14	BEL	Silicified Wernecke Breccia	-5	0.2	1	6	-1	-5	-5	na	2	na
DT	94	13-11	G-233	571500	7199300	106C/14	BEL	Carbonate-veined Fairchild Lake Group	8	0.2	1	4	2	-5	-5	na	1	na
DT	94	13-9	G-231	571500	7199300	106C/14	BEL	Carbonate-altered crackle breccia	-5	0.2	40	5	9	-5	-5	na	2	na
DT	94	13-8	G-230	571500	7199300	106C/14	BEL	"Bleached" Wernecke Breccia	-5	0.2	4	8	5	-5	-5	na	8	na
DT	94	13-2	G-224	571500	7199300	106C/14	BEL	Sulphide-rich Wernecke Breccia	13	0.2	7874	9	16	-5	-5	na	8	na
DT	94	13-3	G-225	571500	7199300	106C/14	BEL	Altered dolomitic siltstone	-5	0.2	3	7	4	-5	-5	na	-1	na
DT	94	13-5	G-227	571500	7199300	106C/14	BEL	Wernecke Breccia with sulphides	-5	0.2	14	8	4	-5	-5	na	1	na
DT	93	166-3b	G-133	572500	7191150	106C/14	PIKA	Supergene oxide zone in Wernecke Breccia	na	2.9	2541	10	22	23	nd	nd	4	nd
DT	94	15-3	G-234	572650	7199650	106C/14	BEL	Rusty quartz vein in dolostone	-5	0.2	54	6	7	15	-5	na	3	na
DT	93	167-2	G-134	572950	7191600	106C/14	PIKA	Diorite, with chalcopyrite	105	1.5	2.0%	14	72	nd	nd	nd	10	nd
DT	94	18-1b	G-235	573400	7198800	106C/14	BEL	Wernecke Breccia	-5	0.2	1	5	4	-5	-5	na	-1	na
DT	93	163-5	G-137	573550	7191400	106C/14	PIKA	Reddened diorite	na	0.3	261	11	34	16	nd	nd	4	nd
DT	93	163-2b	G-135	573550	7191400	106C/14	PIKA	Diorite	na	0.2	214	12	68	nd	nd	nd	5	nd
DT	94	39-4	G-243	573800	7197800	106C/14	JULIE	Sulphide-rich quartz vein in Fairchild L. Gp.	230	3.1	189	9	115	-5	-5	na	2	na
DT	94	40-3b	G-246	573800	7198050	106C/14	JULIE	Pyritic quartz-carbonate vein in Fairchild L. Gp.	420	0.2	18796	8	9	-5	-5	na	-1	na
DT	94	40-4	G-247	573800	7198050	106C/14	JULIE	Very red Wernecke Breccia	8	0.2	19	12	3	-5	-5	na	3	na
DT	94	40-2b	G-245	573800	7198050	106C/14	JULIE	Reddened Wernecke Breccia	5	0.2	41	7	15	-5	-5	na	2	na
DT	94	40-1b	G-244	573800	7198050	106C/14	JULIE	Potassic altered diorite	7	0.2	367	6	94	-5	-5	na	-1	na
DT	94	114-1	G-252	573950	7159850	106C/11	–	Sulphide-rich diorite in Pinguicula Group unit A	-5	0.2	104	24	55	-5	-5	na	-1	na
CW	94	80-1a	G-276	576200	7193800	106C/14	KEY MOUNTAIN	Sulphide-malachite stained dolostone vein	-5	0.2	10406	23	27	-5	-5	na	-1	na
CW	94	104-1a	G-284	578350	7209300	106F/3	–	Malachite veinlets in Pinguicula Group unit A	-5	0.2	2554	12	90	-5	-5	na	-1	na
DT	94	26-1b	G-237	579050	7202900	106C/14	DOWSER	Pyritic crackle Wernecke Breccia	-5	0.2	2	6	-1	-5	-5	na	2	na
DT	94	25-1b	G-236	579100	7201850	106C/14	DOWSER	Metalliferous quartz vein	-5	0.2	1	6	4	-5	-5	na	13	na
DT	94	93-1b	G-250	579350	7195200	106C/14	DOBBY	Altered diorite	-5	0.2	1	13	109	-5	-5	na	-1	na
DT	94	93-2b	G-249	579350	7195200	106C/14	DOBBY	Altered Wernecke Breccia	17	0.2	55	12	4	-5	-5	na	-1	na
CW	94	94-1a	G-277	579450	7197000	106C/14	DOBBY	Malachite-stained clast from Wernecke Breccia	79	36.5	1	9	115	-5	-5	na	79	na

Appendix 4: Assays Table A4-1 (top right side)

Sample no. Geol	Yr.	Number	Bi ppm	Cd ppm	Co ppm	Ni ppm	Ba ppm	Sn ppm	Te ppm	W ppm	Cr ppm	V ppm	Mn ppm	La ppm	Sr ppm	Zr ppm	Sc ppm	Y ppm	Ti %	Al %	Ca %	Fe %	Mg %	K %	Na %	P %
DT	92	138-1b	na	na	na	na	na	na	na	na	na	na	na	na	na	na	na	na	na	na	na	na	na	na	na	na
DT	92	139-5b	na	na	na	na	na	na	na	na	na	na	na	na	na	na	na	na	na	na	na	na	na	na	na	na
DT	92	139-6b	na	na	na	na	na	na	na	na	na	na	na	na	na	na	na	na	na	na	na	na	na	na	na	na
DT	92	149-6b	na	na	na	na	na	na	na	na	na	na	na	na	na	na	na	na	na	na	na	na	na	na	na	na
DT	92	149-8b	na	na	na	na	na	na	na	na	na	na	na	na	na	na	na	na	na	na	na	na	na	na	na	na
DT	92	149-5b	na	na	na	na	na	na	na	na	na	na	na	na	na	na	na	na	na	na	na	na	na	na	na	na
DT	92	149-7b	na	na	na	na	na	na	na	na	na	na	na	na	na	na	na	na	na	na	na	na	na	na	na	na
DT	92	143-1b	na	na	na	na	na	na	na	na	na	na	na	na	na	na	na	na	na	na	na	na	na	na	na	na
DT	92	142-5b	na	na	na	na	na	na	na	na	na	na	na	na	na	na	na	na	na	na	na	na	na	na	na	na
DT	92	77-1b	na	na	na	na	na	na	na	na	na	na	na	na	na	na	na	na	na	na	na	na	na	na	na	na
DT	92	53-2b	na	na	na	na	na	na	na	na	na	na	na	na	na	na	na	na	na	na	na	na	na	na	na	na
CW	92	45-1b	700	0	6	6	24	na	na	7	34	5	554	4	13	6	3	na	nd	0.22	2	2	0.93	0.20	0	0
DT	93	30-1b	nd	nd	18	46	42	na	na	nd	61	119	1476	5	4	4	17	na	0	2.60	2	7	4.19	0.17	0	0
DT	93	113-2	nd	nd	66	123	927	na	na	nd	100	243	668	nd	18	1	19	na	0	4.00	0	8	5.60	0.05	0	0
DT	93	25-5	nd	nd	68	162	23	na	na	nd	91	164	891	2	3	1	16	na	0	3.63	0	6	5.04	0.16	0	0
CW	93	66-1b	nd	nd	3	6	32	na	na	nd	18	8	338	nd	33	3	1	na	nd	0.63	1496	1	1.76	0.07	0	0
DT	93	129-2b	na	na	na	na	na	na	na	na	na	na	na	na	na	na	na	na	na	na	na	na	na	na	na	na
DT	93	126-2b	nd	nd	140	194	60	na	na	nd	55	239	1068	3	3	1	16	na	0	2.53	0	7	3.06	0.15	0	0
CW	93	31-1	2	1	14	55	13	na	na	nd	75	16	83	nd	3	7	1	na	nd	0.65	1	1016	1.35	0.30	0	0
DT	93	120-1b	na	na	na	na	na	na	na	na	na	na	na	na	na	na	na	na	na	na	na	na	na	na	na	na
CW	93	46-1	nd	nd	95	69	19	na	na	6	41	38	692	46	45	1	5	na	0	0.66	2.60	5	0.60	0.25	0	0
CW	93	86-1b	311	nd	123	106	222	na	na	nd	63	52	466	2	4	13	4	na	0	1.87	0	7	2.55	0.10	0	0
CW	93	85-1b	nd	nd	159	11	157	na	na	nd	47	35	4418	1	14	6	5	na	0	0.16	5	5	2.35	0.16	0	0
DT	94	13-4	5	1.0	20	50	59	20	10	20	48	52	2631	2	65	na	na	2	na	1.60	7	2	2	0	0	na
DT	94	13-10	5	1.0	78	28	16	20	10	20	132	14	1759	8	7	na	na	6	na	0.16	2	3	1	0	0	na
DT	94	13-7	5	1.0	12	13	34	20	10	20	41	14	3063	47	14	na	na	5	na	0.23	4	2	1	0	0	na
DT	94	13-6	5	1.0	7	7	18	20	10	20	60	12	2727	82	16	na	na	4	na	0.14	4	2	2	0	0	na
DT	94	13-11	5	1.0	1	2	44	20	10	20	80	30	1217	20	32	na	na	3	na	0.26	5	2	0	0	0	na
DT	94	13-9	5	1.0	24	13	66	20	10	20	54	13	1460	99	1	na	na	7	na	0.69	2	1	0	0	0	na
DT	94	13-8	5	1.0	71	32	15	20	10	20	140	11	2200	19	6	na	na	4	na	0.15	3	3	0	0	0	na
DT	94	13-2	5	1.0	38	25	56	20	10	20	153	14	2902	224	9	na	na	12	na	0.31	2	3	1	0	0	na
DT	94	13-3	5	1.0	10	6	1219	20	10	20	98	44	2564	8	44	na	na	2	na	0.28	3	3	1	0	0	na
DT	94	13-5	5	1.0	12	12	235	20	10	20	118	50	4752	19	12	na	na	4	na	0.34	3	4	0	0	0	na
DT	93	166-3b	nd	nd	109	49	20	na	na	nd	79	8	739	10	6	3	2	na	nd	0.27	1	3	0.11	0.17	0	0
DT	94	15-3	5	1.0	8	16	5	20	10	20	185	6	1526	2	4	na	na	2	na	0.01	2	2	1	0	0	na
DT	93	167-2	nd	nd	128	95	26	na	na	nd	29	212	224	2	3	5	15	na	0	4.55	0	9	6.66	0.05	0	0
DT	94	18-1b	5	1.0	3	5	26	20	10	20	44	19	2219	22	17	na	na	3	na	0.16	6	2	3	0	0	na
DT	93	163-5	nd	nd	148	32	34	na	na	nd	12	330	480	4	10	1	9	na	0	1.69	2	1296	2.36	0.02	0	0
DT	93	163-2b	nd	nd	36	35	29	na	na	nd	28	303	614	7	3	nd	13	na	0	3.44	0	8	4.40	0.05	0	0
DT	94	39-4	5	1.0	21	6	12	20	10	20	112	5	1071	2	6	na	na	4	na	0.28	2	4	0	0	0	na
DT	94	40-3b	5	1.0	27	14	24	20	10	20	92	6	2964	5	15	na	na	15	na	0.02	10	3	6	0	0	na
DT	94	40-4	5	1.0	3	4	51	20	10	20	103	135	2011	3	11	na	na	4	na	0.36	4	5	2	0	0	na
DT	94	40-2b	5	1.0	15	16	26	20	10	20	89	42	2974	17	18	na	na	4	na	0.42	4	3	2	0	0	na
DT	94	40-1b	5	1.0	16	20	29	20	10	20	46	207	906	6	46	na	na	5	na	1.40	6	3	1	0	0	na
DT	94	114-1	5	1.0	27	81	26	20	10	20	274	170	572	1	1	na	na	7	na	2.81	0	5	3	0	0	na
CW	94	80-1a	5	1.0	6	1	33	20	10	20	152	5	9625	1	84	na	na	5	na	0.23	0	8	1	0	0	na
CW	94	104-1a	5	1.0	25	30	296	20	10	20	67	20	502	25	7	na	na	7	na	2.26	0	4	2	0	0	na
DT	94	26-1b	5	1.0	19	14	19	20	10	20	81	6	1341	3	7	na	na	4	na	0.14	3	3	2	0	0	na
DT	94	25-1b	5	1.0	8	12	67	20	10	20	234	13	61	3	4	na	na	3	na	0.53	0	2	0	0	0	na
DT	94	93-1b	5	1.0	31	35	83	20	10	20	142	253	958	16	1	na	na	5	na	2.48	1	5	4	0	0	na
DT	94	93-2b	5	1.0	2	8	69	20	10	20	112	53	1474	59	13	na	na	4	na	0.41	2	4	1	0	0	na
CW	94	94-1a	5	1.0	18	41	68	20	10	20	108	43	56	4	30	na	na	6	na	0.70	0	1	1	0	0	na

Appendix 4: Assays Table A4-1 (top left side)

Sample no. Geol	Yr.	Number	Lab Sample	UTM E	N	Map NTS	Nearest Relevant Mineral Occurrence	Lithologic Description	Au ppb	Ag ppm	Cu ppm	Pb ppm	Zn ppm	As ppm	Sb ppm	Hg ppm	Mo ppm	Tl ppm
DT	92	138-92																
DT	92	139-92																
DT	92	139-92a																
DT	92	140-92																
DT	92	140-92b																
DT	92	140-92c																
DT	92	140-92d																
DT	92	140-92e																
DT	92	77-92																
DT	92	32-92																
CW	92	46-92																
DT	93	30-93																
DT	93	113-2																
DT	93	29-3																
CW	93	66-93																
DT	93	139-93																
DT	93	105-93																
CW	93	83-3																
DT	93	120-93																
CW	93	84-3																
CW	93	86-93																
CW	93	85-93																
DT	94	33-4																
DT	94	73-93																
DT	94	33-1																
DT	94	73-6																
DT	94	73-11																
DT	94	13-5																
DT	94	13-9																
DT	94	13-2																
DT	94	33-5																
DT	94	73-5																
DT	93	166-30																
DT	94	75-3																
DT	93	167-2																
DT	94	38-93																
DT	93	163-5																
DT	93	163-2b																
DT	94	39-4																
DT	94	40-30																
DT	94	40-4																
DT	94	40-2b																
DT	94	40-1b																
DT	94	114-1																
CW	94	30-1a																
CW	94	104-1a																
DT	94	29-1b																
DT	94	25-1b																
DT	94	93-1b																
DT	94	93-2b																
CW	94	94-1a																

Appendix 4: Assays Table A4-1 (top right side)

Sample no.			Bi	Cd	Co	Ni	Ba	Sn	Te	W	Cr	V	Mn	La	Sr	Zr	Sc	Y	Ti	Al	Ca	Fe	Mg	K	Na	P
Geol	Yr.	Number	ppm	ppm	ppm	ppm	ppm	ppm	ppm	ppm	ppm	ppm	ppm	ppm	ppm	ppm	ppm	ppm	%	%	%	%	%	%	%	%
DT	92	138-1b	na	na	na	na	na	na	na	na	na	na	na	na	na	na	na	na	na	na	na	na	na	na	na	na
DT	92	139-5b	na	na	na	na	na	na	na	na	na	na	na	na	na	na	na	na	na	na	na	na	na	na	na	na
DT	92	139-6b	na	na	na	na	na	na	na	na	na	na	na	na	na	na	na	na	na	na	na	na	na	na	na	na
DT	92	140-6b	na	na	na	na	na	na	na	na	na	na	na	na	na	na	na	na	na	na	na	na	na	na	na	na
DT	92	140-8b	na	na	na	na	na	na	na	na	na	na	na	na	na	na	na	na	na	na	na	na	na	na	na	na
DT	92	140-9b	na	na	na	na	na	na	na	na	na	na	na	na	na	na	na	na	na	na	na	na	na	na	na	na
DT	92	140-10b	na	na	na	na	na	na	na	na	na	na	na	na	na	na	na	na	na	na	na	na	na	na	na	na
DT	92	143-1b	na	na	na	na	na	na	na	na	na	na	na	na	na	na	na	na	na	na	na	na	na	na	na	na
DT	92	142-3b	na	na	na	na	na	na	na	na	na	na	na	na	na	na	na	na	na	na	na	na	na	na	na	na
DT	92	21-1b	na	na	na	na	na	na	na	na	na	na	na	na	na	na	na	na	na	na	na	na	na	na	na	na
DT	92	53-2b	na	na	na	na	na	na	na	na	na	na	na	na	na	na	na	na	na	na	na	na	na	na	na	na
CW	92	45-1b	290	2	1	3	24	na	na	1	33	5	334	4	51	6	3	na	140	0.47	2	2	4.93	0.29	0	0
DT	93	38-1b	na	na	na	na	na	na	na	na	na	771	1410	na	3	4	na	na	6	1.61	1	7	4.79	0.17	1	1
DT	93	113-2	na	na	na	211	367	na	na	na	na	1161	1825	na	na	1	na	na	6	4.66	0	8	4.69	0.55	0	0
DT	93	25-5	na	na	na	na	11	na	na	na	na	104	347	2	1	1	na	na	2	1.52	0	1	1.08	0.14	1	0
CW	93	66-1b	na	na	1	3	2	na	na	na	76	8	139	na	na	1	na	na	1	0.63	185	1	1.55	0.02	0	0
DT	93	129-2b	na	na	na	na	na	na	na	na	na	na	na	na	na	na	na	na	na	na	na	na	na	na	na	na
DT	93	126-2b	na	na	565	338	83	na	na	na	2	239	1964	3	3	1	na	na	3	2.11	0	7	1.06	0.16	0	0
CW	93	31-1	2	3	14	5	11	na	na	na	1	42	51	na	3	1	1	na	na	0.61	1	930	1.35	0.43	0	0
DT	93	120-1b	na	na	na	na	na	na	na	na	na	na	na	na	na	na	na	na	na	na	na	na	na	na	na	na
CW	93	86-1	na	na	na	na	71	na	na	1	47	18	220	4	51	1	2	na	2	0.66	230	1	0.66	0.25	0	0
CW	93	86-1b	21	na	23	106	207	na	na	na	53	83	866	3	6	13	3	na	2	1.82	0	7	2.16	0.33	0	0
CW	93	85-1b	na	na	na	19	70	na	na	na	42	6	4400	1	14	6	1	na	0	0.56	1	1	2.2	0.19	0	0
DT	94	13-4	1	1.0	20	10	19	10	10	20	10	42	1007	1	61	na	na	1	na	1.09	1	2	2	0	0	na
DT	94	13-10	1	1.0	12	24	10	10	10	12	12	14	1731	4	1	na	na	1	na	0.92	1	2	1	0	0	na
DT	94	3-7	1	1.0	12	11	14	10	10	10	41	14	1961	47	14	na	na	1	na	0.71	1	2	1	0	0	na
DT	94	13-6	1	1.0	1	1	10	10	10	10	10	12	1111	32	10	na	na	1	na	0.14	1	1	1	0	0	na
DT	94	13-11	1	1.0	1	1	84	10	10	20	10	29	1072	20	37	na	na	1	na	0.55	1	2	1	0	0	na
DT	94	13-9	1	1.0	13	11	10	10	10	20	14	11	1460	10	1	na	na	1	na	0.69	1	1	1	0	0	na
DT	94	13-8	1	1.0	11	10	11	10	10	20	140	11	2380	19	5	na	na	1	na	0.51	1	2	1	0	0	na
DT	94	13-2	1	1.0	20	11	10	10	10	19	10.1	14	2780	224	3	na	na	1	na	0.77	1	2	1	0	0	na
DT	94	13-3	1	1.0	10	6	10.19	10	10	20	10	41	2124	8	11	na	na	1	na	0.59	1	1	1	0	0	na
DT	94	13-1	1	1.0	1	10	11	20	10	10	110	10	4152	74	17	na	na	1	na	2.14	1	4	1	1	0	na
DT	93	146-3b	na	na	603	83	10	na	na	na	29	9	339	10	6	1	2	na	na	0.27	1	1	0.31	0.17	0	0
DT	94	15-3	1	1.0	1	10	1	10	10	20	10	6	5245	2	4	na	na	1	na	0.61	2	2	1	0	0	na
DT	93	162-2	na	na	378	85	35	na	na	na	29	212	324	2	2	1	10	na	0	4.66	0	9	6.66	2.06	0	0
DT	94	18-1b	1	1.0	1	5	10	10	10	20	44	19	2230	10	11	na	na	1	na	0.76	0	1	1	0	0	na
DT	93	163-1	na	na	140	32	34	na	na	na	32	228	860	4	10	1	1	na	0	1.69	2	3.73	2.86	0.62	0	0
DT	93	163-2b	na	na	30	6	11	na	na	na	10	201	374	1	1	na	11	na	0	1.44	0	9	4.82	0.28	0	0
DT	94	39-4	1	1.0	21	6	12	20	10	20	112	5	1021	2	5	na	na	1	na	0.28	2	4	0	0	0	na
DT	94	40-3b	1	1.0	10	14	24	10	10	10	10	6	2164	3	5	na	na	1	na	0.32	10	2	1	0	0	na
DT	94	40-4	1	1.0	1	4	11	20	10	20	111	126	2051	3	17	na	na	1	na	0.38	1	5	1	0	0	na
DT	94	40-2b	1	1.0	15	16	25	20	10	20	20	42	2163	17	10	na	na	1	na	0.47	1	3	1	0	0	na
DT	94	40-1b	1	1.0	10	20	19	20	10	20	6	201	430	6	6	na	na	1	na	1.80	0	1	1	0	0	na
DT	94	114-1	1	1.0	11	21	20	20	10	20	214	130	227	1	3	na	na	1	na	2.93	0	1	1	0	0	na
CW	94	88-1a	1	1.0	8	1	12	20	10	20	10.2	1	3625	1	34	na	na	1	na	0.72	0	2	1	0	0	na
CW	94	104-1a	1	1.0	11	20	276	20	10	20	42	11	420	10	1	na	na	1	na	1.10	0	3	1	0	0	na
DT	94	26-1b	1	1.0	19	14	19	10	10	20	21	6	1161	2	2	na	na	1	na	2.14	1	2	2	0	0	na
DT	94	25-1b	1	1.0	5	11	11	10	10	10	10.8	12	93	1	1	na	na	1	na	0.11	0	1	0	0	0	na
DT	94	33-1b	1	1.0	17	15	91	20	10	20	142	25.1	968	10	1	na	na	1	na	2.48	1	3	3	0	0	na
DT	94	33-2b	1	1.0	1	3	10	10	10	10	10	11	1414	na	12	na	na	1	na	1.47	2	4	1	1	0	na
CW	94	94-1a	1	1.0	10	31	16	20	10	20	100	41	56	4	20	10	na	1	na	0.72	0	2	1	0	0	na

Appendix 4: Assays Table A4-1 (bottom left side)

Sample no. Geol	Yr.	Number	Lab Sample	UTM E	N	Map NTS	Nearest Relevant Mineral Occurrence	Lithologic Description	Au ppb	Ag ppm	Cu ppm	Pb ppm	Zn ppm	As ppm	Sb ppm	Hg ppm	Mo ppm	Tl ppm
DT	94	98-1b	G-251	580000	7199950	106C/14	DOBBY	Cu mineralized diorite	26	0.2	1	11	113	5	5	na	1	na
CW	94	98-1a	G-283	580550	7208450	106C/14	ANOKI	Bleached siltstone with pyrite-quartz veining	7	0.2	31	4	1	5	5	na	3	na
DT	94	11-6	G-217	580750	7201150	106C/14	PORPHYRY	Chloritic quartz albite syenite	48	0.2	3131	12	28	5	5	na	13	na
DT	94	11-12	G-222	580750	7201150	106C/14	PORPHYRY	Crackle brecciated maroon siltstone	5	0.2	1	10	13	5	5	na	1	na
DT	94	11-11	G-293	580750	7201150	106C/14	PORPHYRY	Crackle brecciated maroon siltstone	5	0.2	13	10	54	5	5	na	1	na
DT	94	11-3	G-214	580750	7201150	106C/14	PORPHYRY	Quartz albite syenite	62	0.2	6594	13	28	5	5	na	15	na
DT	94	11-5	G-216	580750	7201150	106C/14	PORPHYRY	Potassic altered quartz albite syenite	8	0.2	185	9	21	5	5	na	2	na
DT	94	11-4	G-215	580750	7201150	106C/14	PORPHYRY	Quartz albite syenite	29	0.2	2763	10	25	5	5	na	13	na
DT	94	11-13	G-223	580750	7201150	106C/14	PORPHYRY	Crackle brecciated maroon siltstone	5	0.2	1	11	12	5	5	na	1	na
DT	94	11-9	G-220	580750	7201150	106C/14	PORPHYRY	Quartz albite syenite from chilled margin	5	0.2	80	11	14	5	5	na	1	na
DT	94	11-8	G-219	580750	7201150	106C/14	PORPHYRY	Quartz albite syenite from chilled margin	40	0.2	3715	12	22	5	5	na	4	na
DT	94	11-7	G-218	580750	7201150	106C/14	PORPHYRY	Quartz albite syenite	18	0.2	2559	11	19	5	5	na	2	na
DT	94	11-10	G-221	580750	7201150	106C/14	PORPHYRY	Crackled maroon siltstone	5	0.2	46	1	17	5	5	na	1	na
CW	94	95-1a	G-278	580960	7209600	106F/3	ANOKI	Metalliferous vein in Pinguicula Gp. unit A	5	0.2	348	4	10	5	5	na	1	na
CW	94	97-1a	G-282	581100	7209800	106C/14	ANOKI	Altered siltstone near Wernecke Breccia	189	1.6	1	19	65	5	12	na	1528	na
CW	94	96-2a	G-279	581200	7209700	106C/14	ANOKI	Potassic altered Wernecke Breccia	5	0.2	231	2	5	5	5	na	3	na
CW	94	96-3a	G-280	581200	7209700	106C/14	ANOKI	Potassic altered Wernecke Breccia	5	0.3	1963	6	6	5	5	na	1	na
CW	94	96-4a	G-281	581200	7209700	106C/14	ANOKI	Hematite/carbonate vein in Quartet Group	5	0.2	35	11	7	5	5	na	1	na
CW	94	27-1a	G-257	581550	7208250	106C/14	ANOKI	Pyritic carbonate vein in chloritic host	18	0.2	4400	8	14	5	5	na	1	na
CW	94	28-6a	G-263	582200	7207650	106C/14	ANOKI	Diorite	5	0.2	1	10	20	5	5	na	1	na
CW	94	28-7a	G-264	582200	7207650	106C/14	ANOKI	Diorite near sedimentary rock contact	5	0.2	9	15	33	5	5	na	1	na
CW	94	28-9a	G-266	582200	7207650	106C/14	ANOKI	Siltstone	5	0.2	4	5	5	5	5	na	1	na
CW	94	28-8a	G-265	582200	7207650	106C/14	ANOKI	Siltstone	10	0.2	75	21	20	5	5	na	1	na
CW	94	28-3a	G-260	582200	7207650	106C/14	ANOKI	Wernecke Breccia	5	0.2	1	10	17	5	5	na	1	na
CW	94	28-1a	G-258A	582200	7207650	106C/14	ANOKI	Chloritic Wernecke Breccia	21	0.2	7660	2	2	5	5	na	29	na
CW	94	28-1a	G-258	582200	7207650	106C/14	ANOKI	Chloritic Wernecke Breccia	5	0.2	2	10	18	5	5	na	1	na
CW	94	28-4a	G-261	582200	7207650	106C/14	ANOKI	Diorite next to Wernecke Breccia	45	0.2	214	11	21	5	5	na	1	na
CW	94	28-5a	G-262	582200	7207650	106C/14	ANOKI	Chloritized diorite	19	0.2	1464	9	39	5	5	na	14	na
CW	94	28-2a	G-259	582200	7207650	106C/14	ANOKI	Wernecke Breccia	8	0.2	4	11	19	5	5	na	1	na
CW	94	21-1a	G-256	582800	7207700	106C/14	ANOKI	Cu-rich carbonate vein in dolostone near breccia	8	20.5	2815	10	159	191	563	na	1	na
DT	94	34-1b	G-242	583000	7201400	106C/14	ANOKI	"Bleached" Wernecke Breccia	39	0.2	604	9	3	5	5	na	15	na
DT	94	32-3	G-240	583150	7206050	106C/14	ANOKI	Pyritic and hematitic carbonate (Gillespie L. Gp.)	5	0.2	1	22	11	5	5	na	1	na
DT	94	32-4b	G-241	583150	7206050	106C/14	ANOKI	Quartz vein in red dolostone (Gillespie L. Gp.)	5	0.2	4	4	2	5	5	na	1	na
CW	94	18-1	G-255	583750	7208200	106C/14	--	Green shale, Tatlya Formation	5	0.2	160	5	4	5	5	na	3	na
DT	94	31-1b	G-238	583750	7206250	106C/14	--	Rusty, pyritic sandstone of basal Pinguicula Gp.	5	0.2	22	8	3	5	5	na	2	na
DT	94	31-3b	G-239	583750	7206250	106C/14	ANOKI	Stained dolostone, Gillespie Lake Group	5	0.2	13	6	6	5	5	na	1	na
CW	94	4-2b	G-268	584400	7202750	106C/14	TETRAHEDRITE CK.	Wernecke Breccia	7	0.2	1	6	1	5	5	na	1	na
CW	94	4-2f	G-272	584400	7202750	106C/14	TETRAHEDRITE CK.	Wernecke Breccia, dolostone-rich	5	0.2	3	5	1	5	5	na	1	na
CW	94	4-2c	G-269	584400	7202750	106C/14	TETRAHEDRITE CK.	Wernecke Breccia matrix	5	0.2	2	9	19	5	5	na	1	na
CW	94	4-2e	G-271	584400	7202750	106C/14	TETRAHEDRITE CK.	Silicified dolostone	5	0.2	2	6	2	5	5	na	1	na
CW	94	4-2a	G-267	584400	7202750	106C/14	TETRAHEDRITE CK.	Wernecke Breccia	5	0.2	1	7	1	5	5	na	1	na
CW	94	4-2d	G-270	584400	7202750	106C/14	TETRAHEDRITE CK.	Wernecke Breccia matrix	49	0.2	1832	11	37	5	5	na	1	na
CW	94	44-1a	G-273	585600	7185750	106C/14	POD	Pink sparry carbonate	5	0.2	2	4	1	5	5	na	1	na
DT	94	62-1b	G-248	586150	7189450	106C/14	POD	Galena-rich stockwork in sparry carbonate	5	0.3	2	964	370	5	5	na	1	na
CW	94	109-1a	G-286	586450	7202250	106C/14	TETRAHEDRITE CK.	Silicified dolostone within Gillespie Lake Group	5	0.2	5	16	17	398	37	na	1	na
CW	94	107-2a	G-285	587000	7201750	106C/14	TETRAHEDRITE CK.	Zebra dolostone clast w/ malachite and azurite	5	0.2	331	3	15	63	5	na	1	na
CW	94	120-1a	G-289	587200	7197200	106C/14	--	Silicified dolostone from Gillespie Lake Group	5	0.2	4089	3	304	21	5	na	10	na
DT	94	146-1b	G-254	588450	7178050	106C/14	--	Hematitic pisolites in Hematite Creek Group	5	0.2	41	35	185	5	5	na	1	na
CW	94	111-1a	G-287	589000	7203200	106C/14	DAN	Vein in Pinguicula unit C	5	7.7	91	23	245	9	26	na	1	na
CW	94	115-1a	G-288	589250	7199750	106C/14	DAN	Vein in Profet dolostone	5	1	2455	1732	>2000	77	>200	na	1	na
CW	94	57-2a	G-274	590300	7201250	106C/14	DAN	Galena in grey carbonate	5	4.7	151	2594	2170	34	45	na	1	na
DT	94	123-1b	G-253	591200	7191450	106C/14	--	Red-stained Quartz arenite	5	0.2	7	15	6	5	5	na	12	na
CW	94	63-3a	G-275	593300	7190700	106C/14	--	Conglomerate, rusty	5	0.2	15	36	124	5	5	na	13	na

Appendix 4: Assays Table A4-1 (bottom right side)

Sample no. Geol Number	Yr.	#	Bi ppm	Cd ppm	Co ppm	Ni ppm	Ba ppm	Sn ppm	Te ppm	W ppm	Cr ppm	V ppm	Mn ppm	La ppm	Sr ppm	Zr ppm	Sc ppm	Y ppm	Ti %	Al %	Ca %	Fe %	Mg %	K %	Na %	P %
DT	94	98-1b	.5	1.0	68	38	11	20	10	20	107	213	250	1	15	na	na	1	na	3.57	0	5	6	0	0	na
CW	94	98-1a	.5	1.0	76	30	24	20	10	20	107	2	14	8	-1	na	na	1	na	0.38	0	3	0	0	0	na
DT	94	11-6	.5	1.0	31	3	13	20	10	20	105	25	603	51	16	na	na	20	na	1.29	3	4	1	0	0	na
DT	94	11-12	.5	1.0	17	25	235	20	10	20	110	61	340	75	9	na	na	8	na	0.89	1	4	1	0	0	na
DT	94	11-11	.5	1.0	25	39	129	20	10	20	114	57	741	121	2	na	na	13	na	1.11	2	4	2	0	0	na
DT	94	11-3	.5	1.0	58	2	23	20	10	20	86	27	555	58	15	na	na	16	na	1.20	3	5	1	0	0	na
DT	94	11-5	.5	1.0	20	2	13	20	10	20	73	23	763	84	34	na	na	20	na	0.81	5	3	1	0	0	na
DT	94	11-4	5	1.0	69	2	28	20	10	20	69	25	566	53	15	na	na	18	na	1.14	3	4	1	0	0	na
DT	94	11-13	.5	1.0	19	28	201	20	10	20	107	50	1310	54	5	na	na	7	na	0.84	3	4	2	0	0	na
DT	94	11-9	.5	1.0	33	10	52	20	10	20	103	52	1119	29	22	na	na	8	na	0.59	4	4	1	0	0	na
DT	94	11-8	.5	1.0	24	9	76	20	10	20	67	33	700	20	32	na	na	14	na	0.87	4	4	1	0	0	na
DT	94	11-7	.5	1.0	38	1	13	20	10	20	78	30	749	55	18	na	na	20	na	0.72	3	4	1	0	0	na
DT	94	11-10	.5	1.0	29	18	85	20	10	20	102	60	1399	271	5	na	na	26	na	0.97	2	4	2	0	0	na
CW	94	95-1a	.5	1.0	69	9	276	20	10	20	84	10	6148	4	150	na	na	6	na	0.50	6	4	2	0	0	na
CW	94	97-1a	12	1.0	6	1	16	20	10	20	58	5	54	3	2	na	na	7	na	0.52	0	3	0	0	0	na
CW	94	96-2a	.5	1.0	1	4	83	20	10	20	59	4	535	31	2	na	na	3	na	0.59	0	1	0	0	0	na
CW	94	96-3a	.5	1.0	3	7	115	20	10	20	81	3	349	27	4	na	na	3	na	0.47	0	2	0	0	0	na
CW	94	96-4a	5	1.0	15	19	181	20	10	20	121	3	3994	15	3	na	na	4	na	0.24	0	5	0	0	0	na
CW	94	27-1a	.5	1.0	77	46	176	20	10	20	92	224	657	10	14	na	na	4	na	2.53	3	4	4	0	0	na
CW	94	28-6a	5	1.0	18	24	67	20	10	20	93	274	1239	10	-1	na	na	3	na	1.69	1	5	3	0	0	na
CW	94	28-7a	.5	1.0	31	23	79	20	10	20	101	342	835	16	1	na	na	4	na	2.46	1	5	4	0	0	na
CW	94	28-9a	.5	1.0	4	8	91	20	10	20	60	30	1772	37	4	na	na	4	na	0.43	3	2	2	0	[illegible]	na
CW	94	28-8a	.5	1.0	39	23	180	20	10	20	86	248	1036	50	15	na	na	8	na	1.55	3	5	2	0	0	na
CW	94	28-3a	.5	1.0	18	32	46	20	10	20	118	64	564	49	-1	na	na	5	na	1.52	1	5	2	0	0	na
CW	94	28-1a	.5	1.0	25	4	159	20	10	20	47	11	375	4	6	na	na	3	na	0.73	1	1	0	1	0	na
CW	94	28-1b	.5	1.0	15	33	66	20	10	20	130	60	656	23	2	na	na	5	na	1.48	1	5	2	0	0	na
CW	94	28-4a	.5	1.0	27	27	38	20	10	20	78	192	1299	16	9	na	na	7	na	1.65	3	4	4	0	0	na
CW	94	28-5a	.5	1.0	41	29	86	20	10	20	55	123	2045	25	27	na	na	15	na	3.08	6	4	4	0	0	na
CW	94	28-2a	.5	1.0	20	32	55	20	10	20	121	71	512	42	-1	na	na	6	na	1.66	1	5	3	0	0	na
CW	94	21-1a	563	1.0	1	1	7	20	10	20	19	12	2545	3	77	na	na	4	na	0.01	>10.00	2	>10.00	0	0	na
DT	94	34-1b	.5	1.0	9	13	56	20	10	20	54	11	3122	12	32	na	na	8	na	0.39	6	3	3	0	0	na
DT	94	32-3	.5	1.0	39	3	16	20	10	20	104	14	4839	-1	5	na	na	3	na	0.03	5	6	4	0	0	na
DT	94	32-4b	.5	1.0	1	8	6	20	10	20	153	12	1871	3	12	na	na	7	na	0.01	6	1	4	0	0	na
CW	94	18-1	.5	1.0	7	5	8	20	10	20	164	5	1726	14	4	na	na	1	na	0.16	1	2	0	0	0	na
DT	94	31-1b	.5	1.0	17	28	84	20	10	20	134	25	78	5	6	na	na	11	na	0.75	1	1	0	1	0	na
DT	94	31-3b	.5	1.0	42	18	16	20	10	20	36	18	2085	4	20	na	na	8	na	0.18	9	1	7	0	0	na
CW	94	4-2b	.5	1.0	3	5	119	20	10	20	64	29	936	31	4	na	na	6	na	0.60	4	2	2	0	0	na
CW	94	4-2f	.5	1.0	3	4	141	20	10	20	51	25	1180	25	7	na	na	6	na	0.40	5	2	3	0	0	na
CW	94	4-2c	.5	1.0	33	37	114	20	10	20	88	269	664	16	2	na	na	5	na	2.44	2	4	5	0	0	na
CW	94	4-2e	.5	1.0	2	3	46	20	10	20	79	37	895	24	3	na	na	6	na	0.29	3	2	2	0	0	na
CW	94	4-2a	.5	1.0	1	3	966	20	10	20	91	43	753	23	15	na	na	5	na	0.41	3	4	2	0	0	na
CW	94	4-2d	.5	1.0	26	35	65	20	10	20	117	287	1026	20	2	na	na	11	na	1.92	2	5	4	0	0	na
CW	94	44-1a	.5	1.0	1	1	4	20	10	20	6	7	472	4	33	na	na	1	na	0.01	>10.00	1	>10.00	0	0	na
DT	94	62-1b	.5	1.0	1	1	25	20	10	20	10	9	1898	4	26	na	na	7	na	0.04	>10.00	1	>10.00	0	0	na
CW	94	109-1a	37	1.0	1	4	1464	20	10	20	182	1	27	1	3	na	na	1	na	0.02	0	2	0	0	0	na
CW	94	107-2a	.5	1.0	1	2	1665	20	10	20	6	7	390	4	40	na	na	1	na	0.02	>10.00	0	>10.00	0	0	na
CW	94	120-1a	.5	1.0	12	37	78	20	10	20	170	3	57	2	1	na	na	3	na	0.13	1	1	0	0	0	na
DT	94	146-1b	.5	1.0	5	20	153	20	10	20	201	58	419	1	8	na	na	3	na	1.04	0	8	0	0	0	na
CW	94	111-1a	26	1.4	1	1	23	20	10	20	7	8	1010	4	27	na	na	1	na	0.04	>10.00	0	>10.00	0	0	na
CW	94	115-1a	>2000	846.9	1	1	2	20	113	>2000	38	3	309	2	3	na	na	1	na	0.02	2	1	1	0	0	na
CW	94	57-2a	45	13.3	1	1	4	20	10	20	4	8	912	4	48	na	na	1	na	0.01	>10.00	0	>10.00	0	0	na
DT	94	123-1b	.5	1.0	1	4	32	20	10	20	223	5	31	3	2	na	na	1	na	0.12	0	1	0	0	0	na
CW	94	63-3a	.5	1.0	2	5	74	20	10	20	235	16	41	2	3	na	na	1	na	0.29	0	2	0	0	0	na

Appendix 4: Assays Table A4-1 (bottom left side)

Sample no. Geol	Yr.	Number	Lab Sample	UTM E	N	Map NTS	Nearest Relevant Mineral Occurance	Lithologic Description	Au ppb	Ag ppm	Cu ppm	Pb ppm	Zn ppm	As ppm	Sb ppm	Hg ppm	Mo ppm	Tl ppm
DT	94	98-1b	G 211	580300	7199500	106C/14	[illegible]	Fe-stained quartz [illegible]	20	0.2	5	15	333	5	5	na	1	na
CW	94	98-1a	G 212	580500	7199400	106C/14	ANOKI	Brecciated siltstone with fine quartz veining	1	0.2	31	4	3	5	5	na	3	na
DT	94	11-6	G 210	580700	7201500	106C/14	POSTHOLE	Chloritic quartz albite syenite	50	0.2	1133	12	29	5	5	na	11	na
DT	94	11-12	G 222	580700	7201100	106C/14	POSTHOLE	Cracked brecciated titanium silicate	5	0.2	5	10	11	5	5	na	1	na
DT	94	11-11	G 221	580700	7201150	106C/14	POSTHOLE	Cracked brecciated titanium silicate	5	0.2	11	10	14	5	5	na	1	na
DT	94	11-3	G 214	580700	7201350	106C/14	POSTHOLE	Quartz albite syenite	60	0.2	6084	11	28	5	5	na	15	na
DT	94	11-5	G 216	580700	7201300	106C/14	POSTHOLE	Brecciated stained quartz albite syenite	5	0.2	786	9	47	5	5	na	4	na
DT	94	11-4	G 215	580700	7201350	106C/14	POSTHOLE	Quartz albite syenite	250	0.2	2863	10	25	5	5	na	13	na
DT	94	11-13	G 223	580700	7201400	106C/14	POSTHOLE	Cracked silica and titanium silicate	5	0.2	5	11	12	5	5	na	1	na
DT	94	11-9	G 208	580700	7201550	106C/14	POSTHOLE	Quartz albite syenite from chilled margin	5	0.2	80	11	14	5	5	na	1	na
DT	94	11-8	G 219	580700	7201600	106C/14	POSTHOLE	Quartz albite syenite from chilled margin	40	0.2	670	12	49	5	5	na	4	na
DT	94	11-7	G 218	580700	7201650	106C/14	POSTHOLE	Quartz albite syenite	10	0.2	2559	11	19	5	5	na	2	na
DT	94	11-10	G 227	580700	7201700	106C/14	POSTHOLE	Cracked titanium silicate	5	0.2	60	11	11	5	5	na	1	na
CW	94	95-1a	G 278	530900	7209600	106C/1	ANOKI	Metasomatic veinlet in intrusive (Quruhn A	5	0.2	83	10	10	5	5	na	1	na
CW	94	97-1a	G 285	541500	7209600	106C/14	ANOKI	Altered basement rock, Wernecke Breccia	100	1.6	5	11	65	5	11	na	11.25	na
CW	94	96-2a	G 279	541000	7209400	106C/14	ANOKI	Hydrothermal altered Wernecke Breccia	5	1	131	2	5	5	5	na	3	na
CW	94	96-3a	G 280	541500	7209700	106C/14	ANOKI	Hydrothermal altered Wernecke Breccia	5	0.2	1041	9	6	5	5	na	1	na
CW	94	96-4a	G 281	541000	7209700	106C/14	ANOKI	Dolomite carbonate vein in Quartet Group	5	0.2	30	11	7	5	5	na	1	na
CW	94	27-1a	G 270	541500	7209250	106C/14	ANOKI	Hydrothermal vein in Wernecke Breccia	10	0.2	1400	9	14	5	5	na	1	na
CW	94	28-6a	G 263	542700	7208300	106C/14	ANOKI	Diorite	5	0.2	1	10	20	5	5	na	1	na
CW	94	28-7a	G 264	542000	7208300	106C/14	ANOKI	Wernecke Sediments/Dark contact	5	0.2	9	15	31	5	5	na	1	na
CW	94	28-9a	G 266	542200	7208600	106C/14	ANOKI	Siltstone	5	0.2	8	5	9	5	5	na	1	na
CW	94	28-8a	G 265	542000	7208600	106C/14	ANOKI	Siltstone	10	0.2	5	21	20	5	5	na	1	na
CW	94	28-3a	G 260	542000	7208400	106C/14	ANOKI	Wernecke breccia	5	0.2	5	10	10	5	5	na	1	na
CW	94	28-1a	G 258	542000	7208600	106C/14	ANOKI	Chloritic Wernecke Breccia	21	0.2	649	2	2	5	5	na	13	na
CW	94	28-1a	G 258	542000	7208600	106C/14	ANOKI	Chloritic Wernecke Breccia	5	0.2	2	10	19	5	5	na	1	na
CW	94	28-4a	G 261	542100	7208600	106C/14	ANOKI	Fenitized Wernecke Breccia	45	0.2	213	11	27	5	5	na	1	na
CW	94	28-5a	G 262	542000	7208400	106C/14	ANOKI	Chloritized diorite	10	0.2	1364	9	19	5	5	na	13	na
CW	94	29-2a	G 274	542000	7208600	106C/14	ANOKI	Wernecke breccia	5	0.2	1	11	14	5	5	na	1	na
CW	94	21-1a	G 216	542400	7207700	106C/14	ANOKI	Fe-rich carbonate vein in siltstone/clast bearing	5	20.4	2305	10	159	191	583	na	1	na
DT	94	34-1b	G 242	583400	7208400	106C/14	ANOKI	Stained rock, Wernecke Breccia	10	0.2	104	9	3	5	5	na	13	na
DT	94	32-3	G 240	583500	7208400	106C/14	ANOKI	Pyritic and hematitic carbonate (Gillespie L. Gp.)	5	0.2	1	23	11	5	5	na	1	na
DT	94	32-4b	G 241	583500	7208400	106C/14	ANOKI	Quartz vein in red dolomite (Gillespie L. Gp.)	5	0.2	4	4	2	5	5	na	1	na
CW	94	18-1	G 255	583700	7208700	106C/14		Green chert, Tatina Formation	5	0.2	160	5	4	5	5	na	1	na
DT	94	31-1b	G 238	583500	7208250	106C/14		Shaly, pyritic sandstone of basal Proterozoic Gp.	5	0.2	27	2	3	5	5	na	1	na
DT	94	31-3b	G 239	583500	7208250	106C/14	ANOKI	Stained dolostone, Gillespie Lake Group	5	0.2	13	6	9	5	5	na	1	na
CW	94	4-2b	G 268	584400	7207750	106C/14	TETRAHEDRITE CK.	Wernecke breccia	1	0.2	1	6	1	5	5	na	1	na
CW	94	4-2f	G 272	584400	7207750	106C/14	TETRAHEDRITE CK.	Wernecke breccia, dolostone rich	5	0.2	1	5	1	5	5	na	1	na
CW	94	4-2c	G 269	584400	7207750	106C/14	TETRAHEDRITE CK.	Wernecke breccia matrix	5	0.2	2	9	19	5	5	na	1	na
CW	94	4-2e	G 271	584400	7207750	106C/14	TETRAHEDRITE CK.	Silicified dolostone	5	0.2	2	6	3	5	5	na	1	na
CW	94	4-2a	G 267	584400	7207750	106C/14	TETRAHEDRITE CK.	Wernecke breccia	5	0.2	1	1	1	5	5	na	1	na
CW	94	4-2d	G 270	584400	7207750	106C/14	TETRAHEDRITE CK.	Wernecke breccia matrix	89	0.2	5882	11	11	5	5	na	1	na
CW	94	44-1a	G 273	585400	7198150	106C/14	POD	Vein quartz carbonate	5	0.2	2	3	1	5	5	na	1	na
DT	94	62-1b	G 248	586150	7198650	106C/14	POD	Calcite-rich stockwork in quartz carbonate	2	0.2	2	364	170	5	5	na	1	na
CW	94	109-1a	G 286	586400	7202750	106C/14	TETRAHEDRITE CK.	Silicified dolostone within Gillespie Lake Group	1	0.2	5	56	72	239	11	na	1	na
CW	94	107-2a	G 285	587000	7201750	106C/14	TETRAHEDRITE CK.	Altered dolostone clast w/ malachite and azurite	3	0.2	111	3	55	93	5	na	1	na
CW	94	120-1a	G 293	587000	7197200	106C/14		Silicified dolostone from Gillespie Lake Group	1	0.2	4391	1	344	25	1	na	19	na
DT	94	146-1b	G 254	586450	7193650	106C/14	--	Hematitic pebbles in Hematite Creek Group	3	0.2	47	35	185	5	5	na	1	na
CW	94	111-1a	G 287	589400	7203700	106C/14	DWN	Skarn in Pinguicula Unit C	5	1	37	23	284	9	25	na	1	na
CW	94	115-1a	G 288	589650	7199950	106C/14	DWN	Skarn in Proviet dolostone	5	1	2906	1732	2444	31	108	na	1	na
CW	94	57-2a	G 274	590900	7200700	106C/14	DWN	Calcite in skarn carbonate	1	4.1	167	2644	2130	14	35	na	1	na
DT	94	123-1b	G 253	591200	7191850	106C/14	--	Red stained Quartz syenite	3	0.2	2	15	6	5	5	na	12	na
CW	94	63-3a	G 275	590350	7190700	106C/14		Carbonate vein	1	0.1	75	30	134	5	5	na	10	na

Appendix 4: Assays Table A4-1 (bottom right side)

Sample no. Geol	Yr.	Number	Bi ppm	Cd ppm	Co ppm	Ni ppm	Ba ppm	Sn ppm	Te ppm	W ppm	Cr ppm	V ppm	Mn ppm	La ppm	Sr ppm	Zr ppm	Sc ppm	Y ppm	Ti %	Al %	Ca %	Fe %	Mg %	K %	Na %	P %
DT	94	98-1b	1	1.0	18	35	11	20	10	20	197	215	268	1	15	na	na	1	na	0.62	0	5	6	0	0	na
CW	94	98-1a	1	1.0	16	30	24	20	10	20	102	2	14	8	1	na	na	1	na	0.68	0	3	0	0	0	na
DT	94	11-6	1	1.0	21	1	13	20	10	20	105	20	103	1	70	na	na	15	na	1.73	1	4	1	0	0	na
DT	94	11-12	1	1.0	17	61	230	20	10	20	110	61	140	15	9	na	na	8	na	0.89	1	4	1	0	0	na
DT	94	11-11	1	1.0	31	61	170	20	10	20	114	51	141	1.1	3	na	na	11	na	1.11	2	4	2	0	0	na
DT	94	11-3	1	1.0	18	2	21	20	10	20	86	22	110	8	10	na	na	15	na	1.70	1	3	1	0	0	na
DT	94	11-5	1	1.0	11	2	10	20	10	20	11	2.5	161	8	15	na	na	20	na	0.81	1	3	1	0	0	na
DT	94	11-4	1	1.0	29	1	25	20	10	20	84	31	390	12	11	na	na	16	na	1.14	1	4	1	0	0	na
DT	94	11-13	1	1.0	15	15	37	20	10	20	102	30	1130	14	5	na	na	1	na	0.84	1	3	1	0	0	na
DT	94	11-9	1	1.0	12	33	52	20	10	20	100	52	3110	14	23	na	na	8	na	0.99	1	4	1	0	0	na
DT	94	11-8	1	1.0	21	1	30	20	10	20	57	21	700	13	11	na	na	19	na	1.10	1	3	1	0	0	na
DT	94	11-7	1	1.0	19	1	10	20	10	20	78	30	649	11	10	na	na	10	na	0.97	1	4	1	0	0	na
DT	94	11-10	1	1.0	14	10	30	20	10	20	50	44	1196	7.1	3	na	na	14.1	na	0.91	2	3	1	0	0	na
CW	94	96-1a	1	1.0	3.0	1	2.0	20	10	20	84	15	1110	4	110	na	na	5	na	0.56	1.4	4	1	0	0	na
CW	94	97-1a	10	1.0	2	1	10	20	10	20	10	1	18	1	3	na	na	1	na	0.10	0	1	0	0	0	na
CW	94	96-2a	1	1.0	1	1	6.5	20	10	20	24	4	130	15	2	na	na	3	na	0.79	0	1	0	0	0	na
CW	94	96-3a	1	1.0	1	1	11.5	20	10	20	37	1	345	7.1	4	na	na	1	na	0.41	0	1	0	0	0	na
CW	94	96-4a	1	1.0	11	10	192	20	10	20	121	1	2094	10	1	na	na	8	na	0.68	0	3	0	0	0	na
CW	94	27-1a	1	1.0	1	10	1.0	20	10	20	10	2.5	1.0	10	10	na	na	1	na	2.3	1	1	1	0	0	na
CW	94	29-6a	1	1.0	15	25	62	20	10	20	91	228	1230	10	1	na	na	1	na	1.61	1	3	3	0	0	na
CW	94	29-7a	1	1.0	11	15	74	20	10	20	101	120	835	10	1	na	na	1	na	1.40	1	3	3	0	0	na
CW	94	29-9a	1	1.0	4	1	37	20	10	20	66	81	1110	11	4	na	na	1	na	0.81	1	2	2	0	0	na
CW	94	29-8a	1	1.0	10	10	100	20	10	20	90	150	1660	20	11	na	na	1	na	1.55	1	3	2	0	0	na
CW	94	29-3a	1	1.0	16	10	45	20	10	20	110	54	554	10	1	na	na	1	na	1.32	1	3	2	0	0	na
CW	94	28-1a	1	1.0	11	1	110	20	10	20	81	11	110	8	6	na	na	1	na	0.73	1	1	1	1	0	na
CW	94	28-1a	1	1.0	11	10	80	20	10	20	120	40	605	11	7	na	na	1	na	1.10	1	3	2	0	0	na
CW	94	28-4a	1	1.0	11	10	11	20	10	20	10	10	1210	10	1	na	na	1	na	2.10	1	4	3	0	0	na
CW	94	28-5a	1	1.0	17	20	86	20	10	20	10	121	2080	20	21	na	na	15	na	1.98	0	4	4	0	0	na
CW	94	28-2a	1	1.0	10	10	10	20	10	20	121	1	157	10	1	na	na	1	na	1.10	1	1	1	0	0	na
CW	94	21-1a	100	1.0	1	1	1	20	10	20	10	1.0	1540	1	11	na	na	1	na	0.01	>10.00	2	>10.00	0	0	na
DT	94	34-1b	1	1.0	1	11	10	20	10	20	1	11	1107	12	10	na	na	1	na	0.11	1	1	1	0	0	na
DT	94	32-3	1	1.0	10	1	10	20	10	20	104	14	4039	1	1	na	na	1	na	0.01	1	1	1	0	0	na
DT	94	32-4b	1	1.0	1	1	1	20	10	20	10	1	1907	1	10	na	na	1	na	0.01	1	1	1	0	0	na
CW	94	18-1	1	1.0	7	1	1	20	10	20	104	1	1705	14	4	na	na	1	na	0.16	1	2	1	0	0	na
DT	94	31-1b	1	1.0	11	25	41	20	10	20	114	11	10	1	1	na	na	11	na	0.15	1	1	2	1	0	na
DT	94	31-3b	1	1.0	41	10	10	20	10	20	10	10	2060	1	10	na	na	1	na	0.16	1	1	1	0	0	na
CW	94	4-2b	1	1.0	1	1	119	20	10	20	14	10	10	11	1	na	na	1	na	0.02	1	2	1	0	0	na
CW	94	4-2f	1	1.0	1	1	111	20	10	20	11	10	1580	10	1	na	na	1	na	0.40	1	2	1	0	0	na
CW	94	4-2c	1	1.0	11	10	114	20	10	20	10	10	1640	10	1	na	na	1	na	2.44	2	4	1	0	0	na
CW	94	4-2e	1	1.0	1	1	10	20	10	20	10	10	1085	14	1	na	na	1	na	0.71	1	2	2	0	0	na
CW	94	4-2a	1	1.0	1	1	140	20	10	20	11	11	1.1	10	10	na	na	1	na	0.11	1	1	1	0	0	na
CW	94	4-2d	1	1.0	24	15	60	20	10	20	117	20.7	1826	10	11	na	na	11	na	1.10	2	5	4	0	0	na
CW	94	44-1a	1	1.0	1	1	1	20	10	20	1	1	472	1	10	na	na	1	na	0.01	>10.00	1	>10.00	0	0	na
DT	94	62-1b	1	1.0	1	1	25	20	10	20	10	1	1098	1	10	na	na	1	na	0.04	>10.00	1	>10.00	0	0	na
CW	94	109-1a	11	1.0	1	1	164	20	10	20	10	1	11	1	1	na	na	1	na	0.02	1	2	1	0	0	na
CW	94	107-2a	1	1.0	1	2	160	20	10	20	1	1	80	1	10	na	na	1	na	0.02	>10.00	2	>10.00	0	0	na
CW	94	120-1a	1	1.0	10	10	10	20	10	20	10	1	11	1	1	na	na	1	na	0.11	1	1	1	0	0	na
DT	94	146-1b	1	1.0	1	10	110	20	10	20	101	10	439	1	1	na	na	1	na	1.01	1	3	3	0	0	na
CW	94	111-1a	10	1.0	1	1	10	20	10	20	1	1	1060	1	10	na	na	1	na	0.01	>10.00	2	>10.00	1	0	na
CW	94	115-1a	1000	340.0	1	1	1	20	111	>10.00	10	1	109	1	1	na	na	1	na	0.02	1	1	1	0	0	na
CW	94	57-2a	10	1.0	1	1	1	20	10	20	1	1	10	1	10	na	na	1	na	0.01	>10.00	1	>10.00	0	0	na
DT	94	123-1b	1	1.0	1	1	10	20	10	20	10.1	1	17	1	1	na	na	1	na	0.12	1	1	1	0	0	na
CW	94	63-3a	1	1.0	1	1	1	20	10	20	1.0	1	1	1	1	na	na	1	na	0.01	1	1	1	0	0	na